High-precision electroweak experiments: A global search for new physics beyond the Standard Model

Paul Langacker, Mingxing Luo, and Alfred K. Mann

Department of Physics, University of Pennsylvania, Philadelphia, Pennsylvania 19104-6396

This paper provides a theoretical framework for the high-precision ($\leq 1\%$) electroweak experiments that are likely to be done in the next ten years. The authors have collected the Standard Model (SM) predictions of 14 weak neutral-current observables and 15 W and Z properties to the one-loop level and have calculated the deviations that would be caused by ten general types of possible new physics that enter at the tree or loop level. Certain experiments appear to have special promise as probes of the new physics considered here. Most importantly, a systematic procedure is introduced that provides a prescription for the analysis of future experimental data and the means of delineating the nature of new physics if quantitative deviations from SM predictions are observed.

CONTENTS

I. INTRODUCTION AND MOTIVATION

The purpose of this paper is to provide a theoretical framework for the high-precision weak-interaction experiments that are likely to be done in the next ten years.[1] These experiments, each designed to have a precision of the order of one percent or better, will test the electroweak interaction component of the Standard Model (SM), the Glashow-Weinberg-Salam theory (Weinberg, 1967, Salam, 1969, Glashow *et al.*, 1970), to high precision, and might possibly detect new physics beyond the SM. They will provide a complementary alternative to the more direct method of studying higher-energy phenomena to find departures from the SM.

The establishment of the SM is one of the major accomplishments in particle physics during the past 20 years. The SM is mathematically self-consistent and is compatible with all known experimental data, including a wide variety of low-energy neutral-current processes (see, for example, Kim *et al.*, 1981; Amaldi *et al.*, 1987; Costa *et al.*, 1988; Fogli and Haidt, 1988; Langacker and Mann, 1989; Langacker, 1990a, 1991a; Langacker and Luo, 1991a). But there are questions that cannot be answered satisfactorily within the framework of the SM (see, for example, Langacker, 1989b and 1990b). For example, why are there so many undetermined free parameters (21 of them)? Why is the gauge structure a product of three gauge groups rather than just a single one? Why are there three generations, etc.?

If we believe that all the fundamental forces can be unified by one gauge group, and that physical parameters should be determined by the theory itself rather than

[1]This paper is based on and updated from M. Luo's Ph.D. thesis, University of Pennsylvania, UPR-0446T, 1990.

having to be put in by hand, then we need to seek a more fundamental theory, which is not subject to these shortcomings and which will reduce to the SM at present energies. To do so, we construct new theories and models, such as grand unified theories, supersymmetry, and superstrings. Experimentally, we try also to detect new physical phenomena that might be induced by such underlying new physics. One direct way is to push the center-of-mass energy higher in experiments, i.e., to build higher-energy colliders. There is, however, a complementary approach, which is relatively inexpensive and technically feasible. It is based on the observation that the precision of present electroweak experiments will be substantially improved in the next decade. If there exists physics beyond the SM, there might be remnants of that physics at present energies that would cause small deviations of various physical quantities from the SM values. The deviations would be too small to be observed given the present experimental errors, but might become amenable to more precise experiments.

In the next ten years, there will be performed a series of high-precision experiments relating to the properties of the Z and W bosons and to weak neutral-current observables (Altarelli *et al.*, 1989; Langacker, 1989b, 1990b). The Z-boson mass has already been measured very precisely at the e^+e^- collider LEP (Large Electron Position Project) at CERN; the world-averaged value of M_Z is now 91.177±0.031 GeV (Dydak, 1990; Fernandez, 1990). The Z total and partial widths, the forward-backward and possibly polarization asymmetries in e^+e^- collisions [SLC (see Blochus *et al.*, 1986 and Swartz, 1987); LEP (see Ellis and Peccei, 1986 and Alexander *et al.*, 1988; Altarelli *et al.*, 1989)], and the W-boson mass [LEP 200 (see Ellis and Peccei, 1988, Vol. 2); CDF (see Abe *et al.*, 1990); UA2 (see Aitti *et al.*, 1990)] have been or will be measured with high but somewhat less precision. High-precision measurements of neutrino-electron scattering [LCD (see Allen *et al.*, 1988); CHARM II (see Geiregat *et al.*, 1989)], atomic parity violation (Bouchiat and Pottier, 1986; (Bouchiat, 1990), deep-inelastic neutrino scattering (Bolton *et al.*, 1990), and other neutral-current processes are all likely to be performed. With these forthcoming experimental data, the electroweak part of the SM can once again be verified, to see whether it is still a correct theory or simply a good approximation at low energy and low experimental accuracy. In this paper we investigate these possibilities by putting the theoretical models and experimental possibilities together. We explore how experimental data will constrain theories and how theories may guide future experiments. Specifically, this paper attempts to provide a general formalism for the global analysis of such high-precision electroweak experiments. [Previous studies with similar aims are given in SLC (see Blochus *et al.*, 1986 and Swartz, 1987); LEP (see Ellis and Peccei, 1986 and Alexander *et al.*, 1988); Boudjema *et al.*, 1988, 1989; Lynn *et al.*, 1988); and Renard and Verzegnassi, 1989.] We focus on weak neutral-current phenomena, Z-pole physics, and the W mass. The implications of charged current experiments are reviewed in Rosner (1990), and LEP 200 measurements in Ellis and Peccei (1988, Vol. 2).

With the improvement of experimental precision, another important physical phenomenon will be brought into more serious consideration, namely, radiative corrections within the SM. The radiative corrections are generally small; they are usually of the order of a few percent of the Born approximation value. But some of them can be large; e.g., the radiative corrections to the masses of W and Z bosons are as large as 4 percent. These contributions are sensitive to the top quark mass m_t (Veltman, 1977; Chanowitz *et al.*, 1978), and have been used to set an upper limit, $m_t < O(200\ \text{GeV})$ (Langacker, 1989a; Ellis, and Fogli, 1988, 1990; Langacker and Luo, 1991a). With one percent experimental errors, the radiative corrections for physical observables will be crucial: the SM predictions of physical observables with radiative corrections are essential to the verification of the SM itself, and, furthermore, they must be included if one is to use the observables to search for small deviations due to new physics. It is therefore necessary to calculate the radiative corrections as accurately as possible. We have included radiative corrections at the one-loop level to all of the SM predictions in our analysis.[2] Note that the SM is now established as correct to an excellent first approximation. Hence we can apply the SM radiative corrections, treating any new physics (whether it enters at tree or loop level) as a perturbation.

In detail, the physical quantities considered here include the masses of Z and W bosons; partial widths of the

[2]Radiative corrections to weak neutral-current phenomena have been carried out in great detail. A partial list includes early work (Marciano, 1979; Passarino and Veltman, 1979); the origin and early development of the on-shell scheme (Marciano and Sirlin, 1980, 1981; Sirlin, 1980, 1984); the $\overline{\text{MS}}$ scheme (Sarantakos *et al.*, 1983; Marciano and Sirlin, 1983, 1984b; Blondel, 1989; Sirlin, 1989, 1990; Fanchiotti and Sirlin, 1990); the relations between the on-shell scheme and the $\overline{\text{MS}}$ scheme (Marciano, 1990a, 1990b; Degrassi *et al.*, 1991; Degrassi and Sirlin, 1991); and the * scheme (Lynn *et al.*, 1986; Kennedy and Lynn, 1989; Kennedy *et al.*, 1989). For a review, see Lynn and Wheater (1984) and Hollik (1990). For the Z-decay widths, especially the top contribution to the $b\bar{b}$ width, see Akhundov *et al.*, (1986), Beenakker and Hollik (1988), and Bernabeu *et al.* (1990). For the Z line shape, see Bardin *et al.* (1988, 1989); Berends, Burgers, Hollik, and van Neervan (1988); Berends, van Neervan, and Burgers (1988); Riemann and Sachwitz (1988); and Borelli (1990). For the M_Z-M_W relation, see Marciano and Sirlin (1984a) and Hioki (1983, 1989, 1991). For higher-order effects, see Albert *et al.* (1980); Consoli *et al.* (1983); Jegerlehner (1986a); Kniehl *et al.* (1988, 1988a, 1988b; see also Kniehl and Kuhn, 1989 and 1990 and Kniehl, 1990a, 1990b); Borrelli, (1990); Djouadi *et al.* (1990); and Riemann *et al.* (1990). See also Ellis and Peccei (1986), Alexander *et al.* (1988), Blochus *et al.* (1986), Swartz (1987), and Altarelli *et al.* (1989).

Z boson; e^+e^- asymmetries at the Z pole and slightly off the Z pole; νe cross-section ratios; atomic parity violation; and νN deep-inelastic scattering. The observables considered, their expectations in the SM, and their present and projected experimental uncertainties are given in Table I. We consider several types of new physics that can be constrained or detected by precision experiments; these are listed in Table II. They include five general types that affect the neutral current and boson mass observables at the tree level (lowest order): extra Z bosons (Durkin and Langacker, 1986; Amaldi *et al.*, 1987; Costa *et al.*, 1988; del Aguila, Moreno, and Quiros, 1989, 1990, 1991; Altarelli, Casalbuoni, Dominici, Feruglio, and Gatto, 1990a, 1990b; Altarelli, Casalbuoni, Feruglio, and Gatto, 1990a, 1990b; Cvetic and Langacker, 1990; Gonzales-Garcia and Valle, 1990a, 1990b, 1991; Layssac *et al.*, 1990; Langacker and Luo, 1991b; Mahanthappa and Mohapatra, 1991), nonstandard Higgs

TABLE I. The observables considered in this article, their SM predictions, and their present and future experimental uncertainties (including theoretical uncertainties where they are important). The SM predictions use the observed value of M_Z and assume $m_t = 100$ GeV, and $M_H = 100$ GeV. g_L^2, g_R^2, R_ν, θ_L, and θ_R are quantities measured in νN scattering; g_V^e, g_A^e, $\sigma_\nu/\sigma_{\bar\nu}$, and $\sigma_\nu/(\sigma_{\bar\nu}+\sigma_\nu)$ are relevant to νe scattering; $C_{1\pm}$, C_{2pm} are measured in atomic parity violation, muonic atoms, and lN scattering; $A_{\rm LR}$, $A_{\rm FB}$, and $A_{\rm pol}$ are asymmetries at the Z pole; and the Γ's are the partial and total Z widths. The e^+e^- asymmetries slightly off the Z pole are briefly considered in Sec. V.

Quantities O_a	O_a^{SM}	(present) O_a^{exp}	(present) ΔO_a^{exp}	(present) $\Delta \sin^2\theta_W^{exp}$	(future) ΔO_a^{exp}	(future) $\Delta \sin^2\theta_W^{exp}$
$M_Z(GeV)$	—	91.177	0.031	0.0004	0.02	0.0003
$M_W(GeV)$	79.983	80.1	0.3	0.0018	0.105	0.0006
g_L^2	0.300	0.2977	0.0042	0.0057	—	—
g_R^2	0.030	0.0317	0.0034	0.013	—	—
R_ν	0.312	—	—	—	0.001	0.002
θ_L	2.46	2.50	0.03	—	—	—
θ_R	5.18	4.59	0.44	—	—	—
g_V^e	−0.036	−0.045	0.022	0.011	—	—
g_A^e	−0.504	−0.513	0.025	—	—	—
$\sigma_\nu/\sigma_{\bar\nu}$	1.152	1.083	0.10	0.012	0.046	0.005
$\sigma_\nu/(\sigma_{\bar\nu}+\sigma_\nu)$	0.146	—	—	—	0.0026	0.0025
C_{1+}	0.129	0.126	0.003	0.01	0.0013	0.003
$C_{1+}(iso)$	0.129	—	—	—	0.0003	0.0009
C_{1-}	−0.36	−0.45	0.1	0.07	—	—
C_{2p}	−0.014	—	—	—	0.046	—
$C_{2p}(1)$	−0.014	—	—	—	0.0046	—
C_{2m}	−0.054	—	—	—	0.11	0.03
$2C_{1u}+C_{1d}$	−0.033	—	—	—	0.004	0.002
$A_{LR}(SLC)$	0.131	—	—	—	0.0066	0.0008
$A_{LR}(LEP)$	0.131	—	—	—	0.0044	0.0005
$A_{FB}^{pol}(c)$	0.473	—	—	—	0.025	0.01
$A_{FB}(c)$	0.062	—	—	—	0.007	0.0017
$A_{FB}^{pol}(b)$	0.697	—	—	—	0.02	0.04
$A_{FB}(b)$	0.091	0.11	0.04	0.007	0.0054	0.001
$A_{FB}^{pol}(\mu)$	0.098	—	—	—	0.009	0.0015
$A_{FB}(\mu)$	0.013	0.024	0.007	0.004	0.0035	0.002
$A_{pol}(\tau)$	0.131	—	—	—	0.01	0.0014
$\Gamma_{inv}(GeV)$	0.499	0.482	0.016	0.007	—	—
$\Gamma_{ll}(GeV)$	0.0835	0.0839	0.0007	0.0016	—	—
$\Gamma_{c\bar c}(GeV)$	0.296	0.235	0.038	0.02	0.03	0.016
$\Gamma_{b\bar b}(GeV)$	0.377	0.372	0.064	0.03	0.04	0.018
$\Gamma_Z(GeV)$	2.484	2.497	0.015	0.001	—	—

TABLE II. The types of new physics considered in this paper.

Tree level physics:	extra Z: χ, ψ, η, Z_{LR}
	non-standard Higgs representations
	leptoquarks: type I, type II
	extra fermions: $u'_{L,R}$, $d'_{L,R}$, $e'_{L,R}$, $\nu'_{L,R}$
	compositeness: four-fermi contact operators
Loop level physics:	m_t, M_H
	extra fermions
	S-T parameters: gauge boson self-energies
	two Higgs doublets
	supersymmetry

representations (Lee, 1972), leptoquarks (Pati and Salam, 1974; Shanker, 1982; Buchmuller and Wyler, 1986b; Hall and Randall, 1986; Buchmuller *et al.*, 1987; Herczeg, 1989; Langacker and Rückl, 1991), extra fermions (Langacker and London, 1988a, 1988b; del Aguila, Garrido, and Miquel, 1990; Maalampi and Roos, 1990; Nardi and Roulet, 1990), and four-fermi contact operators associated with compositeness.[3]

Other types of new physics only affect the observables in higher order, i.e., via the radiative corrections. They include additional nondegenerate or degenerate multiplets of heavy fermions (Bertolini and Sirlin, 1984; van der Bij and Hoogeveen, 1987), additional Higgs doublets (Toussaint, 1978; Einhorn *et al.*, 1981; Bertolini, 1986; Hollik, 1986, 1988; Denner *et al.*, 1990) and supersymmetry (Eliasson, 1984; Lim *et al.*, 1984; Lynn, 1984; Grifols and Sola, 1985; Barbieri *et al.*, 1990; Bilal *et al.*, 1990; Drees and Hagiwara, 1990). Most of these examples of new physics modify low-energy physics only through W, Z, γ, and γ-Z self-energy diagrams; these can be parametrized by three parameters in addition to the weak angle $\sin^2\theta_W$ (Lynn *et al.*, 1986; Golden and Randall, 1991; Holdom and Terning, 1990; Kennedy and Langacker, 1990, 1991; Altarelli and Barbieri, 1991; Marciano and Rosner, 1990; Peskin and Takeuchi, 1990; Altarelli and Barbieri, 1991; Golden and Randall, 1991). The unknown top quark and Higgs boson masses, m_t and M_H, enter predictions of the observables through radiative corrections. We include these in Table II even though they are not technically "new physics," because the techniques for constraining them are similar to those in the search for new physics and because they lead to complications in the analysis. The deviations from the SM due to the possible new physics in Table II are calculated numerically with only a single coupling strength parameter left adjustable. Comparison of these theoretical results with the projected experimental errors delineates which experiments are sensitive to which type of new physics and at what level.[4]

We emphasize that testing the SM and searching for new physics requires the comparison of a number of precise experiments. Most observables are not absolute predictions of the SM, but depend on $\sin^2\theta_W$. Any single experimental result can usually be accommodated by choosing $\sin^2\theta_W$ appropriately. However, comparison of the values of $\sin^2\theta_W$ obtained by a number of experiments probes for physics beyond the SM which would lead to differences in the effective values extracted. Such global studies are also needed to simultaneously constrain m_t and M_H. If a series of high-precision experiments yield equal values for $\sin^2\theta_W$ (within experimental and theoretical uncertainties), then the SM is successfully tested at that level and limits can be set on the possible contributions of new physics.

On the other hand, observed deviations would be evidence for new physics. In this case one wants as much information as possible to distinguish with clarity the different kinds of new physics, and also to separate the effects of the new physics from the unknown m_t and M_H. We describe two schemes to distinguish one type of new physics from another that serve as a prescription for the analysis of future high-precision experiments. One possibility is to use the $\sin^2\theta_W$ values from the different experiments. The pattern of deviations of the various $\sin^2\theta_W$ from each other may be a distinguishing feature. Another and more powerful possibility is to compare the observables directly with the SM predictions. Again, the pattern of deviations is a diagnostic of the type of new physics. In either case, the most sensitive probe for new physics involves the totality of experiments. The high-precision electroweak experiments of the future and the theoretical framework of this paper comprise one method to probe incisively and exhaustively for any weakness in the SM, and to recognize and identify it if found.

The paper is organized as follows: Following this introductory section, we provide a general formalism for the analysis in Sec. II, Sec. III is a survey of high-precision experiments, and in Sec. IV are discussed the various types of new physics and their effects on the observables: In Secs. V and VI are collected in tabular and graphical form the numerical results of the calculations and the comparison with experimental possibilities. The conclusions are in Sec. VII.

II. FORMALISM

Consider a physical observable O_a—for example, the mass of the Z boson or a cross section—and denote its

[3]For a general discussion of effective operators, see Eichten *et al.* (1983), Rückl (1983), Buchmuller and Wyler (1986a), and Randall and Chivukula (1989).

[4]Our goal is to explore the sensitivity of different experiments to the various types of new physics. Hence we consider one type of new physics a time. The possibility of cancellation between effects should be kept in mind, but should not be a major criterion in the design of experiments.

experimental value as $O_a^{\rm exp}$ and the theoretical prediction as O_a^T. Then, within experimental and theoretical uncertainties,

$$O_a^T = O_a^{\rm exp} \tag{1}$$

if both theory and experiment are correct (the superscript T will be omitted in the following for convenience).

Since the exact theory is not known, we start from the SM as a good approximation. Instead of the exact O_a, we have the SM prediction $O_a^{\rm SM}$. Were the SM the true theory, then

$$O_a \equiv O_a^{\rm SM} = O_a^{\rm exp} \ . \tag{2}$$

If it is not, and there exists new physics i beyond the SM, then

$$O_a = O_a^{\rm SM} + \Delta O_a^i \ , \tag{3}$$

where ΔO_a^i is the contribution to O_a of the new physics i. We assume that contributions from new physics are small compared with that from the SM, and that they can be calculated perturbatively. If there exist several types of new physics, they should be summed:

$$O_a = O_a^{\rm SM} + \sum_i \Delta O_a^i \ . \tag{4}$$

In general, $O_a^{\rm SM}$ depends on the SU(2)×U(1) gauge structure. It also depends on the free parameters of the theory. In the GWS (Glashow-Weinberg-Salam) theory, if the masses of the fermions can be neglected, there are three free parameters, namely,

$$\alpha, \quad G_F, \quad \sin^2\theta_W \ , \tag{5}$$

where $\alpha = 1/(137.0359895 \pm 0.0000061)$ is the QED coupling constant, defined in terms of Thomson scattering; $G_F = 1.16637 \pm 0.00002) \times 10^{-5}$ GeV^{-2} is the Fermi weak-interaction coupling constant, determined by the muon lifetime τ_μ; and θ_W is the weak mixing angle. $\sin^2\theta_W$ is the single unspecified parameter in the electroweak theory, representing the mixing between the SU(2) and U(1) sectors. At tree level, $\sin^2\theta_W$ is given by $g'^2/(g'^2+g^2)$, where g and g' are, respectively, the SU(2) and U(1) gauge coupling constants.

When higher-order terms are included, one must define a renormalized $\sin^2\theta_W$. One possibility is the on-shell definition $\sin^2\theta_W^M$. Within the context of the Standard Model $\sin^2\theta_W^M$ is defined as $1 - M_W^2/M_Z^2$, where M_W and M_Z are the measured masses. A useful generalization to a wider class of theories, which we adopt, is $\sin^2\theta_W^M \equiv 1 - M_{W,\rm SM}^2/M_{Z,\rm SM}^2$, where $M_{W,\rm SM}$ and $M_{Z,\rm SM}$ are the masses of W and Z before applying any shifts due to new physics but including higher-order terms (Marciano and Sirlin, 1980; Sirlin, 1980, 1984). For most purposes this is a very convenient definition, although it is somewhat awkward for dealing with a heavy top quark. Another possibility[5] is the $\overline{\rm MS}$ definition (see, for example, Sarantakos *et al.*, 1983; Sirlin, 1989, 1990; Marciano, 1990a, 1990b; Degrassi and Sirlin, 1991; Degrassi *et al.*, 1991) $\sin^2\hat{\theta}_W \equiv g'^2/(g'^2+g^2)$, where the $(n-4)^{-1}$ poles in dimensional regularization and some associated constants $(\log 4\pi - \gamma_E)$ are subtracted from g' and g. It is convenient to evaluate the couplings at the scale $Q^2 = M_Z^2$. The two definitions are related by $\sin^2\hat{\theta}_W(M_z) = C(m_t, M_H)\sin^2\theta_W^M$, where $C = 1.013$ for $m_t = M_H = 100$ GeV. These definitions should yield the same predictions if some appropriate summations of high-order terms are taken (Degrassi *et al*, 1991; Degrassi and Sirlin, 1991). However, since we are dealing with deviations from the SM and only to the lowest order of perturbation, our analysis is essentially independent of which definition of $\sin^2\theta_W$ is used.

Both O_a and $O_a^{\rm SM}$ can be expressed as functions of $\sin^2\theta_W$,

$$O_a = O_a(\sin^2\theta_W) \quad \text{and} \quad O_a^{\rm SM} = O_a^{\rm SM}(\sin^2\theta_W) \ , \tag{6}$$

where $\sin^2\theta_W$ represents either $\sin^2\theta_W^M$ or $\sin^2\hat{\theta}_W$, depending on the renormalization scheme used. To get around our ignorance of the exact value of $\sin^2\theta_W$, we define an effective $\sin^2\theta_W^a$ for each O_a as follows:

$$O_a(\sin^2\theta_W) = O_a^{\rm SM}(\sin^2\theta_W^a) \tag{7}$$

with

$$\sin^2\theta_W^a = \sin^2\theta_W + \Delta\sin^2\theta_W^a \ . \tag{8}$$

That is, $\sin^2\theta_W^a$ is the value extracted from $O_a^{\rm exp}$ assuming the validity of the SM, while $\Delta\sin^2\theta_W^a$ is the shift away from the true $\sin^2\theta_W$ due to new physics. From Eqs. (4), (6), and (7) we have

$$\Delta\sin^2\theta_W^a = \frac{\sum_i \Delta O_a^i}{\left.\dfrac{dO_a^{\rm SM}}{dx}\right|_{x^a}} \ , \tag{9}$$

where $x^a = \sin^2\theta_W^a$. The validity of the SM requires that all $\Delta\sin^2\theta_W^a$ should vanish and all of the $\sin^2\theta_W^a$ should be equal to $\sin^2\theta_W$ (within uncertainties). The $\sin^2\theta_W^a$ would differ from one another if there were new physics beyond the SM. Thus one way to test the SM is simply to compare the values of $\sin^2\theta_W^a$ extracted from measurements of different physical quantities O_a.

However, not all physical quantities are sensitive to $\sin^2\theta_W$. For example, the axial couplings of the electron, neutrino, and quarks are essentially independent of $\sin^2\theta_W$; so is the forward-backward asymmetry of low-energy electron-positron scattering,which is mainly sensitive to the axial couplings. Some physical information would be lost if we only pursued this course—it is important to have predictions of the physical quantities themselves. We therefore consider two analyses: one in which the O_a are compared directly and one in which the extracted $\sin^2\theta_W^a$ are compared. In the former all information is included, while the latter is easier to use.

[5]A third possibility, the * definition, is operationally very similar to the $\overline{\rm MS}$ scheme. See the references in Footnote 2.

However, to study the O_a we need a numerical estimate of $\sin^2\theta_W$ to compute the SM prediction. Even for the comparison of different $\sin^2\theta_W^a$, it is easier to study their differences from a single reference value of $\sin^2\theta_W$ than from the differences between the $\sin^2\theta_W^a$ themselves.

There are two reasonable choices for the estimate of $\sin^2\theta_W$: one is the world average value (Langacker 1990a, 1991a; Langacker and Luo, 1991a) $\sin^2\theta_W^{\rm avg}=0.2261\pm0.0036$ (on-shell) or $\sin^2\theta_W^{\rm avg}=0.2325\pm0.0009$ ($\overline{\rm MS}$), where the uncertainty is mainly from the uncertainty in the contribution of the top quark mass m_t to the radiative corrections. $\sin^2\theta_W^{\rm avg}$ is dominated by the extremely precise measurement of the mass of the Z boson. Consequently, another possibility is to use the reference value $\sin^2\theta_W^Z$ extracted from M_Z (see Footnote 2):

$$M_Z^2=\frac{(37.2803\ \text{GeV})^2}{\rho\sin^2\theta_W^Z\cos^2\theta_W^Z(1-\Delta r)}\ , \tag{10}$$

where ρ and Δr are calculable radiative corrections depending on m_t, M_H, and the renormalization scheme. Both $\sin^2\theta_W^{\rm avg}$ and $\sin^2\theta_W^Z$ may be shifted from the true $\sin^2\theta_W$ by new physics, and that shift must be taken into account in the analysis. This is easier to do for $\sin^2\theta_W^Z$, since it comes from a single measured quantity, and therefore $\sin^2\theta_W^Z$ is used in this paper. The experimental uncertainty in $\sin^2\theta_W^Z$ is also dominated by the uncertainties in m_t and M_H in making the radiative corrections; the uncertainty is only ±0.0004 for fixed m_t and M_H (see Sec. III.A). We will take $\sin^2\theta_W^Z=0.2306\pm0.0004$ (on-shell) or $\sin^2\theta_W^Z=0.2334\pm0.0004$ ($\overline{\rm MS}$) as our estimator, the value corresponding to $m_t=100$ GeV and $M_H=100$ GeV. The effect of variations of m_t and M_H will be treated separately as if they were new physics.

Expressing the equations above in terms of $\sin^2\theta_W^Z$, we have

$$\sin^2\theta_W^a=\sin^2\theta_W^Z+\Delta\sin^2\theta_W^{(a;Z)} \tag{11}$$

with

$$\Delta\sin^2\theta_W^{(a;Z)}=\Delta\sin^2\theta_W^a-\Delta\sin^2\theta_W^Z\ ; \tag{12}$$

i.e., $\Delta\sin^2\theta_W^{(a;Z)}$ represents both the shift in $\sin^2\theta_W^a$ and in $\sin^2\theta_W^Z$ due to new physics. A nonzero $\Delta\sin^2\theta_W^{(a;Z)}$ (i.e., beyond uncertainties) would indicate new physics. Equations (9), (11), and (12) are the basic results for the $\sin^2\theta_W$ analysis. The value of $\Delta\sin^2\theta_W^{(a;Z)}$ obtained from experiments by the differences between the measured and the SM values shown in Eq. (11) can be compared with the predictions from (9) and (12) for each type of new physics.

The numerical values of $\sin^2\theta_W^a$ in the on-shell and $\overline{\rm MS}$ schemes may be significantly different (e.g., 0.003 for $m_t=100$ GeV). However, the *differences* $\Delta\sin^2\theta_w^{(a;Z)}$ are the same in both schemes up to negligible terms of order $(C(m_t,M_H)-1)\Delta\sin^2\theta_W^{(a;Z)}$.

For the analysis based directly on the observables $O_a(\sin^2\theta_W)$, one uses

$$O_a(\sin^2\theta_W)=O_a^{\rm SM}(\sin^2\theta_W)+\sum_i\Delta O_a^i\ . \tag{13}$$

But,

$$O_a^{\rm SM}(\sin^2\theta_W)=O_a^{\rm SM}(\sin^2\theta_W^Z)-\left.\frac{dO_a^{\rm SM}}{dx}\right|_{x^Z}\Delta\sin^2\theta_W^Z\ , \tag{14}$$

so

$$\begin{aligned}O_a(\sin^2\theta_W)&=O_a^{\rm SM}(\sin^2\theta_W^Z)-\left.\frac{dO_a^{\rm SM}}{dx}\right|_{x^Z}\Delta\sin^2\theta_W^Z\\&\quad+\sum_i\Delta O_a^i\\&=O_a^{\rm SM}(\sin^2\theta_W^Z)+\Delta O_a\ .\end{aligned} \tag{15}$$

We shall refer to the SM prediction as

$$O_a^{\rm SM}(\sin^2\theta_W^Z)\ , \tag{16}$$

while the contribution from the new physics is

$$\Delta O_a=-\left.\frac{dO_a^{\rm SM}}{dx}\right|_{x^Z}\Delta\sin^2\theta_W^Z+\sum_i\Delta O_a^i\ . \tag{17}$$

At the one-loop level, ΔO_a is independent of the renormalization scheme. Again, the first term in ΔO_a represents the difference between the (assumed) value of $\sin^2\theta_W^Z$ and the true $\sin^2\theta_W$, while the second term is the direct effect of the new physics on O_a. The calculated $O_a(\sin^2\theta_W)$ in Eq. (15) are the quantities to be directly compared with experiment. The experimental values of ΔO_a obtained from (15) can therefore be compared with the predictions for each type of new physics calculated by Eqs. (8) through (17).

There is no straightforward way to calculate the right-hand side of Eq. (17), because the true theory is absent. The best that one can do is to build models with the guidance of some physical principles and start from them. Reasonable models should reduce to the SM at the present energies; their remnants are presumably small and can, as a consequence, be treated as perturbations.

The general types of new physics treated in this paper break down to 27 separate, possible new-physics contributions. The deviations ΔO_a^i from the SM due to these contributions are calculated numerically, and the results are collected in Sec. V. The effects of different values of m_t and M_H, the top quark mass and the Higgs boson mass, respectively, are also given in Sec. V.

III. PHYSICAL OBSERVABLES AND THEIR MEASUREMENTS

In this section we discuss the physical observables, the methods to measure them, and the predictions of the SM (including radiative corrections). The discussions are summarized in Table I, which gives the SM predictions $O_a^{\rm SM}(\sin^2\theta_W^Z)$ for 29 observables and the present and anti-

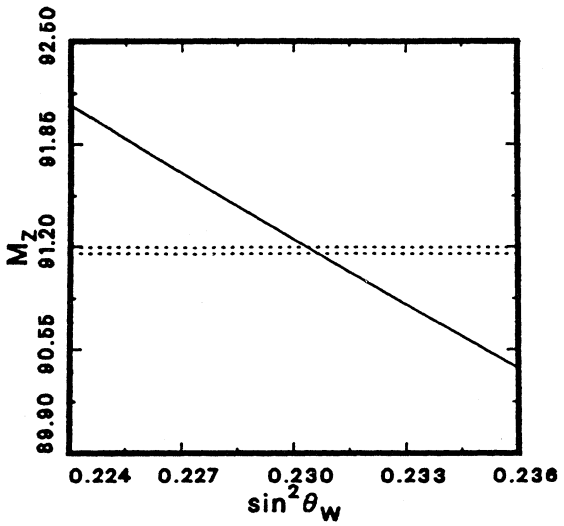

FIG. 1. M_Z vs $\sin^2\theta_W$ for $m_t = M_H = 100$ GeV. $\sin^2\theta_W$ represents $\sin^2\theta_W^M = 0.987 \sin^2\hat{\theta}_W(M_Z)$. The dashed lines are the projected one-standard-deviation range in the observable.

cipated experimental[6] and theoretical errors (1σ). The various $\sin^2\theta_W$ dependences of the observables are shown in Figs. 1–29 for $m_t = M_H = 100$ GeV, along with the projected uncertainties in their determination. One sees in certain instances in Figs. 1–29 the advantages of directly comparing measured and predicted values of observables rather than extracted values of $\sin^2\theta_W$.

Physical observables:

(a) Masses of the intermediate vector bosons Z, W: M_Z, M_W.

(b) Low-energy effective ν_μ-quark coupling coefficients $\epsilon_L(u)$, $\epsilon_R(u)$, $\epsilon_L(d)$, and $\epsilon_R(d)$, and some of their specific combinations directly extracted from experiments.

(c) Low-energy effective ν_μ-electron coupling coefficients g_V^e, g_A^e.

Related are two important ratios of neutrino-electron elastic-scattering cross sections:

$$\frac{\sigma_{\nu_\mu e\to\nu_\mu e}}{\sigma_{\bar{\nu}_\mu e\to\bar{\nu}_\mu e}}, \quad \frac{\sigma_{\nu_\mu e\to\nu_\mu e}}{\sigma_{\bar{\nu}_\mu e\to\bar{\nu}_\mu e}+\sigma_{\nu_e e\to\nu_e e}}.$$

(d) Coefficients for atomic parity violation and parity-violating e-hadron scattering C_{1u}, C_{2u}, C_{1d}, C_{2d}, and their combinations.

(e) Asymmetries of e^+e^- scattering at the Z pole (and slightly off the pole):

[6]For the present purpose of studying sensitivities it is sufficient to ignore correlations between the observables. They must of course be included in the final analysis of actual data. In practice, the only important correlations for the observables in Table I are among Γ_Z, $\Gamma_{l\bar{l}}$, and $\Gamma_{\rm inv}$.

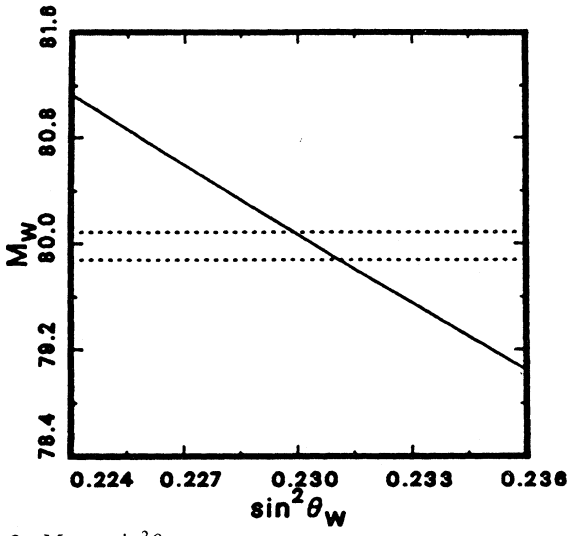

FIG. 2. M_W vs $\sin^2\theta_W$.

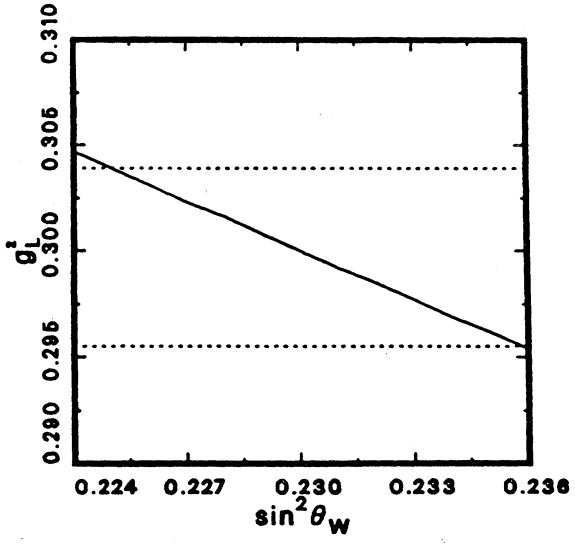

FIG. 3. g_L^2 vs $\sin^2\theta_W$.

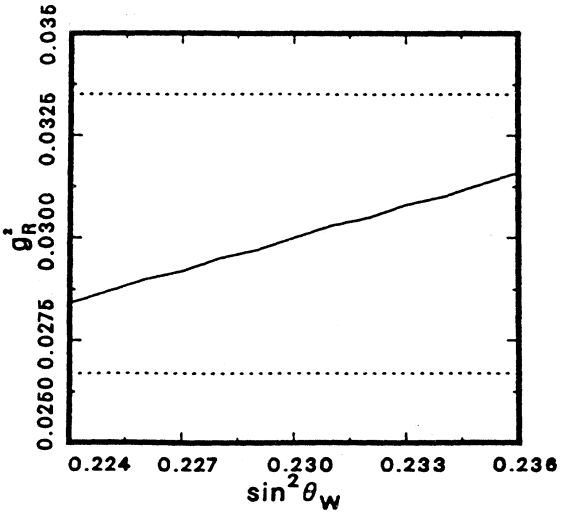

FIG. 4. g_R^2 vs $\sin^2\theta_W$.

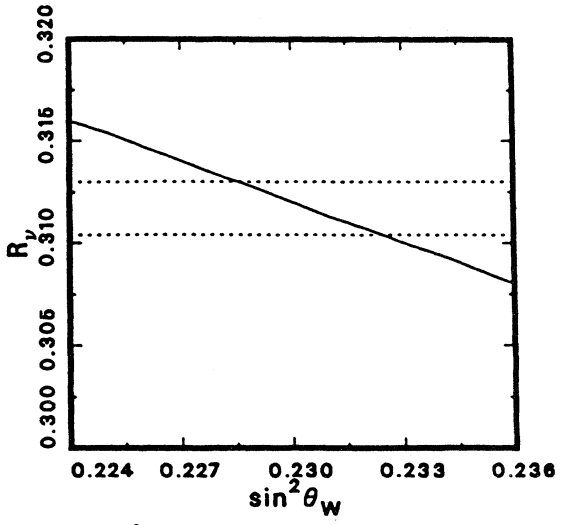

FIG. 5. R_ν vs $\sin^2\theta_W$.

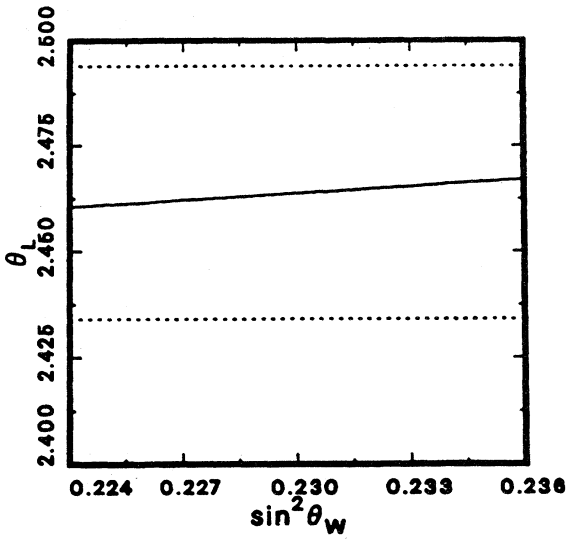

FIG. 6. θ_L vs $\sin^2\theta_W$.

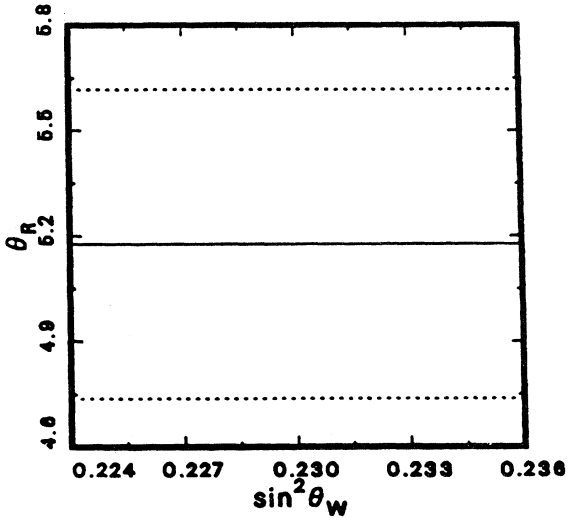

FIG. 7. θ_R vs $\sin^2\theta_W$.

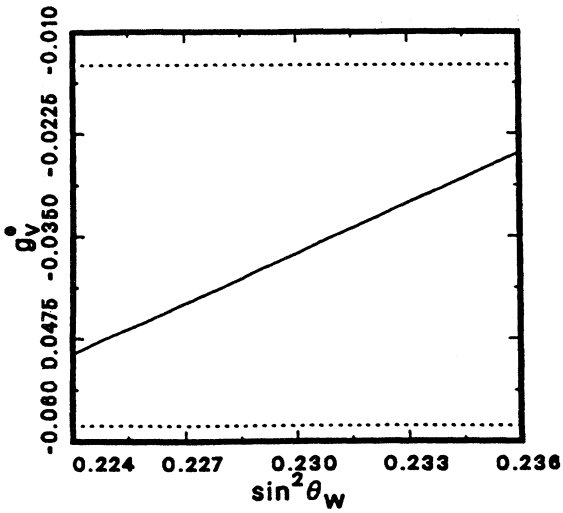

FIG. 8. g_V^e vs $\sin^2\theta_W$.

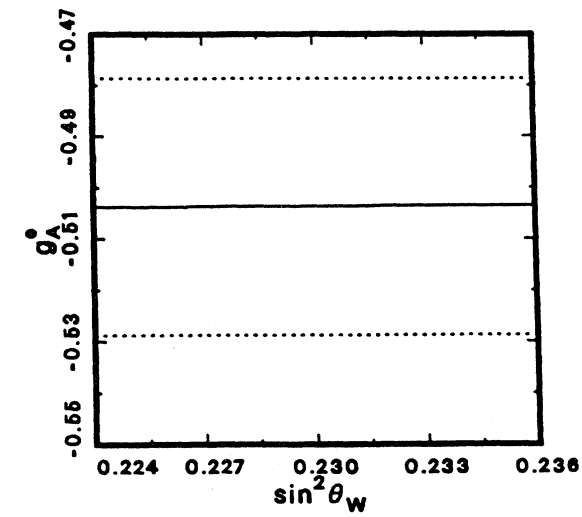

FIG. 9. g_A^e vs $\sin^2\theta_W$.

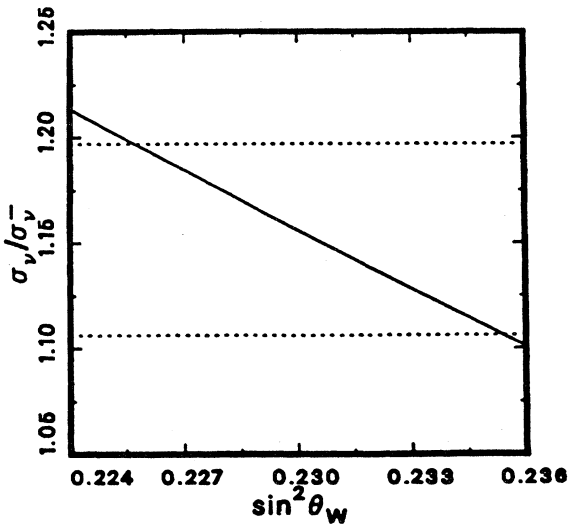

FIG. 10. $\sigma_{\nu_\mu e}/\sigma_{\bar\nu_\nu e}$ vs $\sin^2\theta_W$.

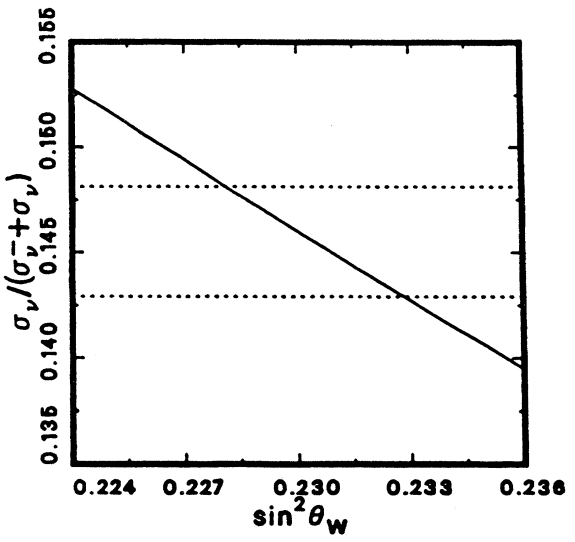

FIG. 11. $\sigma_{\nu_\mu e}/(\sigma_{\bar{\nu}_\mu e}+\sigma_{\nu_e e})$ vs $\sin^2\theta_W$.

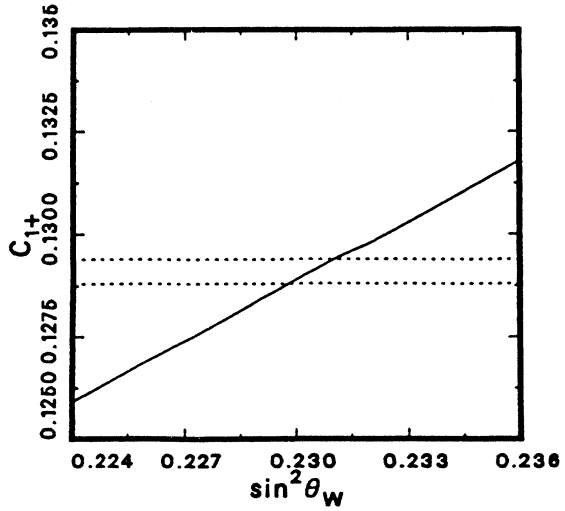

FIG. 12. C_{1+} vs $\sin^2\theta_W$.

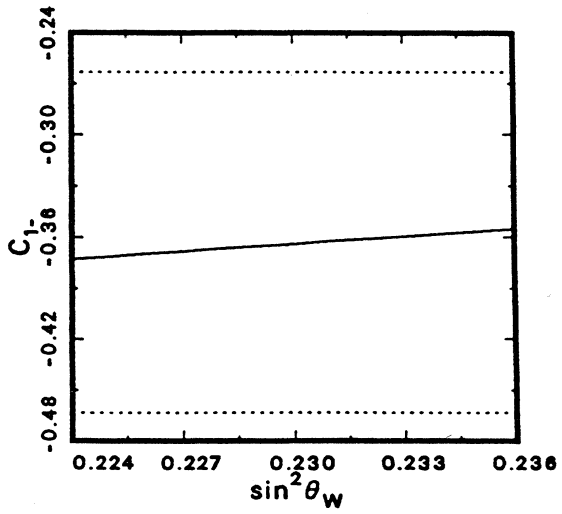

FIG. 13. C_{1-} vs $\sin^2\theta_W$.

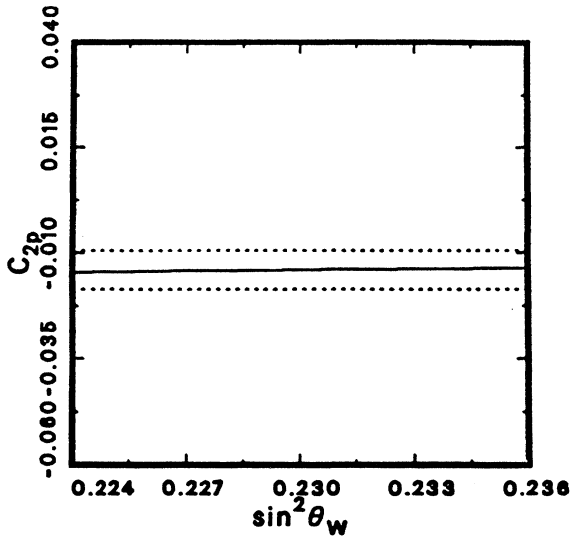

FIG. 14. C_{2p} vs $\sin^2\theta_W$.

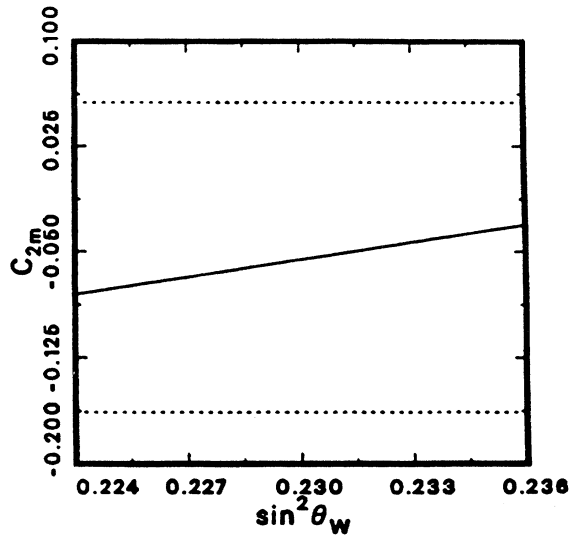

FIG. 15. C_{2m} vs $\sin^2\theta_W$.

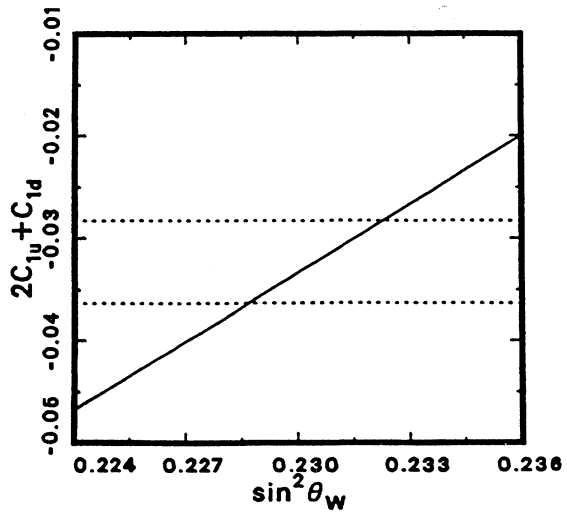

FIG. 16. $2C_{1u}+C_{1d}$ vs $\sin^2\theta_W$.

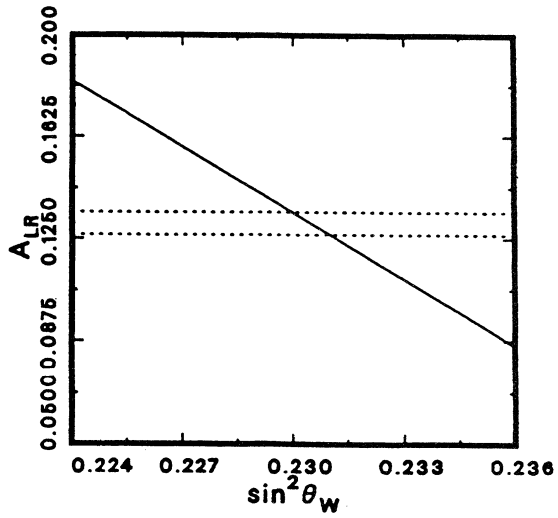

FIG. 17. $A_{\rm LR}$ vs $\sin^2\theta_W$.

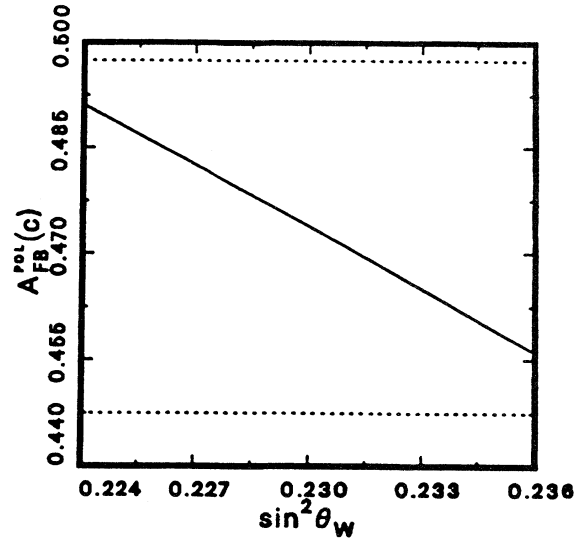

FIG. 18. $A_{\rm FB}^{\rm pol}(c)$ vs $\sin^2\theta_W$.

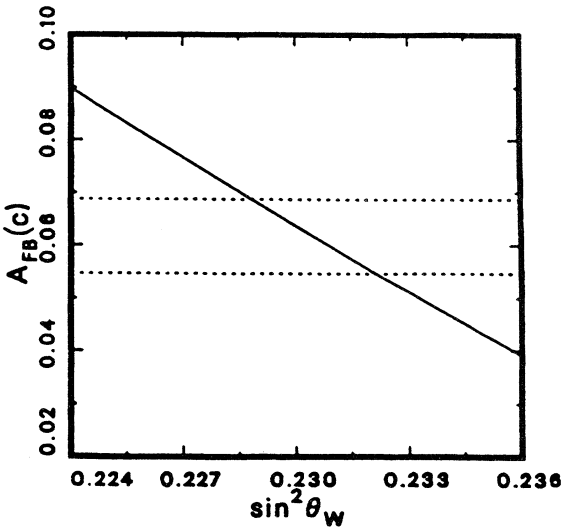

FIG. 19. $A_{\rm FB}(c)$ vs $\sin^2\theta_W$.

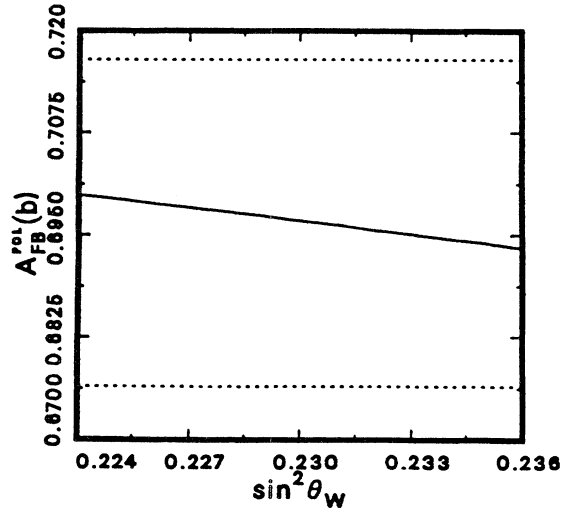

FIG. 20. $A_{\rm FB}^{\rm pol}(b)$ vs $\sin^2\theta_W$.

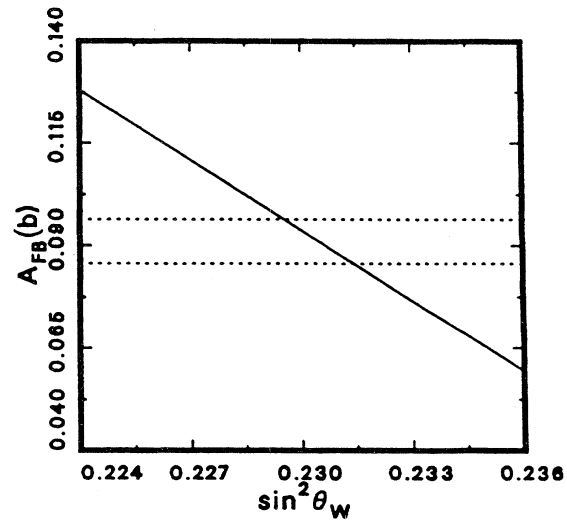

FIG. 21. $A_{\rm FB}(b)$ vs $\sin^2\theta_W$.

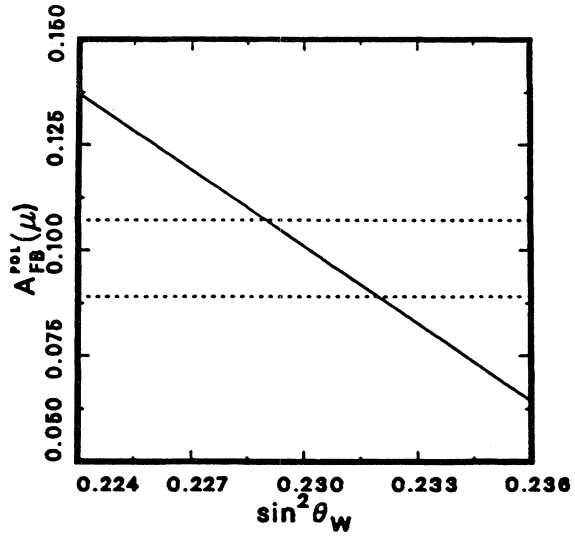

FIG. 22. $A_{\rm FB}^{\rm pol}(\mu)$ vs $\sin^2\theta_W$.

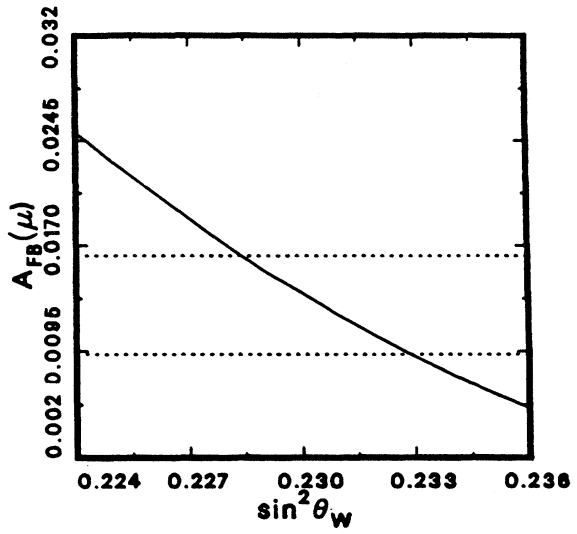

FIG. 23. $A_{\rm FB}(\mu)$ vs $\sin^2\theta_W$.

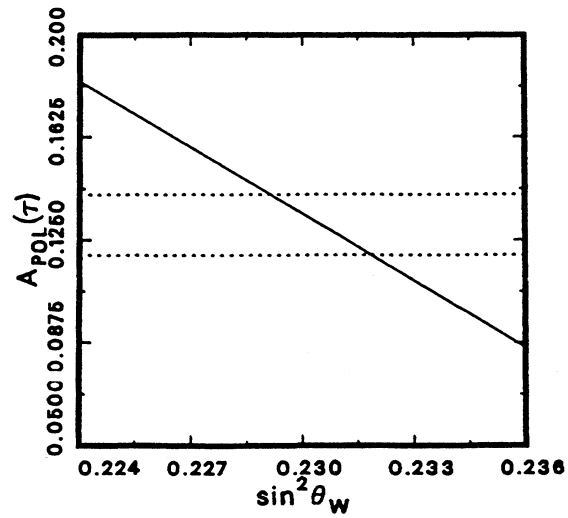

FIG. 24. $A_{\rm pol}(\tau)$ vs $\sin^2\theta_W$.

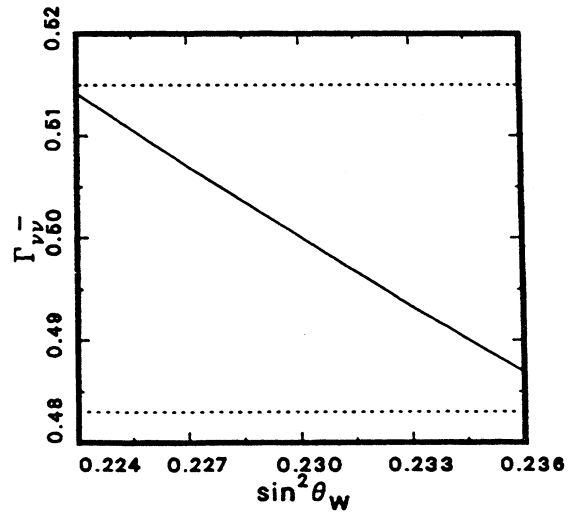

FIG. 25. $\Gamma_{\rm inv}$ vs $\sin^2\theta_W$.

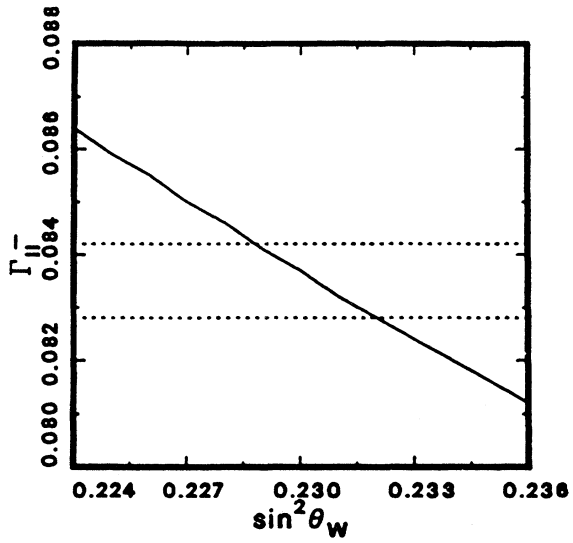

FIG. 26. $\Gamma_{l\bar{l}}$ vs $\sin^2\theta_W$.

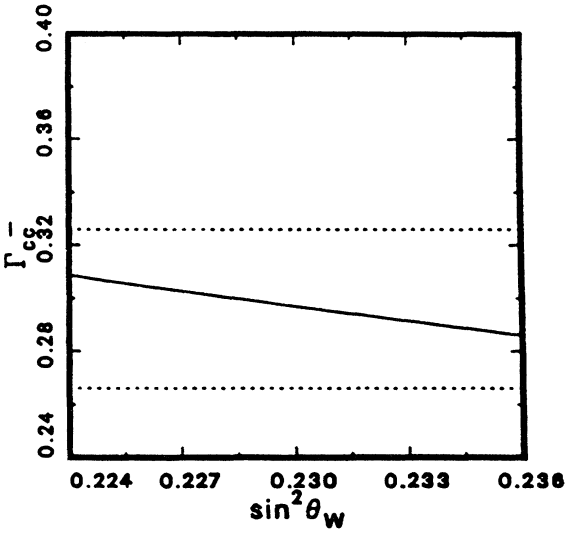

FIG. 27. $\Gamma_{u\bar{u}}$ vs $\sin^2\theta_W$.

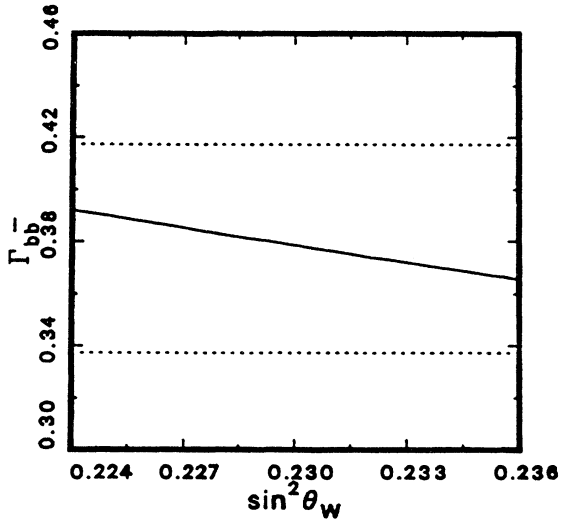

FIG. 28. $\Gamma_{d\bar{d}}$ vs $\sin^2\theta_W$.

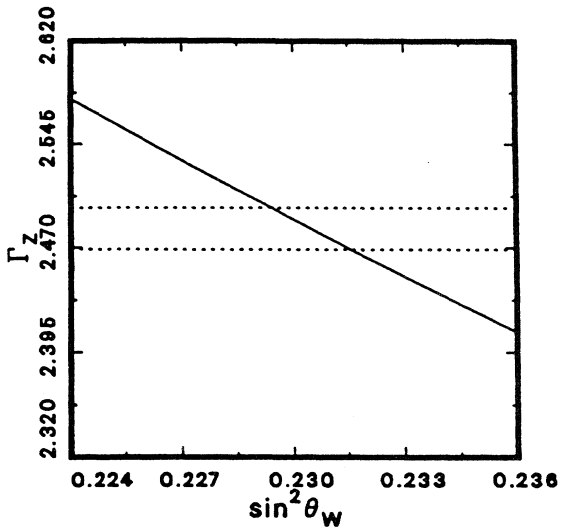

FIG. 29. Γ_Z vs $\sin^2\theta_W$.

(i) left-right asymmetry with initial longitudinally polarized electron beams, A_{LR};

(ii) forward-backward asymmetries of final-state fermions: $A_{FB}(f)$, $f=u,d,\mu$;

(iii) mixed forward-backward asymmetries of final-state fermions with initial polarized electrons:

$$A_{FB}^{pol}(f), \quad f=u,d,\mu \ ;$$

(iv) final-state polarization asymmetry of the τ lepton, $A_{pol}(\tau)$.

(f) Z-decay widths:

(i) partial Z decay widths: $\Gamma_{f\bar{f}}$; $f=\nu,e,u,d$;

(ii) inclusive Z decay width: Γ_Z.

These observables are selected because they have reasonably high probability of being measured with high precision ($\lesssim 1\%$) in the coming decade. Certain other observables, such as forward-backward asymmetries in $\bar{p}p \to Z \to l^+l^-$, are closely related to those considered here.

A. M_Z, M_W

In the SM, weak interactions are mediated by three gauge bosons: $W^\pm$ and Z. They acquire masses through the Higgs mechanism once the SU(2)×U(1) gauge symmetry is spontaneously broken. In the minimal SM, these masses are predicted to be[2] (see, for example, Sirlin, 1980; Marciano, 1990a, 1990b; Degrassi *et al.*, 1991)

$$M_Z^2=\frac{\pi\alpha/\sqrt{2}G_F}{\rho\cos^2\theta_W\sin^2\theta_W(1-\Delta r)} \tag{18}$$

and

$$M_W^2=\frac{\pi\alpha/\sqrt{2}G_F}{\sin^2\theta_W(1-\Delta r)} \ , \tag{19}$$

to the one-loop level. In Eq. (18), Δr and $\rho-1$ are radiative correction parameters that depend on m_t, M_H, and the renormalization scheme. In particular, Δr represents the radiative corrections relating μ decay, neutral-current reactions, and $M_{W,Z}$, while $\rho=M_W^2/M_Z^2\cos^2\theta_W$ is affected by isospin-violating W and Z self-energy corrections. In the on-shell scheme $\rho=1$ by definition, with these effects absorbed into the value of $\sin^2\theta_W$. For small m_t, Δr is largely controlled by the running of α^{-1} from $\alpha^{-1}(0)\simeq 137.036$ to $\alpha^{-1}(M_Z^2)\simeq 128$. One has

$$\frac{1}{1-\Delta r}\simeq\frac{\alpha(M_Z)}{\alpha(0)}\simeq 1.07 \ , \tag{20}$$

so that $\Delta r\simeq 0.07$. The value of Δr in the on-shell scheme, Δr_M, is particularly sensitive to large m_t from W and Z self-energy corrections; one expects $\Delta r_M=0.0576\pm0.0009$ (0.0187 ± 0.0009) for $m_t=100$ (200) GeV, both for $M_H=100$ GeV. In the $\overline{\text{MS}}$ scheme $\Delta r\to\Delta\hat{r}_W$ is insensitive to m_t, while $\rho\to\hat{\rho}=1.0036$ (1.0159) for $m_t=100$ (200) GeV, $M_H=100$ GeV.

The four LEP experiments–ALEPH, DELPHI, L3, and OPAL—yield the extremely precise value $M_Z=91.177\pm0.031$ GeV (Dydak, 1990; Fernandez, 1990), where the uncertainty is essentially the uncertainty in the LEP energy, ±0.030 GeV. This value of M_Z together with the assumed values $m_t=100$ GeV and $M_H=100$ GeV are used as the input parameters in the numerical calculations that follow and are referred to as the *standard input parameters* (SIP) in the remainder of the paper. With these inputs $\sin^2\theta_W^Z=0.2306\pm0.0004$ (on-shell) or 0.2334 ± 0.0004 ($\overline{\text{MS}}$). The experimental error of 0.031 GeV in M_Z corresponds to an error of 0.0002 in $\sin^2\theta_W^Z$. However, the theoretical uncertainty (for fixed m_t and M_H) in Δr is 0.0009 from hadronic corrections to the photon self-energy[7] (Jegerlehner, 1986b; Burckhardt *et al.*, 1988). This causes a theoretical error of 0.0003 in $\sin^2\theta_W^Z$, leading to a total error of 0.0004. The errors in M_Z may eventually be improved to 20 MeV or better, corresponding to a total uncertainty of 0.0003 in $\sin^2\theta_W^Z$.

Since we shall always be comparing measured observables O_a^{exp} with the SM prediction $O_a^{SM}(\sin^2\theta_W^Z)$, the effective uncertainty in each observable O_a is obtained by combining the experimental and theoretical uncertainties (ΔO_a^{exp} and ΔO_a^{th}, respectively) in the determination of O_a itself with the theoretical uncertainty ΔO_a^{pred} in the prediction:

$$\Delta O_a=[(\Delta O_a^{exp})^2+(\Delta O_a^{th})^2+(\Delta O_a^{pred})^2]^{1/2} \ , \tag{21}$$

where

$$\Delta O_a^{pred}=\frac{dO_a^{SM}}{d\sin^2\theta_W}\Delta x^Z \tag{22}$$

[7]There may be additional QCD uncertainties for large m_t (Kniehl, Kühn, and Stuart, 1988a, 1988b; Kniehl, 1990a, 1990b; Halzen, and Kniehl, 1991).

and $\Delta x^Z \simeq 0.0003$ is the uncertainty in $\sin^2\theta_W^Z$. In practice $\Delta O_a^{\rm pred}$ is small compared to the other uncertainties, except possibly for measurements of $A_{\rm LR}$, $A_{\rm FB}(b)$, M_W, and C_{1+}(iso).

The present world-averaged value of M_W is 80.1 ± 0.3 GeV which leads to an error of 0.0018 in $\sin^2\theta_W$ for the SIP, independent of renormalization scheme. This value is dominated by the UA2 measurement of the ratio $M_W/M_Z=0.8831\pm0.0055$ (Alitti *et al.*, 1990), in which the systematic error due to the energy scale is largely canceled, and by the absolute measurement $M_W=79.91\pm0.39$ GeV of CDF (Abe *et al.*, 1990). These values are in excellent agreement with the SM prediction 79.98 ± 0.04 GeV using SIP. One expects improved measurements by three independent techniques: W production at the Tevatron, W exchange at HERA, and the reaction $e^+e^-\to W^+W^-$ in the second phase of LEP (LEP 200). A reasonable projection of the experimental error on M_W is 100 MeV [LEP200 (see Ellis and Peccei, 1988, Vol. 2); Langacker, 1989b, 1990b], which would lead to an error of 0.0006 in $\sin^2\theta_W$. There is an additional theoretical uncertainty of ~ 30 MeV in the prediction due to ΔM_Z and the (correlated) uncertainty in Δr, leading to an effective uncertainty $\Delta M_W=[(\Delta M_W^{\rm exp})^2+(\Delta M_W^{\rm pred})^2]^{1/2}\simeq 105$ MeV and correspondingly $\Delta\sin^2\theta_W\simeq 0.0006$.

B. Low-energy effective neutrino-quark coupling coefficients

In an arbitrary gauge theory, the interaction between neutrinos and quarks involves only V and A currents; i.e., except for negligible Higgs contributions S, P, and T couplings are absent. The low-energy effective Lagrangian can then be written as

$$-L_{\rm eff}=\frac{4G_F}{\sqrt{2}}\sum_{\alpha=1}^{n}\bar{\nu}\gamma^\mu P_L\nu\sum_i[\epsilon_L(i)\bar{q}_i\gamma_\mu P_L q_i+\epsilon_R(i)\bar{q}_i\gamma_\mu P_R q_i]\,, \tag{23}$$

where $P_{L,R}=(1\mp\gamma_5)/2$ are projections onto left- (right-) handed fermions. The expressions for the $\epsilon_{L,R}(i)$ and other parameters in the SM[8] (at tree level) are listed in Table III. The weak interactions of hadrons are complicated by the strong interactions. In elastic scattering, one acquires the form factors of the hadrons; in deep-inelastic scattering, one encounters the quark distributions within the hadrons. Detailed analysis can be found in Kim *et al.* (1981), Amaldi *et al.* (1987), Costa *et al.* (1988), Fogli and Haidt (1988), Langacker and Mann (1989), Langacker (1990a, 1991a), and Langacker and Luo (1991a). The quantities extracted from experiments are the following combinations of the $\epsilon_{L,R}$:

$$g_L^2=\epsilon_L^2(u)+\epsilon_L^2(d)\,, \tag{24}$$

$$g_R^2=\epsilon_R^2(u)+\epsilon_R^2(d)\,, \tag{25}$$

$$\theta_L=\tan^{-1}\epsilon_L(u)/\epsilon_L(d)\,, \tag{26}$$

$$\theta_R=\tan^{-1}\epsilon_R(u)/\epsilon_R(d)\,. \tag{27}$$

Using the SIP, $g_L^2=0.2997$, $g_R^2=0.0301$, $\theta_L=2.46$, and $\theta_R=5.18$.

Measurements of $\epsilon_{L,R}$ are significant accomplishments of the second and the third generation weak neutral-current experiments. In particular, measurements of the deep-inelastic-scattering cross-section ratios

$$R_\nu=\frac{\sigma(\nu_\mu N\to\nu_\mu X)}{\sigma(\nu_\mu N\to\mu^- X)},\quad R_{\bar\nu}=\frac{(\bar\sigma_\mu N\to\bar\nu_\mu X)}{\sigma(\bar\nu_\mu N\to\mu^+ X)} \tag{28}$$

TABLE III. Standard Model predictions (at the tree level) for the neutral-current observables. The chiral couplings are $\epsilon_L(i)=I_{3L}(i)-q_i\sin^2\theta_W$ and $\epsilon_R(i)=-q_i\sin^2\theta_W$, where $I_{3L}(i)$ and q_i are, respectively, the 3rd component of weak isospin and electric charge of fermion i. The effect of radiative corrections is to introduce form factors and new terms, e.g., $\epsilon_L(u)\to\rho_{\rm NC}^{(\nu;h)}(\frac{1}{2}-\frac{2}{3}\kappa^{(\nu;h)}\sin^2\theta_W)+\lambda_{uL}$ where $\rho_{\rm NC}^{(\nu;h)}=\kappa^{(\nu;h)}=1$ and $\lambda_{uL}=0$ at the tree level. The corrections depend on the kinematic variables, m_t, and M_H, and on the renormalization scheme. The full one-loop corrections are included in our numerical analysis.

Quantity	Expression
$\epsilon_L(u)=(g_V^u+g_A^u)/2$	$\frac{1}{2}-\frac{2}{3}\sin^2\theta_W$
$\epsilon_R(u)=(g_V^u-g_A^u)/2$	$-\frac{2}{3}\sin^2\theta_W$
$\epsilon_L(d)=(g_V^d+g_A^d)/2$	$-\frac{1}{2}+\frac{1}{3}\sin^2\theta_W$
$\epsilon_R(d)=(g_V^d-g_A^d)/2$	$\frac{1}{3}\sin^2\theta_W$
g_L^2	$\epsilon_L^2(u)+\epsilon_L^2(d)$
g_R^2	$\epsilon_R^2(u)+\epsilon_R^2(d)$
θ_L	$\tan^{-1}\epsilon_L(u)/\epsilon_L(d)$
θ_R	$\tan^{-1}\epsilon_R(u)/\epsilon_R(d)$
$\epsilon_L(e)=(g_V^e+g_A^e)/2$	$-\frac{1}{2}+\sin^2\theta_W$
$\epsilon_R(e)=(g_V^e-g_A^e)/2$	$\sin^2\theta_W$
$R_{\nu/\bar\nu}$	$\frac{\epsilon_L^2(e)+\epsilon_R^2(e)/3}{\epsilon_L^2(e)/3+\epsilon_R^2(e)}$
$R_{\nu/\bar\nu\nu_e}$	$\frac{\epsilon_L^2(e)+\epsilon_R^2(e)/3}{(\epsilon_L(e)+1)^2+\epsilon_R^2(e)/3+\epsilon_L^2(e)/3+\epsilon_R^2(e)}$
$C_{1u}=2g_A^e g_V^u$	$-\frac{1}{2}+\frac{4}{3}\sin^2\theta_W$
$C_{2u}=2g_V^e g_A^u$	$-\frac{1}{2}+2\sin^2\theta_W$
$C_{1d}=2g_A^e g_V^d$	$\frac{1}{2}-\frac{2}{3}\sin^2\theta_W$
$C_{2d}=2g_V^e g_A^d$	$\frac{1}{2}-2\sin^2\theta_W$

[8]For radiative corrections, see Marciano and Sirlin (1980).

on approximately isoscalar targets yield precise values of g_L^2 and g_R^2. Most theoretical uncertainties involving structure functions and systematic uncertainties concerning the neutrino flux cancel in the ratio. In the simple parton model

$$R_\nu = g_L^2 + g_R^2 r, \quad R_{\bar\nu} = g_L^2 + \frac{g_R^2}{r} , \tag{29}$$

where

$$r = \frac{\sigma(\bar\nu_\mu N \to \mu^+ X)}{\sigma(\nu_\mu N \to \mu^- X)} \simeq \frac{\frac{1}{3}+\epsilon}{1+\epsilon/3} \tag{30}$$

is the ratio of charged current cross sections and $\epsilon \simeq 0.125$ is the ratio of the fraction of the nucleon's momentum carried by antiquarks to that carried by quarks. In practice, many small corrections for quark mixing, s and c sea, the c-quark threshold, Q^2 evolution of structure functions, etc., must be applied to Eq. (29). R_ν has been measured[9] to 1% at CERN and Fermilab. Deep-inelastic scattering from nonisoscalar nuclei or in experiments in which the target nucleon can be identified as p and n, as well as elastic-scattering experiments, yields additional information on θ_L and θ_R. The present experimental values are (Kim *et al.*, 1981; Amaldi *et al.*, 1987; Costa *et al.*, 1988; Fogli and Haldt, 1988; Langacker and Mann, 1989; Langacker, 1990a, 1991a; Langacker and Luo, 1991a) $g_L^2 = 0.2977 \pm 0.0042$, which leads to $\Delta \sin^2\theta_W = 0.0057$; $g_R^2 = 0.0317 \pm 0.0034$ ($\Delta \sin^2\theta_W = 0.013$); $\theta_L = 2.50 \pm 0.03$ ($\Delta \sin^2\theta_W = 0.05$); $\theta_R = 4.59^{+0.44}_{-0.27}$, which is not sensitive to $\sin^2\theta_W$. The uncertainties in g_L^2 and g_R^2 and the corresponding $\sin^2\theta_W$ values are dominated by theoretical uncertainties and incomplete knowledge of certain physical quantities, especially the threshold for c-quark production in the charged current denominators. From deep-inelastic scattering, $\Delta \sin^2\theta_W = \pm 0.003 \pm [0.005]$ for fixed m_t and M_H, where the second uncertainty follows from a realistic estimate of the error in charm production in $\nu_\mu(d,s) \to \mu^- c$, which is obtained from neutrino-induced dimuon production ($c \to \mu^+ X$) (Amaldi *et al.*, 1987; Brock, 1988; Shaevitz, 1990).

There may be future deep-inelastic experiments using a high-energy ν_μ beam, e.g., at Fermilab (Bolton *et al.*, 1990). At high energies the theoretical uncertainties will be reduced and one may obtain a measurement of $R_\nu \simeq g_L^2 + 0.4 g_R^2$ corresponding to $\Delta \sin^2\theta_W = 0.002$ or better.

C. Low-energy effective ν_μ-electron coupling coefficients

The effective Lagrangian of the ν_μ-electron interaction assumes the following general form at low energy:

$$-L_{\rm eff}^{\nu_\mu e} = \frac{2G_F}{\sqrt{2}} \bar\nu_\mu \gamma^\mu P_L \nu_\mu \bar e \gamma_\mu (g_V^e - g_A^e \gamma_5) e , \tag{31}$$

with the SM expressions[10] for $g_{V,A}^e$ given in Table III. The $\nu_\mu e$ interaction is essentially an axial-vector transition, since $g_V = -\frac{1}{2} + 2\sin^2\theta_W$ is very small for $\sin^2\theta_W \simeq 0.23$. Other quantities proportional to the vector part of the Zee vertex are suppressed by the same factor, e.g., the C_2 coefficients of atomic parity violation and the asymmetries in $e^+e^- \to \mu^+\mu^-$ at the Z pole (see later in this section). g_A is sensitive to $\sin^2\theta_W$ and is predicted to be exactly $-\frac{1}{2}$ in the SM at tree level. With the SIP, $g_V = -0.0361$ and $g_A = -0.5037$. Their present experimental values are (Kim *et al.*, 1981; Amaldi *et al.*, 1987; Costa *et al.*, 1988; Fogli and Haidt, 1988; Langacker and Mann, 1989; Langacker, 1990a, 1991a; Langacker and Luo, 1991a) $g_V = -0.045 \pm 0.022$, which leads to $\Delta \sin^2\theta_W = 0.01$; $g_A = -0.513 \pm 0.025$. The measurement of the ratio g_V/g_A is expected to be improved, but not the separate values.

This interaction is not complicated by strong-interaction effects. Here we emphasize two types of experiments that minimize possible systematic errors and that, with sufficient statistics, would yield precise values of the measured quantities. One measurement is of the ratio

$$R_{\nu/\bar\nu} = \frac{\sigma_{\nu_\mu e \to \nu_\mu e}}{\sigma_{\bar\nu_\mu e \to \bar\nu_\mu e}} . \tag{32}$$

With the SIP, $R_{\nu/\bar\nu} = 1.152$. The experimental difficulty in making a precise measurement of $R_{\nu/\bar\nu}$ arises from the necessity of separate normalization of the ν_μ and $\bar\nu_\mu$ fluxes. The present error of $R_{\nu/\bar\nu}$ is 0.1, which leads to an uncertainty of 0.01 in $\sin^2\theta_W$. The future error of $R_{\nu/\bar\nu}$ [CHARM II (see Geiregat *et al.*, 1989)] is projected to be 0.05, which leads $\Delta \sin^2\theta_W = 0.005$.

Another type of experiment would measure the ratio [LCD (see Allen *et al.*, 1988)]

$$R_{\nu/\bar\nu\nu_e} = \frac{\sigma_{\nu_\mu e \to \nu_\mu e}}{\sigma_{\bar\nu_\mu e \to \bar\nu_\mu e} + \sigma_{\nu_e e \to \nu_e e}} . \tag{33}$$

With the SIP's, $R_{\nu/\bar\nu\nu_e} = 0.1455$. $R_{\nu/\bar\nu\nu_e}$ is about $\frac{1}{8}$ of $R_{\nu/\bar\nu}$ rather than $\frac{1}{2}$, the reason being that $\sigma_{\nu_e e \to \nu_e e}$ is much larger than $\sigma_{\nu_\mu e \to \nu_\mu e}$ due to the charged current contribution. The advantage of this experiment is that it is self-normalizing. If the neutrinos from charged-pion decays at rest are employed, the systematic uncertainty in $R_{\nu/\bar\nu\nu_e}$ can be reduced to 2% or less, which would lead to an error of 0.0025 in $\sin^2\theta_W$, as given in the LCD (Large Čerenkov Detector) proposal at Los Alamos.

[9]Recent results include CHARM (see Allaby *et al.*, 1987), CDHS (see Blondel *et al.*, 1990b), FFM (see Mattison *et al.*, 1990), and CCFR (see Reutens *et al.*, 1990).

[10]For radiative corrections, see Sarantakos *et al.* (1983).

D. Atomic parity-violation coupling constants

In the GWS theory of the electroweak interaction, for each γ channel there is always a Z channel accompanying it, as is shown in Fig. 30. At high energy, both channels are comparable. But at low energy, the Z channel is suppressed by a factor of q^2/M_Z^2 where q is the momentum transfer. Nevertheless, this tiny effect can be detected if it is enhanced by some mechanism and if experiments can be performed with high precision. One such effect is manifested in the atomic parity-violation phenomenon caused by the Z-channel interaction between an electron and nucleus in an atom. Nuclei and electrons are bound by electromagnetic interactions that do not violate parity. But the accompanying Z channel has both a vector piece and an axial-vector piece, so there are V, A cross terms that violate parity (see Bouchiat and Pottier, 1986; Noecker, 1988; Dzuba *et al.*, 1989; Blundell *et al.*, 1990; Bouchiat, 1990; Hartley and Sandars, 1990; for radiative corrections, see Marciano and Sirlin, 1983, 1984a). In general, the cross terms can written as

$$-L^{eH}=-\frac{G_F}{\sqrt{2}}\sum_i (C_{1i}\bar{e}\gamma_\mu\gamma_5 e\bar{q}_i\gamma^\mu q_i + C_{2i}\bar{e}\gamma_\mu e\bar{q}_i\gamma^\mu\gamma_5 q_i)\ . \tag{34}$$

The following combinations are the quantities extracted from experiments: $C_{1+}=0.666C_{1u}+0.747C_{1d}$, $C_{1-}=0.747C_{1u}-0.666C_{1d}$, $C_{2p}=C_{2u}+C_{2d}$, and $C_{2m}+C_{2u}-C_{2d}$, where the combination C_{1+} corresponds to parity violation in the cesium atom. The magnitude of the C_{2i} are much smaller than those of the C_{1i}, as mentioned above. Given the SIP, $C_{1+}=0.1291$, $C_{1-}=-0.3633$, $C_{2p}=-0.0140$, $C_{2m}=-0.0537$.

There are several ways to observe the effects of L^{eH} experimentally. One is by the scattering of longitudinally polarized electrons on nuclei. The SLAC polarized $e^{\uparrow\downarrow}D\to eX$ deep-inelastic asymmetry experiment (Prescott *et al.*, 1979) was crucial in establishing the validity of the SM in the late 1970s. Subsequent experiments have measured polarization asymmetries in muon-carbon deep-inelastic scattering (Argento *et al.*, 1983, 1984), and in electron-carbon (Souder *et al.*, 1990) and electron-beryllium elastic or quasielastic scattering (Heil *et al.*, 1989). On the other hand, L^{eH} will mix the energy levels of an atom with different parities. That mixing can be detected by observing the difference of the induced transition rates of an atom when the polarization of an incident laser beam exciting the atom is changed. Successful experiments in cesium with errors of a few percent have been done in Boulder and Paris (Noecker *et al.*, 1988). The theoretical predictions involving high Z atoms have also been improved recently to the 1% level, because, for example, cesium involves a single electron outside of a tightly bound core, allowing an accurate calculation of the necessary matrix elements (Dzuba *et al.*, 1989, Blundell *et al.*, 1990; Hartley and Sandars, 1990). One now has

$$Q_W\equiv -376C_{1u}-422C_{1d} = -71.04\pm1.58\pm[0.88]\ , \tag{35}$$

for the effective weak charge in cesium, where the first (second) uncertainty is experimental (theoretical). This is to be compared with the Standard Model prediction for cesium $Q_W^{Cs}=-73$, almost independent of m_t. A third way to measure the effect of L^{eH} is by optical rotation.

The present experimental values of the coefficients are $C_{1+}=0.126\pm0.003$, which leads to $\Delta\sin^2\theta_W=0.009$, and $C_{1-}=-0.45\pm0.10$, which leads to $\Delta\sin^2\theta_W=0.07$. C_{2p} and C_{2m} are poorly determined. The experimental error of C_{1+} may soon be reduced to $<0.5\%$. The total error would then be dominated by the theoretical uncertainty of $\sim1\%$, which would lead to $\Delta\sin^2\theta_W=0.003$. Future measurements involving different isotopes of cesium or other elements may allow determinations of the C_1's from ratios of measurements in which the atomic matrix elements cancel. We project two uncertainties for C_{1+}: a 1% uncertainty expected soon (C_{1+}) and a later possible 0.2% uncertainty from the use of different isotopes [C_{1+}(iso)][11]. The present precision of C_{1-} will probably not improve very much.

The C_1 coefficients are enhanced relative to those of C_2 in heavy atoms, because the C_1 matrix elements are coherent with respect to the nucleons, while the C_2 terms involve the nuclear spin (Bouchiat and Pittier, 1986; Bouchiat, 1990). It is therefore difficult to extract C_{2u} and C_{2d} from experiments in heavy atoms, and, in addition, there are no immediate prospects for measurements of atomic parity violation in hydrogen or other light elements. However, there is a proposal to measure parity violation in muonic boron atoms at PSI (Paul Scherrer Institute) (Missimer and Simons, 1985, 1990, Langacker, 1991b). If this experiment is realized, linear combinations of C_1 and C_2 coefficients can be measured to 10% or better. A 10% measurement would lead to $\Delta C_{2p}=0.046$ and $\Delta C_{2m}=0.11$. Better measurements of μB may be possible in the future. We shall therefore consider possible determinations of C_{2p} and C_{2m} in 10%

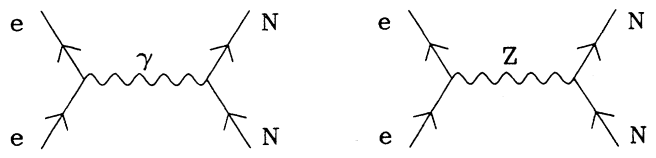

FIG. 30. One-photon and Z-exchange contributions to the electron-nucleus interaction.

[11]We utilize C_1(iso) for simplicity. In practice, other functions of the C_i are likely to be measured. For example, from measurements on isotopes, one may obtain $C_{1r}=C_{1+}/(4C_{1d}+2C_{1u})$, with $\Delta C_{1r}=0.443\Delta C_{1+}+0.15\Delta C_{1-}$.

measurements (C_{2p}, C_{2m}) as well as a possible determination $\Delta C_{2p}=0.005$ in a 1% measurement [$C_{2p}(1)$]. These would not yield a precise determination of $\sin^2\theta_W$, but are sensitive to certain types of new physics in the analysis based on the observables. It should be cautioned that there may be theoretical ambiguities in the interpretation, due to the strange quark sea and to nuclear anapole moment effects (Kim *et al.*, 1981; Kaplan and Manohar, 1988; Frantsuzov and Khriplovich, 1988; Beck, 1989; Campbell *et al.*, 1989; Bouchiat and Piketty, 1991). The constraints on the C_1's from a 1% μB measurement are similar to the expectation of a 1% Cs experiment.

There will be measurements of the electron and quark couplings to the Z in $e^-p\to e^-X$ at HERA (Hadron-Elektron Ring Anlage) Because of uncertainties associated with the quark distributions and other QCD effects, it is not apparent what accuracy will be attained. Sensitivity to new physics should be qualitatively similar to the other experiments discussed with appropriate scaling of errors. A future e^-C asymmetry measurement at the Bates (MIT) accelerator could possibly determine $C_{1u}+C_{1d}$ to 1%. The implications would be similar to a 1% cesium measurement but with completely different systematic errors (Souder *et al.*, 1990). Finally, high statistics $e^{\uparrow\downarrow}p$ experiments at CEBAF (Continuous Electron Beam Accelerator Facility) might measure the combination $2C_{1u}+C_{1d}$ to 10% [CEBAF (see Siegel, 1987)], implying $\Delta\sin^2\theta_W\simeq 0.002$. Since this has a different isospin structure than the other projected experiments, we include it in our projections.

E. Asymmetries of e^+e^- scattering at the Z pole

During the 1980s, measurements of the cross sections and forward-backward asymmetries in $e^+e^-\to\mu^+\mu^-$, $\tau^+\tau^-$, $\bar{b}b$, $\bar{c}c$, hadrons, etc. well below the Z pole at PEP, PETRA, and TRISTAN have been important tests of the SM (see Kiesling, 1988; de Boer, 1989; Marshall, 1989; Mori *et al.*, 1989; Abe, 1990; see also Amaldi *et al.*, 1987). At present and in the future $e^+e^-\to\bar{f}f$ at the Z pole at LEP, and SLC (Stanford Linear Collider) will allow much more precise tests.

It is straightforward to calculate the cross sections of $e^+e^-\to\bar{f}f$ for various final-state $f\bar{f}$'s to first order. Taking into account the Z and single-photon annihilation channels (if $f=e$ or ν_e, there are additional t-channel diagrams) for different helicities of initial and final states, we have (see Blochus *et al.*, 1986; Ellis and Peccei, 1986; Peskin, 1987; Swartz, 1987; Alexander *et al.*, 1988; Altarelli *et al.*, 1989; see also the references in Footnote 2)

$$\frac{d\sigma}{d\Omega}(e_L^-e_R^+\to f_L\bar{f}_R)=C_f\frac{\alpha^2}{4s}(1+\cos\theta)^2|f_{\rm LL}|^2\,, \tag{36}$$

$$\frac{d\sigma}{d\Omega}(e_L^-e_R^+\to f_R\bar{f}_L)=C_f\frac{\alpha^2}{4s}(1-\cos\theta)^2|f_{\rm LR}|^2\,, \tag{37}$$

$$\frac{d\sigma}{d\Omega}(e_R^-e_L^+\to f_L\bar{f}_R)=C_f\frac{\alpha^2}{4s}(1-\cos\theta)^2|f_{\rm RL}|^2\,, \tag{38}$$

$$\frac{d\sigma}{d\Omega}(e_R^-e_L^+\to f_R\bar{f}_L)=C_f\frac{\alpha^2}{4s}(1+\cos\theta)^2|f_{\rm RR}|^2\,, \tag{39}$$

where

$$C_f=\begin{cases}1, & f=\text{leptons},\\ 3, & f=\text{quarks}\end{cases} \tag{40}$$

is the color factor and

$$f_{ij}=-Q_f+\frac{s}{s-M_Z^2+is\Gamma_Z/M_Z}\frac{E_i(e)E_j(f)}{\sin^2\theta_W\cos^2\theta_W}\,, \tag{41}$$

where s is the square of the total center-of-mass energy, $\{ij\}=\{LL\},\{LR\},\{RL\},\{RR\}$, and

$$E_L(f)=\frac{V_f+A_f}{2}\,, \tag{42}$$

TABLE IV. Standard Model tree-level expressions for Z-pole observables. In the SM at the tree level the Z couplings $A_f=I_{3L}(f)$ and $V_f=I_{3L}(f)-2q_f\sin^2\theta_W$ coincide with the low-energy parameters $g_{A,V}^f$ relevant to $\nu f\to\nu f$ (Table III). However, in most extensions of the SM, $A_f\neq g_A^f$, $V_f\neq g_V^f$. $C_f=1$ (3) for leptons (quarks) is the color factor. These expressions reproduce the full SM predictions (including radiative corrections) as a function of M_Z, m_t, and M_H to 5 percent if the $\overline{\rm MS}$ value of $\sin^2\hat{\theta}_W(M_Z)$, corresponding to the given M_Z, m_t, M_H, is substituted. However, we include the full one-loop corrections in our numerical values.

Quantity	Expression
A_e	$-\frac{1}{2}$
V_e	$-\frac{1}{2}+2\sin^2\theta_W$
A_ν	$\frac{1}{2}$
V_ν	$\frac{1}{2}$
A_u	$\frac{1}{2}$
V_u	$\frac{1}{2}-\frac{4}{3}\sin^2\theta_W$
A_d	$-\frac{1}{2}$
V_d	$-\frac{1}{2}+\frac{2}{3}\sin^2\theta_W$
$\mathcal{A}_f$	$\frac{2V_fA_f}{V_f^2+A_f^2}$
A_{LR}	$\mathcal{A}_e$
$A_{FB}(f)$	$\frac{3}{4}\mathcal{A}_e\mathcal{A}_f$
$A_{FB}^{\rm pol}(f)$	$\frac{3}{4}\mathcal{A}_f$
$A_{\rm pol}(\tau)$	$\mathcal{A}_\tau$
$\Gamma_{Z\to f\bar{f}}$	$C_f\frac{G_F}{6\pi\sqrt{2}}M_Z^3[(V_f)^2+(A_f)^2]$

$$E_R(f)=\frac{V_f-A_f}{2}\ , \tag{43}$$

are the couplings of $f_{L,R}$ to the Z. The SM expressions for the vector and axial couplings[12] V_f and A_f are given in Table IV. In the following, we shall use these formulas to derive expressions for various Z-pole asymmetries in the SM. Except for a comment at the end, we only consider asymmetries at the Z pole, where most of the data-taking is expected. There the cross section is largest. Moreover, the electromagnetic contribution is negligible because it is 90° out of phase with the Z amplitude and does not interfere.

(a) The left-right asymmetry with longitudinally polarized initial electrons is given by

$$A_{\rm LR}=\frac{\sigma(e_L^-e^+\to\sum_f f\bar f)-\sigma(e_R^-e^+\to\sum_f f\bar f)}{\sigma(e_L^-e^+\to\sum_f f\bar f)+\sigma(e_R^-e^+\to\sum_f f\bar f)}\ , \tag{44}$$

where the summation runs through all fermion pairs $f\bar f$ comprising the final states. $A_{\rm LR}$ is small but sensitive to $\sin^2\theta_W$, so its precise measurement will provide an excellent determination of $\sin^2\theta_W$. In particular, the extracted $\sin^2\hat\theta_W(M_Z)$ is insensitive to m_t and M_H. It is also a reliable quantity theoretically, because uncertainties from initial-state radiative corrections cancel in the ratio. Within the SIP, $A_{\rm LR}=0.1306$. The projected experimental error of $A_{\rm LR}$ at LEP is (see Blochus *et al.*, 1986; Ellis and Peccei, 1986; Peskin, 1987; Swartz, 1987; Alexander *et al.*, 1988; Altarelli *et al.*, 1989; see also the references in Footnote 2) 0.003 if LEP goes ahead with polarization, corresponding to an error of 0.0003 in $\sin^2\theta_W$. At SLC, an error in $A_{\rm LR}$ of 0.006 is expected. However, we must fold in the theoretical error $\Delta A_{\rm LR}^{\rm pred}\simeq 0.0028$ in the SM prediction of $A_{\rm LR}$, from ΔM_Z and the uncertainty in Δr. The effective error is therefore $\Delta A_{\rm LR}\simeq 0.0041$ (LEP) or 0.0066 (SLC), corresponding to $\Delta\sin^2\theta_W\simeq 0.0005$ (0.0008).

Physically, $A_{\rm LR}$ is a measure of the interference of the vector V_e and axial A_e parts of the *Zee* vertex, which can be seen from the tree-level expression

$$A_{\rm LR}=\frac{2V_eA_e}{V_e^2+A_e^2}\equiv\mathcal{A}_e\ . \tag{45}$$

The radiative corrections modify the SM predictions for $A_{\rm LR}$ and other observables slightly. The one-loop corrections are included in our numerical values. The small magnitude of $A_{\rm LR}$ is due to the suppression of the vector part of the *Zee* vertex, as discussed above.

[12]In the SM at the tree level, one has $V_e=g_V^e$, $A_e=g_A^e$, etc. However, we distinguish between (V_e, A_e), which are the couplings to the Z, and (g_V^e, g_A^e), which are coefficients of the νe interaction, because they are different for most extensions of the SM.

(b) The forward-backward asymmetries of final-state fermions are

$$A_{\rm FB}(f)=\frac{\left[\int_{\cos\theta>0}-\int_{\cos\theta<0}\right]d\Omega\frac{d\sigma}{d\Omega}(e^+e^-\to\bar ff)}{\left[\int_{\cos\theta>0}+\int_{\cos\theta<0}\right]d\Omega\frac{d\sigma}{d\Omega}(e^+e^-\to\bar ff)}\ , \tag{46}$$

with $f=u,d,\mu$, etc. Here θ is the angle between the directions of the incoming electron and outgoing fermion f. All of the $A_{\rm FB}(f)$ are small and monotonically decrease with $\sin^2\theta_W$. The reason for this can be seen from their tree-level expressions:

$$A_{\rm FB}(f)=\frac{3}{4}\frac{2V_eA_e}{4(V_e)^2+(A_e)^2}\frac{2V_fA_f}{(V_f)^2+(A_f)^2}\equiv\frac{3}{4}\mathcal{A}_e\mathcal{A}_f\ . \tag{47}$$

We see $A_{\rm FB}$ is the product of V-A interference of both initial and final fermions. The first factor is exactly $A_{\rm LR}$ so it is not surprising that the $A_{\rm FB}$ have small values. In the case of the muon, $A_{\rm FB}(\mu)=\frac{3}{4}(A_{\rm LR})^2$. With the SIP, $A_{\rm FB}(c)=0.0617$, $A_{\rm FB}(b)=0.0910$, and $A_{\rm FB}(\mu)=0.0128$.

The experimental errors of $A_{\rm FB}$ are projected[13] to be (see Blochus *et al.*, 1986; Ellis and Peccei, 1986; Peskin, 1987; Swartz, 1987; Alexander *et al.*, 1988; Altarelli *et al.*, 1989; see also the references in Footnote 2) $\Delta A_{\rm FB}(\mu)=0.0035$, or $\Delta\sin^2\theta_W=0.0023$; $\Delta A_{\rm FB}(c)=0.0070$, or $\Delta\sin^2\theta_W=0.0017$; $\Delta A_{\rm FB}(b)=0.0054$, or $\Delta\sin^2\theta_W=0.0010$.

(c) If polarization becomes available, then the FB asymmetry for $e^+e^-\to\bar ff$ with a polarized e^- becomes

$$A_{\rm FB}(f)=\frac{3}{4}\frac{\mathcal{A}_e+P_e}{1+P_e\mathcal{A}_e}\mathcal{A}_f \tag{48}$$

in place of (47), where P_e is the electron polarization. This would allow a more precise determination of $\mathcal{A}_f$ than in the unpolarized case. It is more convenient, however, to introduce a mixed FB asymmetry in which the polarization direction is reversed [Blondel *et al.* (1988)]:

$$A_{\rm FB}^{\rm pol}(f)=\frac{\sigma_{\rm FB}^L(f)-\sigma_{\rm FB}^R(f)}{2\sigma}\ , \tag{49}$$

where

$$\sigma_{\rm FB}^{LR}(f)=\left[\int_{\cos\theta>0}-\int_{\cos\theta<0}\right]d\Omega\frac{d\sigma}{d\Omega}(e_{L,R}^-e^+\to f\bar f)\ , \tag{50}$$

$$\sigma=\int d\Omega\frac{d\sigma}{d\Omega}(e^-e^+\to f\bar f)\ . \tag{51}$$

[13]Experimentally, only the asymmetries of heavy quarks are measured accurately, since it is difficult to identify light flavor quarks at high energy.

All of the $A_{FB}^{pol}(f)$ monotonically decrease with $\sin^2\theta_W$. Their tree-level expressions are

$$A_{FB}^{pol}=\frac{3}{4}\frac{2V_fA_f}{(V_f)^2+(A_f)^2}=\frac{3}{4}\mathcal{A}_f\ , \tag{52}$$

which again measures the V-A interference of the final fermions, but without the suppression factor from A_{LR}. With the SIP, $A_{FB}^{pol}(\mu)=0.0980$, $A_{FB}^{pol}(c)=0.4725$, $A_{FB}^{pol}(b)=0.6965$. The expected experimental errors of A_{FB}^{pol} are (see Blochus *et al.*, 1986; Ellis and Peccei, 1986; Peskin, 1987; Swartz, 1987; Alexander *et al.*, 1988; Altarelli *et al.*, 1989; see also the references in Footnote 2) $\Delta A_{FB}^{pol}(\mu)=0.009$, or $\Delta\sin^2\theta_W=0.0015$; $\Delta A_{FB}^{pol}(c)=0.03$, or $\Delta\sin^2\theta_W=0.01$; $\Delta A_{FB}^{pol}(b)=0.02$, or $\Delta\sin^2\theta_W=0.04$.

(d) Final-state polarization asymmetries of the τ lepton: still another way to measure the V-A interference of the final fermions is to measure the decay asymmetries resulting from the polarization of the final-state fermions. It is difficult to measure the spins of quarks and light leptons, since quarks are always wrapped in jets and light leptons penetrate detectors easily. But it can be done for heavy leptons, namely, the τ's, via their decay distributions. Define:

$$A_{pol}(\tau)=\frac{\sigma(e^-e^+\to\tau_L^-\tau^+)-\sigma(e^-e^+\to\tau_R^-\tau^+)}{\sigma(e^-e^+\to\tau_L^-\tau^+)+\sigma(e^-e^+\to\tau_R^-\tau^+)}\ . \tag{53}$$

In the SM, $A_{pol}(\tau)=\mathcal{A}_\tau$, where we expect $\mathcal{A}_\tau=\mathcal{A}_e$ by the family universality of weak interactions, so the same V, A interference effect is measured. $\Delta A_{pol}(\tau)$ is projected to be 0.01 (see Blochus *et al.*, 1986; Ellis and Peccei, 1986; Peskin, 1987; Swartz, 1987; Alexander *et al.*, 1988; Altarelli *et al.*, 1989; see also the references in Footnote 2), which leads to an error of 0.0014 in $\sin^2\theta_W$.

The forward-backward asymmetries and the τ-polarization asymmetry will be measured at LEP within the next few years. It remains to be seen whether polarization asymmetries are measured at LEP and with what accuracy. Certainly the time scale is much larger. The accuracy to be expected at SLC is also uncertain. As will be seen in Sec. V for many types of new physics, A_{LR} and the other asymmetries in e^+e^- scattering at the Z pole are particularly sensitive observables.

F. Z-decay widths

(a) Partial Z-decay widths. The Z decays into lepton and quark pairs with different widths:

$$\Gamma_{f\bar f};\quad f=\nu,e,u,d,\ldots\ . \tag{54}$$

The tree-level predictions (ignoring fermion masses) are

$$\Gamma_{Z\to\nu\bar\nu}=\frac{G_F}{6\pi\sqrt{2}}M_Z^3[(V_\nu)^2+(A_\nu)^2]\ , \tag{55}$$

$$\Gamma_{Z\to e^+e^-}=\frac{G_F}{6\pi\sqrt{2}}M_Z^3[(V_e)^2+(A_e)^2]\ , \tag{56}$$

$$\Gamma_{Z\to u\bar u}=\frac{3G_F}{6\pi\sqrt{2}}M_Z^3[(V_u)^2+(A_u)^2]\ , \tag{57}$$

$$\Gamma_{Z\to d\bar d}=\frac{3G_F}{6\pi\sqrt{2}}M_Z^3[(V_d)^2+(A_d)^2]\ . \tag{58}$$

The formulas (55)–(58) must be supplemented with QCD, QED, and electroweak radiative corrections, as well as fermion mass corrections. By writing the coefficient $g^2M_Z/4\sqrt{2}\cos^2\theta_W$ as $G_FM_Z^3$, many of the electroweak corrections are automatically incorporated. Most of the sensitivity to $\sin^2\theta_W$ of the widths is due to the M_Z^3 coefficient rather than to the explicit $\sin^2\theta_W$ dependence of the vector couplings. One can therefore view the widths as indirect determinations of M_Z, to be compared with the directly measured value $M_z=91.177\pm0.031$ GeV.

With the SIP, $\Gamma_{b\bar b}=0.3773$ GeV, $\Gamma_{c\bar c}=0.2959$ GeV, $\Gamma_{e\bar e}=0.0835$ GeV, $\Gamma_{\nu\bar\nu}=0.1663$ GeV. The precision of $\Gamma_{b\bar b}$ and $\Gamma_{c\bar c}$ is expected to be 10%; i.e., $\Delta\Gamma_{bb}=40$ MeV, $\Delta\sin^2\theta_W=0.018$; $\Delta\Gamma_{c\bar c}=30$ MeV, $\Delta\sin^2\theta_W=0.02$.

The experimental leptonic width is the averaged width of e, μ, and τ; we denote it as $\Gamma_{l\bar l}$. At present,[14] $\Gamma_{l\bar l}=83.9\pm0.7$ MeV (Dydak, 1990; Fernandez, 1990), which leads to $\Delta\sin^2\theta_W=0.002$. The width into unobserved (invisible) particles, Γ_{inv} is determined by the difference of the total Z width (see below) and the Z width into observable particles (hadrons and charged particles). In the SM, $\Gamma_{inv}=3\Gamma_{\nu\bar\nu}=499.0$ MeV. The present experimental value is $\Gamma_{inv}=482\pm16$ MeV (Dydak, 1990; Fernandez, 1990), which leads to $\Delta\sin^2\theta_W=0.007$. The value of Γ_{inv} is not expected to be improved very much in the future.[14] An independent measurement of Γ_{inv} is the observation of single-photon events in e^+e^- collisions a little off the Z pole. That experiment is expected to have an error of 35 MeV, which is less accurate but which would have different systematic errors.

(b) Inclusive Z-decay width. The total or inclusive Z-decay width is the summation of all the partial widths of fermions. That is,

$$\Gamma_Z=3\Gamma_{Z\to\nu\bar\nu}+3\Gamma_{Z\to e^+e^-}+2\Gamma_{Z\to u\bar u}+3\Gamma_{Z\to d\bar d}\ , \tag{59}$$

where the coefficients are due to the three families (the t is too massive to contribute). This quantity is measured by the shape of the energy dependence of the total cross section of the e^+e^- collision around the Z pole. With the SIP, $\Gamma_Z=2.484$ GeV. Experimentally, $\Gamma_Z=2.497\pm0.015$ GeV (Dydak, 1990; Fernandez, 1990), which leads to $\Delta\sin^2\theta_W=0.001$. This number is not expected to improve substantially.[14]

[14]See the Addendum for an updated-discussion.

G. Off-Z-pole observables

The e^+e^- observables at the Z pole will provide a superb test of the SM. They are sensitive to any type of new physics that shifts the Z mass or changes its couplings, such as Z-Z' mixing or mixing between ordinary and exotic fermions. However, they are insensitive to other types of new physics, such as new four-fermi operators induced by compositeness, new Z' bosons that have little mixing with the Z, or leptoquarks. This is partly due to the fact that the Z amplitude is $\simeq 90°$ out of phase with respect to the new physics at the pole, so there is no interference. By measuring e^+e^- observables slightly off the pole, one has the possibility of first-order effects due to interference between the SM and new-physics amplitudes (Cvetic and Lynn, 1987; Cvetic and Langacker, 1990). However, one cannot go very far from the pole without severely reducing the event rates. Hence in Sec. V we discuss the sensitivity of e^+e^- observables at $s-M_Z^2 \simeq M_Z\Gamma_Z$, where the SM cross sections are only reduced by a factor of 2 from their values on the Z pole. We assume, rather optimistically, that the various asymmetries can be measured with the same accuracy as on-shell. We do, however, separate the polarization asymmetries into definite final states to enhance sensitivity to specific types of new physics. The projected statistical uncertainties are increased accordingly.

One expects interference effects due to new physics of strength λ to be of order

$$\frac{s-M_Z^2}{M_Z^2}\lambda \simeq \frac{\Gamma_Z}{M_Z}\lambda \ . \tag{60}$$

Hence the combined effects of needing to go off-shell while still maintaining a reasonable cross section lead to a suppression by $\Gamma_Z/M_Z \simeq 0.03$. Nevertheless, several of the SM asymmetries, in particular $A_{\rm LR}$ and $A_{\rm FB}(\mu)$, are small due to the presence of factors $V_e \simeq -0.036$. Hence the effects of new physics off-shell may be enhanced in these cases if the new physics does *not* have suppressed vector couplings.

H. Forward-backward asymmetries in $p\bar{p} \to Z \to l^+l^-$

Recently the CDF (Collider Detector at Fermilab) collaboration (Hurst, 1990) has measured the forward-backward asymmetry $A_{\rm FB}(\bar{p}p \to e^+e^-)$ in $\bar{p}p \to Z \to l^+l^-$. [In practice, they increase their sensitivity by including e^+e^- pairs somewhat away from the Z pole, where the Z and virtual-photon (Drell-Yan) amplitudes can interfere (Rosner, 1987, 1989)]. The on-shell asymmetry is just a weighted average of the forward-backward asymmetries in $\bar{u}u \to e^+e^-$ and $\bar{d}d \to e^+e^-$, which could in principle be separated by observing how the asymmetry varies with rapidity. The $\bar{f}f \to e^+e^-$ asymmetry is given by the same expression as the $e^+e^- \to \bar{f}f$ asymmetry $A_{\rm FB}(f)$ in (47). Thus

$$A_{\rm FB}(\bar{p}p \to e^+e^-) = \alpha A_{\rm FB}(u) + \beta A_{\rm FB}(d) \ , \tag{61}$$

where the coefficients α and β are calculable and of order unity. The change due to each type of new physics can be determined from the change in $A_{\rm FB}(u)$ and $A_{\rm FB}(d)$. These in turn are the same as or related in an obvious way to the changes in $A_{\rm FB}(c)$ and $A_{\rm FB}(b)$ for the types of new physics considered in this paper.

For ~ 1000 Z's the uncertainty in $A_{\rm FB}(\bar{p}p \to e^+e^-)$ would be $\simeq 0.03$, which is considerably larger than the projected uncertainties of 0.007 and 0.0054 in $A_{\rm FB}(c)$ and $A_{\rm FB}(b)$, respectively.

IV. NEW PHYSICS

A. The new physics of extra Z bosons

1. Generalities

Extra intermediate vector bosons (IVBs) beside the SM prediction of the W and Z are universal in grand unification theories (GUTs) that incorporate the SM. They arise naturally because the extension from the SM to GUTs introduces larger gauge groups with more group generators and more IVBs. Usually the large mass scale of GUTs renders these IVBs ultraheavy and irrelevant to physics in the laboratory (Georgi and Glashow, 1974; Langacker, 1981, 1988; Ross, 1985).

However, there can be extra IVBs that do not acquire masses when the GUT is broken. They may develop masses by other Higgs fields at low energy, e.g., in the TeV range. In that case, we may either see them directly in the Superconducting Super Collider, Large Hadron Collider, or Tevatron, or find their effects at present energies when high-precision experiments are performed in the next decade.

In this paper we study one class of such IVBs: extra neutral Z bosons. If the SM is correct in first order, the effects of extra Z bosons are small perturbations. If there are $n-1$ extra Z bosons, then the gauge group is $SU(2)\times \prod_{\alpha=1}^{n} U(1)_\alpha$. A formalism to describe the effects on neutral-current phenomena was developed several years ago (Durkin and Langacker, 1986). In general, the couplings between the U(1) bosons and the fermions are arbitrary. That gives too many free parameters from which to draw strong conclusions. On the other hand, in the spirit of grand unification we take the U(1)'s as relics of an underlying non-Abelian gauge group, in which there is only one overall coupling constant and the fermions charges in one irreducible representation are related (Durkin and Langacker, 1986; Amaldi *et al.*, 1987; Costa *et al.*, 1988; del Aguila, Moreno, and Quiros, 1990, 1991; Altarelli, Casalbuoni, Dominici, Feruglio, and Gatto, 1990a, 1990b; Altarelli, Casalbuoni, Feruglio, and Gatto, 1990a, 1990b; Cvetic and Langacker, 1990; Gonzales-Garcia and Valle, 1990a, 1990b, 1991; Layssac *et al.*, 1990; Langacker and Luo, 1991b; Mahanthappa

and Mohapatra, 1991). Then the couplings of the extra Z's are predicted (the strength may depend on the GUT breaking pattern). When the $SU(2)\times U(1)^n$ symmetry is broken, the IVBs acquire masses. The SM predictions are changed by the mixing caused by the diagonalization of the gauge boson mass matrix and by the exchange of the extra Z's. In this paper we take the $E(6)$ model as an important example. We also consider the extra Z boson in $SU(2)_L\times SU(2)_R\times U(1)$ models (Mohapatra, 1986; Langacker and Umasanakar, 1989).

2. Formalism

We extend the SM electroweak gauge group $SU(2)\times U(1)$ to $SU(2)\times\prod_{\alpha=1}^{n}U(1)_\alpha$ to incorporate $n-1$ extra Z's. We assume that all left-handed fermions transform as SU(2) doublets, and all right-handed fermions as SU(2) singlets, and we identify the $U(1)_1$ changes with the weak hypercharges $Y=Q-T_{3L}$ of the SM. (This can always be done without loss of generality by an appropriate rotation on the U(1) gauge fields.) The other $U(1)_\alpha$ charges therefore do not overlap with the electric charge Q, and their overall coupling constants are to be determined by the underlying gauge group. The mass matrix of the Z's is to be determined by Higgs fields that break $SU(2)\times U(1)^n$ down to U(1).

After spontaneous symmetry breaking, the neutral-current interaction is[15]

$$-L_{\rm NC}=eJ^\mu_{em}A_\mu+\sum_{\alpha=1}^{n}g_\alpha J^\mu_\alpha Z^0_{\alpha\mu}\ . \tag{62}$$

Here

$$-L^{\rm SM}_{\rm NC}=eJ^\mu_{em}A_\mu+g_1J^\mu_1Z^0_{1\mu} \tag{63}$$

is the SM prediction, with $g_1^2=g^2+g'^2$, and $Z^0_\alpha(\alpha\geq 2)$ are new heavy bosons. The currents are

$$\begin{aligned}J^\mu_\alpha&=\sum_i\bar\psi_i\gamma^\mu[\epsilon^{(\alpha)}_L(i)P_L+\epsilon^{(\alpha)}_R(i)P_R]\psi_i\\&=\frac{1}{2}\sum_i\bar\psi_i\gamma^\mu[g_V^{i(\alpha)}-g_A^{i(\alpha)}\gamma_5]\psi_i\ ,\end{aligned} \tag{64}$$

where

$$g^{i(\alpha)}_{V,A}=\epsilon^{(\alpha)}_L(i)\pm\epsilon^{(\alpha)}_R(i)\ , \tag{65}$$

for $\alpha=1,\ldots,n$; $\epsilon^{(1)}_{L,R}(i)$ are the SM predictions of the weak neutral-current coefficients, given in Table III. The mismatch between the mass and gauge group eigenstates of the Z's will cause mixing. The gauge boson mass eigenstates Z_α will be

$$Z_\alpha=\sum_{\beta=1}^{n}U_{\alpha\beta}Z^0_\beta\ , \tag{66}$$

where U is an orthogonal matrix. In terms of the Z_α's.

$$-L_{\rm NC}=eJ^\mu_{em}A_\mu+\sum_{\alpha,\beta=1}^{n}g_\beta U_{\alpha\beta}J^\mu_\beta Z_{\alpha\mu}\ . \tag{67}$$

At low momentum, the effective four-fermion interaction is

$$-L_{\rm eff}=\frac{4G_f}{\sqrt{2}}\sum_{\alpha=1}^{n}\rho_\alpha\left[\sum_{\beta=1}^{n}\frac{g_\beta}{g_1}U_{\alpha\beta}J^\mu_\beta\right]^2\ , \tag{68}$$

where $\rho_\alpha=M_W^2/(M_\alpha^2\cos^2\theta_W)$; M_W is the mass of the W, and M_α the mass of the Z_α.

From now on we only consider the case of one extra Z boson ($n=2$) for simplicity. The generalization to multi-extra Z's is straightforward. The mixing matrix is then

$$U=\begin{bmatrix}\cos\Theta & \sin\Theta\\ -\sin\Theta & \cos\Theta\end{bmatrix}\ . \tag{69}$$

The presence of the Z_2^0 manifests itself through (a) a change in the Z_1 couplings due to mixing, (b) Z_2 exchange, and (c) a reduction in the Z_1 mass because of mixing. We introduce the following notation to simplify the forthcoming formulas:

$$\rho_{\rm eff}=\rho_1\cos^2\Theta+\rho_2\sin^2\Theta \tag{70}$$

$$w=\frac{g_2}{g_1}\cos\Theta\sin\Theta(\rho_1-\rho_2) \tag{71}$$

$$y=\left[\frac{g_2}{g_1}\right]^2(\rho_1\sin^2\Theta+\rho_2\cos^2\Theta)\ . \tag{72}$$

Clearly, the terms involving ρ_1 (ρ_2) are associated with Z_1 (Z_2) exchange. $\rho_{\rm eff}$ is mainly due to Z_1 exchange, y to Z_2 exchange, and w to Z_1^0-Z_2^0 mixing.

The effective Lagrangian of the neutral-current interactions between massless left-handed neutrinos and quarks and electrons is

$$-L_{\rm eff}=\frac{4G_f}{\sqrt{2}}\bar\nu\gamma^\mu P_L\nu J_\mu\ , \tag{73}$$

where

$$\begin{aligned}J_\mu&=\sum_i\epsilon_L(i)\bar\psi_i\gamma_\mu P_L\psi_i+\epsilon_R(i)\bar\psi_i\gamma_\mu P_R\psi_i\\&=\tfrac{1}{2}\sum_i\bar\psi_i\gamma_\mu(g_v^i-g_A^i\gamma_5)\psi_i\end{aligned} \tag{74}$$

with

$$\begin{aligned}\epsilon_{L,R}(i)&=\epsilon^{(1)}_{L,R}(i)+\delta\epsilon_{L,R}(i)\\&=\rho_{\rm eff}\epsilon^{(1)}_{L,R}(i)+w[\epsilon^{(2)}_{L,R}(i)+2\epsilon^{(2)}_\nu\epsilon^{(1)}_{L,R}(i)]\\&\quad+2y\epsilon^{(2)}_\nu\epsilon^{(2)}_{L,R}(i)\ .\end{aligned} \tag{75}$$

The effective parity-violating interaction between electrons and quarks is

[15]The effects of the extra Z's on the radiative corrections are considered in Degrassi and Sirlin (1989) and Blümlein, Leike, and Riemann (1990). Our purpose is to explore the sensitivity of precise measurements to small tree-level effects induced by the extra Z's. We therefore ignore the smaller effects on the radiative corrections.

$$-L^{eH}=-\frac{G_f}{\sqrt{2}}\sum_i (C_{1i}\bar{e}\gamma_\mu\gamma_5 e\bar{q}_i\gamma^\mu q_i + C_{2i}\bar{e}\gamma_\mu e\bar{q}_i\gamma^\mu\gamma_5 q_i) \tag{76}$$

with

$$C_{1i}=C_{1i}^{(1)}+\delta C_{1i} =2\rho_{\rm eff}g_A^{e(1)}g_V^{i(1)}+2w\,[g_A^{e(1)}g_V^{i(2)}+g_A^{e(2)}g_V^{i(1)}] +2yg_A^{e(2)}g_V^{i(2)}\ , \tag{77}$$

$$C_{2i}=C_{2i}^{(1)}+\delta C_{2i} =2\rho_{\rm eff}g_V^{e(1)}g_A^{i(1)}+2w\,[g_V^{e(1)}g_A^{i(2)}+g_V^{e(2)}g_A^{i(1)}] +2yg_V^{e(2)}g_A^{i(2)}\ . \tag{78}$$

We notice that at low momentum the current structures predicted by the SM are preserved in the presence of one extra Z boson, though the coefficients are changed. Without the extra Z, $\epsilon=\epsilon^{(1)}$, and $C=C^{(1)}$, and we recover the SM predictions.

The partial Z-decay widths are

$$\Gamma_{Z\to\nu\bar{\nu}}=\rho_1\frac{G_F}{6\pi\sqrt{2}}M_Z^3[(V_\nu)^2+(A_\nu)^2]\ , \tag{79}$$

$$\Gamma_{Z\to e^+e^-}=\rho_1\frac{G_F}{6\pi\sqrt{2}}M_Z^3[(V_e)^2+(A_e)^2]\ , \tag{80}$$

$$\Gamma_{Z\to u\bar{u}}=\rho_1\frac{3G_F}{6\pi\sqrt{2}}M_Z^3[(V_u)^2+(A_u)^2]\ , \tag{81}$$

$$\Gamma_{Z\to d\bar{d}}=\rho_1\frac{3G_F}{6\pi\sqrt{2}}M_Z^3[(V_d)^2+(A_d)^2]\ , \tag{82}$$

where

$$V_i=\cos\Theta g_V^{i(1)}+\frac{g_2}{g_1}\sin\Theta g_V^{i(2)}\simeq g_V^{i(1)}+wg_V^{i(2)}\ , \tag{83}$$

$$A_i=\cos\Theta g_A^{i(1)}+\frac{g_2}{g_1}\sin\Theta g_A^{i(2)}\simeq g_A^{i(1)}+wg_A^{i(2)}\ . \tag{84}$$

We can also calculate the cross sections of $e^+e^-\to\bar{f}f$ for various f's ($f\neq e,\nu_e$):

$$\frac{d\sigma}{d\Omega}(e_L^-e_R^+\to f_L\bar{f}_R)=C_f\frac{\alpha^2}{4s}(1+\cos\theta)^2|f_{\rm LL}|^2\ , \tag{85}$$

$$\frac{d\sigma}{d\Omega}(e_L^-e_R^+\to f_R\bar{f}_L)=C_f\frac{\alpha^2}{4s}(1-\cos\theta)^2|f_{\rm LR}|^2\ , \tag{86}$$

$$\frac{d\sigma}{d\Omega}(e_R^-e_L^+\to f_L\bar{f}_R)=C_f\frac{\alpha^2}{4s}(1-\cos\theta)^2|f_{\rm RL}|^2\ , \tag{87}$$

$$\frac{d\sigma}{d\Omega}(e_R^-e_L^+\to f_R\bar{f}_L)=C_f\frac{\alpha^2}{4s}(1+\cos\theta)^2|f_{\rm RR}|^2\ , \tag{88}$$

with

$$f_{ij}=-Q_f+\frac{s}{s-M_{Z_1}^2+is\Gamma_{Z_1}/M_{Z_1}}f_{1ij} +\frac{s}{s-M_{Z_2}^2+is\Gamma_{Z_2}/M_{Z_2}}f_{2ij}\ , \tag{89}$$

and

$$C_f=\begin{cases}1, & f=\text{leptons}\ ,\\ 3, & f=\text{quarks}\end{cases} \tag{90}$$

where $i,j=LL,LR,RL,RR$ and

$$f_{1ij}=\cos^2\Theta\epsilon_i^{(1)}(e)\epsilon_j^{(1)}(f)+(g_2/g_1)\cos\Theta\sin\Theta[\epsilon_i^{(1)}(e)\epsilon_j^{(2)}(f)+\epsilon_i^{(2)}(e)\epsilon_j^{(1)}(f)]+(g_2^2/g_1^2)\sin^2\Theta\epsilon_i^{(2)}(e)\epsilon_j^{(2)}(f)/\sin^2\theta_W\cos^2\theta_W\ , \tag{91}$$

$$f_{2ij}=\sin^2\Theta\epsilon_i^{(1)}(e)\epsilon_j^{(1)}(f)-(g_2/g_1)\cos\Theta\sin\Theta[\epsilon_i^{(1)}(e)\epsilon_j^{(2)}(f)+\epsilon_i^{(2)}(e)\epsilon_j^{(1)}(f)]+(g_2^2/g_1^2)\cos^2\Theta\epsilon_i^{(2)}(e)\epsilon_j^{(2)}(f)/\sin^2\theta_W\cos^2\theta_W\ . \tag{92}$$

If experiments are performed at the Z_1 resonance, then both the extra Z channel and the EM channel will be suppressed; so the asymmetries are

$$A_{\rm LR}=\frac{2V_eA_e}{(V_e)^2+(A_e)^2}\ , \tag{93}$$

$$A_{\rm FB}(f)=\frac{3}{4}\frac{2V_eA_e}{(V_e)^2+(A_e)^2}\frac{2V_fA_f}{(V_f)^2+(A_f)^2}\ , \tag{94}$$

$$A_{\rm FB}^{\rm pol}(F)=\frac{3}{4}\frac{2V_fA_f}{(V_f)^2+(A_f)^2}\ , \tag{95}$$

$$A_{\rm pol}(f)=\frac{2V_fA_f}{(V_f)^2+(A_f)^2}\ , \tag{96}$$

where V_i and A_i are given in Eqs. (83) and (84). In the asymmetries, the extra Z manifests itself only through mixing between different Z bosons. If there is no mixing, no significant deviations will be observed from the SM expressions. This is because the Z_2 exchange is $\pi/2$ out of phase at the Z_1 pole if $i\Gamma_{Z_2}/M_{Z_2}$ is neglected. When off the Z_1 pole, there are first-order contributions from the Z_2 channel, as will be discussed in Sec. V.

3. Mass and mixing parameters

For definite Z_2^0 couplings (including g_2) all of the observables are functions of ρ_1, ρ_2, Θ, and $\sin^2\theta_W$, or, equivalently, M_1, M_2, Θ, and[16] $\sin^2\theta_W$. Actually, these

[16]There is no ambiguity in the definition of $\sin^2\theta_W$ in the presence of the extra Z_2^0 if the $\overline{\rm MS}$ definition is used. For the on-shell definition, we must define $\sin^2\theta_W^M=1-M_W^2/M_0^2$.

are not all independent. One has (Langacker, 1984)

$$\tan^2\Theta=\frac{M_0^2-M_1^2}{M_2^2-M_0^2}\ , \tag{97}$$

where M_0 is the SM value for M_Z in the absence of mixing. Equation (97) follows easily from the diagonalization of the Z_1^0-Z_2^0 mass mixing matrix. Hence mixing reduces the value of M_Z from the SM value:

$$M_1^2=M_0^2-\tan^2\Theta(M_2^2-M_0^2)\ . \tag{98}$$

We assume that the SM is approximately correct. In that case Θ and $\rho_2\equiv M_W^2/M_2^2\cos^2\theta_W\simeq M_1^2/M_2^2$, or, more generally,

$$\hat{\Theta}\equiv\frac{g_2}{g_1}\Theta\ , \tag{99}$$

$$\hat{\rho}_2\equiv\frac{g_2^2}{g_1^2}\rho_2\simeq\frac{g_2^2}{g_1^2}\frac{M_1^2}{M_2^2}\ , \tag{100}$$

are small parameters that characterize the extra Z_2 (the Z_2^0 couplings must also be specified). Θ, M_1^2, and M_2^2 are obtained by diagonalizing the Z_1^0-Z_2^0 mass matrix:

$$M^2=\begin{pmatrix} 2g_1^2\sum_i I_{i3}^2|\langle\phi_i\rangle|^2 & 2g_1g_2\sum_i I_{i3}Q_i|\langle\phi_i\rangle|^2 \\ 2g_1g_2\sum_i I_{i3}Q_i|\langle\phi_i\rangle|^2 & 2g_2^2\sum_i Q_i^2|\langle\phi_i\rangle|^2 \end{pmatrix} \equiv\begin{pmatrix} M_0^2 & c \\ c & M_S^2 \end{pmatrix}\ , \tag{101}$$

where $\langle\phi_i\rangle$ is the VEV of a Higgs field ϕ_i with 3-component of weak isospin I_{i3} and J_2^0 charge Q_i. To obtain $\hat{\rho}_2\ll 1$ and small mixing, one requires $M_S^2\gg|M_0^2|$, $|c|$; i.e., there must be an SU(2)-singlet Higgs with large VEV. Then

$$M_1^2\simeq M_0^2-\frac{c^2}{M_S^2}\ , \tag{102}$$

$$M_2^2\simeq M_S^2\ , \tag{103}$$

$$\rho_2\simeq\frac{M_1^2}{M_2^2}\simeq\frac{M_0^2}{M_S^2}\ , \tag{104}$$

and

$$\Theta\simeq-\frac{c}{M_S^2}\simeq-\frac{c}{M_0^2}\rho_2\ . \tag{105}$$

Hence Θ and ρ_2 are not really independent, but are related by a factor $-c/M_0^2$ that characterizes the model and that is typically of order unity (or zero). This is because both Θ and ρ_2 are generated by the same SU(2)-nonsinglet Higgs fields.

It is convenient to define a quantity

$$C=-\frac{g_1}{g_2}\frac{c}{M_0^2}=-\frac{\sum_i I_{i3}Q_i|\langle\phi_i\rangle|^2}{\sum_i I_{i3}^2|\langle\phi_i\rangle|^2}\ , \tag{106}$$

so that

$$\hat{\Theta}\equiv C\hat{\rho}_2\ . \tag{107}$$

In some models the quantum numbers are such that there is a definite prediction for C. In other cases there is a range, depending on a ratio of VEV's. We will illustrate a number of specific values of C and the J_2^0 couplings.

In terms of C and $\hat{\rho}_2$, the mass relation in (102) becomes

$$\rho_1=\frac{M_W^2}{M_1^2\cos^2\theta_W}\simeq 1+C^2\hat{\rho}_2\ , \tag{108}$$

while the effective neutral couplings are

$$\rho_{\rm eff}\simeq\rho_1,\quad w\simeq C\hat{\rho}_2,\quad y\simeq\hat{\rho}_2\ ; \tag{109}$$

i.e., to leading order in small quantities, these represent Z_1 exchange, Z_1^0-Z_2^0 mixing in Z_1 exchange, and Z_2 exchange, respectively.

4. E(6) models

E(6) and its subgroup SO(10) are natural extensions of the SU(5) model (Georgi and Glashow, 1974; Langacker, 1981, 1988; Robinett, 1982; Robinett and Rosner, 1982a, 1982b; Ross, 1985) with all fermions in a given family assigned to the same representation. More recently, simple versions of E(6), in which all matter supermultiplets transform as 27-plets (i.e., no higher-dimensional representations of fermions and scalars), have become especially popular through the inspiration of superstring theory (Ross, 1988). The phenomenological implications and the expectations for directly producing and detecting the new Z's in E(6) models are described in Langacker, Robinett, and Rosner (1984) and del Aguila, Moreno, and Quiros (1989, 1990).

Both $SU(3)_C\times SU(2)_L\times U(1)_Y$ and SU(5) are groups with rank 4, while $E(6)$ has rank 6. There are therefore two extra neutral Z bosons, one or both of which may be sufficiently light [O(TeV)] to be observed experimentally, either by direct production or through precision experiments. We shall consider the case that a single extra Z is light enough to be relevant. The types of U(1) symmetries that will survive at the TeV scale depend on the pattern of spontaneous symmetry breaking. The following are three important symmetry-breaking patterns, and their corresponding bosons will be considered in this article:

(a)

$$E(6)\underset{M_6}{\rightarrow}SO(10)\times U(1)_\psi\ , \tag{110}$$

$$SO(10)\underset{M_{10}}{\rightarrow}SU(5)\times U(1)_\chi\ , \tag{111}$$

$$\mathrm{SU}(5) \underset{M_5}{\rightarrow} \mathrm{SU}(3)_C \times \mathrm{SU}(2)_L \times \mathrm{U}(1)_Y \ , \tag{112}$$

where M_6, M_{10}, and M_5 are superheavy scales ($>10^{14}$ GeV).

(b) many superstring-inspired models break directly to a rank-5 group by

$$\mathrm{E}(6) \underset{M_6}{\rightarrow} \mathrm{SU}(3)_C \times \mathrm{SU}(2)_L \times \mathrm{U}(1)_Y \times \mathrm{U}(1)_\eta \ , \tag{113}$$

where $Q_\eta = \sqrt{\frac{3}{8}} Q_\chi - \sqrt{\frac{5}{8}} Q_\psi$. However, a general[17] E(6) Z boson is an arbitrary combination of Z_χ and Z_ψ:

$$Z_2^0 = \cos\beta Z_\chi + \sin\beta Z_\psi \ , \tag{114}$$

where β is a mixing angle.

(c)

$$\mathrm{SO}(10) \underset{M_{10}}{\rightarrow} \mathrm{SU}(3)_C \times \mathrm{SU}(2)_L \times \mathrm{SU}(2)_R \times \mathrm{U}(1)_{B-L} \ , \tag{115}$$

$$\mathrm{SU}(2)_R \times \mathrm{U}_{B-L} \underset{M_{\mathrm{LR}}}{\rightarrow} \mathrm{U}(1)_Y \ , \tag{116}$$

where B and L, are respectively, baryon and lepton number. M_{LR} could be very large or it could be in the TeV range or smaller. Of course, $\mathrm{SU}(2)_L \times \mathrm{SU}(2)_R \times \mathrm{U}(1)_{B-L}$ (LR) models can be considered outside of the SO(10) context. We shall consider the χ, ψ, η, and Z_{LR} as typical examples of E(6)-inspired extra Z bosons.

The fermions in one family are assigned to a 27-plet of E(6); their couplings to the χ, ψ, and η are listed in Table V. The corresponding currents are

$$J^\mu_{Z_2^0} = \bar{\Psi}_L \gamma^\mu Q_{Z_{2L}^0} \Psi_L + \bar{\Psi}_R \gamma^\mu Q_{Z_{2R}^0} \Psi_R \ . \tag{117}$$

For the LR model, the current orthogonal to the SM U(1) is

$$J^\mu_{\mathrm{LR}} = \sqrt{3/5} \left[\alpha J^\mu_{3R} - \frac{1}{2\alpha} J^\mu_{B-L} \right] , \tag{118}$$

where J_{3R} is the third component of $\mathrm{SU}(2)_R$. J_{3R} is constructed so that all of the right-handed fermions are doublets and all the left-handed fermions are singlets. In Eq. (118)

$$\alpha = \left[\frac{1-(1+g_L^2/g_R^2)\sin^2\theta_W}{g_L^2/g_R^2 \sin^2\theta_W} \right]^{1/2} . \tag{119}$$

In the special case of left-right symmetry ($g_L = g_R$),

$$\alpha = \left[\frac{1-2\sin^2\theta_W}{\sin^2\theta_W} \right]^{1/2} \simeq 1.53 \ . \tag{120}$$

The coupling constant of the extra U(1) is

$$g_2 = \sqrt{\tfrac{5}{3}} \sin\theta_W g_1 \lambda_g^{1/2} \ , \tag{121}$$

[17]This is the most general case if E(6) directly breaks to a direct product of the SM and a group containing the extra U(1).

TABLE V. Couplings of the Z_χ^0, Z_ψ^0, and Z_η^0 to a 27-plet of E(6). The SO(10) and SU(5) representations are also indicated. The couplings are shown for the left-handed (L) particles and antiparticles. The couplings of the right-handed particles are minus those of the corresponding L antiparticles. The D is an exotic SU(2)-singlet quark with charge $-\frac{1}{3}$. $(E^0, E^-)_{L,R}$ is an exotic lepton doublet with vector SU(2) couplings. N and S are new Weyl neutrinos which may have large Majorana masses.

$SO(10)$	$SU(5)$	$2\sqrt{10}Q_\chi$	$\sqrt{24}Q_\psi$	$2\sqrt{15}Q_\eta$
16	$10\ (u, d, \bar{u}, e^+)_L$	−1	1	−2
	$5^*(\bar{d}, \nu, e^-)_L$	3	1	1
	$1\bar{N}_L$	−5	1	−5
10	$5\ (D, \bar{E}^0, E^+)_L$	2	−2	4
	$5^*(\bar{D}, E^0, E^-)_L$	−2	−2	1
1	$1S_L^0$	0	4	−5

where $g_1 = \sqrt{g^2 + g'^2}$ and λ_g is a number of order unity (Robinett, 1982; Robinett and Rosner, 1982a, 1982b). For Z_{LR}, $\lambda_g = 1$ by construction. For χ, ψ and η, λ_g depends on the pattern of the symmetry breaking, with λ_g typically in the range $\frac{2}{3}$ to 1 [$\lambda_g = 1$ if E(6) or SO(10) breaks in one step to $\mathrm{SU}(3)_C \times \mathrm{SU}(2)_L \times \mathrm{U}(1)_Y \times \mathrm{U}(1)'$].

In E(6) models in which high-dimensional Higgs representations are allowed, there is no real prediction for M^2 in (101) or for C. However, in the superstring-inspired models, the Higgs fields that break the electroweak symmetry are restricted to 27-plets (with the same quantum numbers as the fermions in Table V) or singlets. In particular, that implies that the neutral color-singlet Higgs fields are either $\mathrm{SU}(2)_L$ singlets or doublets; the latter have the same U(1)′ charges as the ν, E^0, or $\bar{E}^0$ in Table V. The expressions for $C = \hat{\Theta}/\hat{\rho}_2$ in terms of $x \equiv \langle \phi_\nu \rangle$, $\bar{v} \equiv \langle \phi_{\bar{E}^0} \rangle$, and $v = \langle \phi_{E^0} \rangle$ are listed for the χ, ψ, and η models in Table VI. It is usually assumed that $x = 0$, because $\langle \phi_\nu \rangle \neq 0$ would cause severe problems with charged current universality if ϕ_ν were the scalar partner of the ν_e, ν_μ, or ν_τ ($x \neq 0$ could occur for scalar 27-plets that are not the SUSY partners of the ordinary fermions). It is also usually assumed that $\bar{v}/v > 1$ for the η and ψ models, since the t and b masses are proportional to $\bar{v}$ and v, respectively.

The Z_{LR} must be treated separately. There are two popular choices. In the first [LR(1)], one introduces Higgs fields that transform as

$$\Phi = (2, \bar{2}, 0), \quad \delta_L = (2, 1, \tfrac{1}{2}), \quad \delta_R = (1, 2, \tfrac{1}{2}) \tag{122}$$

with respect to the $\mathrm{SU}(2)_L \times \mathrm{SU}(2)_R \times \mathrm{U}(1)_{B-L}$ group (Mohapatra, 1986; Langacker and Umasankar, 1989). These can be accommodated in a 27-plet of $E(6)$, with the neutral components identified as ($\Phi \leftrightarrow E^0, \bar{E}^0$), ($\delta_L \leftrightarrow \nu$), and ($\delta_R \leftrightarrow N$). Φ, δ_L, and δ_R develop VEVs after spontaneous symmetry breaking, leading to the expressions

TABLE VI. Expressions for $C \equiv \hat{\Theta}/\hat{\rho}_2$ in the χ, ψ, and η E(6) models as a function of $x = \langle \phi_\nu \rangle$, $\bar{v} = \langle \phi_{\bar{E}^0} \rangle$, and $v = \langle \phi_{E^0} \rangle$. The values or ranges for $x = 0$ and for ($x = 0, \bar{v}/v > 1$) are also shown. The $SU(2)_L \times SU(2)_R \times U(1)_{B-L}$ model LR(1) can be accommodated in a 27-plet of E(6). The range allows $x \neq 0$, as is relevant for nonsupersymmetric versions. LR(2) invokes Higgs triplets and cannot be acommodated in a 27-plet. $\langle \Delta_L^0 \rangle = 0$ is assumed.

Model	C	$C(x=0)$	$C(x=0, \bar{v}/v > 1)$
χ	$\frac{2}{\sqrt{10}} \frac{\lvert\bar{v}\rvert^2+\lvert v\rvert^2-3/2\lvert x\rvert^2}{\lvert\bar{v}\rvert^2+\lvert v\rvert^2+\lvert x\rvert^2}$	$\frac{2}{\sqrt{10}}$	$\frac{2}{\sqrt{10}}$
ψ	$-\sqrt{\frac{2}{3}} \frac{\lvert\bar{v}\rvert^2-\lvert v\rvert^2+\lvert x\rvert^2/2}{\lvert\bar{v}\rvert^2+\lvert v\rvert^2+\lvert x\rvert^2}$	$\sqrt{\frac{2}{3}}[-1,1]$	$\sqrt{\frac{2}{3}}[-1,0]$
η	$\frac{4}{\sqrt{15}} \frac{\lvert\bar{v}\rvert^2-\lvert v\rvert^2/4-\lvert x\rvert^2/4}{\lvert\bar{v}\rvert^2+\lvert v\rvert^2+\lvert x\rvert^2}$	$\frac{4}{\sqrt{15}}[-\frac{1}{4},1]$	$\frac{4}{\sqrt{15}}[\frac{3}{8},1]$
Model	C	**range**	
LR(1)	$\sqrt{\frac{3}{5}}\alpha \frac{\lvert\bar{v}\rvert^2+\lvert v\rvert^2-\lvert x\rvert^2/\alpha^2}{\lvert\bar{v}\rvert^2+\lvert v\rvert^2+\lvert x\rvert^2}$	$\sqrt{\frac{3}{5}}[-\frac{1}{\alpha},\alpha]_{\overrightarrow{SUSY}}\sqrt{\frac{3}{5}}\alpha$	
LR(2)	$\sqrt{\frac{3}{5}}\alpha$	$\sqrt{\frac{3}{5}}\alpha_{\overrightarrow{g_L=g_R}}\sqrt{\frac{3}{5}}\frac{\sqrt{\cos 2\theta_W}}{\sin\theta_W}$	

for C in Table VI. The LR model is usually considered without supersymmetry, i.e., δ_L is not the SUSY partner of the leptons. In that case there is no restriction on x, and C can vary from $-\sqrt{\frac{3}{5}}(1/\alpha)$ to $\sqrt{\frac{3}{5}}\alpha$. The supersymmetric version with $x=0$ has $C=\sqrt{\frac{3}{5}}\alpha$.

Another popular model [LR(2)] introduces Higgs fields:

$$\Phi=(2,\bar{2},0), \quad \Delta_L=(3,1,1), \quad \Delta_R=(1,3,1) . \tag{123}$$

Δ_L and Δ_R are not in the 27-plet of $E(6)$ (Mohapatra and Senjanovic, 1980, 1981). Δ_L and Δ_R are popular in non-string models, since they can generate Majorana masses for the neutrinos. We assume that the neutral field in Δ_L has a negligible VEV due to the stringent constraint from the ρ_0 parameter discussed below. Then $C=\sqrt{\frac{3}{5}}\alpha$. In the special case of left-right symmetry ($g_L=g_R$), this becomes $\sqrt{\frac{3}{5}}\sqrt{\cos 2\theta_W}/\sin\theta_W$, so that $\Theta/\rho_2 = g_2 C/g_1 = \sqrt{\cos 2\theta_W} \simeq 0.735$.

TABLE VII. The present limits at 95 percent C.L. on the masses of extra Z bosons from direct searches and indirect constraints from Z and W properties and weak neutral-current data. The indirect constraints are for three cases: (a) $\rho_0 = M_W^2/M_Z^2 \cos^2\theta_W = 1$ (at tree level), with $\lambda \equiv |\bar{v}/v|^2$ fixed, corresponding to Higgs fields in 27-plets of E(6) with $x=0$; (b) $\rho_0=1$, corresponding to Higgs doublets with arbitrary coupling to Z_2^0; and (c) $\rho_0 \neq 1$, corresponding to a completely arbitrary Higgs sector.

Sources	χ	ψ	η	LR
CDF prelim	259	166	189	305
$\lambda = 0$	559	540	180	801
$\lambda = 1$	559	149	451	801
$\lambda = 5$	559	509	650	801
$\lambda = \infty$	559	631	752	801
$\rho_0 = 1$	333	147	169	386
ρ_0 free	333	149	167	383

The present limits on M_2 from weak neutral current data are shown in Table VII; they are typically in the range several hundred GeV, although for some values of C they are much stronger (Durkin and Langacker, 1986; Amaldi *et al.*, 1987; Costa *et al.*, 1988; del Aguila, Moreno, and Quiros, 1990, 1991; Altarelli, Casalbuoni, Dominici, Feruglio, and Gatto, 1990a, 1990b; Altarelli, Casalbuoni, Feruglio, and Gatto, 1990a, 1990b; Cvetic and Langacker, 1990; Gonzales-Garcia and Valle, 1990a, 1990b, 1991; Langacker, 1991a; Layssac *et al.*, 1990; Langacker and Luo, 1991b; Mahanthappa and Mohapatra, 1991). Direct production limits from $\bar{p}p$ collisions are comparable or somewhat weaker. Future precision experiments should extend the sensitivity up to $O(1$ TeV), while at the SSC it should ultimately be possible to produce and detect extra Z's up to several TEV (Langacker, Robinett, and Rosner, 1984; del Aguila, Moreno, and Quiros, 1989, 1990), though at the upper end of the range there will be little ability to discriminate between the kinds of Z's.

B. The new physics of extra scalar bosons

1. Introduction

It is always possible to incorporate scalar bosons into gauge theories without spoiling the symmetry. However, we still have not seen any, so they are usually ignored in the SM with the exception of one SU(2) scalar doublet

employed to realize the Higgs mechanism. After spontaneous symmetry breaking, one scalar particle remains. SU(3) is not broken in QCD, so no colored scalar bosons are introduced.

But scalar bosons often cannot be avoided in theories beyond the SM. In grand unification theories, more scalar bosons must be introduced to break the symmetries via the Higgs mechanism (Langacker, 1981, 1988; Ross, 1985). In technicolor theories there are no elementary scalars, but scalars are generated as bound states (Holdom, 1985, 1987; Appelquist *et al.*, 1986, Haber, 1990). In supersymmetry, two Higgs doublets are required, and for each ordinary fermion there is a scalar partner (Eliasson, 1984; Lim *et al.*, 1984; Lynn, 1984; Nilles, 1984, 1990; Grifols and Sola, 1985; Haber and Kane, 1985; Barbieri *et al.*, 1990; Bilal *et al.*, 1990; Drees and Hagiwara, 1990).

Scalars may have either color or weak charges. If (color-singlet) scalars that carry nonstandard SU(2) charges [i.e., SU(2) triplets] also develop vacuum expectation values, then the pattern of the spontaneous symmetry breaking will be changed. In particular, the tree-level parameter

$$\rho_0=\frac{M_W^2}{M_Z^2\cos^2\theta_W} \tag{124}$$

will be different from unity so that the nonstandard Higgs fields manifest themselves at tree level. The value of ρ_0 is especially interesting because large classes of superstring theories predict $\rho_0=1$; i.e., they cannot accommodate nonstandard Higgs fields (Cvetic and Langacker, 1990).

Additional Higgs doublets do not change the SM prediction $\rho_0=1$. However, they affect the radiative corrections to the SM if there are large splittings between the masses of the physical Higgs scalars. These loop effects will be discussed in Sec. IV.E.

There are also many possible types of colored bosons. We shall consider one example, leptoquarks. They are color triplets that change quarks to leptons (or antileptons) and vice versa when they are emitted or absorbed (Pati and Salam, 1974; Shanker, 1982; Buchmuller and Wyler, 1986b; Hall and Randall, 1986; Buchmuller *et al.*, 1987; Herczeg, 1989; Langacker and Rückl, 1991). They have many experimental consequences, but we only consider effects on neutral-current phenomena.

2. Nonstandard Higgs fields

Gauge invariance (i.e., renormalizability) does not allow gauge bosons to have intrinsic masses. The observed short-range phenomena of the weak interactions are due to the weak charges of the vacuum. When weak gauge bosons propagate, they constantly interact with the vacuum, so effective masses are generated. The Higgs mechanism is one dynamical way to give the vacuum weak charges (Englert and Brout, 1964; Guralnik *et al.*, 1964; Higgs, 1964, 1966; Kibble, 1967).[18]

All of the weak gauge bosons belong to one SU(2) representation and they interact with the same vacuum; so the masses of W and Z should be related. The relation is characterized by the ρ_0 parameter, defined in Eq. (124).

If the symmetry breaking is realized via elementary Higgs bosons, the vacuum either acquires weak charges when the Higgs bosons condense, or receives vacuum expectation values (VEVs). The masses of Z and W will depend on both the weak charges of the Higgs bosons and their VEVs. Assuming that electromagnetic $U(1)$ gauge symmetry is unbroken (i.e., that only neutral Higgs fields acquire VEVs), one has

$$\rho_0=\frac{\sum_i (I_i^2-I_{i3}^2+I_i)|\langle\phi_i\rangle|^2}{\sum_i 2I_{i3}^2|\langle\phi_i\rangle|^2}\ , \tag{125}$$

where $\langle\phi_i\rangle$ is the VEV of a Higgs field ϕ_i with weak isospin and third-component I_i and I_{i3}, respectively. If there are only Higgs doublets in the theory (regardless of how many), as in the SM, then $\rho_0=1$. But if there are other multiplets of Higgs fields that have $I>\frac{1}{2}$, then in general $\rho_0\neq 1$.

The direct effect[19] of ρ_0 on observables is that
(a) the SM prediction for M_Z is modified by

$$M_Z\to\frac{1}{\sqrt{\rho_0}}M_Z^{\rm SM}\ ; \tag{126}$$

(b) the SM expressions for WNC amplitudes should be multiplied by ρ_0:

$$\epsilon_{L,R}(i)\to\rho_0\epsilon_{L,R}^{\rm SM}(i)\ , \tag{127}$$

$$g_{V,A}^{i}\to\rho_0 g_{V,A}^{i,{\rm SM}}\ , \tag{128}$$

$$C_{ij}\to\rho_0 C_{ij}^{\rm SM}\ ; \tag{129}$$

(c) the predictions for $\Gamma_{Z\to\bar{f}f}$ are multiplied by ρ_0:

$$\Gamma_{Z\to\bar{f}f}\to\rho_0\Gamma_{Z\to\bar{f}f}^{\rm SM}\ . \tag{130}$$

Of course, (b) and (c) are consequences of (a). The Z-pole couplings V_i, A_i are not affected.

If the true value of $\sin^2\theta_W$ were known, these would be the only changes in the SM predictions. Recall, however, that we have taken

---

[18]For standard and nonstandard Higgs fields, see Chanowitz (1988) and Gunion *et al.* (1990).

[19]In the $\overline{\rm MS}$ scheme the definition of $\sin^2\hat{\theta}_W(M_Z)$ is unaffected. In the on-shell scheme, one must in principle introduce a new definition for $\sin^2\theta_W$, such as $\sin^2\theta_W^M=(\pi\alpha/\sqrt{2}G_F)/M_W^2(1-\Delta r_M)$. In practice these ambiguities and any other effects of the $\rho_0\neq 1$ physics on the radiative corrections are of $O(\alpha(\rho_0-1))$, and are therefore negligible compared to the tree-level ($O(\rho_0-1)$) effects for which we are searching. We also ignore any tree-level exchanges mediated by new Higgs fields, since their couplings to ordinary fermions are tiny.

$$\sin^2\theta_W^Z=\frac{1}{2}\left[1-\left[1-\frac{4\pi\alpha/\sqrt{2}G_F}{M_Z^2(1-\Delta r_M)}\right]^{1/2}\right], \quad (131)$$

using the on-shell scheme, or $1-\Delta r_M\to\hat{\rho}(1-\Delta\hat{r}_W)$ in the $\overline{\rm MS}$ scheme. Since the Z mass is measured very precisely, so is $\sin^2\theta_W^Z$. For $\rho_0\neq 1$, $\sin^2\theta_W^Z$ differs from the true $\sin^2\theta_W$ by

$$\sin^2\theta_W^Z=\sin^2\theta_W+(\rho_0-1)\frac{\sin^2\theta_W\cos^2\theta_W}{\cos^2\theta_W-\sin^2\theta_W}. \quad (132)$$

Our predictions of physical quantities O_a will be shifted by an amount

$$\Delta O_a=\frac{\partial O_a}{\partial\sin^2\theta_W}(\sin^2\theta_W-\sin^2\theta_W^Z)+\Delta O_a^\rho, \quad (133)$$

where $\Delta O_a^\rho=0$ if O_a has no explicit dependence on ρ_0; $\Delta O_a^\rho=(\rho_0-1)O_a^{\rm SM}$ if O_a has a linear dependence on ρ_0, etc. The numerical results of the shifts are shown below in Table XIX.

The present uncertainty in ρ_0 (for fixed m_t, M_H) is around ± 0.005. That can be improved by a factor of $\simeq 3$ by future experiments. As will be discussed below, different values of m_t and new scalar or fermion multiplets with large mass splittings affect the observables via radiative corrections in a way that is very similar to the tree-level effects of ρ_0-1. That means that the ρ_0 constraints apply as well to a number of types of new physics. On the other hand, the possibility of cancellations between ρ_0-1 and these other effects, while somewhat unlikely, cannot be eliminated.

3. The SU(5) leptoquarks

a. Generalities

It is possible to write SU(3)×SU(2)×U(1) invariant couplings of leptoquarks to the ordinary quarks and leptons for a wide variety of leptoquarks, which differ in spin (0 or 1), fermion numbers (i.e., whether they couple quarks to leptons or antileptons), weak isospin, and charge. Here we shall consider a specific model as an illustrative example: those which are predicted in the SU(5) unification theory (Pati and Salam, 1974; Shanker, 1982; Buchmuller and Wyler, 1986b; Hall and Randall, 1986; Buchmuller *et al.*, 1987; Herczeg, 1989; Langacker and Rückl, 1991).

In SU(5), fermions are assigned to the **5*** and **10** representations, so scalars coupled to fermion pairs should be in the representation **5**, **5***, **10**, **15**, **45**, **45***, or **50** (Buchmuller and Wyler, 1986b). An interesting type of LQ comes from the superstring-inspired $E(6)$ model, in which both fermions and scalars are assigned to 27-plets. The scalars with the quantum numbers of the D_L and $\bar{D}_L$ in Table V can have leptoquark couplings. These transform as **5**, **5*** under SU(5) subgroup and are the SU(5) partners of the Higgs doublets [analogs of $(E^0,\bar{E}^0)$ which break SU(2)×U(1)]. Leptoquarks may in general carry SU(2) charges; but in our present example they do not.

In the standard SU(5) model, leptoquarks must be nearly as heavy as the GUT scale to suppress the proton decay rate. That is because SU(5) symmetry implies both leptoquark and diquark couplings. But we can also have relatively light leptoquarks, by suppressing the couplings between the LQ and quark pairs to stabilize the proton. By doing so, the SU(5) symmetry is violated. This is suggested by some superstring-inspired models (Buchmuller and Wyler, 1986b; Ross, 1988).

By lowering the mass of the leptoquarks, they will be phenomenologically relevant. They will change the predictions of some old phenomena and produce new ones. Phenomena related to the charged current and flavor-changing processes have been discussed[20] in Buchmuller and Wyler (1986b). In the following, we shall deal with weak neutral-current-related phenomena.

Since LQ's carry color, they will not affect pure leptonic precesses; thus $\nu e\to\nu e$ will not be affected. LQ's will not mix with the weak intermediate bosons, which are colorless, so the masses of W and Z bosons will not be changed.

On the other hand, LQ's may affect e^+e^- collisions. The cross sections and asymmetries of quark-pair final states at low (PEP-PETRA-TRISTAN) energies will be changed. But they will not affect the e^+e^- physics at the Z pole significantly—like the contributions from the EM channel and extra Z bosons, they do not interfere with the ordinary Z amplitude and are therefore small. (First-order effects will be present at energies slightly away from the Z pole.)

So for the physical quantities considered in this paper, only the neutrino-quark interaction coefficients and the atomic parity-violation coefficients will be changed.

b. Formalism

If the LQ's are heavier than the weak scale, then their full dynamics will not be important. Only two things will be relevant to our discussion: the Yukawa couplings between the fermions and the LQ's, and the LQ mass matrix. They will determine the effective coupling at the present energy level and are left as free parameters to be determined by experiments.

In the E_6 model each 27-plet of scalars has an isoscalar color triplet $S^{\alpha l}$ and its antiparticle $S^l_{c\alpha}$, where α is the color index and l labels the 27-plet.[21] The Yukawa couplings are (suppressing the color index α)

---

[20]Several equations in that paper were corrected in Langacker and Rückl (1991).

[21]We shall follow the conventions of Langacker and Rückel (1991). The $S^{\alpha l}$ and $S^l_{c\alpha}$ have the quantum number of the D_L and $\bar{D}_L$ in Table V.

$$-L=[\eta^l_{Lmn}\bar{q}^{\,c}_{mR}i\tau_2 l_{nL}+\eta^l_{Rmn}\bar{u}^{\,c}_{mL}e_{nR}]S_l+\text{h.c.}$$
$$=[\eta^l_{Lmn}(\bar{u}^{\,c}_{mR}e_{nL}-\bar{d}'^{\,c}_{mR}\nu_{nL})+\eta^l_{Rmn}\bar{u}^{\,c}_{mL}e_{nR}]S_l$$
$$+\text{h.c.} \tag{134}$$

where

$$\tau_2 q^c_R=\tau_2\begin{bmatrix}u^c_R\\ d^c_R\end{bmatrix}$$

are the right-handed antiquark doublets,

$$l_L=\begin{bmatrix}\nu_L\\ e_L\end{bmatrix}$$

are the left-handed lepton doublets, u^c_L are the left-handed anti-up quarks,[22] and e_R are the right-handed leptons; m and n are family indices, and η^l_{Lmn} and η^l_{Rmn} are coupling constants to be predicted by specific models. d'_{mL} are SU(2) eigenstates that are related to the mass eigenstates by the Kobayashi-Maskawa-Cabibbo matrix A_{KMC}:

$$d'_{mL}=A^{mk}_{KMC}d_{kL}\ . \tag{135}$$

For simplicity, let us consider the case of one leptoquark with one family of quarks and one family of leptons; then the above Lagrangian is much simplified:

$$-L=[\eta_L\bar{q}^{\,c}_R i\tau_2 l_L+\eta_R\bar{u}^{\,c}_L e_R]S+\text{H.c.}$$
$$=[\eta_L(\bar{u}^{\,c}_R e_L-\bar{d}^{\,c}_R\nu_L)+\eta_R\bar{u}^{\,c}_L e_R]S+\text{H.c.} \tag{136}$$

There are only two coupling constants, η_L and η_R.

In Born approximation, the effective four-fermion interaction at low energy is

$$-L^{\text{LQ}}_{\text{eff}}=-L_{\text{LL}}-L_{\text{RR}}-L_{\text{RL}} \tag{137}$$

where

$$-L_{LL}=\frac{|\eta_L|^2}{2M_S^2}(-\bar{u}_L\gamma^\mu u_L\bar{e}_L\gamma_\mu e_L-\bar{d}_L\gamma^\mu d_L\bar{\nu}_L\gamma_\mu\nu_L$$
$$+\bar{u}_L\gamma^\mu d_L\bar{e}_L\gamma_\mu\nu_L+\bar{d}_L\gamma^\mu u_L\bar{\nu}_L\gamma_\mu e_L), \tag{138}$$

$$-L_{RR}=\frac{|\eta_R|^2}{2M_S^2}[-\bar{u}_R\gamma^\mu u_R\bar{e}_R\gamma_\mu e_R]\ , \tag{139}$$

$$-L_{RL}=\frac{\eta_L\eta_R^*}{2M_S^2}(\bar{u}_R u_L\bar{e}_R e_L+\bar{u}_R\sigma^{\mu\nu}u_L\bar{e}_R\sigma_{\mu\nu}e_L$$
$$-\bar{u}_R d_L\bar{e}_R\nu_L-\bar{u}_R\sigma^{\mu\nu}d_L\bar{e}_R\sigma_{\mu\nu}\nu_L)$$
$$+\text{H.c.}\ ; \tag{140}$$

M_S is the leptoquark mass, and $\sigma_{\mu\nu}=[\gamma_\mu,\gamma_\nu]/4$.

We see that the SU(5) LQ's induce both neutral and charged currents. There can also be flavor-changing neutral currents (FCNC). In our simple model with one leptoquark, and assuming the absence of FCNC, only one coefficient of ν-q coupling is directly affected; it is that of the left-handed d quark:

$$\delta\epsilon_L(d)=-\frac{\sqrt{2}|\eta_L|^2}{8M_S^2G_F}\ . \tag{141}$$

However, the most precise measurements of the ν-q couplings are presently from the neutral current to charged current ratios R_ν and $R_{\bar{\nu}}$. The experimental values of the $\epsilon_{L,R}(u)$ and $\epsilon_{L,R}(d)$ are extracted from the data assuming the SM value for the charged current cross sections. From Eq. (138), it is obvious that the WCC cross sections are affected by $-L_{LL}$ as well, i.e., $\sigma_{\text{WCC}}\to(1+K_L)^2\sigma^{\text{SM}}_{\text{WCC}}$, where $K_L=\sqrt{2}|\eta_L|^2/8M_S^2G_F$. Hence the shift in the apparent (measured) values of the ϵ's is

$$\delta\epsilon_L(d)=-[\epsilon_L(d)+1]K_L\ , \tag{142}$$

$$\delta_\epsilon=-K_L\epsilon\ , \tag{143}$$

where the second expression applies to $\epsilon_L(u)$, $\epsilon_R(u)$, and $\epsilon_R(d)$. Of course, the ϵ's are determined by ν_μ and $\bar{\nu}_\mu$ scattering. Hence the constraints in Eqs. (142) and (143) apply to the couplings involving the (u,d) and the (ν_μ,μ^-).

For the atomic parity-violation coefficients, only the parts related to the u-type quarks are changed:[23]

$$\delta C_{1u}=\delta C_{2u}=-\frac{\sqrt{2}}{8M_s^2G_F}[|\eta_L|^2-|\eta_R|^2]\ . \tag{144}$$

Since C_{1u} and C_{2u} will be measured by atomic parity violation and muonic atoms, respectively, δC_{1u} (δC_{2u}) refers to leptoquarks coupling to the first (second) family of leptons. Other implications of leptoquarks, involving FCNC, $\pi_{e2}/\pi_{\mu2}$, charged current universality, direct production, etc., are discussed in Buchmuller and Wyler, (1986b); Buchmuller *et al.* (1987); Herczeg (1989); and Langacker and Rückl (1991).

In particular, the absence of the FCNC places stringent constraints [i.e., $M_S>O(10-100$ TeV], but only if flavor-changing currents are present. Similarly, the ratio $\pi_{e2}/\pi_{\mu2}$ implies $M_S>O(10)$ TeV if η_L and η_R are *both* significant ($|\eta_L\eta_R|\geq 4\pi\alpha$). HERA will be able to observe leptoquarks up to $\sim$300 GeV directly, even for very small couplings. The WNC observables will be sensitive into the TeV region, independent of the existence of flavor-changing coupling or whether $|\eta_L\eta_R|=0$.

[22]The charge-conjugate fields are defined as $\psi^c_{L(R)}=C\bar{\psi}^T_{R(L)}$, where C is the charge-conjugate matrix, defined by $C\gamma_\mu C^{-1}=-\gamma_\mu^T$.

[23]Terms in L_{RL} do not contribute to atomic parity violation in the nonrelativistic limit.

C. The new physics of extra fermions

1. Introduction

In the SM there are three families of fermions. Each family consists of one neutrino, one charged lepton, and two quarks. Their strong, weak, and electric charges are assigned to accommodate observations.

From the theoretical point of view, however, the selection of fermions in the SM is rather arbitrary; gauge invariance places no restrictions on the number or kind of fermion representations except for the cancellations of anomalies. Actually, most extensions of the SM predict the existence of extra fermions (Langacker and London, 1988a, 1988b; del Aguila, Garrido, and Miquel, 1990; Maalampi and Roos, 1990; Nardi and Roulet, 1990). For instance, in the E(6) model, fermions in one family are assigned to a 27-plet, which includes the 15 ordinary fermions and 12 extra ones, as shown in Table V. In this article we shall not consider the actual production of new heavy fermions. Rather, we shall focus on their mixing with the known light particles. This can affect weak universality, lead to induced right-handed currents, and affect the relations between the Fermi constant and $M_{W,Z}$.

For the convenience of discussion, we shall define fermions to have *canonical* SU(2)×U(1) assignments if the left-handed components are SU(2) doublets and their right-handed components are SU(2) singlets; these fermions are called *ordinary* fermions; otherwise, fermions are said to have *noncanonical* assignments and are called *exotic* fermions. The canonical fermions should obey the Gell-Mann-Nishijima relation if exotic electric charges are excluded.

For most extensions of the SM, the extra fermions can be divided into several types:

(a) *Sequential fermions* have canonical SU(2)×U(1) assignments. They differ from the fermions in the SM only by their masses. Usually these fermions are introduced in a whole family. These have no effects on the WNC and the Z-pole observables at the tree level, but do affect the loop corrections (see Sec. IV.E).

(b) *Mirror fermions* have opposite charge assignments from the canonical fermions: the left-handed components are SU(2) singlets; the right-handed components are SU(2) doublets. Usually they are also introduced in a whole family.

(c) *Vector-doublet fermions* have both their left- and right-handed components as SU(2) doublets.

(d) *Vector-singlet fermions* have both their left- and right-handed components as SU(2) singlets.

(e) *SU(2)-singlet Weyl neutrinos.*

(f) Fermions in higher-dimensional SU(2) representations.

(g) Fermions with exotic electric charges and colors.

For the 12 extra fermions in the E(6) model, we have one vector-singlet D quark, D_L, D_R; one vector-doublet lepton:

$$\begin{pmatrix} E^0 \\ E^- \end{pmatrix}_L, \quad \begin{pmatrix} E^0 \\ E^- \end{pmatrix}_R ;$$

and two Weyl neutrinos $\bar{N}_L$, S_L^0.

We shall consider the mixing between ordinary fermions and the exotic right-handed SU(2) doublets and left-handed SU(2) singlets, which modifies the neutral-current couplings of the light particles. Assuming the absence of significant flavor-changing neutral currents, the remaining effects can be parametrized in a way that is almost model independent. We shall follow the formalism scheme developed in Langacker and London (1988a, 1988b).

2. Results and discussion

Arbitrary mixing between ordinary and exotic fermions will in general induce flavor-changing neutral currents between the light fermions at a rate that is much larger than is allowed by observation (Langacker and London, 1988a, 1988b; Maalampi and Roos, 1990). To avoid this, one must assume that that each mass-eigenstate light fermion ψ_L^i or ψ_R^i mixes with a unique heavy partner. Let us assume that that is the case. Define $c_L^i = \cos\theta_L^i$ and $s_R^i = \sin\theta_R^i$, where $\theta_{L(R)}^i$ are the left (right) mixing angles of ψ_L^i or ψ_R^i with its heavy partner. $\theta_{L(R)}^i$ are in principle independent variables, but in most models one expects $\theta^2 = O((m/M)^\sigma)$, where m and M are, respectively, the masses of the ordinary and heavy fermions, and σ is typically 1–2, depending on the model. The largest mixings are therefore expected for the c, b, and τ, for which $\theta^2 \sim 0.01$ is quite plausible.

Let us introduce the neutral-current couplings:

$$\hat{\epsilon}_L(i) = I_{i3}(c_L^i)^2 - \sin^2\theta_W q_i \ , \tag{145}$$

$$\hat{\epsilon}_R(i) = I_{i3}(s_R^i)^2 - \sin^2\theta_W q_i \ , \tag{146}$$

$$\hat{g}_{V,A}(i) = \hat{\epsilon}_L(i) \pm \hat{\epsilon}_R(i) \ , \tag{147}$$

where $(I_{i3}, q_i) = (\frac{1}{2}, \frac{2}{3})$, $(-\frac{1}{2}, -\frac{1}{3})$, $(\frac{1}{2}, 0)$, and $(-\frac{1}{2}, -1)$ for u quarks, d quarks, neutrinos, and charged leptons, respectively. The direct effects of fermion mixings are contained in the $\hat{\epsilon}_{L,R}$ factors. However, the mixing also affects the charged current processes used to normalize the WNC rates and to determine G_F. In particular, the apparent Fermi constant $G_F = 1.16637 \times 10^{-5}$ GeV^{-2}, determined from muon decay assuming the validity of the SM, differs from the true Fermi constant $\hat{G}_F$ due to the reduction in the strength by factors c_L^i in the effective four-fermi interaction of muon decay:

$$G_F = \hat{G}_F c_L^e c_L^{\nu_e} c_L^\mu c_L^{\nu_\mu} \ . \tag{148}$$

Let us define

$$F(s^2) = \left[\frac{\hat{G}_F}{G_F} \right]^{1/2} . \tag{149}$$

Then, for small mixing,

$$F(s^2)=1+\tfrac{1}{4}[(s_L^e)^2+(s_L^{\nu_e})^2+(s_L^{\mu})^2+(s_L^{\nu_\mu})^2] . \quad (150)$$

We shall consider the following changes in observables induced by ordinary-exotic mixing.[24]

(a) The masses of the W and the Z bosons:

$$M_W=\frac{(\pi\alpha/\sqrt{2}\hat{G}_F)^{1/2}}{\sin\theta_W(1-\Delta r)^{1/2}} =\frac{(\pi\alpha/\sqrt{2}G_F)^{1/2}}{\sin\theta_W(1-\Delta r)^{1/2}}[2-F(s^2)] , \quad (151)$$

$$M_Z=\frac{M_W}{\sqrt{\rho}\cos\theta_W} , \quad (152)$$

where the $2-F$ is due to the shift in the apparent Fermi constant. The M_W/M_Z ratio is not affected at tree level by the extra fermions; however, the $\sin^2\theta_W^Z$ determined from M_Z differs from the true value of $\sin^2\theta_W$:

$$\sin^2\theta_W^Z=\sin^2\theta_W+\Delta\sin^2\theta_W^Z \quad (153)$$

where

$$\Delta\sin^2\theta_W^Z=2\frac{\sin^2\theta_W\cos^2\theta_W}{\cos^2\theta_W-\sin^2\theta_W}[F(s^2)-1] . \quad (154)$$

(b) Low-energy ν_μ-q couplings:

$$\epsilon_{L,R}(i)=F_1(s^2,\kappa)\hat{\epsilon}_{L,R}(i);\quad i=u,d , \quad (155)$$

where $F_1(s^2,\kappa)$ depends on the mixing of neutrinos and how $\epsilon_{L,R}$ are extracted from the data. If $\epsilon_{L,R}$ are extracted from the ratios

$$R_\nu=\frac{\sigma_{\nu N\to\nu X}}{\sigma_{\nu N\to\mu^- X}},\quad R_{\bar\nu}=\frac{\sigma_{\bar\nu N\to\bar\nu X}}{\sigma_{\bar\nu N\to\mu^+ X}} , \quad (156)$$

measured for (approximately) isoscalar targets and for proton targets, then (Langacker and London, 1988a)

$$F_1(s^2,\kappa)=\frac{1-\frac{\Lambda_\mu}{2}(s_L^{\nu_\mu})^2}{1-(s_L^\mu)^2-(s_L^{\nu_\mu})^2-\mathrm{Re}(\kappa_{ud})} , \quad (157)$$

where Λ_μ varies between 0 and 4 depending on the types of extra neutrinos, and κ is the contribution due to the induced right-handed charged current. We shall display the formulas for arbitrary Λ_μ and the analogous Λ_e, but will use $\Lambda_{\mu,e}=2$ in the numerical results, corresponding to mixing with an SU(2)-singlet neutrino.

(c) Low-energy ν_μ-e couplings:

$$g_{V,A}^e=F_2(s^2)\hat{g}_{V,A}^e , \quad (158)$$

where

$$F_2(s^2)=\frac{1-\frac{\Lambda_\mu}{2}(s_L^{\nu_\mu})^2}{1-(s_L^\mu)^2-(s_L^{\nu_\mu})^2} . \quad (159)$$

For high-energy ν_μ-e couplings,

$$g_{V,A}^e=F_1(s^2,\kappa)\hat{g}_{V,A}^e . \quad (160)$$

The difference between the low- and high-energy couplings is due to the normalization method used in experiments.

Similarly, the $\nu_e e$ coupling is (including both the neutral and charged channel)

$$g_{V,A}^{\prime e}=F_e\left[\hat{g}_{V,A}^e+\frac{(c_L^e)^2(c_L^{\nu_e})^2}{1-\frac{\Lambda_e}{2}(s_L^{\nu_e})^2}\right] , \quad (161)$$

where

$$F_e=\frac{1-\frac{\Lambda_e}{2}(s_L^{\nu_e})^2}{N} , \quad (162)$$

where N depends on the normalization method.

In the ratio $R_{\nu/\bar\nu}=\sigma_{\nu_\mu e}/\sigma_{\bar\nu_\mu e}$, the F factors cancel,

$$R_{\nu/\bar\nu}=\frac{\hat{\epsilon}_L^2(e)+\hat{\epsilon}_R^2(e)/3}{\hat{\epsilon}_L^2(e)/3+\hat{\epsilon}_R^2(e)} . \quad (163)$$

In the ratio $R_{\nu/\nu\bar\nu}=\sigma_{\nu_\mu e}/(\sigma_{\nu_e e}+\sigma_{\bar\nu_\mu e})$ there are some residues of F factors,

$$R_{\nu/\nu\bar\nu}=\frac{[\hat{\epsilon}_L^2(e)+\hat{\epsilon}_R^2(e)/3]}{\frac{\hat{\epsilon}_L^2(e)}{3}+\hat{\epsilon}_R^2(e)+F_{e/\mu}\left\{\left[\hat{\epsilon}_L(e)+(c_L^e)^2(c_L^{\nu_e})^2\left[1+\frac{\Lambda_e}{2}(s_L^{\nu_e})^2\right]\right]^2+\frac{\hat{\epsilon}_R^2(e)}{3}\right\}} , \quad (164)$$

where

$$F_{e/\mu}=\frac{1-\Lambda_e(s_L^{\nu_e})^2}{1-\Lambda_\mu(s_L^{\nu_\mu})^2} . \quad (165)$$

(d) Atomic parity-violation coefficients:

$$C_{1i}=[F(s^2)]^2 2\hat{g}_A^e\hat{g}_V^i \quad (166)$$

$$C_{2i}=[F(s^2)]^2 2\hat{g}_V^e\hat{g}_A^i , \quad (167)$$

where $i=u,d$.

(e) The asymmetries on the Z pole are given by the SM expressions with couplings replaced by the couplings $\hat{\epsilon}$ or $\hat{g}$. The left-right asymmetry with longitudinally polarized initial electrons is

[24]Further observable consequences in the purely charged current sector are discussed in Langacker and London (1988a, 1988b) and Maalampi and Roos (1990).

$$A_{\rm LR}=\frac{2\hat{g}_A(e)\hat{g}_V(e)}{\hat{g}^2_A(e)+\hat{g}^2_V(e)}=\frac{\hat{\epsilon}^2_L(e)-\hat{\epsilon}^2_R(e)}{\hat{\epsilon}^2_L(e)+\hat{\epsilon}^2_R(e)}\ , \tag{168}$$

which differs from the SM prediction $A_{\rm LR}^{\rm SM}$ by

$$\Delta A_{\rm LR}=A_{\rm LR}-A_{\rm LR}^{\rm SM}$$
$$=\frac{2\epsilon_L(e)\epsilon_R(e)}{[\epsilon^2_L(e)+\epsilon^2_R(e)]^2}[\epsilon_R(e)(s^e_L)^2+\epsilon_L(e)(s^e_R)^2]\ . \tag{169}$$

The forward-backward asymmetries of final-state fermions with polarization of the initial electrons are

$$A_{\rm FB}^{\rm pol}(f)=\frac{3}{4}\frac{2\hat{g}_A(f)\hat{g}_V(f)}{\hat{g}^2_A(f)+\hat{g}^2_V(f)}$$
$$=\frac{3}{4}\frac{\hat{\epsilon}^2_L(f)-\hat{\epsilon}^2_R(f)}{\hat{\epsilon}^2_L(f)+\hat{\epsilon}^2_R(f)}\ , \tag{170}$$

which differs from the SM prediction $A_{\rm FB}^{\rm pol,SM}$ by

$$\Delta A_{\rm FB}^{\rm pol}(f)=A_{\rm FB}^{\rm pol}(f)-A_{\rm FB}^{\rm pol,SM}(f)$$
$$=-I_{f3}\frac{3\epsilon_L(f)\epsilon_R(f)}{[\epsilon^2_L(f)+\epsilon^2_R(f)]^2}$$
$$\times[\epsilon_R(f)(s^f_L)^2+\epsilon_L(f)(s^f_R)^2] \tag{171}$$

where I_{f3} is defined following Eq. (147).

The forward-backward asymmetries of final-state fermions are

$$A_{\rm FB}(f)=\frac{3}{4}\frac{2\hat{g}_A(e)\hat{g}_V(e)}{\hat{g}^2_A(e)+\hat{g}^2_V(e)}\frac{2\hat{g}_A(f)\hat{g}_V(f)}{\hat{g}^2_A(f)+\hat{g}^2_V(f)}$$
$$=A_{\rm LR}A_{\rm FB}^{\rm pol}(f)\ , \tag{172}$$

which differs from the SM prediction $A_{\rm FB}^{\rm SM}$ by

$$\Delta A_{\rm FB}(f)=A_{\rm LR}\Delta A_{\rm FB}^{\rm pol}(f)+A_{\rm FB}^{\rm pol}(f)\Delta A_{\rm LR}\ . \tag{173}$$

The final-state polarization asymmetries of the fermions are

$$A_{\rm pol}(f)=\tfrac{4}{3}A_{\rm FB}^{\rm pol}(f)\ . \tag{174}$$

In the special case of the τ lepton,

$$\Delta A_{\rm pol}(\tau)=A_{\rm pol}(\tau)-A_{\rm pol}^{\rm SM}(\tau)$$
$$=\frac{2\epsilon_L(e)\epsilon_R(e)}{[\epsilon^2_L(e)+\epsilon^2_R(e)]^2}[\epsilon_R(e)(s^\tau_L)^2+\epsilon_L(e)(s^\tau_R)^2]\ , \tag{175}$$

which differs from $\Delta A_{\rm LR}$, since one does not expect the mixing to be the same for different families.

(f) The partial Z widths are

$$\Gamma_{Z\to f\bar{f}}=C_f[F(s^2)]^2\frac{G_F}{6\pi\sqrt{2}}M_Z^3[\hat{g}^{f2}_V+\hat{g}^{f2}_A]\ , \tag{176}$$

where $C_f=1$ for leptons and $C_f=3$ for quarks, and $f=u$, c, d, s, b, e, μ, τ, ν_e, ν_μ, and ν_τ. Again, there is no reason to expect family universality in the mixing angles. The total Z width is

$$\Gamma_Z=\sum_f\Gamma_{Z\to f\bar{f}}\ . \tag{177}$$

D. Compositeness

No hint has been seen of lepton or quark form factors or other signs of compositeness. Nevertheless, it is possible that the leptons and quarks have a substructure if the compositeness scale Λ is very large [$\Lambda>O(1\ {\rm TeV})$]. One consequence should be the generation by constituent interchange diagrams in Fig. 31 of four-fermi or other effective operators at energies small compared to Λ. These must be SU(3)×SU(2)×U(1) invariant, since new physics at the scale $\Lambda\gg M_Z$ must preserve the low-energy symmetries.

One can write a great many invariant operators,[3] including those which generate FCNC; S, P, and T operators; and those which contribute to both charged and neutral-current phenomena. Even restricting to V, A operators that affect WNC processes only, there are many possibilities, such as $\bar{l}_{\mu L}\gamma^\mu l_{\mu L}\bar{q}_L\gamma_\mu q_L$, $\bar{l}_{eL}\gamma^\mu l_{eL}\bar{q}_L\gamma_\mu q_L$, and $\bar{l}_{\mu L}\gamma^\mu l_{\mu L}\bar{l}_{eL}\gamma_\mu l_{eL}$, where $l_{\mu L}=(\nu_{\mu L}\ \mu^-_L)^T$, $l_{eL}=(\nu_{eL}\ e^-_L)^T$, and $q_{eL}=(u_L\ d_L)^T$. Other operators can be generated by the replacements $q_L\to(u_R$ or $d_R)$, $l_{\mu L}\to\mu_R$, or $l_{eL}\to e_R$.

As typical examples of those operators that can best be measured, we shall consider

$$-L_1=\pm\frac{4\pi}{\Lambda_1^2}\bar{l}_{\mu L}\gamma^\mu l_{\mu L}\bar{q}_L\gamma_\mu q_L\ , \tag{178}$$

$$-L_2=\pm\frac{4\pi}{\Lambda_2^2}\bar{\nu}_{\mu L}\gamma^\mu\nu_{\mu L}\bar{e}_L\gamma_\mu e_L\ , \tag{179}$$

$$-L_3=\pm\frac{4\pi}{\Lambda_3^2}\bar{e}_L\gamma^\mu e_L\bar{q}_L\gamma_\mu q_L\ , \tag{180}$$

where in $L_{2,3}$ we have only displayed the parts of the operators that can be well measured in the experiments considered here. The coefficients define the scale Λ_i. This can be qualitatively interpreted as the mass of the exchanged constituents, since no coupling constants are required for the diagrams in Fig. 31 (i.e., the effective coupling is $g^2_{\rm eff}/4\pi=1$).

Such four-fermi operators do not affect M_W or M_Z and their contributions to Z-pole observables are second or-

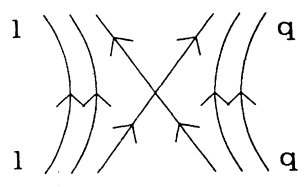

FIG. 31. Constituent interchange diagrams, leading to an effective four-fermi eq interaction.

der. For the operators considered here, the changes are

$$\delta\epsilon_L(u)=\delta\epsilon_L(d)=\delta C_{2u}=\delta C_{2d}=\pm\frac{\sqrt{2}}{G_F}\frac{\pi}{\Lambda_1^2}\ , \quad (181)$$

$$\delta g_V^e=\delta g_A^e=\pm\frac{\sqrt{2}}{G_F}\frac{\pi}{\Lambda_2^2}\ , \quad (182)$$

$$\delta C_{1u}=\delta C_{1d}=\pm\frac{\sqrt{2}}{G_F}\frac{\pi}{\Lambda_3^2} \quad (183)$$

(we have assumed that $C_{2u,d}$ will be measured in muonic atoms). $\delta g_{V,A}^e$ are only relevant to $\nu_\mu(\bar{\nu}_\mu)e$ scattering, not to $\nu_e(\bar{\nu}_e)e$.

From Table XXX below we see that precision experiments may have sensitivity to Λ in the 20 TeV range, while limits from colliders should be in the (1–10) TeV range [Eichten *et al.*, 1984; SLC (see Blochus *et al.*, 1986 and Swartz, 1987); LEP (see Ellis and Peccei, 1986 and Alexander *et al.*, 1988); Martyn, 1987]. Such operators yield small first-order effects in e^+e^- asymmetries slightly off the Z pole, as will be discussed in Sec. V.

E. New physics through radiative corrections

1. Overview

So far we have concentrated on those types of new physics that would manifest themselves via tree-level effects. In this section we shall discuss those that affect only the neutral current and W and Z observables through radiative corrections. As usual, these types of new physics are related to a high mass scale, since they are not observed at the present energy level. According to the decoupling theorem (Appelquist and Carazzone, 1975), most types of heavy physics affect low-energy observables only through inverse powers of the heavy scale and therefore have little effect, except possibly for mediating rare processes. However, the decoupling theorem does not hold if the heavy physics breaks the symmetries of the low-energy theory (Kennedy, 1991). One famous example is the large mass splitting between the b and t quarks, which breaks weak isospin. In that case, the heavy top quark does not decouple; its effects on low-energy predictions actually increase quadratically as $O(G_F m_t^2)$.

Studies of such effects began with the pioneering work of Veltman, who introduced the famous ρ parameter (Veltman, 1977; Chanowitz *et al.*, 1978);. This describes the effects of large splittings between the masses of members of the same SU(2) multiplets, such as m_t-m_b or mass differences involving new multiplets of heavy fermions or bosons. Such splittings break the vector part of the SU(2) symmetry and affect the M_W/M_Z ratio. Recently, several groups have considered the effects of heavy degenerate multiplets of fermions, such as those occurring in technicolor theories (Bertolini and Sirlin, 1984; van der Bij and Hoogeveen, 1987; Peskin and Takeuchi, 1990; Golden and Randall, 1991). These break the SU(2) axial symmetry and lead to a shift in both M_Z and M_W relative to the SM predictions.

Several authors have shown that the effects (for neutral current and W, Z observables) of all types of heavy physics that enter only through self-energy diagrams can be parametrized in terms of three parameters, $h_V=T$, h_{AW}, and h_{AZ}, where h_V (h_A) refers to the breaking of the vector (axial) part (Lynn *et al.*, 1986; Holdom and Terning, 1990; Kennedy and Langacker, 1990, 1991; Marciano and Rosner, 1990; Peskin and Takeuchi, 1990; Altarelli and Barbieri, 1991; Golden and Randall, 1991) of SU(2). In most cases, the axial parameters are approximately equal, $h_{AW}\sim h_{AZ}=S$. The existing the future constraints have been described in Kennedy and Langacker, (1990, 1991). In particular, it was shown (Marciano and Rosner, 1990) that atomic parity violation sets rather stringent limits on S. In this section we shall review these general constraints and give several specific applications: the sensitivity to the t quark and Higgs masses within the SM, extra fermion multiplets, the theory with two Higgs doublets, and the minimal supersymmetric Standard Model (MSSM).

2. Formalism for heavy multiplets

Electroweak radiative corrections in weak neutral-current phenomena can be divided into three classes: vertex diagrams, box diagrams, and gauge boson self-energy diagrams.[2,25] All of these diagrams have been calculated and have been incorporated in our analysis. Their effects can be absorbed into (process-dependent) effective parameters ρ, κ, and λ, where ρ multiplies the tree-level expression for WNC amplitudes, κ multiplies $\sin^2\theta_W$, and λ is a (small) additive shift. That is, the tree-level amplitude $F^a(\sin^2\theta_W^0)$ for process a is replaced by $\rho^a F^a(\kappa^a\sin^2\theta_W)+\lambda^a$.

Similarly, radiative corrections due to heavy new physics can also be divided into vertex, box, and gauge boson self-energy diagrams. Contributions from vertex and box diagrams are usually tiny because of the weak couplings between the new physics and ordinary particles. Due to the decoupling theorem, the self-energies can also be ignored if there is no symmetry breaking. If there is symmetry breaking, the effects of the self-energies can be de-

[25]There are also QED corrections in which real or virtual photons are attached to charged particles in all possible ways. These depend on experimental cuts and acceptances and are generally subtracted from the data by the experimenters. QED vacuum polarization diagrams, however, should be included with the electroweak corrections.

scribed by three additional parameters defined as[26]

$$\Delta\rho(0)=\frac{A_{ZZ}^{\rm new}(0)}{M_Z^2}-\frac{A_{WW}^{\rm new}(0)}{M_W^2}\ , \tag{184}$$

$$\Delta_Z(M_Z^2)=\left[\frac{A_{ZZ}^{\rm new}(M_Z^2)-A_{ZZ}^{\rm new}(0)}{M_Z^2}\right]_{\overline{\rm MS}}\ , \tag{185}$$

$$\Delta_W(M_W^2)=\left[\frac{A_{WW}^{\rm new}(M_W^2)-A_{WW}^{\rm new}(0)}{M_W^2}\right]_{\overline{\rm MS}}\ , \tag{186}$$

where $A_{ZZ}^{\rm new}(q^2)$ and $A_{WW}^{\rm new}(q^2)$ are, respectively, the contributions from various types of new physics to the self-energies of the Z and W bosons at momentum transfer q^2; the subscript $\overline{\rm MS}$ refers to minimal subtraction, with the 't Hooft mass scale $\mu=M_Z$. $\Delta_\rho(0)$ breaks weak isospin, while $\Delta_{Z,W}$ are related to wave-function renormalization and preserve weak isospin (Lynn *et al.*, 1986; Holdom and Terning, 1990; Kennedy and Langacker, 1990, 1991; Marciano and Rosner, 1990; Peskin and Takeuchi, 1990; Altarelli and Barbieri, 1991; Golden and Randall, 1991). It is convenient to introduce dimensionless parameters $h_{V,A}$ (or T,S) by[27]

$$\alpha h_V=\alpha T=4\sqrt{2}G_F\Delta_\rho(0)\ , \tag{187}$$

$$h_{AZ}=S_Z=-16\pi\Delta_Z(M_Z^2)/M_Z^2\ , \tag{188}$$

$$h_{AW}=S_W=-16\pi\Delta_W(M_W^2)/M_W^2\ . \tag{189}$$

The self-energies are defined with coupling constants removed so that one expects h_V, h_{AZ}, and h_{AW} to be of order unity if there is new physics. We can then express the shifts of all the physical observables in terms of these parameters (Kennedy and Langacker, 1990). In particular,

$$M_Z^2\to M_{Z,\rm SM}^2\frac{1-\alpha h_V}{1-4\sqrt{2}G_F M_{Z,\rm SM}^2 h_{AZ}/16\pi}\ , \tag{190}$$

$$M_W^2\to M_{W,\rm SM}^2\frac{1}{1-4\sqrt{2}G_F M_{W,\rm SM}^2 h_{AW}/16\pi}\ , \tag{191}$$

$$\Gamma_Z\to\frac{1}{1-\alpha h_V}\Gamma_Z^{\rm SM}(M_Z)\ , \tag{192}$$

$$\Gamma_W\to\Gamma_W^{\rm SM}(M_W)\ , \tag{193}$$

$$\epsilon_{L,R}(i)\to\frac{1}{1-\alpha h_V}\epsilon_{L,R}^{\rm SM}(i)\ , \tag{194}$$

where $M_{Z,\rm SM}^2$, $M_{W,\rm SM}^2$, $\Gamma_Z^{\rm SM}$, $\Gamma_W^{\rm SM}$, and $\epsilon_{L,R}^{\rm SM}(i)$ are the SM expressions ($\Gamma_Z^{\rm SM}\propto G_F M_Z^3$ is to be expressed in terms of the *physical* M_Z rather than $M_{Z,\rm SM}$. Similarly, $\Gamma_W^{\rm SM}\propto G_F M_W^3$ is expressed in terms of the *physical* M_W).

We see that h_{AZ} and h_{AW} only affect the masses of Z and W, respectively. The role of h_{AW} is limited to one observable, M_W, and the same would be the case for h_{AZ} if the exact value of $\sin^2\theta_W$ were known independently. However, since that is not the case and we use the experimental value of M_Z as an input parameter to determine the apparent $\sin^2\theta_W$, the effects of h_{AZ} will propagate and induce artificial shifts in other physical observables. Comparing with Sec. IV.B, we see that h_V has effects identical to those of tree-level weak isospin breaking, i.e., to $\rho_0\neq 0$ due to nonstandard Higgs bosons. In fact, we can loosely think of h_V as a radiative correction to ρ_0. The effects of both ρ_0 and h_V can thus be absorbed into one effective ρ parameter:

$$\rho_{\rm eff}=\frac{\rho_0}{1-\alpha h_V}\ . \tag{195}$$

Thus there is no way to discriminate between ρ_0 and h_V from the WNC and W, Z observables considered in this paper.

A global fit to the existing neutral-current and Z and W data shows (for $\rho_0=1$) $-1.2<h_V<0.9$, $-3.5<h_{AZ}<1.0$, $-4.4<h_{AW}<2.4$ at 90 percent confidence level (Kennedy and Langacker, 1990, 1991).

3. m_t and M_H

In the $\overline{\rm MS}$ scheme (see, for example, Sarantakos *et al.*, 1983; Sirlin, 1989, 1990; Marciano, 1990a, 1990b; Degrassi and Sirlin, 1991; Degrassi *et al.*, 1991),[28] the W and Z masses in the SM are

$$M_W^2=\frac{\pi\alpha/\sqrt{2}G_F}{\sin^2\hat\theta_W(1-\Delta\hat r_W)}\ , \tag{196}$$

$$M_Z^2=\frac{M_W^2}{\hat\rho\cos^2\hat\theta_W}\ . \tag{197}$$

For large m_t, $\hat\rho$ increases quadratically,

$$\hat\rho\sim 1+\Delta\rho_t \tag{198}$$

where

$$\Delta\rho_t=\frac{3G_F m_t^2}{8\sqrt{2}\pi^2}\simeq 0.0031\left[\frac{m_t}{100\ \text{GeV}}\right]^2\ . \tag{199}$$

The formulas for Γ_Z and $\epsilon_{L,R}(i)$ are multiplied by $\hat\rho$.

---

[26]The definitions given here are slightly different from those in Kennedy and Langacker (1990), due to the different definitions of $\sin^2\theta_W$.

[27]In many cases $h_{AZ}\simeq h_{AW}\equiv S$, but we allow $h_{AZ}\neq h_{AW}$ for completeness.

[28]In the on-shell scheme (Marciano and Sirlin, 1980; Sirlin, 1980, 1984), $\sin^2\theta_W^M=1-M_W^2/M_Z^2$, the effect of m_t is included in the definition of $\sin^2\theta_W^M$ and therefore propagates into the $\sin^2\theta_W^M$ dependence of all formulas. Γ_z and $\epsilon_{L,R}(i)$ are still proportional to $1+\Delta\rho_t$. In addition, the form factor κ that multiplies $\sin^2\theta_W^M$ in the vertices has a term $\kappa\sim 1+\Delta\rho_t/\tan^2\theta_W$, while Δr_M defined by $M_W^2=(\pi\alpha/\sqrt{2}G_F)/[\sin^2\theta_W^M(1-\Delta r_M)]$ contains $\Delta r_M\sim\Delta r_0-\Delta\rho_t/\tan^2\theta_W$.

There is additional logarithmic dependence in $\Delta\hat{r}_W$, $\hat{\rho}$, Γ_Z, $\epsilon_{L,R}(i)$, and the Z-pole observables that is included in the analysis but is not displayed here. Finally, the $Z\to b\bar{b}$ vertex has a strong m_t dependence (see Akhundov *et al.*, 1986; Beenakker and Hollik, 1988; Bernabeu *et al.*, 1990; and Blondel, 1990) from the vertex diagrams in Fig. 32. These actually cause $\Gamma_{Z\to b\bar{b}}$ to decrease with m_t.

Clearly, the quadratic $\Delta\rho_t$ dependence has effects identical to nonstandard Higgs fields, ρ_0. Equivalently, these effects can be incorporated in the general $h_{V,A}$ formalism by a contribution

$$\alpha h_V(m_t)=\Delta\rho_t \ . \tag{200}$$

It is even possible to incorporate the logarithmic corrections as contributions to h_{AW} and h_{AZ}. However, we will treat m_t separately in order to properly correlate the quadratic and logarithmic terms and also to include the $\Gamma_{Z\to b\bar{b}}$ vertex.

Present data are mainly sensitive to $\Delta\rho_t$ and lead to the upper limit[2] $m_t<194$ (202) GeV at 90 (95) C.L. If one allows $\rho_0<1$, then m_t and ρ_0 can compensate in $\rho_{\rm eff}=\rho_0(1+\Delta\rho_t)$ and one obtains the weaker limit (Langacker and Luo, 1991a) $m_t<O(300)$ GeV from the logarithmic dependence and $\Gamma_{Z\to b\bar{b}}$. Improved measurements of $\Gamma_{b\bar{b}}$ and $A_{\rm FB}(b)$ will allow a better separation between ρ_0 and m_t.

The SM Higgs mass M_H affects $\hat{\rho}$, $\Delta\hat{r}_W$, and other observables in a rather complicated (logarithmic) way. For $M_H\geq M_Z$ the leading terms can be incorporated as logarithmic contributions to h_V, $h_{\rm AW}$, and h_{AZ}. In order to include the correlations we shall treat M_H separately. Present data to not constrain M_H, but in the future $A_{\rm LR}$ may give a reasonable constraint if m_t is known independently. The effects of M_H are small but not completely negligible. For large M_H they yield a contribution

$$-\frac{3\alpha}{8\pi\cos^2\theta_W}\ln\frac{M_H}{M_W} \tag{201}$$

to $\rho_{\rm eff}$. This is negative and can in principle weaken the limit on m_t (since $\Delta\rho_t>0$). However, even for $M_H=1$ TeV, the contribution is only ~-0.003, too small to have a major effect.

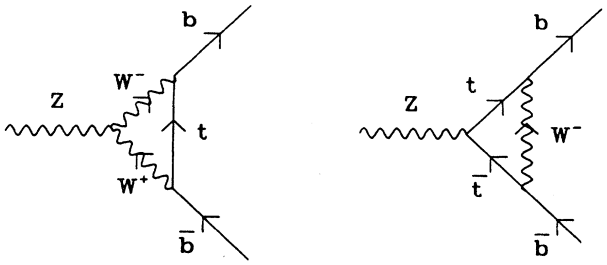

FIG. 32. Vertex corrections to $Z\to b\bar{b}$.

4. Additional SU(2) multiplets

Heavy doublets[29] of new fermions or scalars yield quadratic contributions to h_V similar to m_t,

$$\alpha h_V=\frac{G_F}{8\sqrt{2}\pi^2}(3\Delta m_q^2+\Delta m_l^2+\Delta m_S^2) \ , \tag{202}$$

where

$$\Delta m_q^2=m_{t'}^2+m_{b'}^2-\frac{2m_{t'}^2m_{b'}^2}{m_{t'}^2+m_{b'}^2}\ln\frac{m_{t'}}{m_{b'}}\geq(m_{t'}-m_{b'})^2 \tag{203}$$

represents the effects of a fourth (t',b') quark doublet; the factor of 3 is due to color. A similar formula holds for leptons (Δm_l^2) and for nondegenerate complex scalar doublets (Δm_S^2). These terms are positive, so the presence of nondegenerate doublets *strengths* the upper limit on m_t. In fact, one can approximately reinterpret the upper limit on m_t as

$$m_t^2+\Delta m_q^2+\tfrac{1}{3}\Delta m_l^2+\tfrac{1}{3}\Delta m_S^2<(194\ {\rm GeV})^2 \ . \tag{204}$$

Heavy degenerate fermion multiplets contribute to $h_{AW,Z}$ if they are chiral. The perturbative contribution is (Kennedy and Langacker, 1990, 1991)

$$h_{AW}=h_{AZ}=\sum_i[I_{3L}(i)-I_{3R}(i)]^2\frac{N_C}{3\pi} \ , \tag{205}$$

where the sum extends over the members of the multiplets, and $N_C=1(3)$ for leptons (quarks) is the color factor. Technicolor theories contain additional technifamilies. The perturbative result in Eq. (205) is not valid because it neglects the strong technicolor interactions. Peskin and Takeuchi (1990) have used a scaled-up QCD analysis to estimate

$$h_{AW}\simeq h_{AZ}\sim N_{TG}\begin{cases}0.4+0.08(N_{TC}-4)\\ 2.1+0.49(N_{TC}-4)\end{cases} \tag{206}$$

for a class of technicolor models, where N_{TG} and N_{TC} are the number of technigenerations and technicolors, respectively. The first line is for a single SU(2) doublet of techniquarks, while the second is for a full generation. Equation (206) does not apply to walking technicolor models (Holdom, 1985, 1987).

5. Two Higgs doublets

The theoretical and phenomenological implications of additional Higgs doublets have been discussed extensive-

[29]The effects of additional SU(2) multiplets are discussed in detail in Toussaint (1978), Einhorn *et al.* (1981), Bertolini and Sirlin (1984), Bertolini (1986), van der Bij and Hoogeveen (1987), Hollik (1986, 1988), and Denner *et al.* (1990).

ly (Toussaint, 1978; Einhorn *et al.*, 1981; Bertolini and Sirlin, 1984; Bertolini, 1986; Hollik, 1986, 1988; van der Bij and Hoogeveen, 1987; Chanowitz, 1988; Denner *et al.*, 1990; Gunion *et al.*, 1990). Even one extra Higgs doublet complicates the theory significantly; assuming *CP* symmetry and a discrete symmetry to eliminate Higgs-mediated FCNC, there are still four extra scalar bosons and five extra free parameters, not including Higgs self-interactions. Fortunately, the situation is much simplified if we are only interested in their contributions to the gauge boson self-energies. To one-loop level these depend only on the scalar masses and mixing angles, not on their self-interactions The dominant effects are in the ρ (or $\hat{\rho}$) parameter, i.e., in αh_V. We concentrate on these; more detailed discussions may be found in Toussaint (1978), Einhorn *et al.* (1981), Bertolini and Sirlin (1984), Bertolini (1986), Hollik (1986, 1988), van der Bij and Hoogeveen (1987), Chanowitz (1988), Denner *et al.* (1990), and Gunion *et al.* (1990).

Consider two doublets Φ_1 and Φ_2 and choose a basis such that

$$\Phi_1=\frac{1}{\sqrt{2}}\begin{bmatrix}0\\ v+\phi_1\end{bmatrix},\qquad \Phi_2=\begin{bmatrix}\phi^+\\ \frac{1}{\sqrt{2}}(\phi_2+i\phi_3)\end{bmatrix}, \tag{207}$$

where ϕ_1 and ϕ_2 are two scalars related to the mass eigenstates with masses $M_{1,2}$ by a mixing angle[30] $\alpha-\beta$; ϕ_3 is the pseudoscalar[31] with a mass M_3; and ϕ^+ is the charged Higgs with a mass M_+. For large masses, the contribution to the ρ parameter due to these particles is given approximately by

$$\alpha h_V=\Delta\rho_{2H}=\frac{G_F}{8\sqrt{2}\pi^2}[\sin^2(\alpha-\beta)F(M_+^2,M_3^2,M_1^2)+\cos^2(\alpha-\beta)F(M_+^2,M_3^2,M_2^2)], \tag{208}$$

where

$$F(a,b,c)=a+\frac{bc}{b-c}\ln\frac{b}{c}-\frac{ab}{a-c}\ln\frac{a}{b}-\frac{ac}{a-c}\ln\frac{a}{c}. \tag{209}$$

$\Delta\rho_{2H}$ is small unless there are large mass splittings. For $M_+>M_{1,2,3}$ or $M_+<M_{1,2,3}$; one has $\Delta\rho_{2H}>0$. This is the same sign as $\Delta\rho_t$, so the limits on m_t are strengthened in these cases. In particular, for $M=M_+\gg M_{1,2,3}$, or $M\sim M_1\sim M_2\sim M_3\gg M_+$, one has

$$\Delta\rho_{2H}\sim\frac{G_F}{8\sqrt{2}\pi^2}M^2. \tag{210}$$

In order to weaken the limits on m_t one requires $\Delta\rho_{2H}<0$. This can only occur for $M_{1,2}<M_+<M_3$ and $M_3<M_+<M_{1,2}$. Numerical calculations show that the largest negative $\Delta\rho_{2H}$ occurs for $M_1\sim M_2\sim 0$, $M_+\sim 0.56M_3$ or $M_3\sim 0$, $M_+\sim 0.56M_{1,2}$ (Denner, *et al.*, 1990). Then

$$\Delta\rho_{2H}\sim-\frac{G_F}{8\sqrt{2}\pi^2}0.216M^2 \tag{211}$$

where $M=M_3$ or $M_{1,2}$. There is therefore a small region of parameter space in which $\Delta\rho$ could weaken the m_t limits. However, masses $\gg 1$ TeV would be needed for significant effects, since the relevant quantity is

$$\Delta\rho_t+\Delta\rho_{2H}\sim\frac{G_F}{8\sqrt{2}\pi^2}(3m_t^2-0.216M^2). \tag{212}$$

Such large masses would require large self-interaction, so that perturbation theory breaks down.

Even allowing very large masses, only a small corner of parameter space permits a significant $\Delta\rho_{2H}<0$. To see this, consider for simplicity the case $M_1=M_2$. Then one can write $M_{1,2}^2=M^2\sin\theta\sin\phi$, $M_3^2=M^2\sin\theta\cos\phi$, $M_+^2=M^2\cos\theta$. Then

$$\Delta\rho_{2H}=\frac{G_FM^2}{8\sqrt{2}\pi^2}F \tag{213}$$

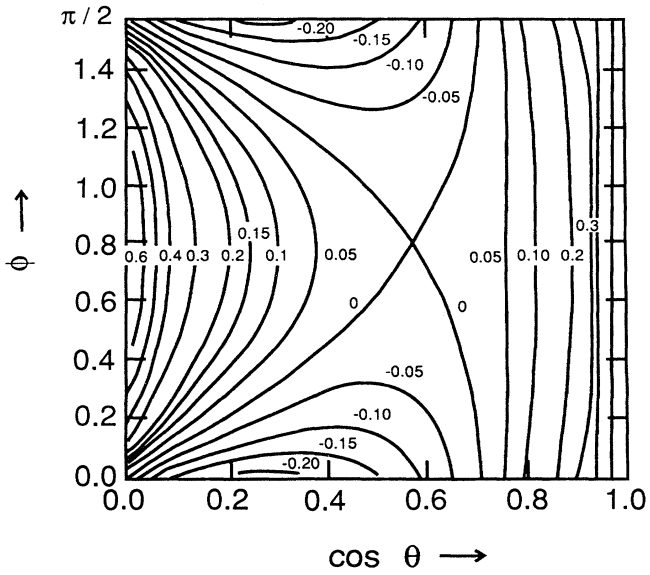

FIG. 33. Contours of F as a function of $\cos\theta$ and ϕ. $F\to 1$ for $\cos\theta\to 0$ or 1. F is negative for a significant range of intermediate values. However, the magnitude is very small except for a tiny region of parameter space around $\cos\theta\sim 0.2-0.4$, $\phi\sim 0$ or $\pi/2$.

[30]Here α and β are two mixing angles between the Higgs fields. If we choose a basis in which Φ_1' gives masses to d-type quarks and Φ_2' gives masses to u-type, then $\tan\beta=|\langle\Phi_2'\rangle|/|\langle\Phi_1'\rangle|$ and α is the mixing angle relating the neutral scalars in Φ_1' and Φ_2' to the mass eigenstates.

[31]We are ignoring *CP* violation, so there is no mixing of ϕ_3 with $\phi_{1,2}$.

with $-0.216 \leq F \leq 1$, to be compared with the top quark contribution $\Delta\rho_t = 3G_F m_t^2/8\sqrt{2}\pi^2$. F is shown as a function of ϕ and $\cos\theta$ in Fig. 33. It is seen that the fraction of the parameter space for which $\Delta\rho_{2H}$ is sufficiently large to significantly weaken the m_t limit is very small.

6. Supersymmetry

Direct searches at colliders are more promising for searching for supersymmetric extensions of the SM than are indirect searches via precision experiments. Nevertheless, there exist several analyses which suggest that indications of supersymmetry could be observed in the experiments considered here (Eliasson, 1984; Lim *et al.*, 1984; Lynn, 1984; Grifols and Sola, 1985; Barbieri *et al.*, 1990; Bilal *et al.*, 1990; Drees and Hagiwara, 1990).

There are several possible manifestations of supersymmetry. One aspect involves the Higgs sector. Supersymmetry requires the existence of at least two Higgs doublets. However, most viable models imply that $M_1 \sim M_Z$, $M_+ \sim M_2 \sim M_3 \sim M \gg M_Z$. This limit [which corresponds to $\cos(\alpha-\beta) \simeq 0$] is similar to the SM with $M_H \sim M_1 \sim M_Z$. The other Higgs fields decouple. That is, if radiative corrections and direct searches are consistent with $M_H \sim M_Z$, then the SM cannot be distinguished from these classes of SUSY models by this means, while $M_H \gg M_Z$ would eliminate many SUSY models.

Another contribution to the radiative corrections is via nondegenerate scalar quarks. In most viable models, the only significant splitting is between the stop and sbottom scalar quarks. Their contribution to αh_V is of the same form as that for a quark doublet [Eq. (202)].

Finally, there may be non-negligible vertex corrections involving winos, but these have not been studied in detail.

V. NUMERICAL ANALYSIS AND RESULTS

The SM predictions of the observables O_a up to one-loop radiative corrections have been calculated in Sec. III of this paper, along with their measurements and projected experimental errors, $\Delta O_a^{\rm exp}$ and $\Delta \sin^2\theta_W^{\rm exp}$. The effects of a variety of possible types of new physics involving extra Z bosons, extra scalar bosons, extra fermions, compositeness, and types of new physics that enter at the loop level are discussed in Sec. IV, and the formulas for ΔO_a^i and $\Delta \sin^2\theta_W^a$ are given there.[32] The effects of varying m_t and M_H within the SM are also discussed.

The present section collects the numerical results of these calculations in Tables VIII to XXXIV and the accompanying figures (Figs. 34–60). The SM predictions for the quantities in column 1 are given in column 2. Column 3 gives the projected one-standard-deviation experimental errors, $\Delta O_a^{\rm exp}$, which include the theoretical uncertainties when they are significant. The latter include both the theoretical uncertainties in the extraction of $O_a^{\rm exp}$ and the uncertainties in the SM prediction of O_a due to the uncertainty ~ 0.0003 in $\sin^2\theta_W^Z$. The contributions of new physics of type i to each of the observables, ΔO_a^i, is given in column 4. To ensure accuracy, in each case the ΔO_a^i were determined by two independent calculations. The ΔO_a^i depend on a coupling constant,[33] λ, which determines the strength of the new physics. We assume $\lambda = 0.01$ for definiteness in column 4, but λ can be scaled linearly to any value preferred by the reader. In column 5 is the minimum value of λ for a given observable; $\lambda_a^{\rm min}$ is the value necessary to make the new-physics contribution to that observable equal to the projected experimental error. Of course, a one-standard-deviation effect is not sufficient to either establish or exclude a given type of new physics, but it is a reasonable measure of sensitivity. Columns 6 and 7 play the same role for $\sin^2\theta_W^{(a;Z)}$ as columns 3 and 4 do for O_a, and in most cases the values of $\lambda^{\rm min}$ in column 5 are also applicable to the values in columns[34] 6 and 7. We reemphasize that although the central values of $\sin^2\theta_W^a$ extracted from each experiment depend on the renormalization scheme, both the experimental uncertainty $\Delta \sin^2\theta_W^{\rm exp}$ in column 6 and the relative shift $\Delta \sin^2\theta_W^{(a;Z)}$ in column 7 are essentially scheme independent.

Since the assumed values $m_t = 100$ GeV and $M_H = 100$ GeV are used as inputs to the tables, the SM predictions with other values of m_t and M_H may be formally treated as if they were new physics. The changes in $O_a^{\rm SM}(\sin^2\theta_W^Z)$ for various values of M_H and m_t are collected in Tables XXXIII and XXXIV and Figs. 59 and 60.

To see what experiments are sensitive to a given type of new physics i, for each O_a we define the ratio of the calculated deviation from the SM due to the new physics i to the projected experimental error:

$$r_a^i(\lambda) = \frac{|\Delta O_a^i|}{\Delta O_a^{\rm exp}} \ . \tag{214}$$

Although r_a^i itself is dependent on the value of λ, the relative sensitivities, or the relative values of r_a^i for different

[32] The extension of our analysis to other types of new physics is straightforward.

[33] In some cases, such as extra Z bosons, there is more than one extra parameter. However, only one is related to the coupling strength, while the others are of order unity. We pick typical values for the latter parameters for definiteness.

[34] That means that the analyses based on $\sin^2\theta_W$ and on the observables themselves are equivalent. That is true provided that the expected variation in the observable can be described by a reasonable variation in $\sin^2\theta_W$ and that the relation is approximately linear within the experimentally prescribed region. This condition is satisfied by all of the observables in this paper except θ_L, θ_R, g_A^e, and C_{2p}, which are insensitive to $\sin^2\theta_W$ (see Figs. 6, 7, 9, and 14).

O_a, are independent of λ. The larger r_a^i is, the more significantly the ith new physics manifests itself, and the more likely for the new physics i to be seen in experiments measuring O_a. $r_a^i(\lambda)$ is proportional to λ, with $r_a^i(\lambda_a^{\min})=1$.

To see the relative sensitivity of each O_a graphically, we plot $1/\lambda_a^{\min}$ from the numerical results for each type of new physics. As an example, consider Fig. 34, in which the new physics is an extra Z_χ with $C=\sqrt{2/5}$. The x axis is labeled by the physical observables with their explicit definitions to be found in Sec. III. The vertical bars represent the relative values of $1/\lambda_a^{\min}$ for each O_a. The higher the bar, the more sensitive is O_a to the Z_χ. The values of M_{Z_2} corresponding to $1/\lambda^{\min}$ are indicated on the right-hand scale. The height of each bar can be scaled up or down if the precision of the corresponding experiment varies. For example, if the error of M_W is reduced to 50 MeV rather than 100 MeV, then the bar of M_W should be scaled up by a factor of 2. On the other hand, if the error of $A_{\rm LR}$ is 0.006 rather than the projected 0.004, then the bar of $A_{\rm LR}$ should be scaled down accordingly. At the moment, let us take the projected precision seriously. Then we see that R_ν is especially sensitive to this type of Z_λ. Looking back at Table VIII, at $\lambda=0.01$ the deviation in R_ν is some 5 times its projected experimental error, and $\lambda_a^{\min}=0.0019$, corresponding to $M_{Z_2}\simeq 1295$ GeV. M_W, g_L^2, $\sigma_{\nu e}/(\sigma_{\nu_e e}+\sigma_{\bar{\nu}e})$, C_{1+}(iso), $A_{\rm LR}$(LEP), and Γ_Z all have $\lambda^{\min}<0.01$, corresponding to $M_{Z_2}=565$ GeV. Other figures are organized in the same form, and conclusions related to each are presented in the Comments of the corresponding table caption.

A. Treatment of extra Z bosons

There are effectively two extra free parameters in the SM with an extra Z boson, provided the relative fermion couplings are constrained by the underlying non-Abelian gauge group:

$$\hat{\rho}_2=\left[\frac{g_2}{g_1}\right]^2\left[\frac{M_Z}{M_{Z_2}}\right]^2, \tag{215}$$

$$\hat{\Theta}=\frac{g_2}{g_1}\Theta, \tag{216}$$

where M_{Z,Z_2} and $g_{1,2}$ are the masses and coupling constants of the ordinary Z and the extra Z_2, respectively; Θ is the Z_1^0-Z_2^0 mixing angle. Typically, $(g_2/g_1)^2\simeq 5\sin^2\theta_W/3\simeq 0.38$. Both $\hat{\rho}_2$ and $\hat{\Theta}$ are small numbers, but their ratio $C=\hat{\Theta}/\hat{\rho}_2$ is of the order of unity. C depends on the $U(1)_2$ quantum numbers of the Higgs fields which cause the mixing. In our analysis, $\hat{\rho}_2$ is taken to be the free parameter λ and some typical values of C [usually motivated by simple $E(6)$ models as shown in Table VI] are selected for each type of Z_2; these values are given above each of the tables.

The numerical results for extra Z bosons are collected in Tables VIII–XVIII and Figs. 34–44.

B. Treatment of extra scalar bosons

In our treatment of extra scalar bosons, we consider nonstandard Higgs fields and leptoquarks.

1. Nonstandard Higgs boson

In the presence of nonstandard Higgs fields only the prediction of M_Z and quantities related to it are directly affected (except for negligible effects associated with scalar exchange). However, $\sin^2\theta_W^Z$ extracted from M_Z assuming the validity of the SM differs from the true $\sin^2\theta_W$. This gives artificial changes in quantities that are sensitive to $\sin^2\theta_W$ when they are predicted from $\sin^2\theta_W^Z$. These changes and those directly due to $\rho_0\equiv M_W^2/M_Z^2\cos^2\theta_W$ are collected in Table XIX and Fig. 45. We take $\lambda=\rho_0-1$.

2. Leptoquarks

The contributions of leptoquarks are suppressed at the Z pole, as are those of photons. Accordingly, e^+e^- collider experiments at the Z pole will give no information about them. Neither will leptoquarks contribute to pure leptonic processes, since leptoquarks change quarks to leptons and leptons to quarks at tree level. Only the vq coupling constants and atomic parity-violation coefficients can be affected by leptoquarks.

In a general leptoquark theory, there may be many extra parameters. But for the specific SU(5) leptoquark we have chosen for illustration, there are only two relevant parameters:

$$\frac{\sqrt{2}|\eta_L|^2}{8M_S^2G_F}$$

and

$$\frac{\sqrt{2}|\eta_R|^2}{8M_S^2G_F}.$$

The results for $\eta_L\neq 0$ and $\eta_R=0$ (referred to as *type-1 leptoquark*) are in Table XX and Fig. 46, while the results of $\eta_L=0$ and $\eta_R\neq 0$ (referred to as *type-2 leptoquark*) are simply summarized at the top of Table XX. In each case,

$$\lambda=\frac{\sqrt{2}|\eta|^2}{8M_S^2G_F}.$$

C. Treatment of extra fermions

The theories of extra fermions are complicated by many free parameters. To simplify, we separate a general theory with many extra fermions into specific ones with

only one extra fermion. So, we do not deal with a theory with n extra fermions, but n theories with one extra fermion.

Nine specific case are considered:

(a) one extra left-handed u-type quark;
(b) one extra right-handed u-type quark;
(c) one extra left-handed d-type quark;
(d) one extra right-handed d-type quark;
(e) one extra left-handed charged lepton mixed with e_L;
(f) one extra right-handed charged lepton mixed with e_R;
(g) one extra left-handed neutral lepton mixed with ν_e;
(h) one extra left-handed charged lepton mixed with μ;
(i) one extra left-handed neutral lepton mixed with ν_μ.

In each case it is assumed that the extra fermions have exotic weak interactions, e.g., left-handed singlets or right-handed doublets. Their effects are listed in Tables XXI–XXIX and Figs. 47–55.

We take $\lambda=\sin^2\theta$, where θ is the mixing angle between the ordinary and exotic fermions.

D. Treatment of contact operators

We consider three representative cases of four-fermi contact operators:

$$-L_1=\pm\frac{4\pi}{\Lambda_1^2}\bar{l}_{\mu L}\gamma^\mu l_{\mu L}\bar{q}_L\gamma_\mu q_L \ , \tag{217}$$

$$-L_2=\pm\frac{4\pi}{\Lambda_2^3}\bar{\nu}_{\mu L}\gamma^\mu \nu_{\mu L}\bar{e}_L\gamma_\mu e_L \ , \tag{218}$$

$$-L_3=\pm\frac{4\pi}{\Lambda_3^2}\bar{e}_L\gamma^\mu e_L\bar{q}_L\gamma_\mu q_L \ . \tag{219}$$

L_1 will shift the values of $\epsilon_L(u)$, $\epsilon_L(d)$, C_{2u}, and C_{2d}, L_2 those of g_V^e and g_A^e, and L_3 those of C_{1u} and C_{1d}. The results are shown in Table XXX(a) and Fig. 56. We define

$$\lambda=(\sqrt{2}/G_F)(\pi/\Lambda_1^2)=(\sqrt{2}/G_F)(\pi/\Lambda_2^2)$$
$$=(\sqrt{2}/G_F)(\pi/\Lambda_3^2) \ .$$

Then $\lambda=0.01$ corresponds to $\Lambda_1=\Lambda_2=\Lambda_3=6.17$ TeV.

The sensitivity of e^+e^- asymmetries off the Z pole at $s-M_Z^2=M_Z\Gamma_Z$ is shown in Table XXX(b) for a number of representative four-fermi operators generated by new physics. One expects sensitivity to compositeness scales of $O(1$ TeV), which is considerably lower than some of the other observables in Table XXX(a), and to anticipated collider limits [Eichten *et al.*, 1984; Martyn, 1987; LEP200 (see Ellis and Peccei, 1988, Vol. 2)].

In Tables VIII—XVII it is apparent that the e^+e^- observables at the Z pole are strongly affected by mixing between the Z and an extra Z_2 boson. However, there is no sensitivity to a Z_2 if Z_1^0-Z_2^0 mixing is absent. Off the Z pole, an unmixed Z_2 contributes effective four-fermi operators

$$-L=\frac{4\pi}{\Lambda^2}\bar{e}_a\gamma^\mu e_a\bar{f}_b\gamma_\mu f_b \ . \tag{220}$$

where $a,b=L$ or R,

$$\frac{4\pi}{\Lambda^2}=\frac{8G_F}{\sqrt{2}}\frac{M_Z^2}{M_{Z_2}^2}\left[\frac{g_2}{g_1}\right]^2 Q_a(e)Q_b(f) \ , \tag{221}$$

and $Q_{LR}(f)$ are the Z_2 chiral charges defined in Eq. (117) and Table V. For the E(6) and LR-model bosons considered in this paper, the sensitivity is at best to $M_{Z_2}\simeq O(100$–200 GeV), which is poor compared to other indirect observables and direct production at colliders. Thus off-Z-pole e^+e^- asymmetries do not look promising, at least for the types of new physics considered here.

E. Heavy-particle loop contributions

Many types of new physics that enter at the one-loop level affect only the gauge boson self-energies and can be described by the parameters h_V, h_{AW}, and h_{AZ}, as described in Sec. IV.E. h_V is sensitive to nondegenerate SU(2) multiplets which break the vector SU(2) symmetries, including the top quark mass, nondegenerate fourth-family fermions, nondegenerate Higgs multiplets, and $\tilde{b}$-$\tilde{t}$ splitting in supersymmetry. The effects of h_V are equivalent to $\rho_0\neq 1$ in Table XIX, but are repeated for convenience in Table XXXI. h_A in Table XXXII is sensitive to axial-SU(2) breaking, such as that due to the Higgs mass or heavy degenerate chiral fermion multiplets. The latter are expected in technicolor theories.

In this paper, $M_H=100$ GeV and $m_t=100$ GeV are used as inputs for the calculation of radiative corrections. The effects of other values of m_t and M_H are treated as if they are new physics. Most of the effects of a Higgs mass M_H or top quark mass m_t differing from their reference values of 100 GeV can be described by h_V and h_A. However, they are treated separately in order to take the correlations between h_V, h_{AW}, and h_{AZ} properly into account and to include additional m_t dependence from $Z\to\bar{b}b$ vertex diagrams. The effects of $M_H=500$ GeV and 1 TeV are shown in Table XXXIII and Fig. 59. The radiative corrections to physical observables depend logarithmatically on M_H and are generally small. The effects of $m_t=150$ GeV and 200 GeV, shown in Table XXXIV and Fig. 60, are considerably larger due to the dominant $\alpha m_t^2/M_Z^2$ dependence of the ratio M_W^2/M_Z^2 and of quantities that depend on the ratio.

TABLE VIII. Deviations from the SM by an extra Z_χ boson [$C=(2/5)^{1/2}$]. Type: Z_χ. Free parameter: $\lambda=(g_2^2/M_{Z_2}^2)/(g_1^2/M_Z^2)$ with $C=\Theta(g_2/g_1)/\lambda=\sqrt{2/5}$ (Sec. IV.A). g_1, g_2 and M_Z, M_{Z_2} are the coupling constants and masses of the ordinary Z and the extra Z_χ bosons, respectively; Θ is their mixing angle. Inputs: $M_Z=91.177$ GeV, $m_t=100$ GeV, $M_H=100$ GeV ($\sin^2\theta_W^M=0.2306$, $\sin^2\hat{\theta}_W=0.2334$). **Comments:** For the explicit definitions of physical observables, see Sec. III. $\lambda^{\min}$ is the value of λ for which the change ΔO_a is equal to the projected one-standard-deviation experimental error. The inverses of the sixth column $1/\lambda^{\min}$ are plotted in Fig. 34. Following the argument given in the text, the bigger $1/\lambda_a^{\min}$ is, the more likely for Z_χ to be detected by measuring O_a. R_ν is sensitive to this particular Z_χ; it has $\lambda_a^{\min}=0.0019$, which corresponds to $M_{Z_2}=1295$ GeV for $g_2^2/g_1^2=\frac{5}{3}\sin^2\theta_W$. M_W, g_L^2, $\sigma_{\nu e}/(\sigma_{\nu_e e}+\sigma_{\bar{\nu}e})$, C_{1+}(iso), $A_{\rm LR}$(LEP), and Γ_Z all have $\lambda^{\min}<0.01$, corresponding to $M_{Z_2}=565$ GeV.

Quantities	O_a^{SM}	ΔO_a^{exp}	ΔO_a^i $\lambda=0.01$	λ_a^{min}	$\Delta\sin^2\theta_W^{exp}$	$\Delta\sin^2\theta_W^{(a;Z)}$ $\lambda=0.01$
$M_Z(GeV)$	91.1770	0.0200	—	—	0.0003	—
$M_W(GeV)$	79.9832	0.1050	0.2284	0.0046	0.0006	−0.0013
g_L^2	0.2997	0.0042	0.0074	0.0057	0.0057	−0.0100
g_R^2	0.0301	0.0034	−0.0017	0.0202	0.0130	−0.0065
R_ν	0.3117	0.0013	0.0067	0.0019	0.0020	−0.0105
θ_L	2.4640	0.0300	0.0057	0.0529	—	—
θ_R	5.1765	0.4400	−0.0322	0.1366	—	—
g_V^e	−0.0361	0.0220	0.0070	0.0314	0.0110	0.0035
g_A^e	−0.5037	0.0250	0.0000	—	—	—
$\sigma_\nu/\sigma_{\bar{\nu}}$	1.1515	0.0453	−0.0318	0.0143	0.0050	0.0035
$\sigma_\nu/(\sigma_{\bar{\nu}}+\sigma_\nu)$	0.1455	0.0026	−0.0036	0.0072	0.0025	0.0035
C_{1+}	0.1291	0.0013	−0.0005	0.0250	0.0033	−0.0013
$C_{1+}(iso)$	0.1291	0.0003	−0.0005	0.0065	0.0009	−0.0013
C_{1-}	−0.3633	0.1000	−0.0019	0.5289	0.0689	−0.0013
C_{2p}	−0.0140	0.0460	−0.0001	—	—	—
$C_{2p}(1)$	−0.0140	0.0046	−0.0001	0.4494	—	—
C_{2m}	−0.0537	0.1100	−0.0052	0.2122	0.0274	−0.0013
$2C_{1u}+C_{1d}$	−0.0323	0.0040	−0.0026	0.0151	0.0020	−0.0013
$A_{LR}(SLC)$	0.1306	0.0066	−0.0048	0.0142	0.0008	0.0006
$A_{LR}(LEP)$	0.1306	0.0041	−0.0048	0.0090	0.0005	0.0006
$A_{FB}^{pol}(c)$	0.4725	0.0250	0.0050	0.0504	0.0095	−0.0019
$A_{FB}(c)$	0.0617	0.0070	−0.0016	0.0434	0.0017	0.0004
$A_{FB}^{pol}(b)$	0.6965	0.0200	0.0044	0.0450	0.0423	−0.0094
$A_{FB}(b)$	0.0910	0.0054	−0.0028	0.0200	0.0010	0.0005
$A_{FB}^{pol}(\mu)$	0.0980	0.0090	−0.0036	0.0251	0.0015	0.0006
$A_{FB}(\mu)$	0.0128	0.0035	−0.0009	0.0373	0.0023	0.0006
$A_{pol}(\tau)$	0.1306	0.0110	−0.0048	0.0230	0.0014	0.0006
$\Gamma_{inv}(GeV)$	0.4990	0.0160	0.0080	0.0201	0.0070	−0.0035
$\Gamma_{l\bar{l}}(GeV)$	0.0835	0.0007	−0.0004	0.0193	0.0016	0.0008
$\Gamma_{c\bar{c}}(GeV)$	0.2959	0.0300	−0.0001	—	0.0161	0.0001
$\Gamma_{b\bar{b}}(GeV)$	0.3773	0.0400	0.0029	0.1387	0.0184	−0.0013
$\Gamma_Z(GeV)$	2.4837	0.0150	0.0153	0.0098	0.0011	−0.0011

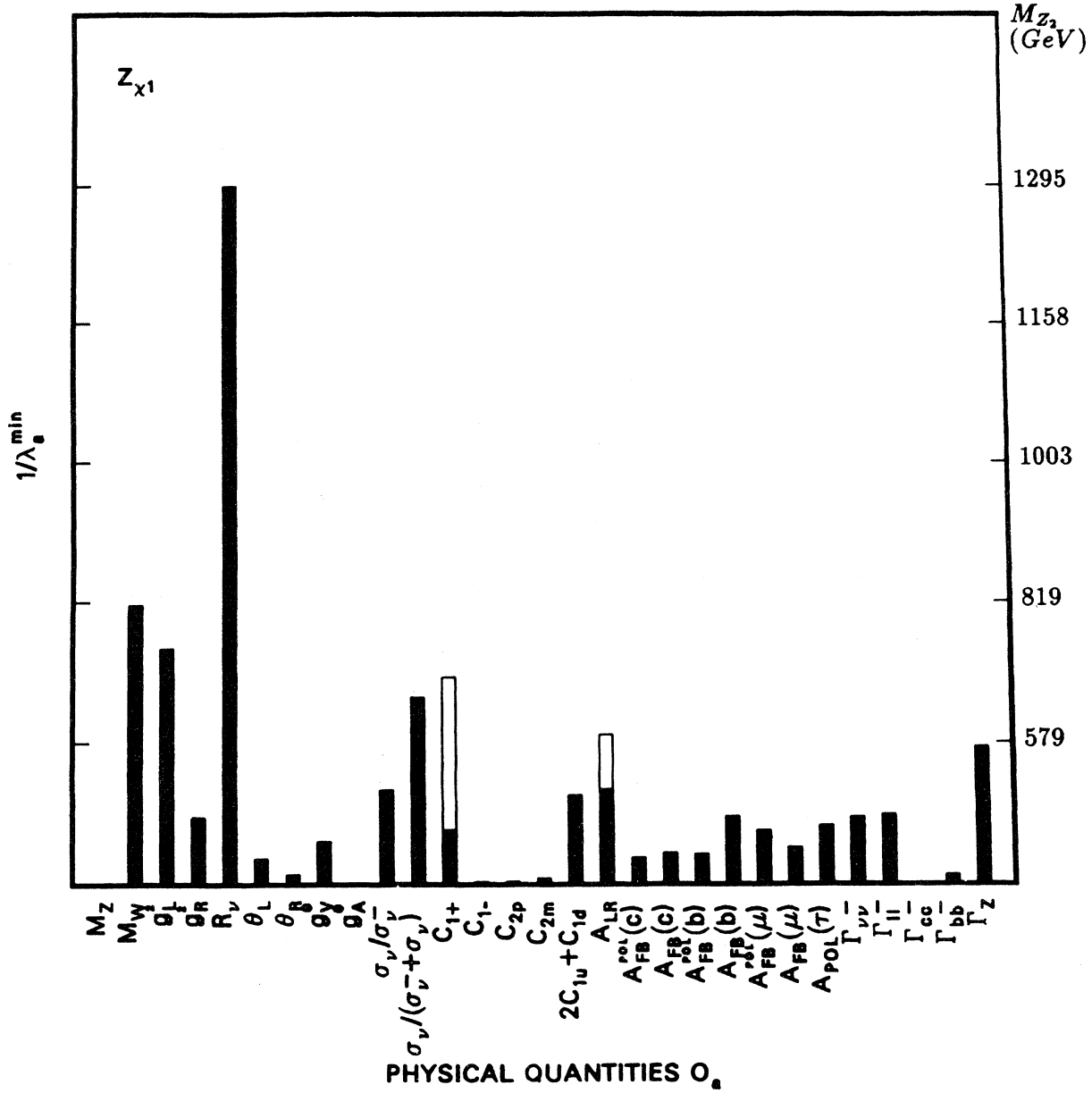

FIG. 34. The new physics of Z_χ with $C=(2/5)^{1/2}$: solid bar for C_{1+} and A_{LR}(SLC); open bar for C_{1+}(iso) and A_{LR}(LEP). The right-hand scale corresponds to M_{Z_2} in GeV.

TABLE IX. Deviations from the SM by an extra Z_χ boson (no mixing). Type: Z_χ. Free parameter: $\lambda=(g_2^2/M_{Z_2}^2)/(g_1^2/M_Z^2)$ with $C=\Theta(g_2/g_1)/\lambda=0$ (Sec. IV.A). g_1, g_2 and M_Z, M_{Z_2} are the coupling constants and masses of the ordinary Z and the extra Z_χ bosons, respectively; Θ is their mixing angle. Inputs: $M_Z=91.177$ GeV, $m_t=100$ GeV, $M_H=100$ GeV ($\sin^2\theta_W^M=0.2306$, $\sin^2\hat{\theta}_W=0.2334$). **Comments:** The inverses of the sixth column $1/\lambda^{\min}$ are plotted in Fig. 35. C_{1+}(iso) has $\lambda^{\min}=0.0011$, corresponding to $M_Z=1700$ GeV, while C_{1+} would be sensitive to $M_{Z_2}\sim 850$ GeV, $\sigma_\nu/(\sigma_{\bar{\nu}}+\sigma_\nu)$ to ~ 780 GeV, and the CEBAF observable $2C_{1u}+C_{1d}$ to ~ 560 GeV.

Quantities	O_a^{SM}	ΔO_a^{exp}	ΔO_a^i $\lambda=0.01$	λ_a^{min}	$\Delta\sin^2\theta_W^{exp}$	$\Delta\sin^2\theta_W^{(a;Z)}$ $\lambda=0.01$
$M_Z(GeV)$	91.1770	0.0200	—	—	0.0003	—
$g_{L\nu}^2$	0.2997	0.0042	0.0002	0.1681	0.0057	−0.0003
$g_{\nu R}^2$	0.0301	0.0034	−0.0012	0.0292	0.0130	−0.0045
R_ν	0.3117	0.0013	−0.0002	0.0591	0.0020	0.0003
θ_L	2.4640	0.0300	0.0039	0.0779	—	—
θ_R	5.1765	0.4400	−0.0193	0.2277	—	—
g_V^e	−0.0361	0.0220	0.0060	0.0367	0.0110	0.0030
g_A^e	−0.5037	0.0250	0.0030	0.0833	—	—
$\sigma_\nu/\sigma_{\bar{\nu}}$	1.1515	0.0453	−0.0262	0.0173	0.0050	0.0029
$\sigma_\nu/(\sigma_{\bar{\nu}}+\sigma_\nu)$	0.1455	0.0026	−0.0050	0.0052	0.0025	0.0048
C_{1+}	0.1291	0.0013	−0.0030	0.0044	0.0033	−0.0076
$C_{1+}(iso)$	0.1291	0.0003	−0.0030	0.0011	0.0009	−0.0076
C_{1-}	−0.3633	0.1000	0.0027	0.3754	0.0689	0.0018
C_{2p}	−0.0140	0.0460	0.0000	—	—	—
$C_{2p}(1)$	−0.0140	0.0046	0.0000	—	—	—
C_{2m}	−0.0537	0.1100	−0.0080	0.1375	0.0274	−0.0020
$2C_{1u}+C_{1d}$	−0.0323	0.0040	−0.0040	0.0100	0.0020	−0.0020

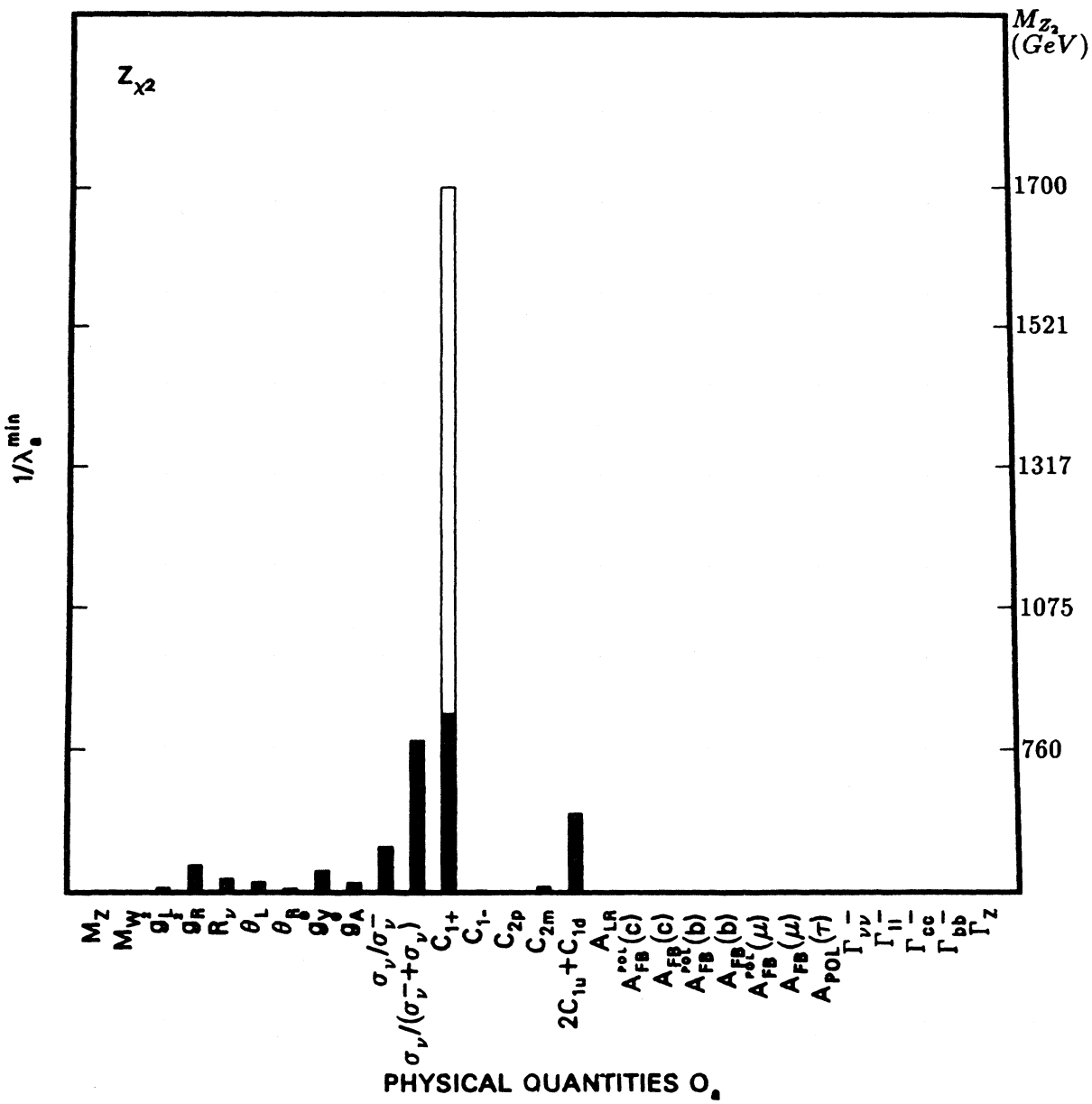

FIG. 35. The new physics of Z_χ with $C=0$: solid bar for C_{1+}, open bar for C_{1+}(iso).

TABLE X. Deviations from the SM by an extra Z_ψ boson [$C=(2/3)^{1/2}$]. Type: Z_ψ. Free parameter: $\lambda=(g_2^2/M_{Z_2}^2)/(g_1^2/M_Z^2)$ with $C=\Theta(g_2/g_1)/\lambda=\sqrt{2/3}$ (Sec. IV.A). g_1, g_2, and M_Z, M_{Z_2} are the coupling constants and masses of the ordinary Z and the extra Z_ψ bosons, respectively; Θ is their mixing angle. Inputs: $M_Z=91.177$ GeV, $m_t=100$ GeV, $M_H=100$ GeV ($\sin^2\theta_W^M=0.2306$, $\sin^2\hat{\theta}_W=0.2334$). **Comments:** The inverses of the sixth column $1/\lambda^{\min}$ are plotted in Fig. 36. For R_ν, $\lambda_a^{\min}=0.0017$, which corresponds to $M_{Z_2}=1370$ GeV for $g_2^2/g_1^2=\frac{5}{3}\sin^2\theta_W$. M_W, C_{1+}(iso), $A_{\rm LR}$, and $A_{\rm FB}(b)$ all have $\lambda_a^{\min}<0.0042$ ($M_{Z_2}>872$ GeV).

Quantities	O_a^{SM}	ΔO_a^{exp}	ΔO_a^i $\lambda=0.01$	λ_a^{min}	$\Delta\sin^2\theta_W^{exp}$	$\Delta\sin^2\theta_W^{(a;Z)}$ $\lambda=0.01$
$M_Z(GeV)$	91.1770	0.0200	—	—	0.0003	—
$M_W(GeV)$	79.9832	0.1050	0.3806	0.0028	0.0006	−0.0022
g_L^2	0.2997	0.0042	0.0072	0.0058	0.0057	−0.0097
g_R^2	0.0301	0.0034	0.0004	0.0805	0.0130	0.0016
R_ν	0.3117	0.0013	0.0074	0.0017	0.0020	−0.0115
θ_L	2.4640	0.0300	−0.0077	0.0391	—	—
θ_R	5.1765	0.4400	−0.0193	0.2276	—	—
g_V^e	−0.0361	0.0220	−0.0047	0.0463	0.0110	−0.0024
g_A^e	−0.5037	0.0250	0.0000	—	—	—
$\sigma_\nu/\sigma_{\bar{\nu}}$	1.1515	0.0453	0.0215	0.0211	0.0050	−0.0024
$\sigma_\nu/(\sigma_{\bar{\nu}}+\sigma_\nu)$	0.1455	0.0026	0.0025	0.0104	0.0025	−0.0024
C_{1+}	0.1291	0.0013	−0.0009	0.0144	0.0033	−0.0023
$C_{1+}(iso)$	0.1291	0.0003	−0.0009	0.0037	0.0009	−0.0023
C_{1-}	−0.3633	0.1000	−0.0031	0.3207	0.0689	−0.0021
C_{2p}	−0.0140	0.0460	−0.0006	0.7992	—	—
$C_{2p}(1)$	−0.0140	0.0046	−0.0006	0.0799	—	—
C_{2m}	−0.0537	0.1100	−0.0092	0.1202	0.0274	−0.0023
$2C_{1u}+C_{1d}$	−0.0323	0.0040	−0.0045	0.0090	0.0020	−0.0022
$A_{LR}(SLC)$	0.1306	0.0066	0.0181	0.0038	0.0008	−0.0023
$A_{LR}(LEP)$	0.1306	0.0041	0.0181	0.0024	0.0005	−0.0023
$A_{FB}^{pol}(c)$	0.4725	0.0250	0.0033	0.0758	0.0095	−0.0013
$A_{FB}(c)$	0.0617	0.0070	0.0090	0.0078	0.0017	−0.0022
$A_{FB}^{pol}(b)$	0.6965	0.0200	0.0027	0.0748	0.0423	−0.0057
$A_{FB}(b)$	0.0910	0.0054	0.0129	0.0042	0.0010	−0.0024
$A_{FB}^{pol}(\mu)$	0.0980	0.0090	0.0136	0.0066	0.0015	−0.0023
$A_{FB}(\mu)$	0.0128	0.0035	0.0035	0.0099	0.0023	−0.0023
$A_{pol}(\tau)$	0.1306	0.0110	0.0181	0.0061	0.0014	−0.0023
$\Gamma_{inv}(GeV)$	0.4990	0.0160	0.0066	0.0241	0.0070	−0.0029
$\Gamma_{l\bar{l}}(GeV)$	0.0835	0.0007	−0.0004	0.0158	0.0016	0.0010
$\Gamma_{c\bar{c}}(GeV)$	0.2959	0.0300	0.0064	0.0469	0.0161	−0.0034
$\Gamma_{b\bar{b}}(GeV)$	0.3773	0.0400	0.0002	—	0.0184	−0.0001
$\Gamma_Z(GeV)$	2.4837	0.0150	0.0186	0.0080	0.0011	−0.0013

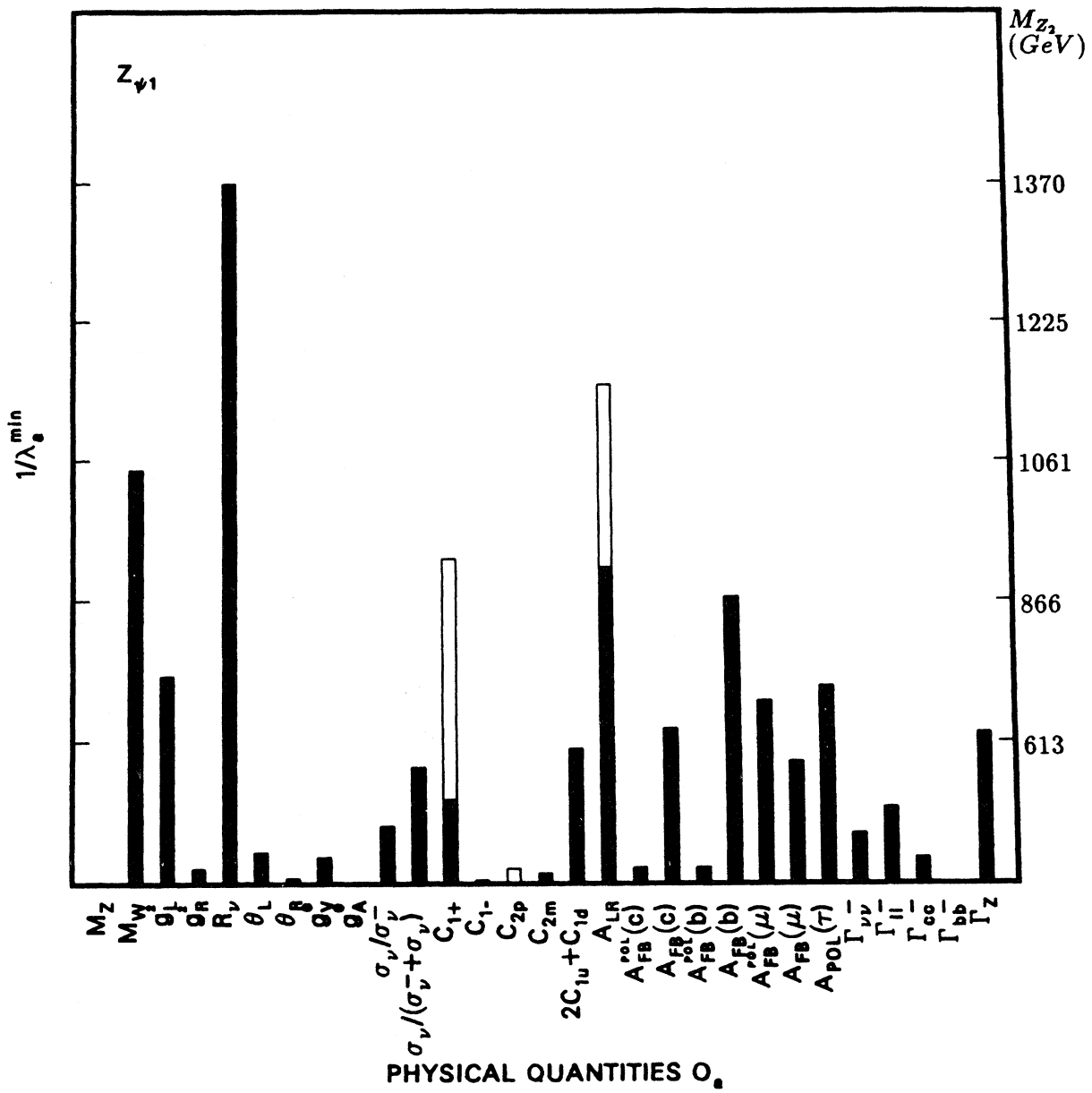

FIG. 36. The new physics of Z_ψ with $C=(2/3)^{1/2}$: solid bar for C_{1+}, C_{2p}, and A_{LR}(SLC); open bar for C_{1+}(iso), $C_{2p}(1)$, and A_{LR}(LEP).

TABLE XI. Deviations from the SM by an extra Z_ψ boson [$C=-(2/3)^{1/2}$]. Type: Z_ψ. Free parameter: $\lambda=(g_2^2/M_{Z_2}^2)/(g_1^2/M_Z^2)$ with $C=\Theta(g_2/g_1)/\lambda=-\sqrt{2/3}$ (Sec. IV.A). g_1, g_2 and M_Z, M_{Z_2} are the coupling constants and masses of the ordinary Z and the extra Z_ψ bosons, respectively; Θ is their mixing angle. Inputs: $M_Z=91.177$ GeV, $m_t=100$ GeV, $M_H=100$ GeV ($\sin^2\theta_W^M=0.2306$, $\sin^2\hat{\theta}_W=0.2334$). **Comments:** The inverses of the sixth column $1/\lambda^{\min}$ are plotted in Fig. 37. $A_{\rm LR}$(LEP) and M_W are most sensitive, both have $\lambda^{\min}\leq 0.0029$, corresponding to $M_{Z_2}>1050$ GeV. R_ν, C_{1+}(iso), $A_{\rm LR}$(SLC), $A_{\rm FB}(b)$, and $\Gamma_{\bar{l}l}$ all have $\lambda^{\min}<0.005$ ($M_{Z_2}>800$ GeV).

Quantities	O_a^{SM}	ΔO_a^{exp}	ΔO_a^i $\lambda=0.01$	λ_a^{min}	$\Delta\sin^2\theta_W^{exp}$	$\Delta\sin^2\theta_W^{(a;Z)}$ $\lambda=0.01$
$M_Z(GeV)$	91.1770	0.0200	—	—	0.0003	—
$M_W(GeV)$	79.9832	0.1050	0.3806	0.0028	0.0006	−0.0022
g_L^2	0.2997	0.0042	0.0038	0.0112	0.0057	−0.0051
g_R^2	0.0301	0.0034	−0.0005	0.0686	0.0130	−0.0019
R_ν	0.3117	0.0013	0.0036	0.0036	0.0020	−0.0056
θ_L	2.4640	0.0300	0.0009	0.3345	—	—
θ_R	5.1765	0.4400	0.0064	0.6828	—	—
g_V^e	−0.0361	0.0220	−0.0045	0.0488	0.0110	−0.0023
g_A^e	−0.5037	0.0250	−0.0033	0.0747	—	—
$\sigma_\nu/\sigma_{\bar{\nu}}$	1.1515	0.0453	0.0193	0.0234	0.0050	−0.0021
$\sigma_\nu/(\sigma_{\bar{\nu}}+\sigma_\nu)$	0.1455	0.0026	0.0045	0.0059	0.0025	−0.0043
C_{1+}	0.1291	0.0013	0.0009	0.0144	0.0033	0.0023
$C_{1+}(iso)$	0.1291	0.0003	0.0009	0.0038	0.0009	0.0023
C_{1-}	−0.3633	0.1000	−0.0081	0.1236	0.0689	−0.0056
C_{2p}	−0.0140	0.0460	0.0004	—	—	—
$C_{2p}(1)$	−0.0140	0.0046	0.0004	0.1184	—	—
C_{2m}	−0.0537	0.1100	−0.0092	0.1202	0.0274	−0.0023
$2C_{1u}+C_{1d}$	−0.0323	0.0040	−0.0048	0.0083	0.0020	−0.0024
$A_{LR}(SLC)$	0.1306	0.0066	0.0162	0.0042	0.0008	−0.0021
$A_{LR}(LEP)$	0.1306	0.0041	0.0162	0.0027	0.0005	−0.0021
$A_{FB}^{pol}(c)$	0.4725	0.0250	0.0083	0.0302	0.0095	−0.0031
$A_{FB}(c)$	0.0617	0.0070	0.0087	0.0080	0.0017	−0.0022
$A_{FB}^{pol}(b)$	0.6965	0.0200	−0.0006	0.3340	0.0423	0.0013
$A_{FB}(b)$	0.0910	0.0054	0.0112	0.0049	0.0010	−0.0020
$A_{FB}^{pol}(\mu)$	0.0980	0.0090	0.0122	0.0074	0.0015	−0.0021
$A_{FB}(\mu)$	0.0128	0.0035	0.0032	0.0110	0.0023	−0.0021
$A_{pol}(\tau)$	0.1306	0.0110	0.0162	0.0068	0.0014	−0.0021
$\Gamma_{inv}(GeV)$	0.4990	0.0160	0.0000	—	0.0070	0.0000
$\Gamma_{l\bar{l}}(GeV)$	0.0835	0.0007	0.0018	0.0039	0.0016	−0.0041
$\Gamma_{c\bar{c}}(GeV)$	0.2959	0.0300	−0.0002	—	0.0161	0.0001
$\Gamma_{b\bar{b}}(GeV)$	0.3773	0.0400	0.0069	0.0582	0.0184	−0.0032
$\Gamma_Z(GeV)$	2.4837	0.0150	0.0255	0.0059	0.0011	−0.0018

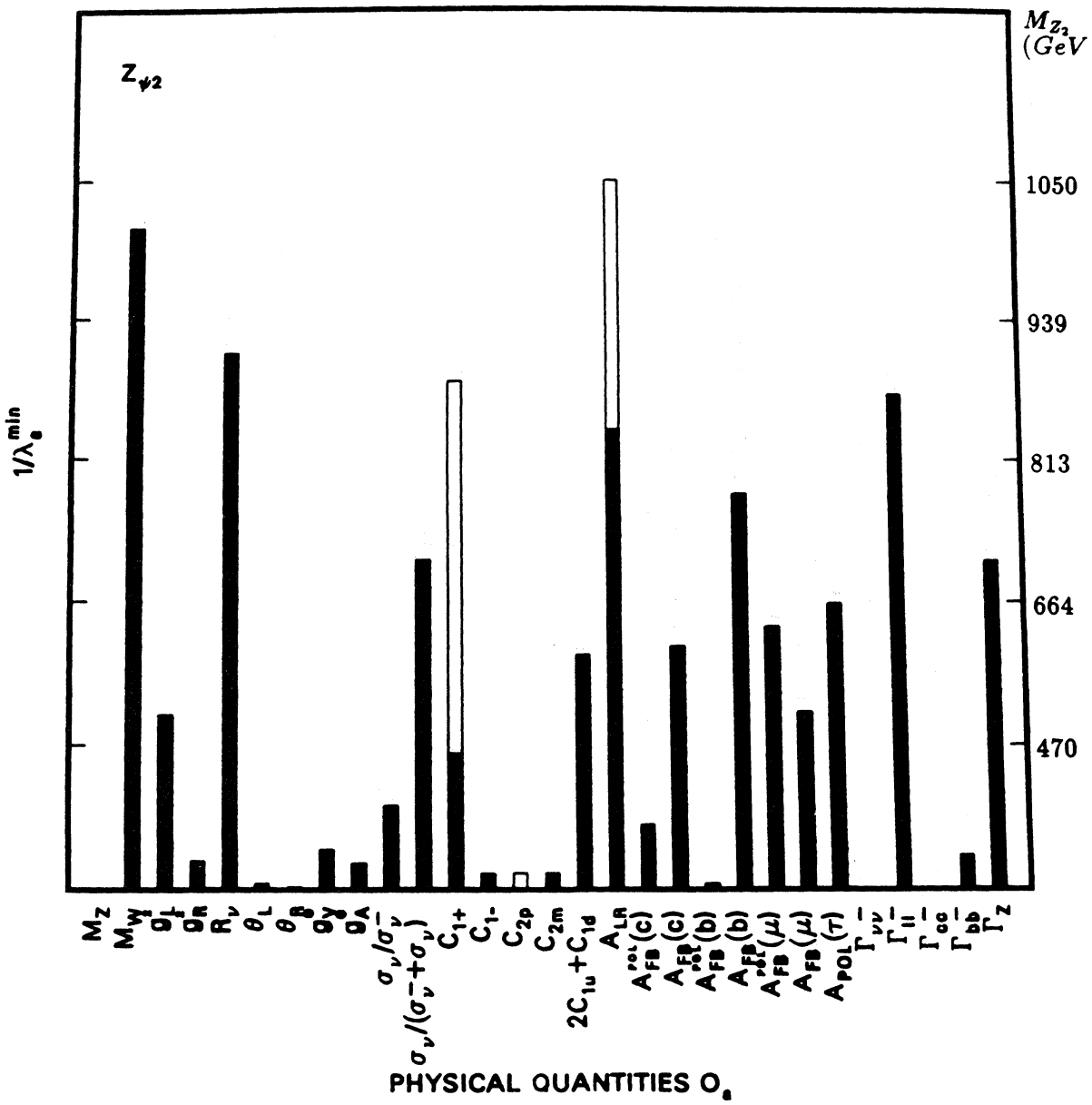

FIG. 37. The new physics of Z_ψ with $C=-(2/3)^{1/2}$: solid bar for C_{1+}, C_{2p}, and A_{LR}(SLC); open bar for C_{1+}(iso), $C_{2p}(1)$, and A_{LR}(LEP).

TABLE XII. Deviations from the SM by an extra Z_ψ boson (no mixing). Type: Z_ψ. Free parameter: $\lambda=(g_2^2/M_{Z_2}^2)/(g_1^2/M_Z^2)$ with $C=\Theta(g_2/g_1)/\lambda=0$ (Sec. IV.A). g_1, g_2 and M_Z, M_{Z_2} are the coupling constants and masses of the ordinary Z and the extra Z_ψ bosons, respectively; Θ is their mixing angle. Inputs: $M_Z=91.177$ GeV, $m_t=100$ GeV, $M_H=100$ GeV ($\sin^2\theta_W^M=0.2306$, $\sin^2\hat{\theta}_W=0.2334$). **Comments:** The inverses of the sixth column $1/\lambda^{\min}$ are plotted in Fig. 38. $Z_\psi(C=0)$ has no effect on Z-pole physics, M_W, or on the atomic parity-violation coefficients. The most likely candidate to see $Z_\psi(C=0)$ is $\sigma_{\nu_\mu e}/(\sigma_{\nu_e e}+\sigma_{\bar{\nu}_\mu e})$; its $\lambda^{\min}=0.025$ corresponds to $M_{Z_2}=357$ GeV.

Quantities	O_a^{SM}	ΔO_a^{exp}	ΔO_a^i $\lambda=0.01$	λ_a^{min}	$\Delta \sin^2\theta_W^{exp}$	$\Delta \sin^2\theta_W^{(a;Z)}$ $\lambda=0.01$
$M_Z(GeV)$	91.1770	0.0200	—	—	0.0003	—
g_L^2	0.2997	0.0042	−0.0001	0.3027	0.0057	0.0002
g_R^2	0.0301	0.0034	0.0001	0.2633	0.0130	0.0005
R_ν	0.3117	0.0013	−0.0001	0.1466	0.0020	0.0001
θ_L	2.4640	0.0300	−0.0021	0.1402	—	—
θ_R	5.1765	0.4400	−0.0064	0.6828	—	—
g_V^e	−0.0361	0.0220	0.0000	—	0.0110	0.0000
g_A^e	−0.5037	0.0250	0.0017	0.1500	—	—
$\sigma_\nu/\sigma_{\bar{\nu}}$	1.1515	0.0453	0.0005	0.8360	0.0050	−0.0001
$\sigma_\nu/(\sigma_{\bar{\nu}}+\sigma_\nu)$	0.1455	0.0026	−0.0010	0.0250	0.0025	0.0010
C_{1+}	0.1291	0.0013	0.0000	—	0.0033	0.0000
$C_{1+}(iso)$	0.1291	0.0003	0.0000	—	0.0009	0.0000
C_{1-}	−0.3633	0.1000	0.0000	—	0.0689	0.0000
C_{2p}	−0.0140	0.0460	0.0000	—	—	—
$C_{2p}(1)$	−0.0140	0.0046	0.0000	—	—	—
C_{2m}	−0.0537	0.1100	0.0000	—	0.0274	0.0000
$2C_{1u}+C_{1d}$	−0.0323	0.0040	0.0000	—	0.0020	0.0000

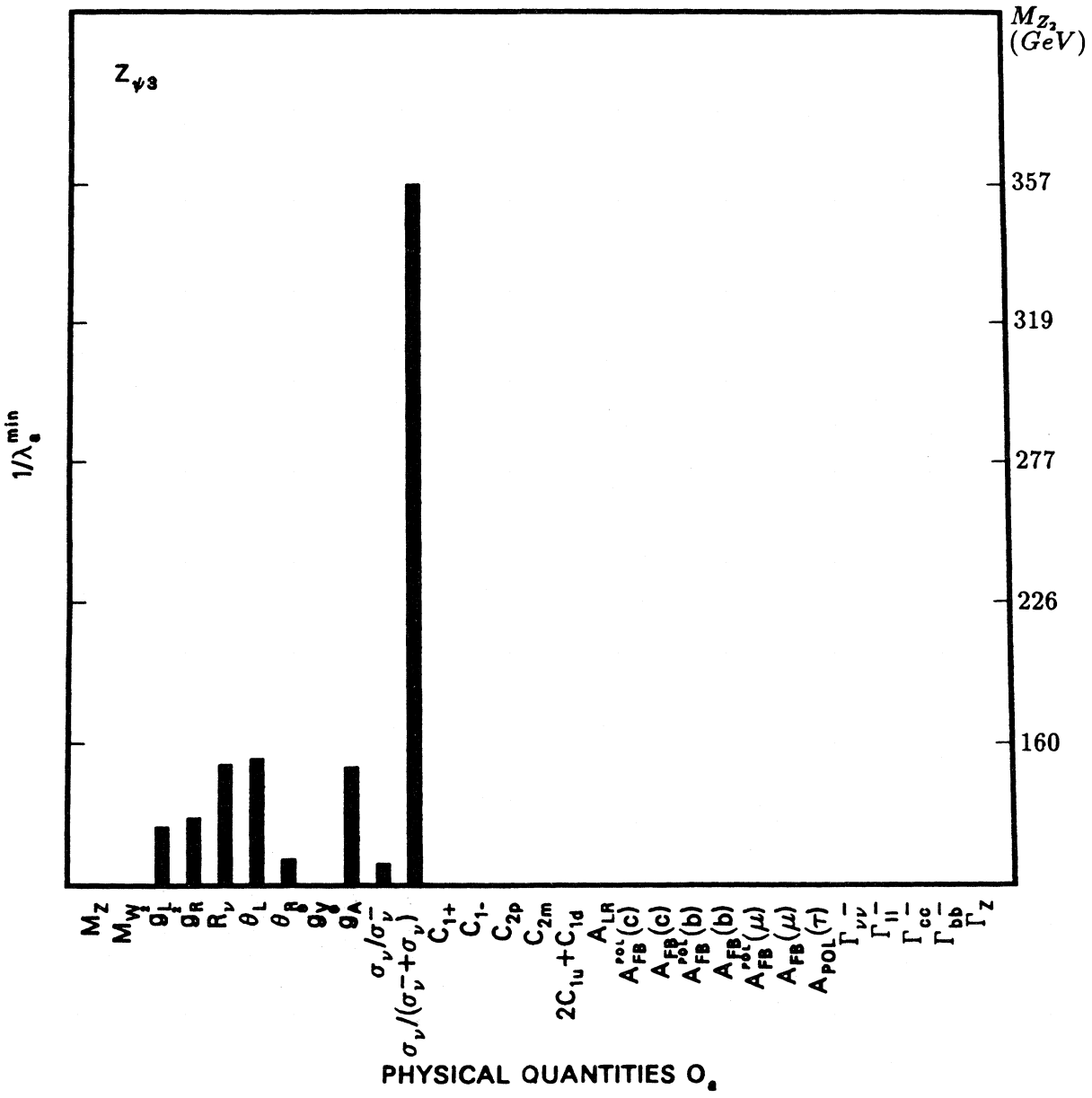

FIG. 38. The new physics of Z_ψ with $C=0$.

TABLE XIII. Deviations from the SM by an extra Z_η boson [$C=-(1/15)^{1/2}$]. Type: Z_η. Free parameter: $\lambda=(g_2^2/M_{Z_2}^2)/(g_1^2/M_Z^2)$ with $C=\Theta(g_2/g_1)/\lambda=-1/\sqrt{15}$ (Sec. IV.A). g_1, g_2 and M_Z, M_{Z_2} are the coupling constants and masses of the ordinary Z and the extra Z_η bosons, respectively; Θ is their mixing angle. Inputs: $M_Z=91.177$ GeV, $m_t=100$ GeV, $M_H=100$ GeV ($\sin^2\theta_W^M=0.2306$, $\sin^2\hat{\theta}_W=0.2334$). **Comments:** The inverses of the sixth column $1/\lambda^{\min}$ are plotted in Fig. 39. $A_{\rm LR}$(LEP) has $\lambda_a^{\min}=0.0075$, which corresponds to $M_{Z_2}=650$ GeV for $g_2^2/g_1^2=\frac{5}{3}\sin^2\theta_W$. $C_{2p}(1)$, $A_{\rm LR}$(SLC), and $A_{\rm FB}(b)$ would be sensitive to M_{Z_2} up to 500–600 GeV.

Quantities	O_a^{SM}	ΔO_a^{exp}	ΔO_a^i $\lambda=0.01$	λ_a^{min}	$\Delta\sin^2\theta_W^{exp}$	$\Delta\sin^2\theta_W^{(a;Z)}$ $\lambda=0.01$
$M_Z(GeV)$	91.1770	0.0200	—	—	0.0003	—
$M_W(GeV)$	79.9832	0.1050	0.0381	0.0276	0.0006	−0.0002
g_L^2	0.2997	0.0042	0.0002	0.2581	0.0057	−0.0002
g_R^2	0.0301	0.0034	−0.0001	0.5993	0.0130	−0.0002
R_ν	0.3117	0.0013	0.0001	0.0912	0.0020	−0.0002
θ_L	2.4640	0.0300	−0.0001	—	—	—
θ_R	5.1765	0.4400	0.0000	—	—	—
g_V^e	−0.0361	0.0220	−0.0004	0.5015	0.0110	−0.0002
g_A^e	−0.5037	0.0250	0.0000	—	—	—
$\sigma_\nu/\sigma_{\bar{\nu}}$	1.1515	0.0453	0.0020	0.2280	0.0050	−0.0002
$\sigma_\nu/(\sigma_{\bar{\nu}}+\sigma_\nu)$	0.1455	0.0026	0.0002	0.1140	0.0025	−0.0002
C_{1+}	0.1291	0.0013	−0.0001	0.1357	0.0033	−0.0002
$C_{1+}(iso)$	0.1291	0.0003	−0.0001	0.0353	0.0009	−0.0002
C_{1-}	−0.3633	0.1000	−0.0003	—	0.0689	−0.0002
C_{2p}	−0.0140	0.0460	−0.0051	0.0899	—	—
$C_{2p}(1)$	−0.0140	0.0046	−0.0051	0.0090	—	—
C_{2m}	−0.0537	0.1100	−0.0060	0.1836	0.0274	−0.0015
$2C_{1u}+C_{1d}$	−0.0323	0.0040	−0.0005	0.0884	0.0020	−0.0002
$A_{LR}(SLC)$	0.1306	0.0066	0.0057	0.0119	0.0008	−0.0007
$A_{LR}(LEP)$	0.1306	0.0041	0.0057	0.0075	0.0005	−0.0007
$A_{FB}^{pol}(c)$	0.4725	0.0250	−0.0004	0.6000	0.0095	0.0002
$A_{FB}(c)$	0.0617	0.0070	0.0026	0.0264	0.0017	−0.0007
$A_{FB}^{pol}(b)$	0.6965	0.0200	−0.0004	0.4524	0.0423	0.0009
$A_{FB}(b)$	0.0910	0.0054	0.0039	0.0140	0.0010	−0.0007
$A_{FB}^{pol}(\mu)$	0.0980	0.0090	0.0043	0.0210	0.0015	−0.0007
$A_{FB}(\mu)$	0.0128	0.0035	0.0011	0.0312	0.0023	−0.0007
$A_{pol}(\tau)$	0.1306	0.0110	0.0057	0.0192	0.0014	−0.0007
$\Gamma_{inv}(GeV)$	0.4990	0.0160	−0.0003	0.4839	0.0070	0.0001
$\Gamma_{l\bar{l}}(GeV)$	0.0835	0.0007	0.0000	0.3435	0.0016	0.0000
$\Gamma_{c\bar{c}}(GeV)$	0.2959	0.0300	0.0016	0.1839	0.0161	−0.0009
$\Gamma_{b\bar{b}}(GeV)$	0.3773	0.0400	−0.0007	0.5916	0.0184	0.0003
$\Gamma_Z(GeV)$	2.4837	0.0150	0.0008	0.1779	0.0011	−0.0001

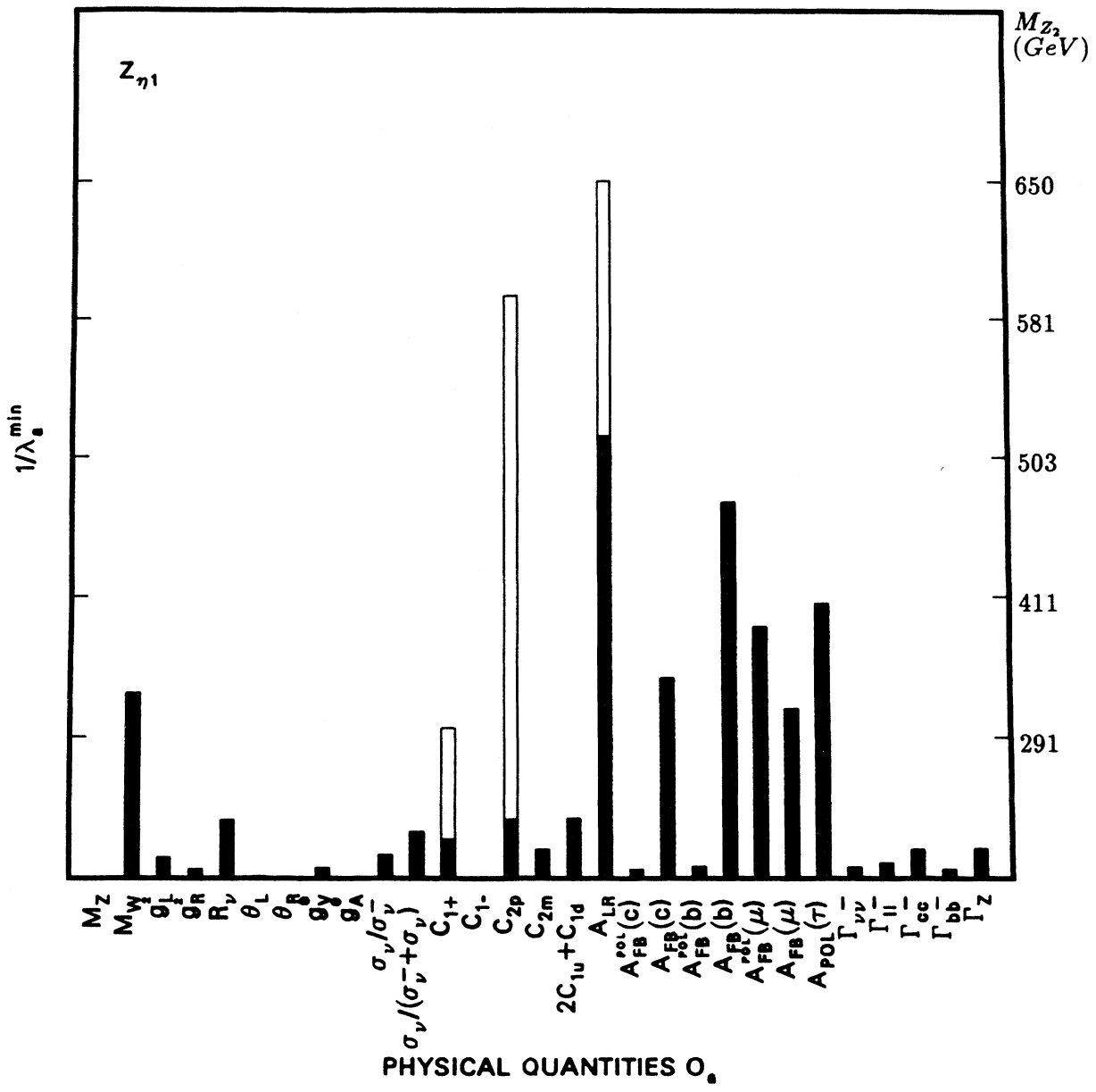

FIG. 39. The new physics of Z_η with $C = -(1/15)^{1/2}$: solid bar for C_{1+}, C_{2p}, and A_{LR}(SLC); open bar for C_{1+}(iso), $C_{2p}(1)$, and A_{LR}(LEP).

TABLE XIV. Deviations from the SM by an extra Z_η boson [$C=(16/15)^{1/2}$]. Type: Z_η. Free parameter: $\lambda=(g_2^2/M_{Z_2}^2)/(g_1^2/M_Z^2)$ with $C=\Theta(g_2/g_1)/\lambda=4/\sqrt{15}$; (Sec. IV.A). g_1, g_2, and M_Z, M_{Z_2} are the coupling constants and masses of the ordinary Z and the extra Z_η bosons, respectively; Θ is their mixing angle. Inputs: $M_Z=91.177$ GeV, $m_t=100$ GeV, $M_H=100$ GeV ($\sin^2\theta_W^M=0.2306$, $\sin^2\hat{\theta}_W=0.2334$). **Comments:** The inverses of the sixth column $1/\lambda^{\min}$ are plotted in Fig. 40. C_{1+}(iso) has $\lambda_a^{\min}=0.0008$, which corresponds to $M_{Z_2}=2000$ GeV. M_W and R_ν would be sensitive up to 1300–1600 GeV.

Quantities	O_a^{SM}	ΔO_a^{exp}	ΔO_a^i $\lambda=0.01$	λ_a^{min}	$\Delta\sin^2\theta_W^{exp}$	$\Delta\sin^2\theta_W^{(a;Z)}$ $\lambda=0.01$
$M_Z(GeV)$	91.1770	0.0200	—	—	0.0003	—
$M_W(GeV)$	79.9832	0.1050	0.6090	0.0017	0.0006	−0.0035
g_L^2	0.2997	0.0042	0.0111	0.0038	0.0057	−0.0150
g_R^2	0.0301	0.0034	−0.0014	0.0243	0.0130	−0.0054
R_ν	0.3117	0.0013	0.0106	0.0012	0.0020	−0.0166
θ_L	2.4640	0.0300	0.0066	0.0457	—	—
θ_R	5.1765	0.4400	0.0000	—	—	—
g_V^e	−0.0361	0.0220	−0.0025	0.0880	0.0110	−0.0013
g_A^e	−0.5037	0.0250	−0.0084	0.0298	—	—
$\sigma_\nu/\sigma_{\bar{\nu}}$	1.1515	0.0453	0.0086	0.0527	0.0050	−0.0009
$\sigma_\nu/(\sigma_{\bar{\nu}}+\sigma_\nu)$	0.1455	0.0026	0.0066	0.0040	0.0025	−0.0063
C_{1+}	0.1291	0.0013	0.0041	0.0032	0.0033	0.0105
$C_{1+}(iso)$	0.1291	0.0003	0.0041	0.0008	0.0009	0.0105
C_{1-}	−0.3633	0.1000	−0.0133	0.0751	0.0689	−0.0092
C_{2p}	−0.0140	0.0460	−0.0047	0.0976	—	—
$C_{2p}(1)$	−0.0140	0.0046	−0.0047	0.0098	—	—
C_{2m}	−0.0537	0.1100	−0.0093	0.1178	0.0274	−0.0023
$2C_{1u}+C_{1d}$	−0.0323	0.0040	−0.0025	0.0163	0.0020	−0.0012
$A_{LR}(SLC)$	0.1306	0.0066	0.0114	0.0059	0.0008	−0.0015
$A_{LR}(LEP)$	0.1306	0.0041	0.0114	0.0038	0.0005	−0.0015
$A_{FB}^{pol}(c)$	0.4725	0.0250	0.0132	0.0189	0.0095	−0.0050
$A_{FB}(c)$	0.0617	0.0070	0.0071	0.0098	0.0017	−0.0018
$A_{FB}^{pol}(b)$	0.6965	0.0200	0.0038	0.0520	0.0423	−0.0081
$A_{FB}(b)$	0.0910	0.0054	0.0085	0.0065	0.0010	−0.0015
$A_{FB}^{pol}(\mu)$	0.0980	0.0090	0.0086	0.0105	0.0015	−0.0015
$A_{FB}(\mu)$	0.0128	0.0035	0.0022	0.0156	0.0023	−0.0015
$A_{pol}(\tau)$	0.1306	0.0110	0.0114	0.0096	0.0014	−0.0015
$\Gamma_{inv}(GeV)$	0.4990	0.0160	0.0080	0.0201	0.0070	−0.0035
$\Gamma_{l\bar{l}}(GeV)$	0.0835	0.0007	0.0014	0.0049	0.0016	−0.0033
$\Gamma_{c\bar{c}}(GeV)$	0.2959	0.0300	−0.0003	0.8861	0.0161	0.0002
$\Gamma_{b\bar{b}}(GeV)$	0.3773	0.0400	0.0098	0.0410	0.0184	−0.0045
$\Gamma_Z(GeV)$	2.4837	0.0150	0.0408	0.0037	0.0011	−0.0030

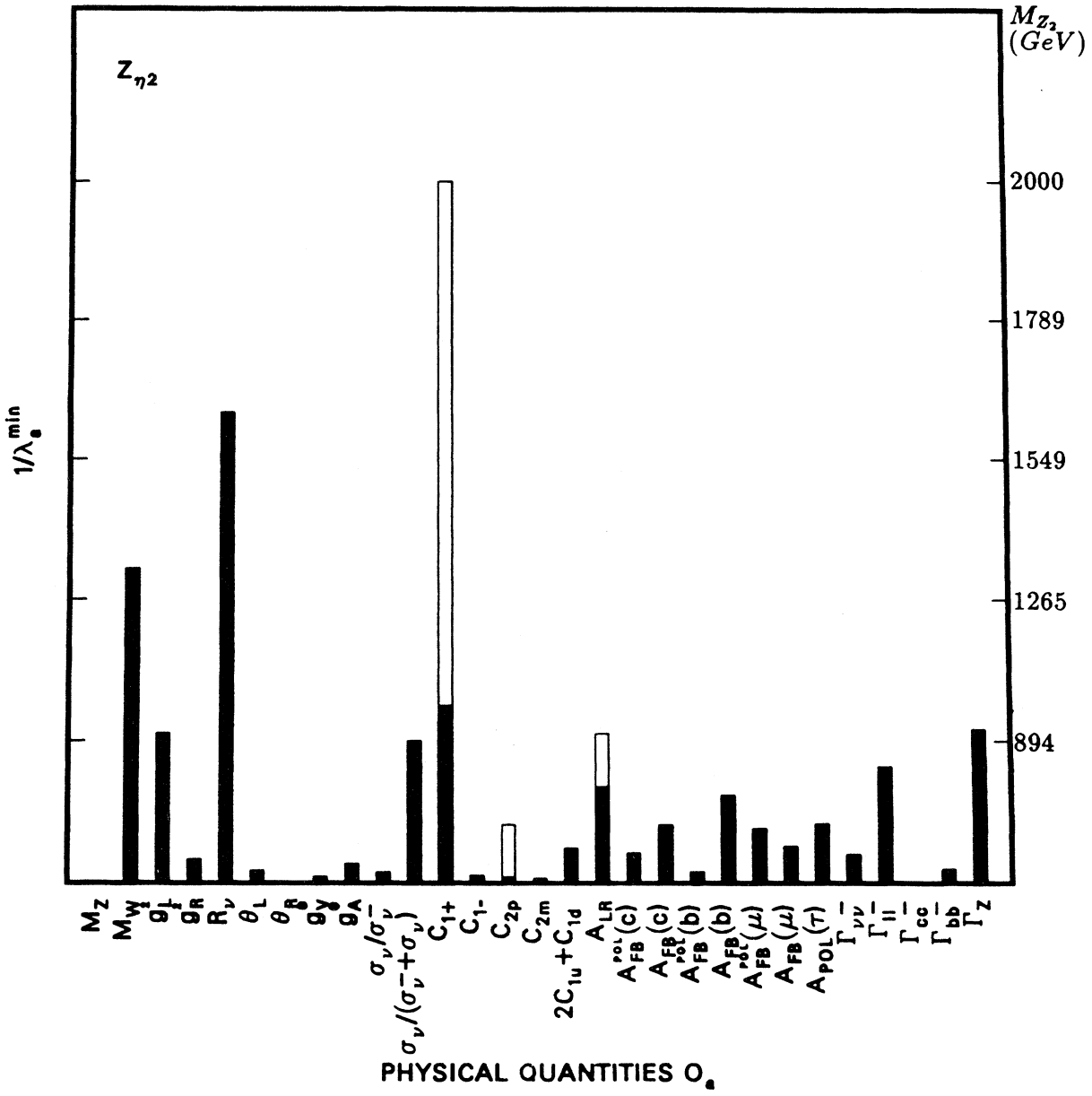

FIG. 40. The new physics of Z_η with $C=(16/15)^{1/2}$: solid bar for C_{1+}, C_{2p}, and A_{LR}(SLC); open bar for C_{1+}(iso), $C_{2p}(1)$, and A_{LR}(LEP).

TABLE XV. Deviations from the SM by an extra Z_η boson (no mixing). Type: Z_η. Free parameter: $\lambda=(g_2^2/M_{Z_2}^2)/(g_1^2/M_Z^2)$ with $C=\Theta(g_2/g_1)/\lambda=0$ (Sec. IV.A). g_1, g_2 and M_Z, M_{Z_2} are the coupling constants and masses of the ordinary Z and the extra Z_η bosons, respectively; Θ is their mixing angle. Inputs: $M_Z=91.177$ GeV, $m_t=100$ GeV, $M_H=100$ GeV ($\sin^2\theta_W^M=0.2306$, $\sin^2\hat{\theta}_W=0.2334$). **Comments:** The inverses of the sixth column $1/\lambda^{\min}$ are plotted in Fig. 41. $Z_\eta(C=0)$ has no effect on Z-pole physics or M_W. A good candidate to see $Z_\eta(C=0)$ is C_{1+}(iso), which has $\lambda^{\min}=0.0045$ corresponding to $M_{Z_2}=840$ GeV. $C_{2p}(1)$ would be sensitive up to 590 GeV.

Quantities	O_a^{SM}	ΔO_a^{exp}	ΔO_a^i $\lambda=0.01$	λ_a^{min}	$\Delta\sin^2\theta_W^{exp}$	$\Delta\sin^2\theta_W^{(a;Z)}$ $\lambda=0.01$
$M_Z(GeV)$	91.1770	0.0200	—	—	0.0003	—
g_L^2	0.2997	0.0042	0.0001	0.3783	0.0057	−0.0001
g_R^2	0.0301	0.0034	−0.0003	0.1314	0.0130	−0.0010
R_ν	0.3117	0.0013	0.0000	—	0.0020	0.0000
θ_L	2.4640	0.0300	0.0017	0.1752	—	—
θ_R	5.1765	0.4400	0.0000	—	—	—
g_V^e	−0.0361	0.0220	0.0010	0.2200	0.0110	0.0005
g_A^e	−0.5037	0.0250	−0.0003	0.7500	—	—
$\sigma_\nu/\sigma_{\bar{\nu}}$	1.1515	0.0453	−0.0046	0.0977	0.0050	0.0005
$\sigma_\nu/(\sigma_{\bar{\nu}}+\sigma_\nu)$	0.1455	0.0026	−0.0003	0.0833	0.0025	0.0003
C_{1+}	0.1291	0.0013	0.0007	0.0174	0.0033	0.0019
$C_{1+}(iso)$	0.1291	0.0003	0.0007	0.0045	0.0009	0.0019
C_{1-}	−0.3633	0.1000	−0.0007	—	0.0689	−0.0005
C_{2p}	−0.0140	0.0460	−0.0050	0.0920	—	—
$C_{2p}(1)$	−0.0140	0.0046	−0.0050	0.0092	—	—
C_{2m}	−0.0537	0.1100	−0.0030	0.3667	0.0274	−0.0007
$2C_{1u}+C_{1d}$	−0.0323	0.0040	0.0010	0.0400	0.0020	0.0005

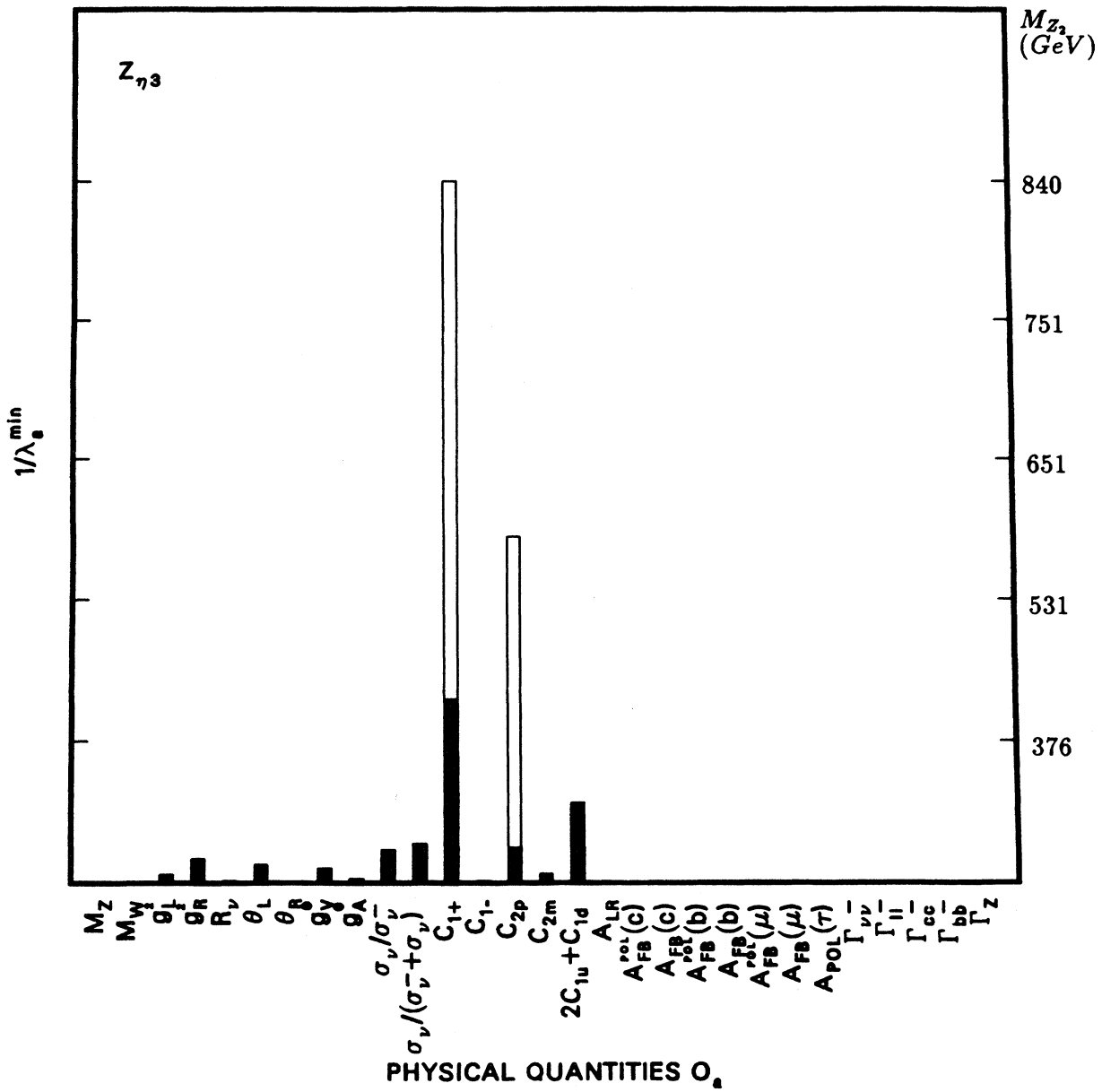

FIG. 41. The new physics of Z_η with $C=0$: solid bar for C_{1+} and C_{2p}; open bar for C_{1+}(iso) and $C_{2p}(1)$.

TABLE XVI. Deviations from the SM by an extra Z_{3R} boson [$C=(3/5)^{1/2}\alpha$]. Type: Z_{3R}. Free parameter: $\lambda=(g_2^2/M_{Z_2}^2)/(g_1^2/M_Z^2)$ with $C=\Theta(g_2/g_1)/\lambda=\sqrt{3/5}\alpha$ (Sec. IV.A). g_1, g_2 and M_Z, M_{Z_2} are the coupling constants and masses of the ordinary Z and the extra Z_{3R} bosons, respectively; Θ is their mixing angle. Note that here $\alpha=[(1-2\sin^2\theta_W)/\sin^2\theta_W]^{1/2}$. Inputs; $M_Z=91.177$ GeV, $m_t=100$ GeV, $M_H=100$ GeV ($\sin^2\theta_W^M=0.2306$, $\sin^2\hat{\theta}_W=0.2334$). **Comments:** The inverses of the sixth column $1/\lambda^{\min}$ are plotted in Fig. 42. R_ν has $\lambda^{\min}=0.0009$, corresponding to $M_{Z_2}\sim 1880$ GeV, and $A_{\rm LR}$(LEP) has $\lambda^{\min}=0.0010$ (1780 GeV). M_W, $A_{\rm LR}$(SLC), C_{1+}(iso), and $A_{\rm FB}(b)$ are sensitive up to 1300–1500 GeV.

Quantities	O_a^{SM}	ΔO_a^{exp}	ΔO_a^i $\lambda=0.01$	λ_a^{min}	$\Delta\sin^2\theta_W^{exp}$	$\Delta\sin^2\theta_W^{(a;Z)}$ $\lambda=0.01$
$M_Z(GeV)$	91.1770	0.0200	—	—	0.0003	—
$M_W(GeV)$	79.9832	0.1050	0.8042	0.0013	0.0006	−0.0046
g_L^2	0.2997	0.0042	0.0157	0.0027	0.0057	−0.0212
g_R^2	0.0301	0.0034	−0.0044	0.0076	0.0130	−0.0172
R_ν	0.3117	0.0013	0.0139	0.0009	0.0020	−0.0218
θ_L	2.4640	0.0300	0.0010	0.2900	—	—
θ_R	5.1765	0.4400	−0.0369	0.1193	—	—
g_V^e	−0.0361	0.0220	−0.0115	0.0192	0.0110	−0.0057
g_A^e	−0.5037	0.0250	−0.0001	—	—	—
$\sigma_\nu/\sigma_{\bar{\nu}}$	1.1515	0.0453	0.0520	0.0087	0.0050	−0.0057
$\sigma_\nu/(\sigma_{\bar{\nu}}+\sigma_\nu)$	0.1455	0.0026	0.0061	0.0043	0.0025	−0.0058
C_{1+}	0.1291	0.0013	−0.0019	0.0069	0.0033	−0.0048
$C_{1+}(iso)$	0.1291	0.0003	−0.0019	0.0018	0.0009	−0.0048
C_{1-}	−0.3633	0.1000	−0.0067	0.1501	0.0689	−0.0046
C_{2p}	−0.0140	0.0460	−0.0002	—	—	—
$C_{2p}(1)$	−0.0140	0.0046	−0.0002	0.2476	—	—
C_{2m}	−0.0537	0.1100	−0.0183	0.0600	0.0274	−0.0046
$2C_{1u}+C_{1d}$	−0.0323	0.0040	−0.0094	0.0042	0.0020	−0.0047
$A_{LR}(SLC)$	0.1306	0.0066	0.0423	0.0016	0.0008	−0.0054
$A_{LR}(LEP)$	0.1306	0.0041	0.0423	0.0010	0.0005	−0.0054
$A_{FB}^{pol}(c)$	0.4725	0.0250	0.0275	0.0091	0.0095	−0.0104
$A_{FB}(c)$	0.0617	0.0070	0.0236	0.0030	0.0017	−0.0058
$A_{FB}^{pol}(b)$	0.6965	0.0200	0.0121	0.0166	0.0423	−0.0255
$A_{FB}(b)$	0.0910	0.0054	0.0310	0.0018	0.0010	−0.0056
$A_{FB}^{pol}(\mu)$	0.0980	0.0090	0.0317	0.0028	0.0015	−0.0054
$A_{FB}(\mu)$	0.0128	0.0035	0.0083	0.0042	0.0023	−0.0054
$A_{pol}(\tau)$	0.1306	0.0110	0.0423	0.0026	0.0014	−0.0054
$\Gamma_{inv}(GeV)$	0.4990	0.0160	0.0130	0.0123	0.0070	−0.0057
$\Gamma_{l\bar{l}}(GeV)$	0.0835	0.0007	−0.0009	0.0077	0.0016	0.0021
$\Gamma_{c\bar{c}}(GeV)$	0.2959	0.0300	0.0014	0.2083	0.0161	−0.0008
$\Gamma_{b\bar{b}}(GeV)$	0.3773	0.0400	0.0067	0.0601	0.0184	−0.0031
$\Gamma_Z(GeV)$	2.4837	0.0150	0.0331	0.0045	0.0011	−0.0024

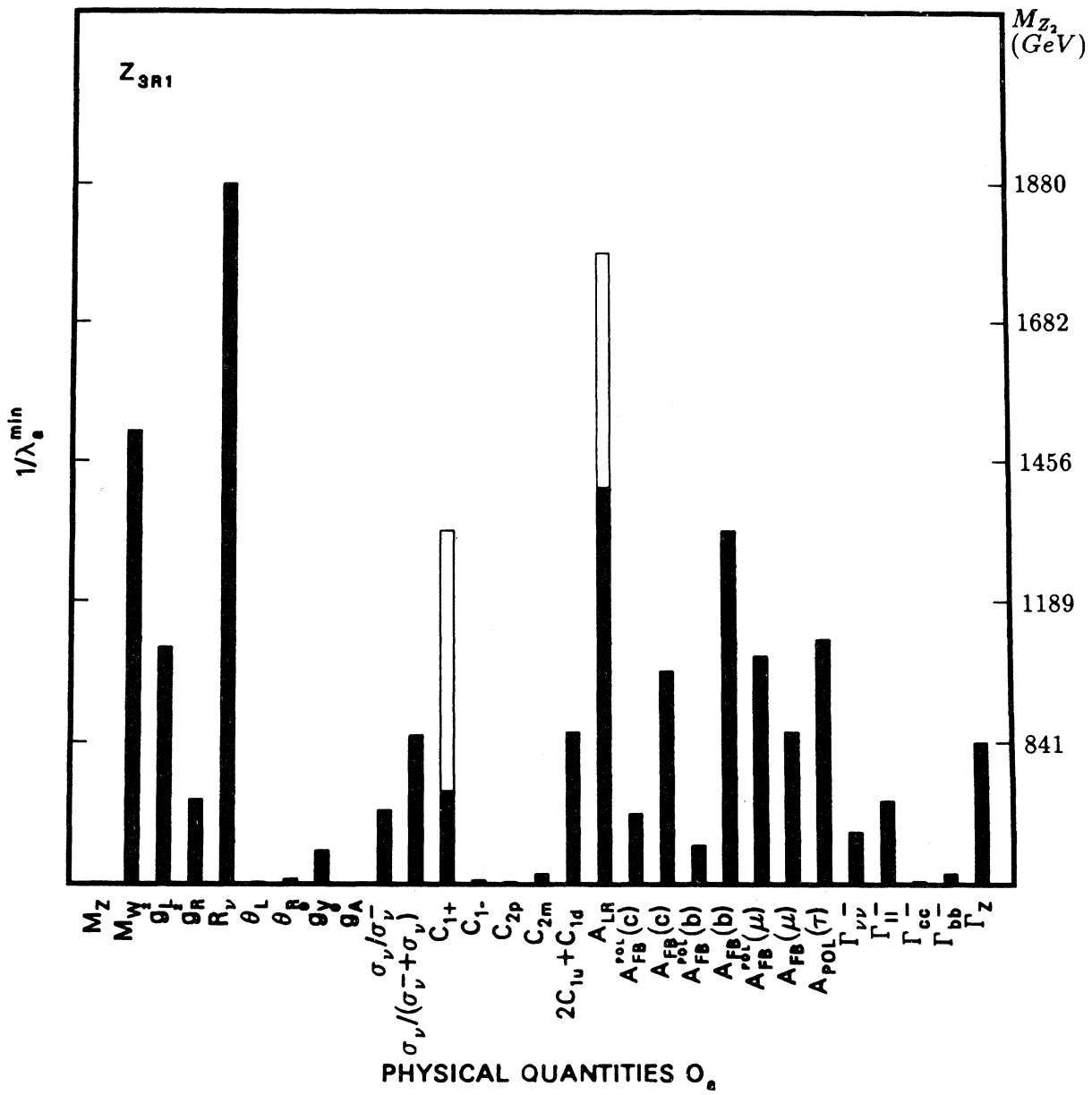

FIG. 42. The new physics of Z_{3R} with $C=(3/5)^{1/2}\alpha$: solid bar for C_{1+} and A_{LR}(SLC); open bar for C_{1+}(iso), and A_{LR}(LEP).

TABLE XVII. Deviations from the SM by an extra Z_{3R} boson [$C=-(3/5)^{1/2}/\alpha$]. Type: Z_{3R}. Free parameter: $\lambda=(g_2^2/M_{Z_2}^2)/(g_1^2/M_Z^2)$ with $C=\Theta(g_2/g_1)/\lambda=-(3/5)^{1/2}/\alpha$ (Sec. IV.A). g_1, g_2 and M_Z, M_{Z_2} are the coupling constants and masses of the ordinary Z and the extra Z_{3R} bosons, respectively; Θ is their mixing angle. Note that here $\alpha=[(1-2\sin^2\theta_W)/\sin^2\theta_W]^{1/2}$. Inputs: $M_Z=91.177$ GeV, $m_t=100$ GeV, $M_H=100$ GeV ($\sin^2\theta_W^M=0.2306$, $\sin^2\hat{\theta}_W=0.2334$). **Comments**: The inverses of the sixth column $1/\lambda^{\min}$ are plotted in Fig. 43. For C_{1+}(iso) in cesium, this extra Z boson has $\lambda^{\min}=0.0008$, corresponding to $M_{Z_2}=2000$ GeV, while for C_{1+}, $\lambda^{\min}=0.0032$, $M_{Z_2}\cong 1000$ GeV.

Quantities	O_a^{SM}	ΔO_a^{exp}	ΔO_a^i $\lambda=0.01$	λ_a^{min}	$\Delta\sin^2\theta_W^{exp}$	$\Delta\sin^2\theta_W^{(a;Z)}$ $\lambda=0.01$
$M_Z(GeV)$	91.1770	0.0200	—	—	0.0003	—
$M_W(GeV)$	79.9832	0.1050	0.1459	0.0072	0.0006	−0.0008
g_L^2	0.2997	0.0042	0.0006	0.0673	0.0057	−0.0008
g_R^2	0.0301	0.0034	−0.0002	0.1563	0.0130	−0.0008
R_ν	0.3117	0.0013	0.0005	0.0238	0.0020	−0.0008
θ_L	2.4640	0.0300	−0.0005	0.6293	—	—
θ_R	5.1765	0.4400	0.0000	—	—	—
g_V^e	−0.0361	0.0220	−0.0017	0.1308	0.0110	−0.0008
g_A^e	−0.5037	0.0250	0.0000	—	—	—
$\sigma_\nu/\sigma_{\bar{\nu}}$	1.1515	0.0453	0.0076	0.0595	0.0050	−0.0008
$\sigma_\nu/(\sigma_{\bar{\nu}}+\sigma_\nu)$	0.1455	0.0026	0.0009	0.0297	0.0025	−0.0008
C_{1+}	0.1291	0.0013	−0.0040	0.0032	0.0033	−0.0103
$C_{1+}(iso)$	0.1291	0.0003	−0.0040	0.0008	0.0009	−0.0103
C_{1-}	−0.3633	0.1000	0.0096	0.1041	0.0689	0.0066
C_{2p}	−0.0140	0.0460	0.0000	—	—	—
$C_{2p}(1)$	−0.0140	0.0046	0.0000	—	—	—
C_{2m}	−0.0537	0.1100	−0.0010	—	0.0274	−0.0002
$2C_{1u}+C_{1d}$	−0.0323	0.0040	−0.0004	0.0891	0.0020	−0.0002
$A_{LR}(SLC)$	0.1306	0.0066	0.0040	0.0170	0.0008	−0.0005
$A_{LR}(LEP)$	0.1306	0.0041	0.0040	0.0108	0.0005	−0.0005
$A_{FB}^{pol}(c)$	0.4725	0.0250	−0.0043	0.0585	0.0095	0.0016
$A_{FB}(c)$	0.0617	0.0070	0.0013	0.0526	0.0017	−0.0003
$A_{FB}^{pol}(b)$	0.6965	0.0200	−0.0038	0.0525	0.0423	0.0081
$A_{FB}(b)$	0.0910	0.0054	0.0023	0.0241	0.0010	−0.0004
$A_{FB}^{pol}(\mu)$	0.0980	0.0090	0.0030	0.0300	0.0015	−0.0005
$A_{FB}(\mu)$	0.0128	0.0035	0.0008	0.0447	0.0023	−0.0005
$A_{pol}(\tau)$	0.1306	0.0110	0.0040	0.0275	0.0014	−0.0005
$\Gamma_{inv}(GeV)$	0.4990	0.0160	−0.0013	0.1262	0.0070	0.0006
$\Gamma_{l\bar{l}}(GeV)$	0.0835	0.0007	0.0012	0.0056	0.0016	−0.0029
$\Gamma_{c\bar{c}}(GeV)$	0.2959	0.0300	0.0034	0.0894	0.0161	−0.0018
$\Gamma_{b\bar{b}}(GeV)$	0.3773	0.0400	0.0017	0.2372	0.0184	−0.0008
$\Gamma_Z(GeV)$	2.4837	0.0150	0.0143	0.0105	0.0011	−0.0010

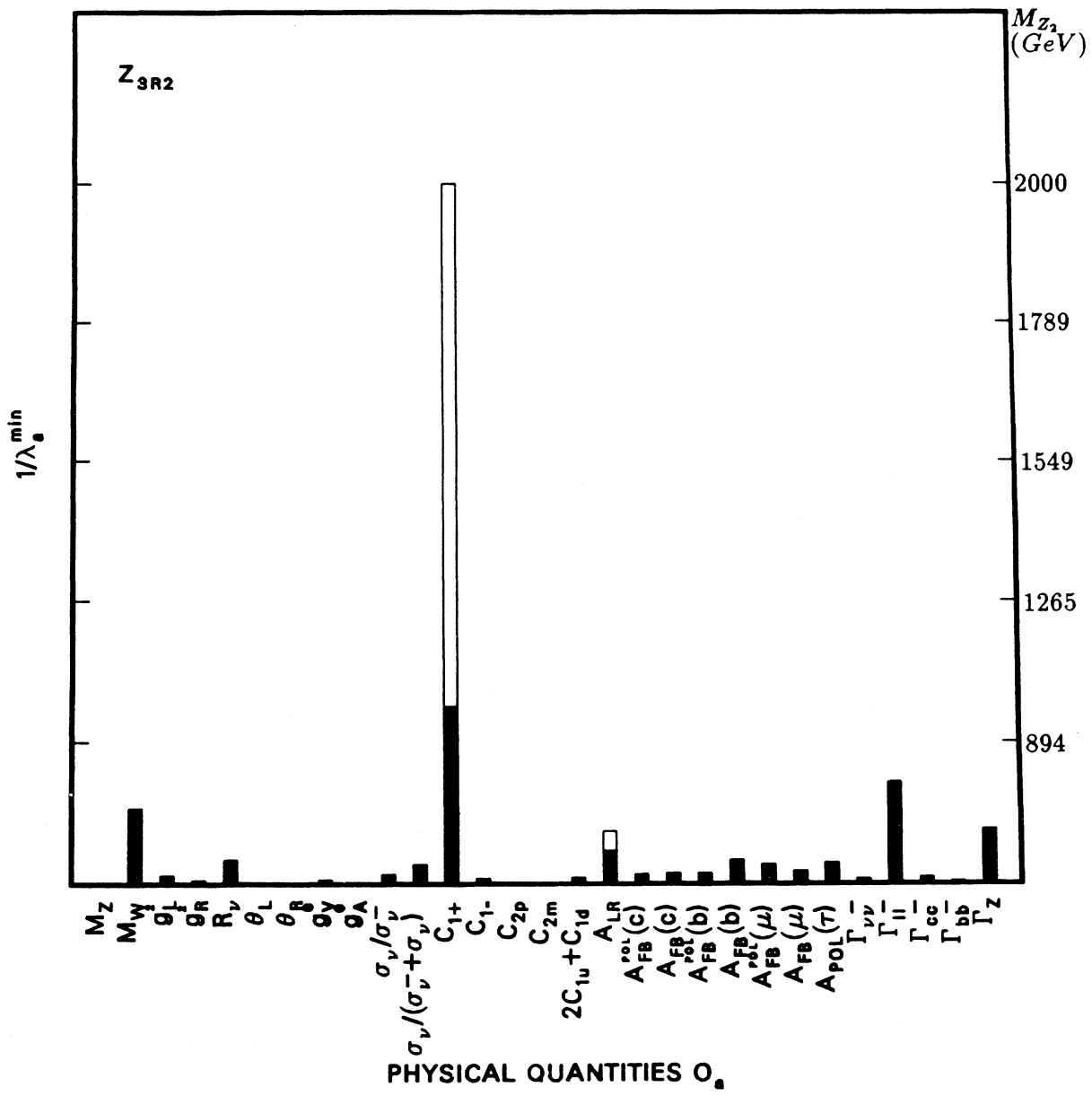

FIG. 43. The new physics of Z_{3R} with $C=-(3/5)^{1/2}/\alpha$: solid bar for C_{1+} and $A_{\rm LR}$(SLC); open bar for C_{1+}(iso) and $A_{\rm LR}$(LEP).

TABLE XVIII. Deviations from the SM by an extra Z_{3R} boson (no mixing). Type: Z_{3R}. Free parameter: $\lambda=(g_2^2/M_{Z_2}^2)/(g_1^2/M_Z^2)$ with $C=\Theta(g_2/g_1)/\lambda=0$ (Sec. IV.A). g_1, g_2, and M_Z, M_{Z_2} are the coupling constants and masses of the ordinary Z and the extra Z_{3R} bosons, respectively; Θ is their mixing angle. Inputs: $M_Z=91.177$ GeV, $m_t=100$ GeV, $M_H=100$ GeV ($\sin^2\theta_W^M=0.2306$, $\sin^2\hat{\theta}_W=0.2334$). **Comments:** The inverses of the sixth column $1/\lambda^{\min}$ are plotted in Fig. 44. $Z_{3R}(C=0)$ has no effect on Z-pole physics or M_W. For C_{1+}(iso), $\lambda^{\min}=0.0010$ corresponding to $M_{Z_2}=1785$ GeV, while for C_{1+}, $\lambda^{\min}=0.0038$, $M_{Z_2}=917$ GeV.

Quantities	O_a^{SM}	ΔO_a^{exp}	ΔO_a^i $\lambda=0.01$	λ_a^{min}	$\Delta\sin^2\theta_W^{exp}$	$\Delta\sin^2\theta_W^{(a;Z)}$ $\lambda=0.01$
$M_Z(GeV)$	91.1770	0.0200	—	—	0.0003	—
g_L^2	0.2997	0.0042	0.0001	0.5921	0.0057	−0.0001
g_R^2	0.0301	0.0034	−0.0013	0.0255	0.0130	−0.0051
R_ν	0.3117	0.0013	−0.0005	0.0277	0.0020	0.0007
θ_L	2.4640	0.0300	0.0011	0.2742	—	—
θ_R	5.1765	0.4400	−0.0110	0.3995	—	—
g_V^e	−0.0361	0.0220	−0.0004	0.4950	0.0110	−0.0002
g_A^e	−0.5037	0.0250	0.0030	0.0833	—	—
$\sigma_\nu/\sigma_{\bar{\nu}}$	1.1515	0.0453	0.0030	0.1516	0.0050	−0.0003
$\sigma_\nu/(\sigma_{\bar{\nu}}+\sigma_\nu)$	0.1455	0.0026	−0.0016	0.0159	0.0025	0.0016
C_{1+}	0.1291	0.0013	−0.0034	0.0038	0.0033	−0.0086
$C_{1+}(iso)$	0.1291	0.0003	−0.0034	0.0010	0.0009	−0.0086
C_{1-}	−0.3633	0.1000	0.0098	0.1021	0.0689	0.0067
C_{2p}	−0.0140	0.0460	0.0000	—	—	—
$C_{2p}(1)$	−0.0140	0.0046	0.0000	—	—	—
C_{2m}	−0.0537	0.1100	0.0021	0.5271	0.0274	0.0005
$2C_{1u}+C_{1d}$	−0.0323	0.0040	0.0010	0.0383	0.0020	0.0005

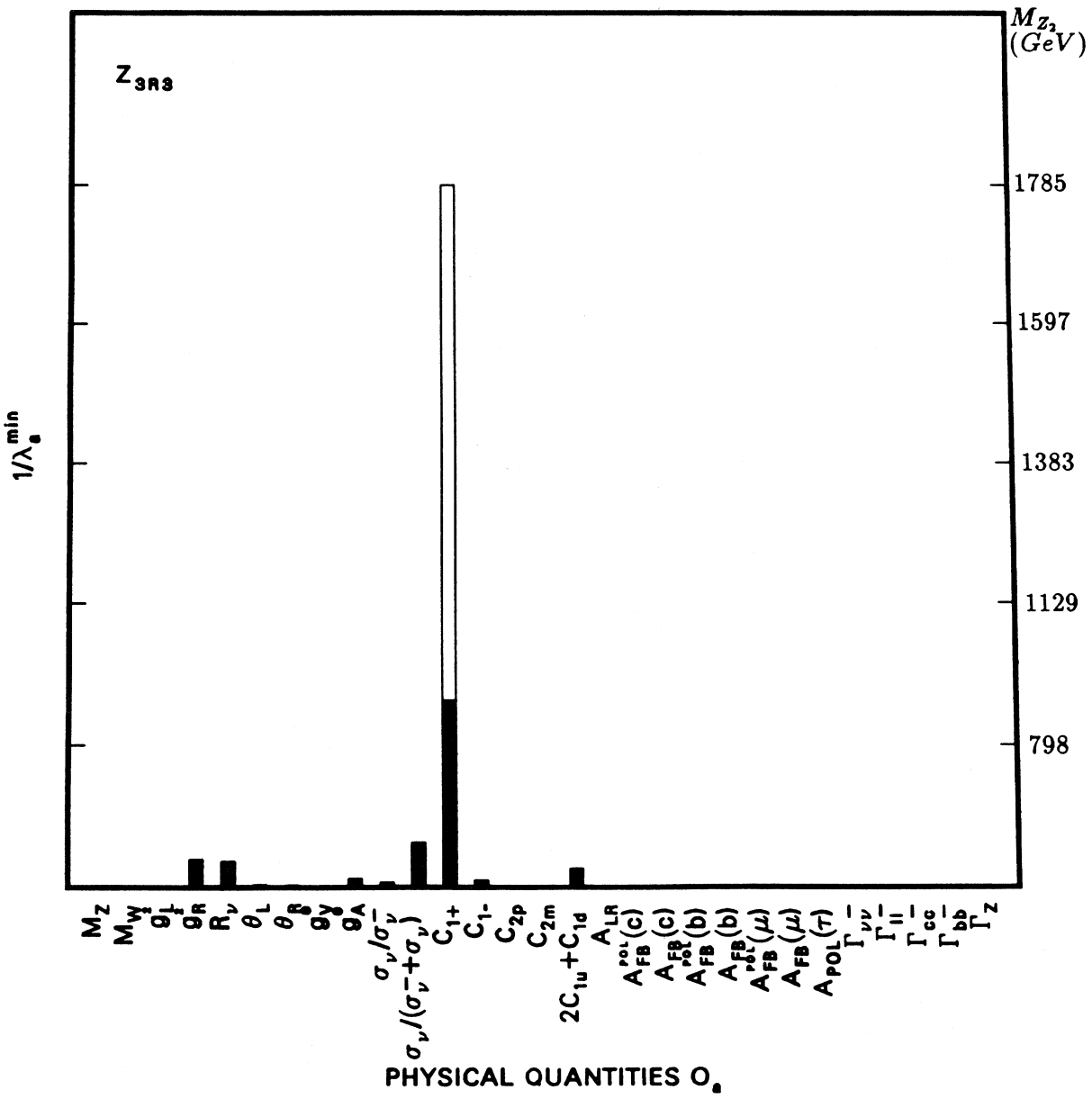

FIG. 44. The new physics of Z_{3R} with $C=0$: solid bar for C_{1+}; open bar for C_{1+}(iso).

TABLE XIX. Deviations from the SM by a nonstandard Higgs field. Type: extra SU(2)-triplet (or higher-dimensional) Higgs field. Free parameter: $\lambda=\rho_0-1$, where $\rho_0=M_W^2/M_Z^2\cos^2\theta_W^M$ (Sec. IV.B). Inputs: $M_Z=91.177$ GeV, $m_t=100$ GeV, $M_H=100$ GeV ($\sin^2\theta_W^M=0.2306$, $\sin^2\hat{\theta}_W=0.2334$). **Comments:** For the explicit definitions of physical observables, see Sec. III. The inverses of the sixth column $1/\lambda^{\min}$ are plotted in Fig. 45. Following the argument given in the text, the bigger $1/\lambda_a^{\min}$ is, the more likely for the vacuum expectation value of the nonstandard Higgs field to be detected by measuring O_a. R_ν, $A_{\rm LR}$(LEP), and M_W have $\lambda^{\min}\sim 0.0015$–$0.0018$, corresponding to $\mathrm{VEV_{NH}}\sim 7$ GeV, while $A_{\rm LR}$(SLC) and $A_{\rm FB}(b)$ have $\lambda^{\min}\sim 0.0026$–$0.0030$, corresponding to $\mathrm{VEV_{NH}}\sim 9$ GeV.

Quantities	O_a^{SM}	ΔO_a^{exp}	ΔO_a^i $\lambda=0.01$	λ_a^{min}	$\Delta\sin^2\theta_W^{exp}$	$\Delta\sin^2\theta_W^{(a;Z)}$ $\lambda=0.01$
$M_Z(GeV)$	91.1770	0.0200	—	—	0.0003	—
$M_W(GeV)$	79.9832	0.1050	0.5709	0.0018	0.0006	−0.0033
g_L^2	0.2997	0.0042	0.0084	0.0050	0.0057	−0.0114
g_R^2	0.0301	0.0034	−0.0002	0.1366	0.0130	−0.0010
R_ν	0.3117	0.0013	0.0083	0.0015	0.0020	−0.0131
θ_L	2.4640	0.0300	−0.0019	0.1608	—	—
θ_R	5.1765	0.4400	0.0000	—	—	—
g_V^e	−0.0361	0.0220	−0.0069	0.0317	0.0110	−0.0035
g_A^e	−0.5037	0.0250	−0.0050	0.0496	—	—
$\sigma_\nu/\sigma_{\bar{\nu}}$	1.1515	0.0453	0.0298	0.0152	0.0050	−0.0033
$\sigma_\nu/(\sigma_{\bar{\nu}}+\sigma_\nu)$	0.1455	0.0026	0.0068	0.0039	0.0025	−0.0065
C_{1+}	0.1291	0.0013	0.0000	—	0.0033	0.0000
$C_{1+}(iso)$	0.1291	0.0003	0.0000	—	0.0009	0.0000
C_{1-}	−0.3633	0.1000	−0.0084	0.1190	0.0689	−0.0058
C_{2p}	−0.0140	0.0460	−0.0001	—	—	—
$C_{2p}(1)$	−0.0140	0.0046	−0.0001	0.3276	—	—
C_{2m}	−0.0537	0.1100	−0.0137	0.0801	0.0274	−0.0034
$2C_{1u}+C_{1d}$	−0.0323	0.0040	−0.0070	0.0058	0.0020	−0.0035
$A_{LR}(SLC)$	0.1306	0.0066	0.0257	0.0026	0.0008	−0.0033
$A_{LR}(LEP)$	0.1306	0.0041	0.0257	0.0017	0.0005	−0.0033
$A_{FB}^{pol}(c)$	0.4725	0.0250	0.0087	0.0288	0.0095	−0.0033
$A_{FB}(c)$	0.0617	0.0070	0.0133	0.0053	0.0017	−0.0033
$A_{FB}^{pol}(b)$	0.6965	0.0200	0.0016	0.1285	0.0423	−0.0033
$A_{FB}(b)$	0.0910	0.0054	0.0181	0.0030	0.0010	−0.0033
$A_{FB}^{pol}(\mu)$	0.0980	0.0090	0.0193	0.0047	0.0015	−0.0033
$A_{FB}(\mu)$	0.0128	0.0035	0.0050	0.0069	0.0023	−0.0033
$A_{pol}(\tau)$	0.1306	0.0110	0.0257	0.0043	0.0014	−0.0033
$\Gamma_{inv}(GeV)$	0.4990	0.0160	0.0050	0.0321	0.0070	−0.0022
$\Gamma_{l\bar{l}}(GeV)$	0.0835	0.0007	0.0010	0.0070	0.0016	−0.0023
$\Gamma_{c\bar{c}}(GeV)$	0.2959	0.0300	0.0046	0.0646	0.0161	−0.0025
$\Gamma_{b\bar{b}}(GeV)$	0.3773	0.0400	0.0053	0.0757	0.0184	−0.0024
$\Gamma_Z(GeV)$	2.4837	0.0150	0.0332	0.0045	0.0011	−0.0024

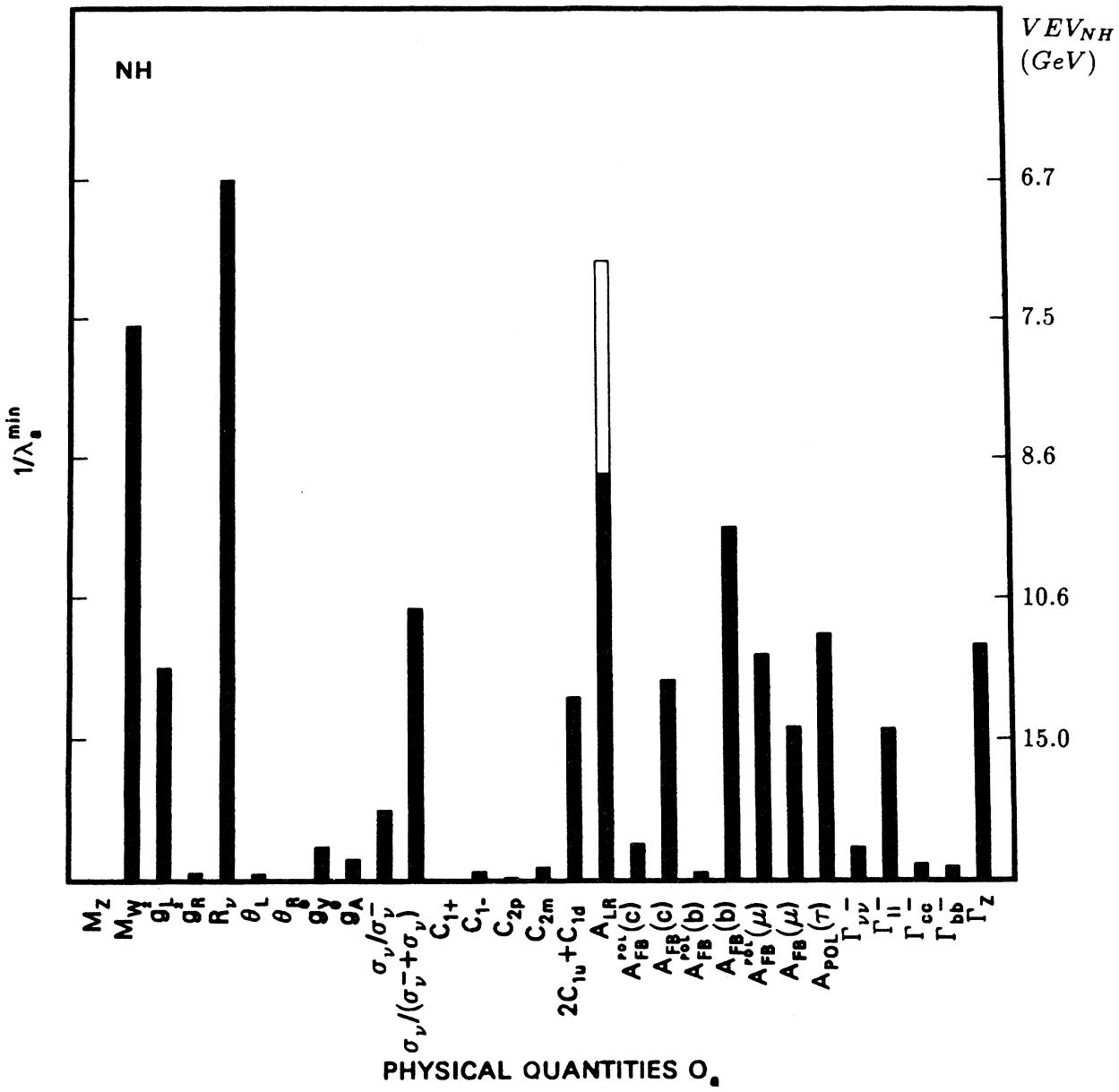

FIG. 45. The new physics of nonstandard Higgs fields: solid bar for A_{LR}(SLC), open bar for A_{LR}(LEP). The right-hand scale corresponds to the VEV of the nonstandard Higgs field in GeV.

TABLE XX. Deviations from the SM by an SU(5) leptoquark ($\eta_L \neq 0$). Type: SU(5) leptoquark. Free parameter: $\lambda = (\sqrt{2}|\eta_L|^2/8M_S^2 G_F)$ ($\eta_L \neq 0$, $\eta_R = 0$; Sec. IV.B). Inputs: $M_Z = 91.177$ GeV, $m_t = 100$ GeV, $M_H = 100$ GeV ($\sin^2\theta_W^M = 0.2306$, $\sin^2\hat{\theta}_W = 0.2334$). **Comments:** For the explicit definitions of physical observables, see Sec. III. The inverses of the sixth column $1/\lambda^{\min}$ are plotted in Fig. 46. Leptoquarks have no effect on Z-pole physics, M_W, and purely leptonic processes. For C_{1+}(iso), $\lambda^{\min} = 0.0005$, corresponding to $(M_S/|\eta_L|) > 5.5$ TeV. C_{1+} and $2C_{1u} + C_{1d}$ are sensitive up to ~ 2.8 TeV. For the leptoquark with $\eta_R \neq 0$, $\eta_L = 0$, only the atomic parity-violation coefficients are affected. The deviations on the C's are the same as those in this table but within minus signs.

Quantities	O_a^{SM}	ΔO_a^{exp}	ΔO_a^i $\lambda = 0.01$	λ_a^{min}	$\Delta \sin^2\theta_W^{exp}$	$\Delta \sin^2\theta_W^{(a;Z)}$ $\lambda = 0.01$
$M_Z(GeV)$	91.1770	0.0200	—	—	0.0003	—
g_L^2	0.2997	0.0042	0.0025	0.0166	0.0057	−0.0034
g_R^2	0.0301	0.0034	−0.0006	0.0565	0.0130	−0.0023
R_ν	0.3117	0.0013	0.0023	0.0056	0.0020	−0.0036
θ_L	2.4640	0.0300	0.0115	0.0262	—	—
C_{1+}	0.1291	0.0013	−0.0067	0.0020	0.0033	−0.0170
$C_{1+}(iso)$	0.1291	0.0003	−0.0067	0.0005	0.0009	−0.0170
C_{1-}	−0.3633	0.1000	−0.0075	0.1339	0.0689	−0.0051
C_{2p}	−0.0140	0.0460	−0.0100	0.0460	—	—
$C_{2p}(1)$	−0.0140	0.0046	−0.0100	0.0046	—	—
C_{2m}	−0.0537	0.1100	−0.0100	0.1100	0.0274	−0.0025
$2C_{1u} + C_{1d}$	−0.0323	0.0040	−0.0200	0.0020	0.0020	−0.0099

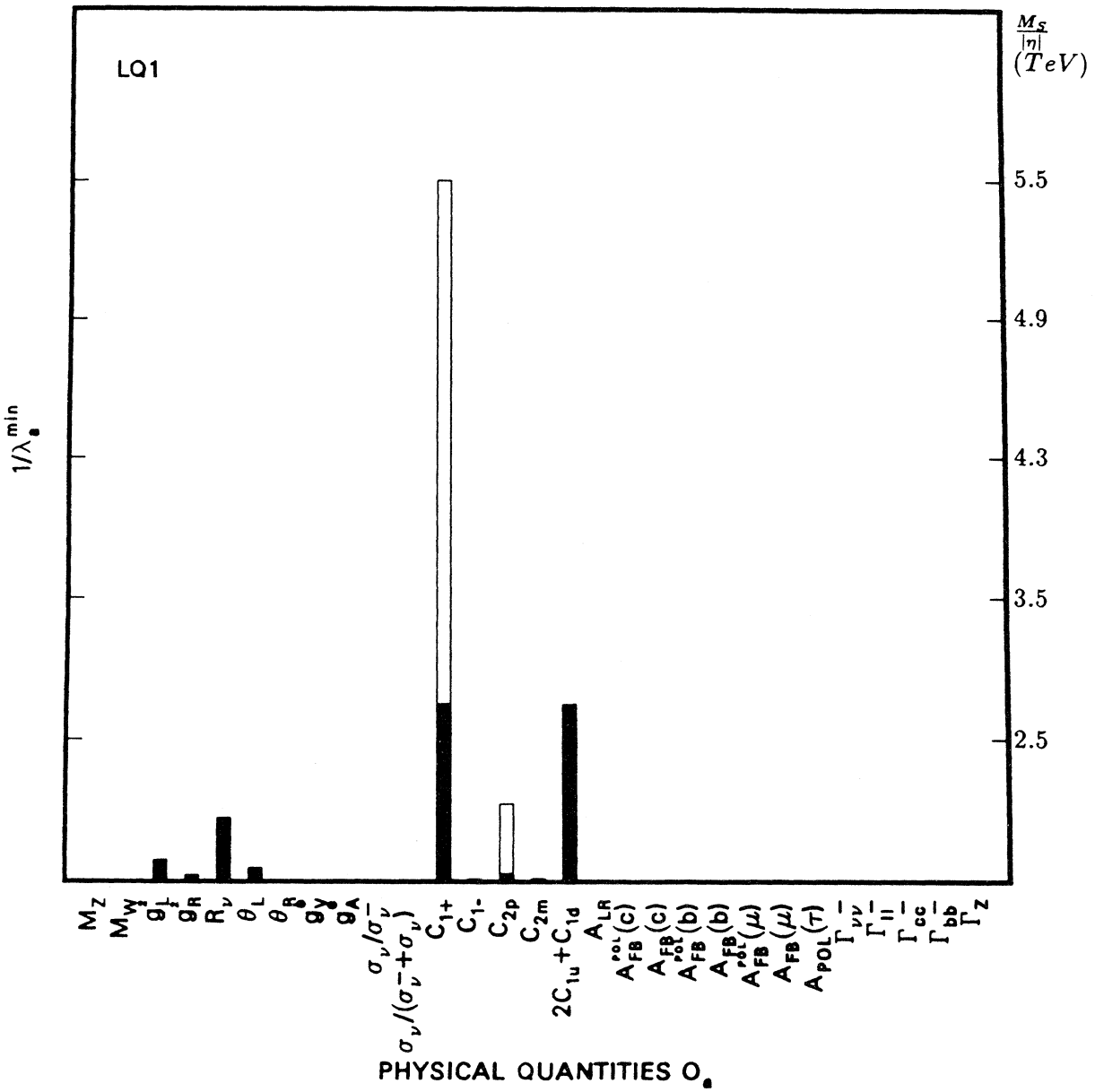

FIG. 46. The new physics of SU(5) leptoquark, type 1: solid bar for C_{1+} and C_{2p}; open bar for C_{1+}(iso) and $C_{2p}(1)$. The right-hand scale corresponds to $M_S/|\eta|$ in TeV.

TABLE XXI. Deviations from the SM by an extra fermion (u_L). Type: extra left-handed $Q=\frac{2}{3}$, SU(2)-singlet quark (Sec. IV.C). Free parameter: $\lambda=\sin^2\theta_L^u$, where θ_L^u is the mixing angle between ordinary and exotic [SU(2)-singlet] left-handed u quark. Inputs: $M_Z=91.177$ GeV, $m_t=100$ GeV, $M_H=100$ GeV ($\sin^2\theta_W^M=0.2306$, $\sin^2\hat{\theta}_W=0.2334$). **Comments:** For the explicit definitions of physical observables, see Sec. III. The deviations of $A_{\rm FB}^{\rm pol}(c)$, $A_{\rm FB}(c)$ and $\Gamma_{c\bar{c}}$ are are due to the mixing between the ordinary c quark and an exotic c quark. For these the mixing angle is $\sin^2\theta_L^c$ rather than $\sin^2\theta_L^u$. The inverses of the sixth column $1/\lambda^{\rm min}$ are plotted in Fig. 47. Following the argument given in the text, the bigger $1/\lambda_a^{\rm min}$ is, the more likely for the extra u_L to be detected by measuring O_a. C_{1+}(iso) is sensitive to $\sin^2\theta_L^u\cong 0.0010$, while R_ν, C_{1+}, and $2C_{1u}+C_{1d}$ have $\lambda^{\rm min}\sim 0.004$.

Quantities	O_a^{SM}	ΔO_a^{exp}	ΔO_a^i $\lambda=0.01$	λ_a^{min}	$\Delta\sin^2\theta_W^{exp}$	$\Delta\sin^2\theta_W^{(a;Z)}$ $\lambda=0.01$
$M_Z(GeV)$	91.1770	0.0200	—	—	0.0003	—
g_L^2	0.2997	0.0042	−0.0034	0.0122	0.0057	0.0046
R_ν	0.3117	0.0013	−0.0034	0.0037	0.0020	0.0054
θ_L	2.4640	0.0300	0.0071	0.0422	—	—
C_{1+}	0.1291	0.0013	0.0034	0.0039	0.0033	0.0085
$C_{1+}(iso)$	0.1291	0.0003	0.0034	0.0010	0.0009	0.0085
C_{1-}	−0.3633	0.1000	0.0038	0.2658	0.0689	0.0026
C_{2p}	−0.0140	0.0460	0.0004	—	—	—
$C_{2p}(1)$	−0.0140	0.0046	0.0004	0.1273	—	—
C_{2m}	−0.0537	0.1100	0.0004	—	0.0274	0.0001
$2C_{1u}+C_{1d}$	−0.0323	0.0040	0.0101	0.0040	0.0020	0.0050
$A_{FB}^{pol}(c)$	0.4725	0.0250	−0.0062	0.0406	0.0095	0.0023
$A_{FB}(c)$	0.0617	0.0070	−0.0008	0.0870	0.0017	0.0002
$\Gamma_{c\bar{c}}(GeV)$	0.2959	0.0300	−0.0068	0.0439	0.0161	0.0037
$\Gamma_Z(GeV)$	2.4837	0.0150	−0.0068	0.0220	0.0011	0.0005

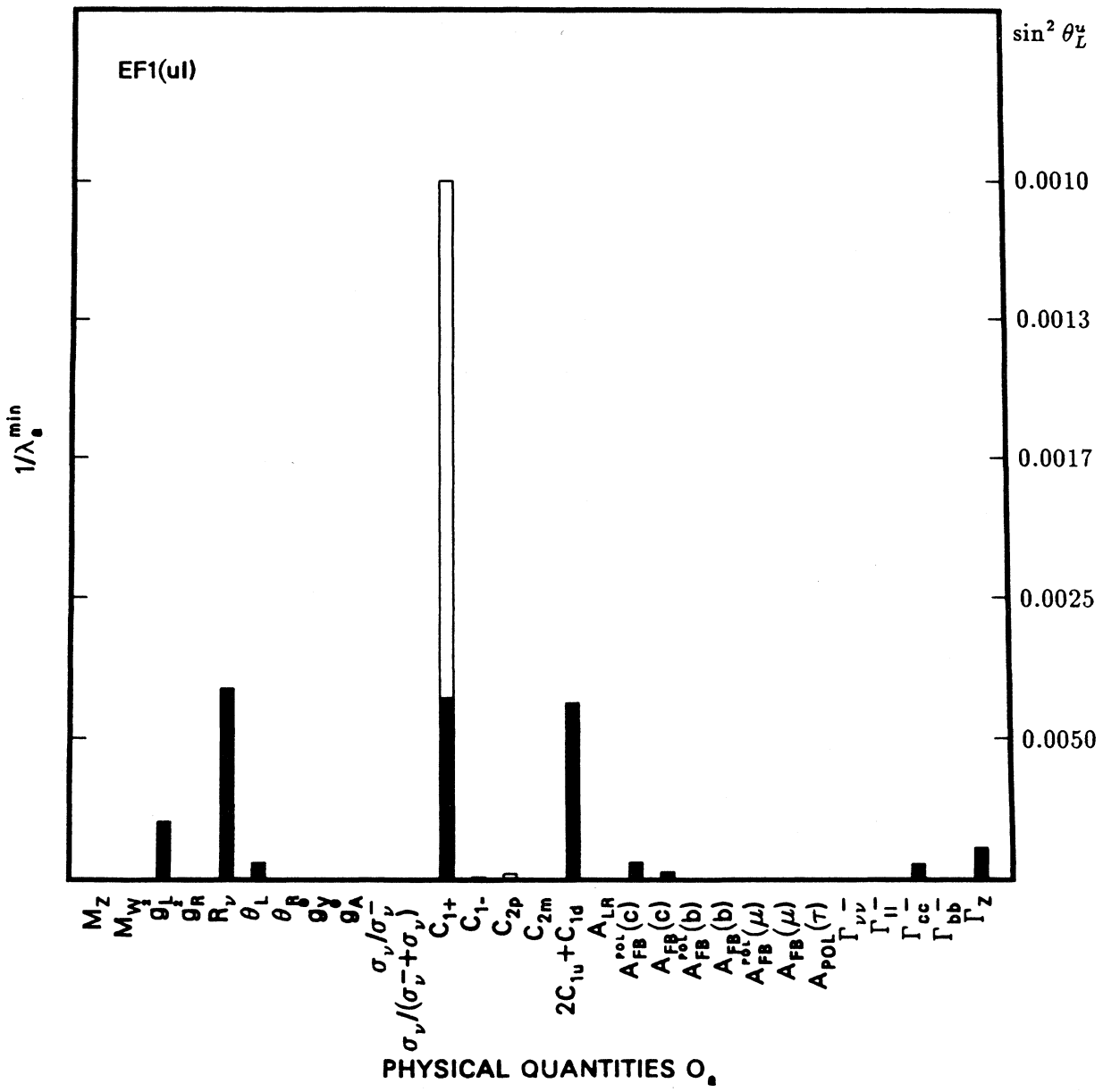

FIG. 47. The new physics of one extra u_L: solid bar for C_{1+} and C_{2p}; open bar for C_{1+}(iso), $C_{2p}(1)$. The right-hand scale corresponds to $\sin^2\theta_L^u$.

TABLE XXII. Deviations from the SM by an extra fermion (u_R). Type: extra right-handed $Q=\frac{2}{3}$, SU(2)-doublet quark (Sec. IV.C). Free parameter: $\lambda=\sin^2\theta_R^u$, where θ_R^u is the mixing angle between ordinary and exotic [SU(2)-doublet] right-handed u quark. Inputs: $M_Z=91.177$ GeV, $m_t=100$ GeV, $M_H=100$ GeV ($\sin^2\theta_W^M=0.2306$, $\sin^2\hat{\theta}_W=0.2334$). **Comments:** The deviations of $A_{\rm FB}^{\rm pol}(c)$, $A_{\rm FB}(c)$ and $\Gamma_{c\bar{c}}$ are due to the mixing between the ordinary c quark and an exotic c quark. For these the mixing angle is $\sin^2\theta_R^c$ rather than $\sin^2\theta_R^u$. The inverses of the sixth column $1/\lambda^{\rm min}$ are plotted in Fig. 48. C_{1+}(iso) has $\lambda^{\rm min}=0.0010$, while $\lambda^{\rm min}\cong 0.004$ for C_{1+} and $2C_{1u}+C_{1d}$.

Quantities	O_a^{SM}	ΔO_a^{exp}	ΔO_a^i $\lambda=0.01$	λ_a^{min}	$\Delta\sin^2\theta_W^{exp}$	$\Delta\sin^2\theta_W^{(a;Z)}$ $\lambda=0.01$
$M_Z(GeV)$	91.1770	0.0200	—	—	0.0003	—
g_R^2	0.0301	0.0034	−0.0016	0.0219	0.0130	−0.0060
R_ν	0.3117	0.0013	−0.0006	0.0206	0.0020	0.0010
θ_R	5.1765	0.4400	0.0129	0.3411	—	—
C_{1+}	0.1291	0.0013	−0.0034	0.0039	0.0033	−0.0085
$C_{1+}(iso)$	0.1291	0.0003	−0.0034	0.0010	0.0009	−0.0085
C_{1-}	−0.3633	0.1000	−0.0038	0.2658	0.0689	−0.0026
C_{2p}	−0.0140	0.0460	0.0004	—	—	—
$C_{2p}(1)$	−0.0140	0.0046	0.0004	0.1273	—	—
C_{2m}	−0.0537	0.1100	0.0004	—	0.0274	0.0001
$2C_{1u}+C_{1d}$	−0.0323	0.0040	−0.0101	0.0040	0.0020	−0.0050
$A_{FB}^{pol}(c)$	0.4725	0.0250	0.0136	0.0184	0.0095	−0.0052
$A_{FB}(c)$	0.0617	0.0070	0.0018	0.0393	0.0017	−0.0004
$\Gamma_{c\bar{c}}(GeV)$	0.2959	0.0300	−0.0031	0.0972	0.0161	0.0017
$\Gamma_Z(GeV)$	2.4837	0.0150	−0.0031	0.0486	0.0011	0.0002

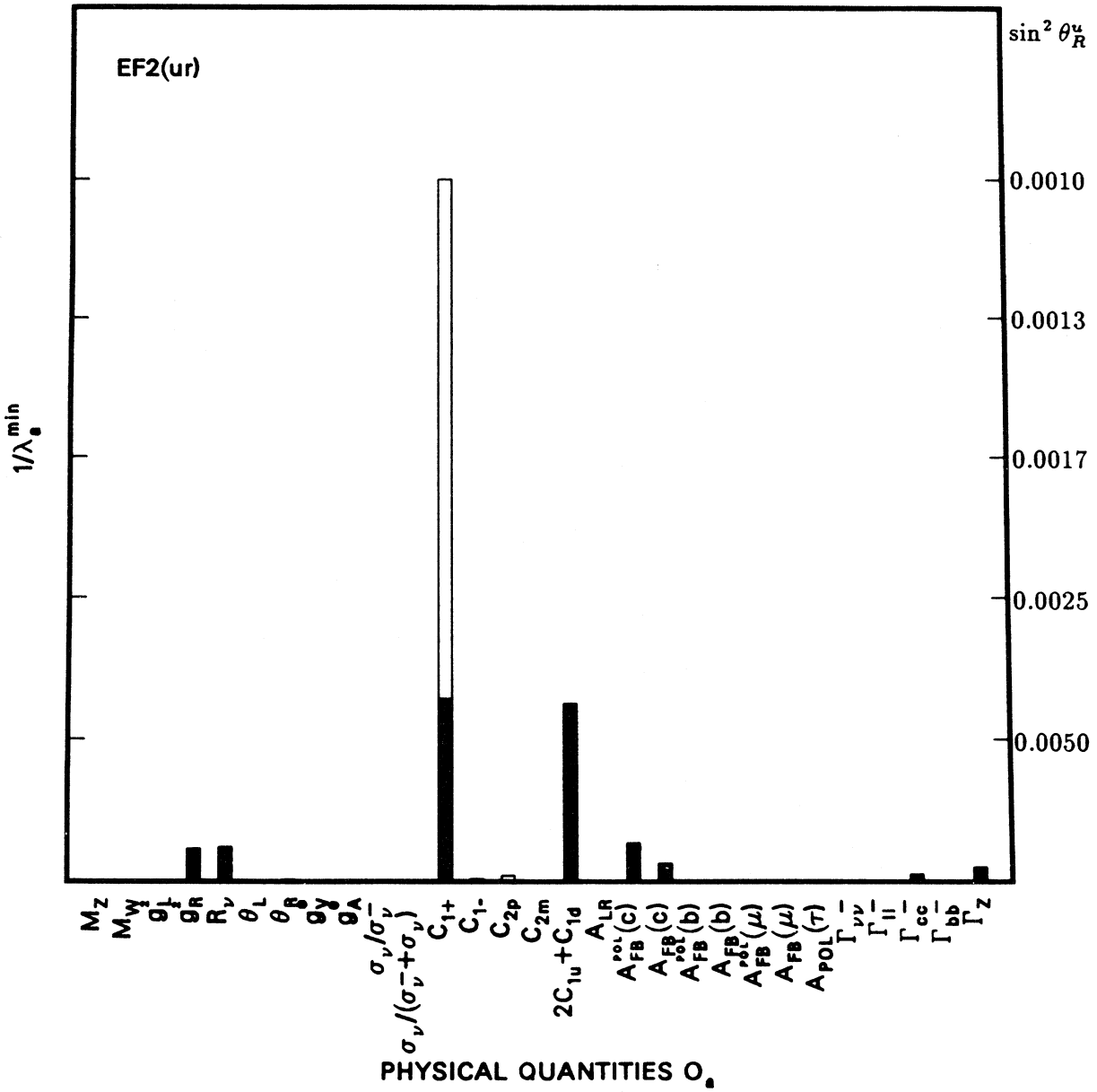

FIG. 48. The new physics of one extra u_R: solid bar for C_{1+} and C_{2p}; open bar for C_{1+}(iso) and $C_{2p}(1)$.

TABLE XXIII. Deviations from the SM by an extra fermion (d_L). Type: extra left-handed $Q=-\frac{1}{3}$, SU(2)-singlet quark (Sec. IV.C). Free parameter: $\lambda=\sin^2\theta_L^d$, where θ_L^d is the mixing angle between ordinary and exotic [SU(2)-singlet] left-handed d quark. Inputs: $M_Z=91.177$ GeV, $m_t=100$ GeV, $M_H=100$ GeV ($\sin^2\theta_W^M=0.2306$, $\sin^2\hat{\theta}_W=0.2334$). **Comments:** The deviations of $A_{\rm FB}^{\rm pol}(b)$, $A_{\rm FB}(b)$ and $\Gamma_{b\bar{b}}$ are due to the mixing between the ordinary b quark and an exotic b quark. For these the mixing angle is $\sin^2\theta_L^b$ rather than $\sin^2\theta_L^d$. The inverses of the sixth column $1/\lambda^{\rm min}$ are plotted in Fig. 49. C_{1+}(iso) has $\lambda^{\rm min}\cong 0.0009$, while $\lambda^{\rm min}\sim 0.003$ for R_ν and C_{1+}.

Quantities	O_a^{SM}	ΔO_a^{exp}	ΔO_a^i $\lambda=0.01$	λ_a^{min}	$\Delta\sin^2\theta_W^{exp}$	$\Delta\sin^2\theta_W^{(a;Z)}$ $\lambda=0.01$
$M_Z(GeV)$	91.1770	0.0200	—	—	0.0003	—
g_L^2	0.2997	0.0042	−0.0043	0.0098	0.0057	0.0057
R_ν	0.3117	0.0013	−0.0043	0.0030	0.0020	0.0067
θ_L	2.4640	0.0300	−0.0057	0.0524	—	—
C_{1+}	0.1291	0.0013	−0.0038	0.0035	0.0033	−0.0096
$C_{1+}(iso)$	0.1291	0.0003	−0.0038	0.0009	0.0009	−0.0096
C_{1-}	−0.3633	0.1000	0.0034	0.2981	0.0689	0.0023
C_{2p}	−0.0140	0.0460	−0.0004	—	—	—
$C_{2p}(1)$	−0.0140	0.0046	−0.0004	0.1273	—	—
C_{2m}	−0.0537	0.1100	0.0004	—	0.0274	0.0001
$2C_{1u}+C_{1d}$	−0.0323	0.0040	−0.0050	0.0079	0.0020	−0.0025
$A_{FB}^{pol}(b)$	0.6965	0.0200	−0.0011	0.1830	0.0423	0.0023
$A_{FB}(b)$	0.0910	0.0054	−0.0001	0.3852	0.0010	0.0000
$\Gamma_{b\bar{b}}(GeV)$	0.3773	0.0400	−0.0085	0.0471	0.0184	0.0039
$\Gamma_Z(GeV)$	2.4837	0.0150	−0.0085	0.0177	0.0011	0.0006

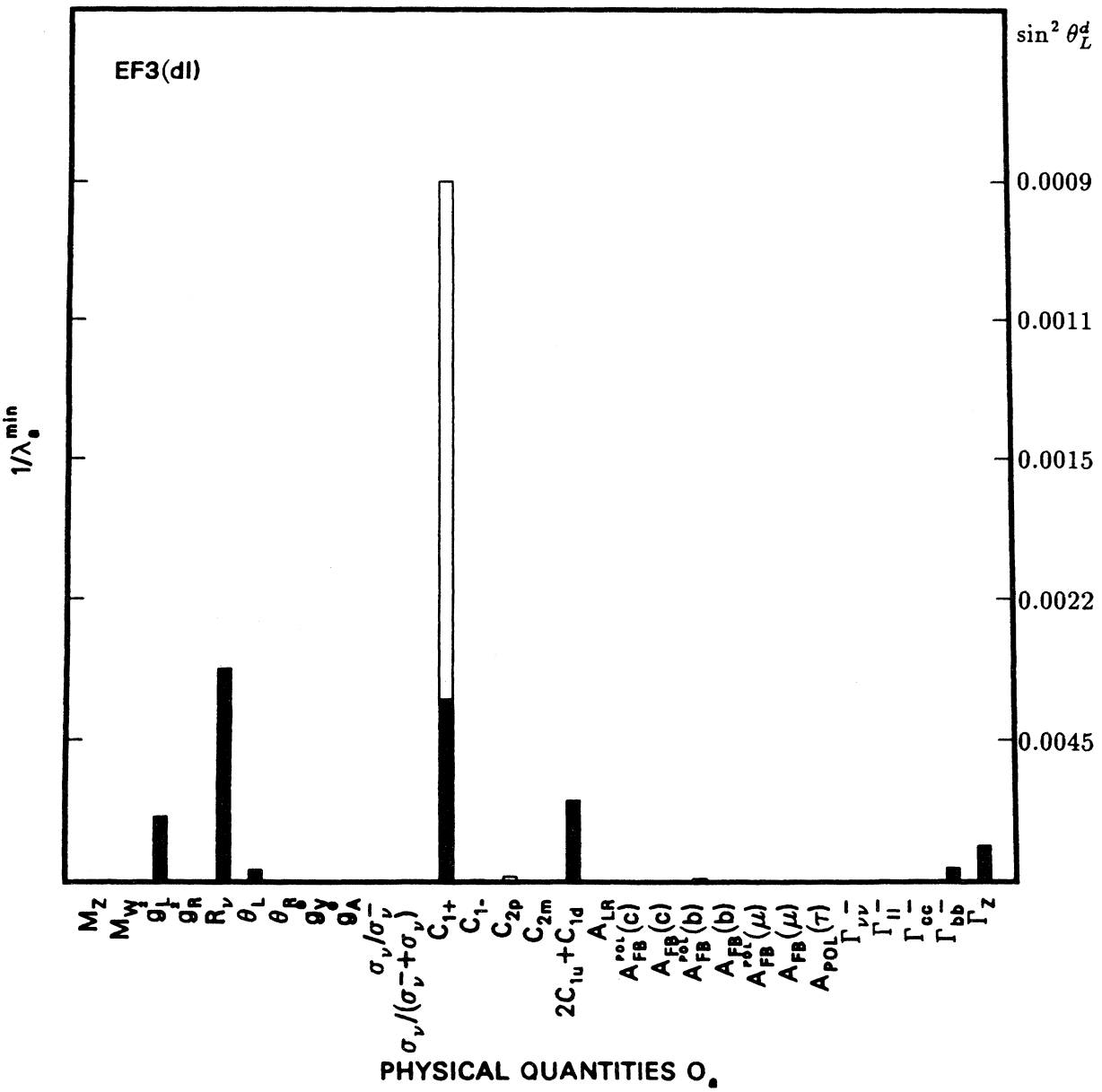

FIG. 49. The new physics of one extra d_L: solid bar for C_{1+} and C_{2p}; open bar for C_{1+}(iso) and $C_{2p}(1)$.

TABLE XXIV. Deviations from the SM by an extra fermion (d_R). Type: extra right-handed $Q=-\frac{1}{3}$, SU(2)-doublet quark (Sec. IV.C). Free parameter: $\lambda=\sin^2\theta_R^d$, where θ_R^d is the mixing angle between ordinary and exotic [SU(2)-doublet] right-handed d quark. Inputs: $M_Z=91.177$ GeV, $m_t=100$ GeV, $M_H=100$ GeV ($\sin^2\theta_W^M=0.2306$, $\sin^2\hat{\theta}_W=0.2334$). **Comments:** The deviations of $A_{\rm FB}^{\rm pol}(b)$, $A_{\rm FB}(b)$ and $\Gamma_{b\bar{b}}$ are due to the mixing between the ordinary b quark and an exotic b quark. For these the mixing angle is $\sin^2\theta_R^b$ rather than $\sin^2\theta_R^d$. The inverses of the sixth column $1/\lambda^{\rm min}$ are plotted in Fig. 50. C_{1+}(iso) has $\lambda^{\rm min}\cong 0.0009$, while $\lambda^{\rm min}\sim 0.0035$ for C_{1+}.

Quantities	O_a^{SM}	ΔO_a^{exp}	ΔO_a^i $\lambda=0.01$	λ_a^{min}	$\Delta\sin^2\theta_W^{exp}$	$\Delta\sin^2\theta_W^{(a;Z)}$ $\lambda=0.01$
$M_Z(GeV)$	91.1770	0.0200	—	—	0.0003	—
g_R^2	0.0301	0.0034	−0.0008	0.0438	0.0130	−0.0030
R_ν	0.3117	0.0013	−0.0003	0.0411	0.0020	0.0005
θ_R	5.1765	0.4400	−0.0258	0.1708	—	—
C_{1+}	0.1291	0.0013	0.0038	0.0035	0.0033	0.0096
$C_{1+}(iso)$	0.1291	0.0003	0.0038	0.0009	0.0009	0.0096
C_{1-}	−0.3633	0.1000	−0.0034	0.2981	0.0689	−0.0023
C_{2p}	−0.0140	0.0460	−0.0004	—	—	—
$C_{2p}(1)$	−0.0140	0.0046	−0.0004	0.1273	—	—
C_{2m}	−0.0537	0.1100	0.0004	—	0.0274	0.0001
$2C_{1u}+C_{1d}$	−0.0323	0.0040	0.0050	0.0079	0.0020	0.0025
$A_{FB}^{pol}(b)$	0.6965	0.0200	0.0060	0.0333	0.0423	−0.0127
$A_{FB}(b)$	0.0910	0.0054	0.0008	0.0702	0.0010	−0.0001
$\Gamma_{b\bar{b}}(GeV)$	0.3773	0.0400	−0.0015	0.2588	0.0184	0.0007
$\Gamma_Z(GeV)$	2.4837	0.0150	−0.0015	0.0970	0.0011	0.0001

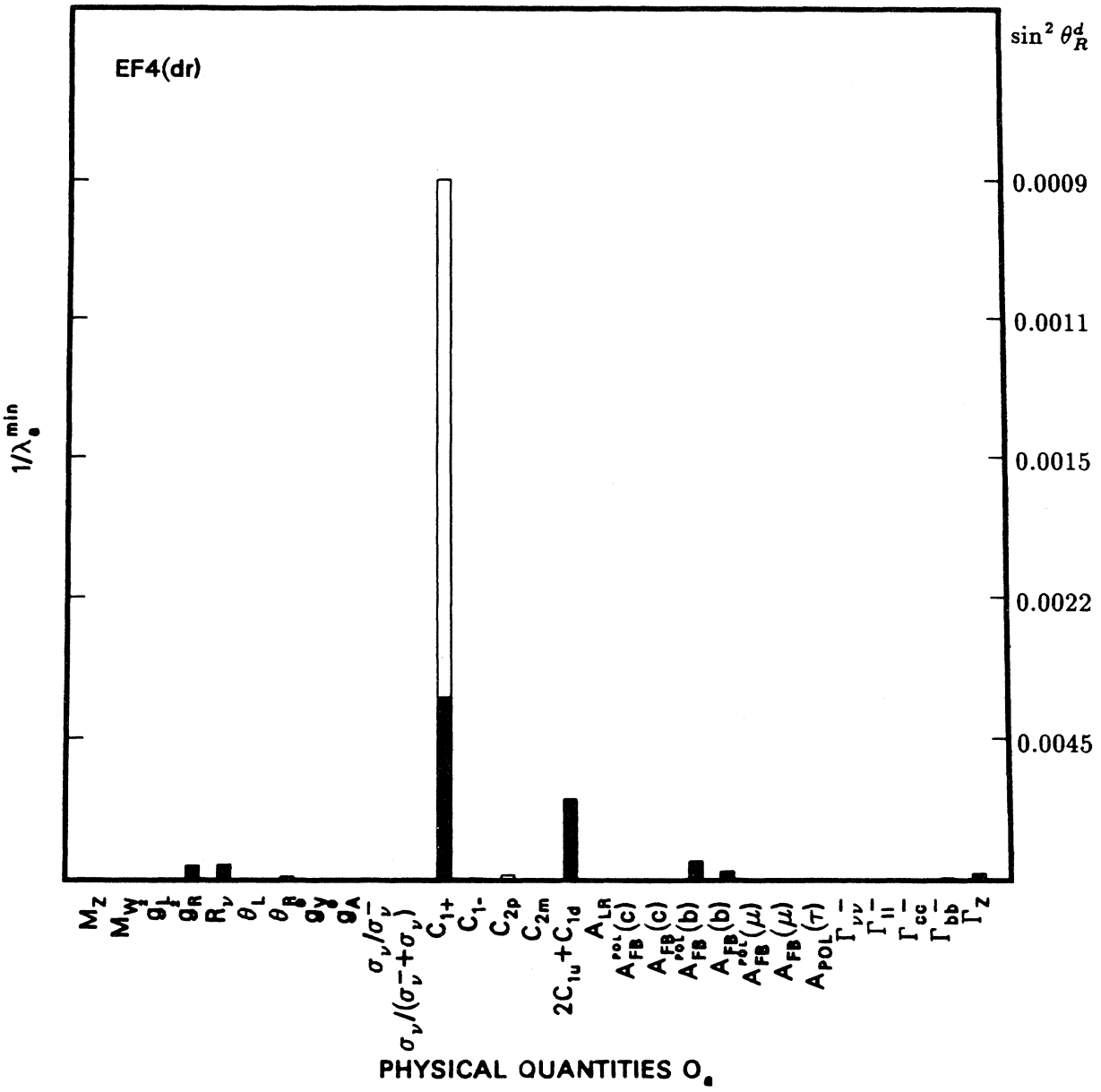

FIG. 50. The new physics of one extra d_R: solid bar for C_{1+} and C_{2p}; open bar for C_{1+}(iso) and $C_{2p}(1)$.

TABLE XXV. Deviations from the SM by an extra fermion (e_L). Type: extra left-handed SU(2)-singlet charged lepton (Sec. IV.C). Free parameter: $\lambda=\sin^2\theta_L^e$, where θ_L^e is the mixing angle between ordinary and exotic [SU(2)-singlet] left-handed electrons. Inputs: $M_Z=91.177$ GeV, $m_t=100$ GeV, $M_H=100$ GeV ($\sin^2\theta_W^M=0.2306$, $\sin^2\hat{\theta}_W=0.2334$). **Comments:** The deviation of $A_{\rm pol}(\tau)$ is due to the mixing between the ordinary τ and an exotic τ-lepton. The mixing angle is $\sin^2\theta_L^\tau$ rather than $\sin^2\theta_L^e$, and there is no shift in $\sin^2\theta_W$. For the mixing between an ordinary and an exotic electron, there are no direct shifts in C_{2p} and C_{2m}, which are measured in μ-atoms; the shifts are due to the shift in $\sin^2\theta_W$ only. $\Gamma_{l\bar{l}}$ is averaged over the e, μ, and τ. $\Gamma_{e\bar{e}}$ is shifted by -0.0012 GeV, including both the direct shift and the $\sin^2\theta_W$ shift. $\Gamma_{\mu\bar{\mu}}$ and $\Gamma_{\tau\bar{\tau}}$ are shifted by 0.0004 GeV due to $\sin^2\theta_W$. The inverses of the sixth column $1/\lambda^{\rm min}$ are plotted in Fig. 51. C_{1+}(iso) is sensitive to $\lambda^{\rm min}=0.0025$, while $\sin^2\theta_L^\tau\cong 0.006$ for $A_{\rm pol}(\tau)$.

Quantities	O_a^{SM}	ΔO_a^{exp}	ΔO_a^i $\lambda=0.01$	λ_a^{min}	$\Delta\sin^2\theta_W^{exp}$	$\Delta\sin^2\theta_W^{(a;Z)}$ $\lambda=0.01$
$M_Z(GeV)$	91.1770	0.0200	—	—	0.0003	—
$M_W(GeV)$	79.9832	0.1050	0.0855	0.0123	0.0006	−0.0005
g_L^2	0.2997	0.0042	0.0012	0.0344	0.0057	−0.0016
g_R^2	0.0301	0.0034	−0.0004	0.0799	0.0130	−0.0016
R_ν	0.3117	0.0013	0.0011	0.0122	0.0020	−0.0016
θ_L	2.4640	0.0300	−0.0009	0.3216	—	—
g_V^e	−0.0361	0.0220	0.0017	0.1287	0.0110	0.0009
g_A^e	−0.5037	0.0250	0.0050	0.0500	—	—
$\sigma_\nu/\sigma_{\bar{\nu}}$	1.1515	0.0453	−0.0061	0.0740	0.0050	0.0007
$\sigma_\nu/(\sigma_{\bar{\nu}}+\sigma_\nu)$	0.1455	0.0026	−0.0007	0.0383	0.0025	0.0007
C_{1+}	0.1291	0.0013	−0.0014	0.0096	0.0033	−0.0034
$C_{1+}(iso)$	0.1291	0.0003	−0.0014	0.0025	0.0009	−0.0034
C_{1-}	−0.3633	0.1000	−0.0005	—	0.0689	−0.0003
C_{2p}	−0.0140	0.0460	−0.0001	—	—	—
$C_{2p}(1)$	−0.0140	0.0046	−0.0001	0.6551	—	—
C_{2m}	−0.0537	0.1100	−0.0069	0.1602	0.0274	−0.0017
$2C_{1u}+C_{1d}$	−0.0323	0.0040	−0.0032	0.0125	0.0020	−0.0016
$A_{LR}(SLC)$	0.1306	0.0066	−0.0053	0.0129	0.0008	0.0007
$A_{LR}(LEP)$	0.1306	0.0041	−0.0053	0.0081	0.0005	0.0007
$A_{FB}^{pol}(c)$	0.4725	0.0250	0.0043	0.0576	0.0095	−0.0016
$A_{FB}(c)$	0.0617	0.0070	−0.0019	0.0363	0.0017	0.0005
$A_{FB}^{pol}(b)$	0.6965	0.0200	0.0008	0.2571	0.0423	−0.0016
$A_{FB}(b)$	0.0910	0.0054	−0.0036	0.0154	0.0010	0.0006
$A_{FB}^{pol}(\mu)$	0.0980	0.0090	0.0096	0.0093	0.0015	−0.0016
$A_{FB}(\mu)$	0.0128	0.0035	0.0007	0.0471	0.0023	−0.0005
$A_{pol}(\tau)$	0.1306	0.0110	−0.0181	0.0061	0.0014	0.0023
$\Gamma_{inv}(GeV)$	0.4990	0.0160	0.0025	0.0641	0.0070	−0.0011
$\Gamma_{l\bar{l}}(GeV)$	0.0835	0.0007	−0.0001	0.0743	0.0016	0.0002
$\Gamma_{c\bar{c}}(GeV)$	0.2959	0.0300	0.0023	0.1293	0.0161	−0.0012
$\Gamma_{b\bar{b}}(GeV)$	0.3773	0.0400	0.0026	0.1514	0.0184	−0.0012
$\Gamma_Z(GeV)$	2.4837	0.0150	0.0148	0.0101	0.0011	−0.0011

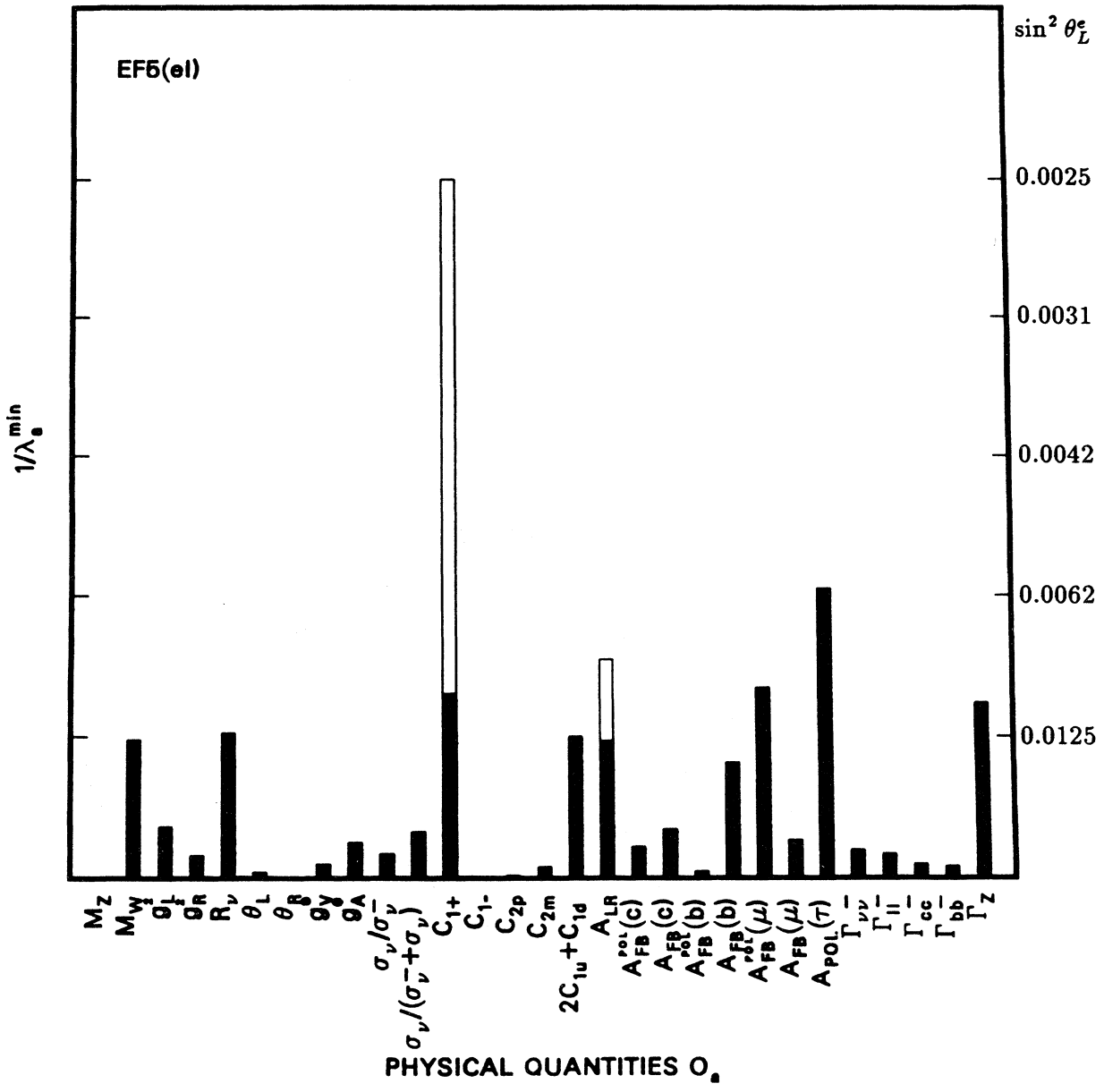

FIG. 51. The new physics of one extra e_L: solid bar for C_{1+} and A_{LR}(SLC); open bar for C_{1+}(iso) and A_{LR}(LEP).

TABLE XXVI. Deviations from the SM by an extra fermion (e_R). Type: extra right-handed SU(2)-doublet charged lepton mixed with ordinary electron (Sec. IV.C). Free parameter: $\lambda=\sin^2\theta_R^e$, where θ_R^e is the mixing angle between ordinary and exotic [SU(2)-doublet] right-handed electron. Inputs: $M_Z=91.177$ GeV, $m_t=100$ GeV, $M_H=100$ GeV ($\sin^2\theta_W^M=0.2306$, $\sin^2\hat{\theta}_W=0.2334$). **Comments:** The deviation of $A_{\rm pol}(\tau)$ is due to the mixing between the ordinary τ and an exotic τ-lepton. The mixing angle is $\sin^2\theta_R^\tau$ rather than $\sin^2\theta_R^e$. C_{2p} and C_{2m} are assumed to be measured in μ-atoms and are therefore not affected. The inverses of the sixth column $1/\lambda^{\rm min}$ are plotted in Fig. 52. $A_{\rm LR}$(LEP) and C_{1+}(iso) would be sensitive to $\sin^2\theta_R^e\sim 0.0021$–$0.0025$, while $\lambda^{\rm min}<0.01$ for C_{1+}, A_{LR}(SLC), $A_{\rm FB}(c)$, $A_{\rm FB}(b)$, and $A_{\rm pol}(\tau)$.

Quantities	O_a^{SM}	ΔO_a^{exp}	ΔO_a^i $\lambda=0.01$	λ_a^{min}	$\Delta\sin^2\theta_W^{exp}$	$\Delta\sin^2\theta_W^{(a;Z)}$ $\lambda=0.01$
$M_Z(GeV)$	91.1770	0.0200	—	—	0.0003	—
g_V^e	−0.0361	0.0220	−0.0050	0.0440	0.0110	−0.0025
g_A^e	−0.5037	0.0250	0.0050	0.0500	—	—
$\sigma_\nu/\sigma_{\bar{\nu}}$	1.1515	0.0453	0.0243	0.0187	0.0050	−0.0027
$\sigma_\nu/(\sigma_{\bar{\nu}}+\sigma_\nu)$	0.1455	0.0026	−0.0005	0.0501	0.0025	0.0005
C_{1+}	0.1291	0.0013	−0.0014	0.0096	0.0033	−0.0034
$C_{1+}(iso)$	0.1291	0.0003	−0.0014	0.0025	0.0009	−0.0034
C_{1-}	−0.3633	0.1000	0.0037	0.2683	0.0689	0.0026
$2C_{1u}+C_{1d}$	−0.0323	0.0040	0.0003	0.1466	0.0020	0.0001
$A_{LR}(SLC)$	0.1306	0.0066	0.0210	0.0032	0.0008	−0.0027
$A_{LR}(LEP)$	0.1306	0.0041	0.0210	0.0021	0.0005	−0.0027
$A_{FB}(c)$	0.0617	0.0070	0.0099	0.0071	0.0017	−0.0025
$A_{FB}(b)$	0.0910	0.0054	0.0146	0.0038	0.0010	−0.0026
$A_{FB}(\mu)$	0.0128	0.0035	0.0021	0.0171	0.0023	−0.0013
$A_{pol}(\tau)$	0.1306	0.0110	0.0210	0.0052	0.0014	−0.0027
$\Gamma_{l\bar{l}}(GeV)$	0.0835	0.0007	−0.0005	0.0135	0.0016	0.0012
$\Gamma_Z(GeV)$	2.4837	0.0150	−0.0016	0.0967	0.0011	0.0001

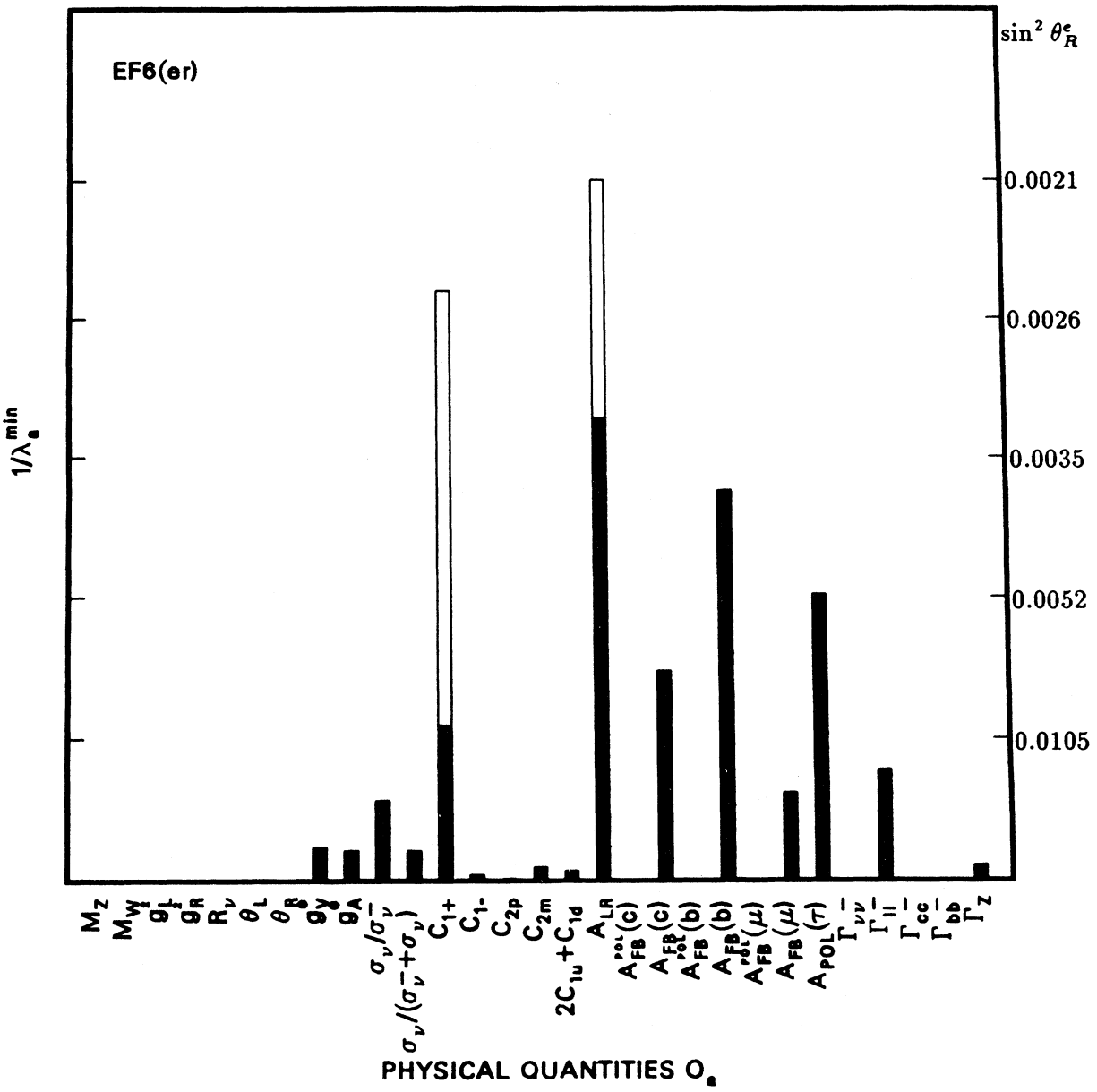

FIG. 52. The new physics of one extra e_R: solid bar for C_{1+} and A_{LR}(SLC); open bar for C_{1+}(iso) and A_{LR}(LEP).

TABLE XXVII. Deviations from the SM by an extra fermion (ν_{eL}). Type: extra left-handed SU(2)-singlet ν_e (Sec. IV.C). Free parameter: $\lambda=\sin^2\theta_L^{\nu_e}$, where $\theta_L^{\nu_e}$ is the mixing angle between ordinary and exotic [SU(2)-singlet] left-handed neutrino. Inputs: $M_Z=91.177$ GeV, $m_t=100$ GeV, $M_H=100$ GeV ($\sin^2\theta_W^M=0.2306$, $\sin^2\hat{\theta}_W=0.2334$). **Comments:** The inverses of the sixth column $1/\lambda^{\min}$ are plotted in Fig. 53. $A_{\rm LR}$(LEP) would be sensitive to $\lambda^{\min}\sim 0.0033$, while $\lambda^{\min}<0.01$ for $\sigma_\nu/(\sigma_{\bar\nu}+\sigma_\nu)$, $A_{\rm LR}$(SLC), $A_{\rm FB}(b)$, and $A_{\rm FB}^{\rm pol}(\mu)$.

Quantities	O_a^{SM}	ΔO_a^{exp}	ΔO_a^i $\lambda=0.01$	λ_a^{min}	$\Delta\sin^2\theta_W^{exp}$	$\Delta\sin^2\theta_W^{(a;Z)}$ $\lambda=0.01$
$M_Z(GeV)$	91.1770	0.0200	—	—	0.0003	—
$M_W(GeV)$	79.9832	0.1050	0.0855	0.0123	0.0006	−0.0005
g_L^2	0.2997	0.0042	0.0012	0.0344	0.0057	−0.0016
g_R^2	0.0301	0.0034	−0.0004	0.0799	0.0130	−0.0016
R_ν	0.3117	0.0013	0.0011	0.0122	0.0020	−0.0016
θ_L	2.4640	0.0300	−0.0009	0.3216	—	—
g_V^e	−0.0361	0.0220	−0.0033	0.0669	0.0110	−0.0016
$\sigma_\nu/\sigma_{\bar\nu}$	1.1515	0.0453	0.0149	0.0304	0.0050	−0.0016
$\sigma_\nu/(\sigma_{\bar\nu}+\sigma_\nu)$	0.1455	0.0026	0.0042	0.0062	0.0025	−0.0041
C_{1+}	0.1291	0.0013	0.0000	—	0.0033	0.0000
$C_{1+}(iso)$	0.1291	0.0003	0.0000	—	0.0009	0.0000
C_{1-}	−0.3633	0.1000	−0.0042	0.2379	0.0689	−0.0029
C_{2p}	−0.0140	0.0460	−0.0001	—	—	—
$C_{2p}(1)$	−0.0140	0.0046	−0.0001	0.6551	—	—
C_{2m}	−0.0537	0.1100	−0.0069	0.1602	0.0274	−0.0017
$2C_{1u}+C_{1d}$	−0.0323	0.0040	−0.0035	0.0115	0.0020	−0.0017
$A_{LR}(SLC)$	0.1306	0.0066	0.0129	0.0053	0.0008	−0.0016
$A_{LR}(LEP)$	0.1306	0.0041	0.0129	0.0033	0.0005	−0.0016
$A_{FB}^{pol}(c)$	0.4725	0.0250	0.0043	0.0576	0.0095	−0.0016
$A_{FB}(c)$	0.0617	0.0070	0.0066	0.0105	0.0017	−0.0016
$A_{FB}^{pol}(b)$	0.6965	0.0200	0.0008	0.2571	0.0423	−0.0016
$A_{FB}(b)$	0.0910	0.0054	0.0091	0.0061	0.0010	−0.0016
$A_{FB}^{pol}(\mu)$	0.0980	0.0090	0.0096	0.0093	0.0015	−0.0016
$A_{FB}(\mu)$	0.0128	0.0035	0.0025	0.0139	0.0023	−0.0016
$\Gamma_{inv}(GeV)$	0.4990	0.0160	−0.0008	0.1947	0.0070	0.0004
$\Gamma_{ll}(GeV)$	0.0835	0.0007	0.0005	0.0139	0.0016	−0.0012
$\Gamma_{c\bar c}(GeV)$	0.2959	0.0300	0.0023	0.1293	0.0161	−0.0012
$\Gamma_{b\bar b}(GeV)$	0.3773	0.0400	0.0026	0.1514	0.0184	−0.0012
$\Gamma_Z(GeV)$	2.4837	0.0150	0.0133	0.0113	0.0011	−0.0010

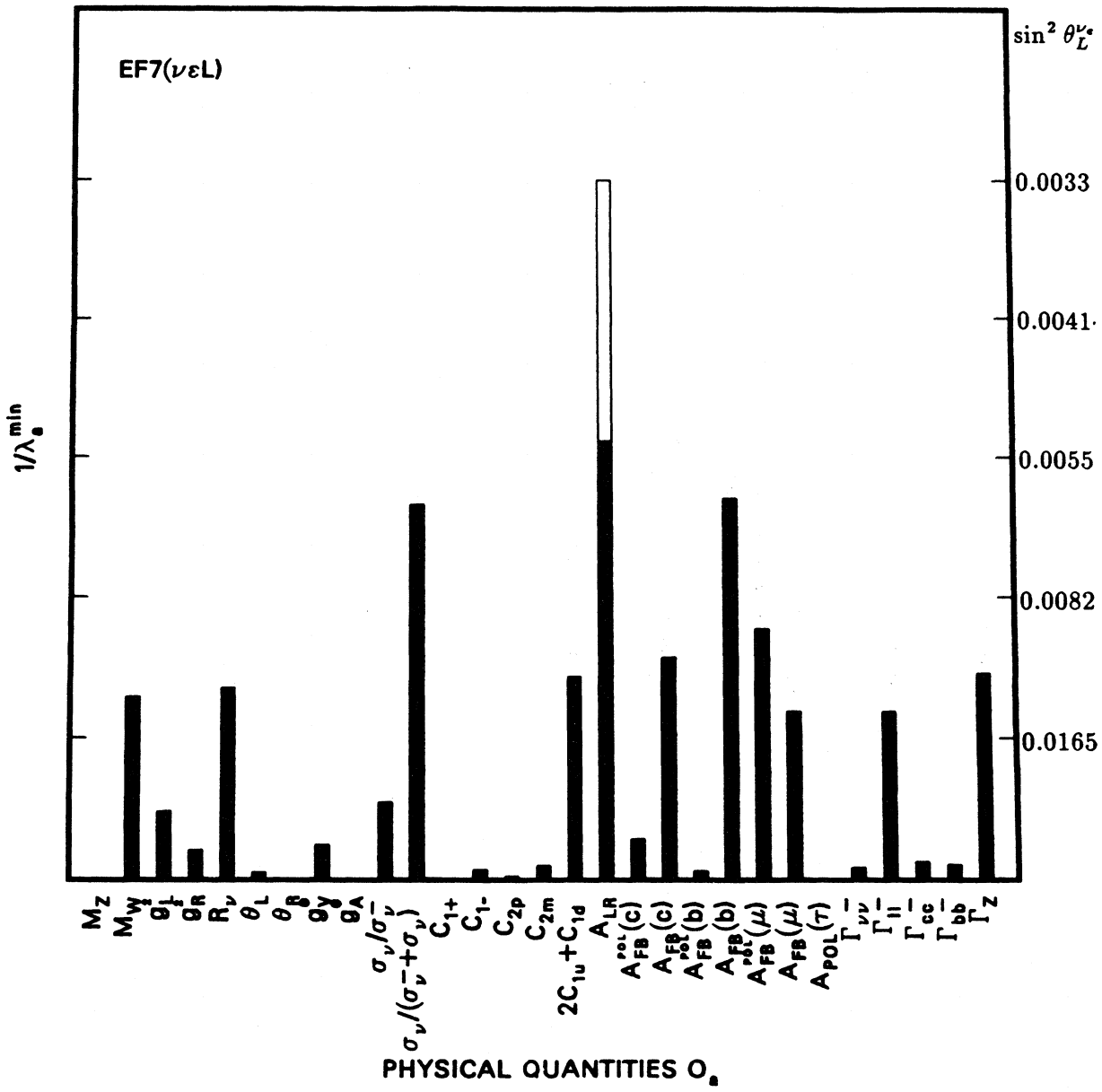

FIG. 53. The new physics of one extra ν_{eL}: solid bar for C_{2p} and $A_{\rm LR}$(SLC); open bar for $C_{2p}(1)$ and $A_{\rm LR}$(LEP).

TABLE XXVIII. Deviations from the SM by an extra fermion (μ_L). Type: extra left-handed SU(2)-singlet charged lepton mixed with ordinary muon (Sec. IV.C). Free parameter: $\lambda=\sin^2\theta_L^\mu$, where θ_L^μ is the mixing angle between ordinary and exotic [SU(2)-singlet] left-handed muon. Inputs: $M_Z=91.177$ GeV, $m_t=100$ GeV, $M_H=100$ GeV ($\sin^2\theta_W^M=0.2306$, $\sin^2\hat{\theta}_W=0.2334$). **Comments:** The inverses of the sixth column $1/\lambda^{\min}$ are plotted in Fig. 54. It is assumed that C_{2p} and C_{2m} are measured in muonic atoms and therefore receive direct contributions from μ_L mixing as well as $\sin^2\theta_W$ effects. $\Gamma_{l\bar{l}}$ is averaged over e, μ, and τ. R_ν would be sensitive to $\sin^2\theta_L^\mu\sim 0.0018$, while $\lambda^{\min}<0.01$ for g_L^2, $A_{\rm FB}(b)$, and $A_{\rm LR}$ at both LEP and SLC. If μ_R is mixed with an exotic [SU(2)-doublet] right-handed lepton, then we have the following shifts: $\Delta C_{2p}=0.0001$, $\Delta C_{2m}=-0.0100$, $\Delta A_{\rm FB}^{\rm pol}(\mu)=0.0157$, $\Delta A_{\rm FB}(\mu)=0.0021$, $\Delta\Gamma_{l\bar{l}}({\rm GeV})=-0.0005$, and $\Delta\Gamma_Z({\rm GeV})=-0.0016$.

Quantities	O_a^{SM}	ΔO_a^{exp}	ΔO_a^i $\lambda=0.01$	λ_a^{min}	$\Delta\sin^2\theta_W^{exp}$	$\Delta\sin^2\theta_W^{(a;Z)}$ $\lambda=0.01$
$M_Z(GeV)$	91.1770	0.0200	—	—	0.0003	—
$M_W(GeV)$	79.9832	0.1050	0.0855	0.0123	0.0006	−0.0005
g_L^2	0.2997	0.0042	0.0072	0.0058	0.0057	−0.0097
g_R^2	0.0301	0.0034	0.0002	0.1924	0.0130	0.0007
R_ν	0.3117	0.0013	0.0073	0.0018	0.0020	−0.0114
θ_L	2.4640	0.0300	−0.0009	0.3216	—	—
g_V^e	−0.0361	0.0220	−0.0037	0.0602	0.0110	−0.0018
g_A^e	−0.5037	0.0250	−0.0050	0.0496	—	—
$\sigma_\nu/\sigma_{\bar{\nu}}$	1.1515	0.0453	0.0149	0.0304	0.0050	−0.0016
$\sigma_\nu/(\sigma_{\bar{\nu}}+\sigma_\nu)$	0.1455	0.0026	0.0017	0.0152	0.0025	−0.0016
C_{1+}	0.1291	0.0013	0.0000	—	0.0033	0.0000
$C_{1+}(iso)$	0.1291	0.0003	0.0000	—	0.0009	0.0000
C_{1-}	−0.3633	0.1000	−0.0042	0.2379	0.0689	−0.0029
C_{2p}	−0.0140	0.0460	−0.0001	—	—	—
$C_{2p}(1)$	−0.0140	0.0046	−0.0001	0.3595	—	—
C_{2m}	−0.0537	0.1100	0.0032	0.3481	0.0274	0.0008
$2C_{1u}+C_{1d}$	−0.0323	0.0040	−0.0035	0.0115	0.0020	−0.0017
$A_{LR}(SLC)$	0.1306	0.0066	0.0129	0.0053	0.0008	−0.0016
$A_{LR}(LEP)$	0.1306	0.0041	0.0129	0.0033	0.0005	−0.0016
$A_{FB}^{pol}(c)$	0.4725	0.0250	0.0043	0.0576	0.0095	−0.0016
$A_{FB}(c)$	0.0617	0.0070	0.0066	0.0105	0.0017	−0.0016
$A_{FB}^{pol}(b)$	0.6965	0.0200	0.0008	0.2571	0.0423	−0.0016
$A_{FB}(b)$	0.0910	0.0054	0.0091	0.0061	0.0010	−0.0016
$A_{FB}^{pol}(\mu)$	0.0980	0.0090	−0.0040	0.0227	0.0015	0.0007
$A_{FB}(\mu)$	0.0128	0.0035	0.0007	0.0471	0.0023	−0.0005
$\Gamma_{inv}(GeV)$	0.4990	0.0160	0.0025	0.0641	0.0070	−0.0011
$\Gamma_{l\bar{l}}(GeV)$	0.0835	0.0007	−0.0001	0.0743	0.0016	0.0002
$\Gamma_{c\bar{c}}(GeV)$	0.2959	0.0300	0.0023	0.1293	0.0161	−0.0012
$\Gamma_{b\bar{b}}(GeV)$	0.3773	0.0400	0.0026	0.1514	0.0184	−0.0012
$\Gamma_Z(GeV)$	2.4837	0.0150	0.0148	0.0101	0.0011	−0.0011

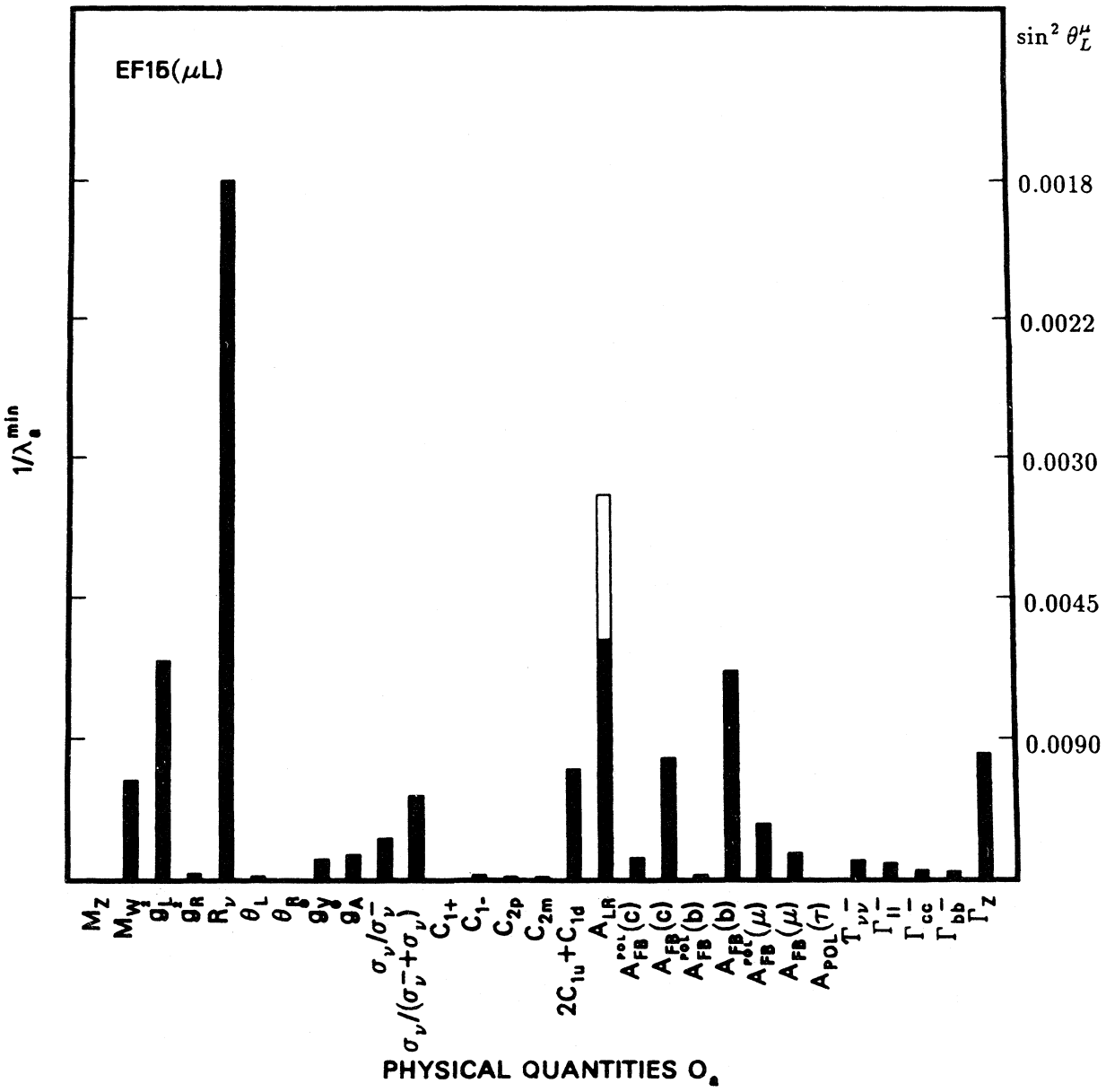

FIG. 54. The new physics of one extra μ_L: solid bar for C_{2p} and A_{LR}(SLC); open bar for $C_{2p}(1)$ and A_{LR}(LEP).

TABLE XXIX. Deviations from the SM by an extra fermion ($\nu_{\mu L}$). Type: extra left-handed SU(2)-singlet ν_μ (Sec. IV.C). Free parameter: $\lambda = \sin^2\theta_L^{\nu_\mu}$, where $\theta_L^{\nu_\mu}$ is the mixing angle between ordinary and exotic [SU(2)-singlet] left-handed ν_μ. Inputs: $M_Z = 91.177$ GeV, $m_t = 100$ GeV, $M_H = 100$ GeV ($\sin^2\theta_W^M = 0.2306$, $\sin^2\hat{\theta}_W = 0.2334$). **Comments:** The inverses of the sixth column $1/\lambda^{\min}$ are plotted in Fig. 55. The minimum λ is ~ 0.0033 for A_{LR}(LEP), while $\lambda^{\min} < 0.01$ for $A_{\rm LR}$(SLC), $A_{\rm FB}(b)$ and $A_{\rm FB}^{\rm pol}(\mu)$.

Quantities	O_a^{SM}	ΔO_a^{exp}	ΔO_a^i $\lambda = 0.01$	λ_a^{min}	$\Delta \sin^2\theta_W^{exp}$	$\Delta \sin^2\theta_W^{(a;Z)}$ $\lambda = 0.01$
$M_Z(GeV)$	91.1770	0.0200	—	—	0.0003	—
$M_W(GeV)$	79.9832	0.1050	0.0855	0.0123	0.0006	−0.0005
g_L^2	0.2997	0.0042	0.0012	0.0344	0.0057	−0.0016
g_R^2	0.0301	0.0034	−0.0004	0.0799	0.0130	−0.0016
R_ν	0.3117	0.0013	0.0011	0.0122	0.0020	−0.0016
θ_L	2.4640	0.0300	−0.0009	0.3216	—	—
g_V^e	−0.0361	0.0220	−0.0033	0.0669	0.0110	−0.0016
$\sigma_\nu/\sigma_{\bar{\nu}}$	1.1515	0.0453	0.0149	0.0304	0.0050	−0.0016
$\sigma_\nu/(\sigma_{\bar{\nu}} + \sigma_\nu)$	0.1455	0.0026	−0.0008	0.0324	0.0025	0.0008
C_{1+}	0.1291	0.0013	0.0000	—	0.0033	0.0000
$C_{1+}(iso)$	0.1291	0.0003	0.0000	—	0.0009	0.0000
C_{1-}	−0.3633	0.1000	−0.0042	0.2379	0.0689	−0.0029
C_{2p}	−0.0140	0.0460	−0.0001	—	—	—
$C_{2p}(1)$	−0.0140	0.0046	−0.0001	0.6551	—	—
C_{2m}	−0.0537	0.1100	−0.0069	0.1602	0.0274	−0.0017
$2C_{1u} + C_{1d}$	−0.0323	0.0040	−0.0035	0.0115	0.0020	−0.0017
$A_{LR}(SLC)$	0.1306	0.0066	0.0129	0.0053	0.0008	−0.0016
$A_{LR}(LEP)$	0.1306	0.0041	0.0129	0.0033	0.0005	−0.0016
$A_{FB}^{pol}(c)$	0.4725	0.0250	0.0043	0.0576	0.0095	−0.0016
$A_{FB}(c)$	0.0617	0.0070	0.0066	0.0105	0.0017	−0.0016
$A_{FB}^{pol}(b)$	0.6965	0.0200	0.0008	0.2571	0.0423	−0.0016
$A_{FB}(b)$	0.0910	0.0054	0.0091	0.0061	0.0010	−0.0016
$A_{FB}^{pol}(\mu)$	0.0980	0.0090	0.0096	0.0093	0.0015	−0.0016
$A_{FB}(\mu)$	0.0128	0.0035	0.0025	0.0139	0.0023	−0.0016
$\Gamma_{inv}(GeV)$	0.4990	0.0160	−0.0008	0.1947	0.0070	0.0004
$\Gamma_{l\bar{l}}(GeV)$	0.0835	0.0007	0.0005	0.0139	0.0016	−0.0012
$\Gamma_{c\bar{c}}(GeV)$	0.2959	0.0300	0.0023	0.1293	0.0161	−0.0012
$\Gamma_{b\bar{b}}(GeV)$	0.3773	0.0400	0.0026	0.1514	0.0184	−0.0012
$\Gamma_Z(GeV)$	2.4837	0.0150	0.0133	0.0113	0.0011	−0.0010

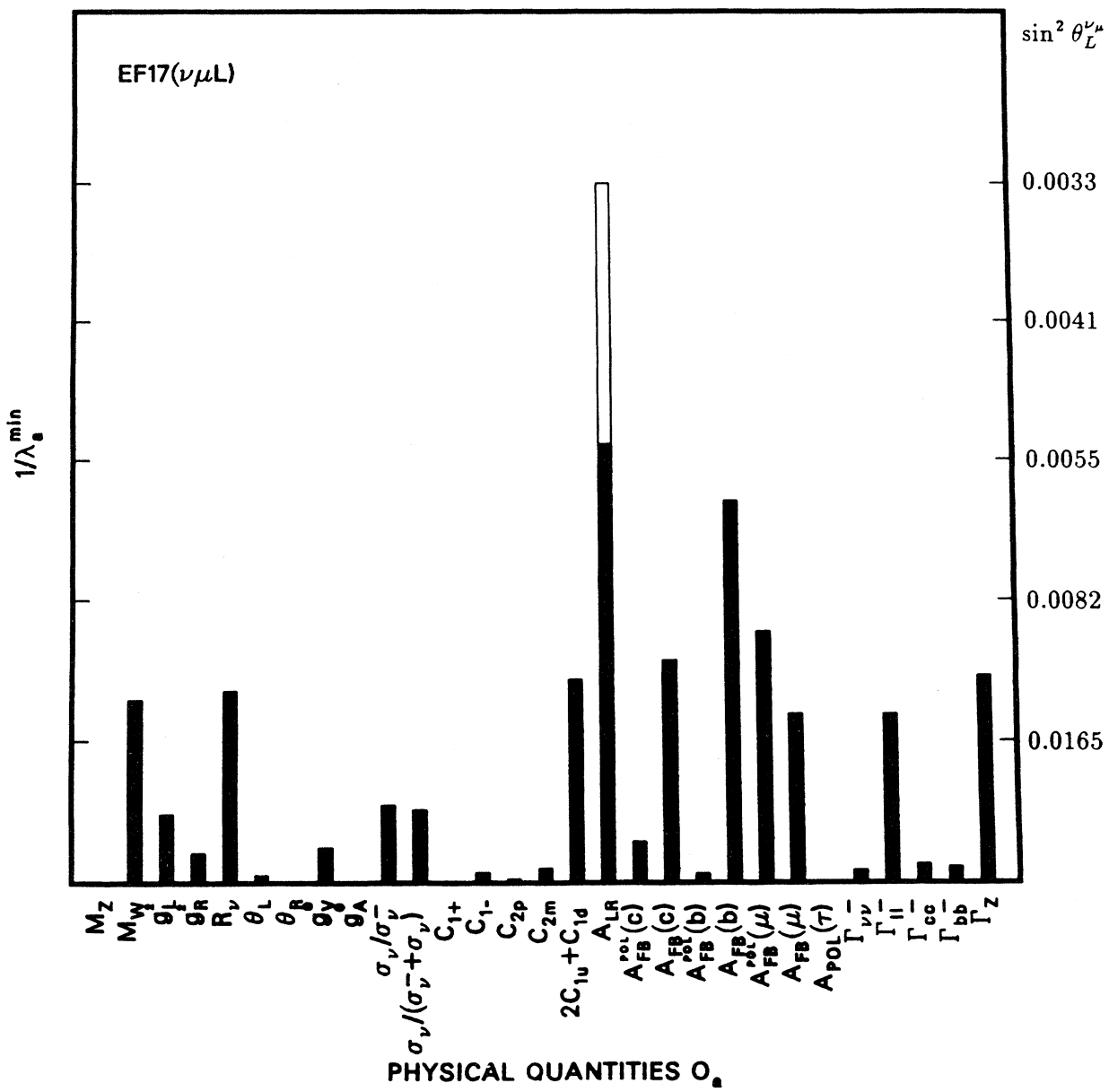

FIG. 55. The new physics of one extra $\nu_{\mu L}$: solid bar for $A_{\rm LR}$(SLC); open bar for $A_{\rm LR}$(LEP).

TABLE XXX(a). Deviations from the SM due to four-Fermi Operators induced by Compositeness. Type: four-fermi operators induced by compositeness of fermions (Sec. IV.D). Free parameter: $\lambda=(\sqrt{2}\pi/G_F\Lambda^2)$. Inputs: $M_Z=91.177$ GeV, $m_t=100$ GeV, $M_H=100$ GeV ($\sin^2\theta_W^M=0.2306$, $\sin^2\hat{\theta}_W=0.2334$). **Comments:** For the explicit definitions of physical observables, see Sec. III. In this table are included three types of operators: (1) $-L_1=\pm(4\pi/\Lambda_1^2)\bar{l}_{\mu L}\gamma^\mu l_{\mu L}\bar{q}_L\gamma_\mu q_L$, which shifts $\epsilon_L(u)$, $\epsilon_L(d)$, C_{2u}, and C_{2d}; (2) $-L_2=\pm(4\pi/\Lambda_2^2)\bar{\nu}_{\mu L}\gamma^\mu\nu_{\mu L}\bar{e}_L\gamma_\mu e_L$, which shifts g_V^e and g_A^e; and (3) $-L_3=\pm(4\pi/\Lambda_3^2)\bar{e}_L\gamma^\mu e_L\bar{q}_L\gamma_\mu q_L$, which shifts C_{1u} and C_{1d}. The deviation pattern of L_1 is plotted in Fig. 56(a). $C_{2p}(1)$ would be sensitive to $\lambda^{\min}=0.0023$, corresponding to $\Lambda_1=12.9$ TeV. The deviation pattern of L_2 is plotted in Fig. 56(b). $\sigma_\nu/(\sigma_{\bar{\nu}}+\sigma_\nu)$ has $\lambda^{\min}=0.0032$ ($\Lambda_2=10.9$ TeV). The deviation pattern of L_3 is plotted in Fig. 56(c). C_{1+}(iso) has $\lambda^{\min}=0.0002$ ($\Lambda_3\cong 44$ TeV).

Quantities	O_a^{SM}	ΔO_a^{exp}	ΔO_a^i $\lambda=0.01$	λ_a^{min}	$\Delta\sin^2\theta_W^{exp}$	$\Delta\sin^2\theta_W^{(a;Z)}$ $\lambda=0.01$
$M_Z(GeV)$	91.1770	0.0200	—	—	0.0003	—
g_L^2	0.2997	0.0042	−0.0017	0.0252	0.0057	0.0022
R_ν	0.3117	0.0013	−0.0017	0.0077	0.0020	0.0026
θ_L	2.4640	0.0300	−0.0257	0.0117	—	—
g_V^e	−0.0361	0.0220	0.0100	0.0220	0.0110	0.0050
g_A^e	−0.5037	0.0250	0.0100	0.0250	—	—
$\sigma_\nu/\sigma_{\bar{\nu}}$	1.1515	0.0453	−0.0421	0.0108	0.0050	0.0046
$\sigma_\nu/(\sigma_{\bar{\nu}}+\sigma_\nu)$	0.1455	0.0026	−0.0082	0.0032	0.0025	0.0078
C_{1+}	0.1291	0.0013	0.0141	0.0009	0.0033	0.0360
$C_{1+}(iso)$	0.1291	0.0003	0.0141	0.0002	0.0009	0.0360
C_{1-}	−0.3633	0.1000	0.0008	—	0.0689	0.0006
C_{2p}	−0.0140	0.0460	0.0200	0.0230	—	—
$C_{2p}(1)$	−0.0140	0.0046	0.0200	0.0023	—	—
$2C_{1u}+C_{1d}$	−0.0323	0.0040	0.0300	0.0013	0.0020	0.0149

TABLE XXX(b). e^+e^- asymmetries away from the Z pole at $s-M_Z^2=M_Z\Gamma_Z$. We have optimistically assumed experimental uncertainties that are the same as the corresponding uncertainties on-shell. $A_{LR}(f)$ is the polarization asymmetry for final states $f\bar{f}$ only. The Lagrangian is of the form $-L=4\pi/\Lambda^2\times$operator. $\lambda^{\min}$ is the value of $\lambda=2^{1/2}\pi/G_F\Lambda^2$ for which the change in the observable is equal to $\Delta O_a^{\exp}$, and $\Lambda_{\min}$ is the corresponding value of Λ.

Quantities	O_a^{SM}	ΔO_a^{exp}	Operator	λ^{min}	$\Lambda_{min}(TeV)$
$A_{LR}(\mu)$	0.1687	0.0100	$\bar{e}_L\gamma_\mu e_L\bar{\mu}_L\gamma^\mu\mu_L$	0.08	2.1
$A_{LR}(c)$	0.1991	0.0090	$\bar{e}_L\gamma_\mu e_L\bar{c}_L\gamma^\mu c_L$	0.07	2.3
$A_{LR}(b)$	0.1818	0.0080	$\bar{e}_L\gamma_\mu e_L\bar{b}_L\gamma^\mu b_L$	0.07	2.3
$A_{FB}^{pol}(c)$	0.5061	0.0250	$\bar{e}_L\gamma_\mu e_L\bar{c}_L\gamma^\mu c_L$	0.67	0.8
$A_{FB}(c)$	0.1440	0.0070	$\bar{e}_L\gamma_\mu e_L\bar{c}_L\gamma^\mu c_L$	0.07	2.3
$A_{FB}^{pol}(b)$	0.7025	0.0200	$\bar{e}_L\gamma_\mu e_L\bar{b}_L\gamma^\mu b_L$	2.98	0.4
$A_{FB}(b)$	0.1365	0.0050	$\bar{e}_L\gamma_\mu e_L\bar{b}_L\gamma^\mu b_L$	0.06	2.6
$A_{FB}^{pol}(\mu)$	0.1266	0.0090	$\bar{e}_L\gamma_\mu e_L\bar{\mu}_L\gamma^\mu\mu_L$	0.10	2.0
$A_{FB}(\mu)$	0.1285	0.0035	$\bar{e}_L\gamma_\mu e_L\bar{\mu}_L\gamma^\mu\mu_L$	0.04	3.1
$A_{pol}(\tau)$	0.1687	0.0110	$\bar{e}_L\gamma_\mu e_L\bar{\tau}_L\gamma^\mu\tau_L$	0.10	1.9

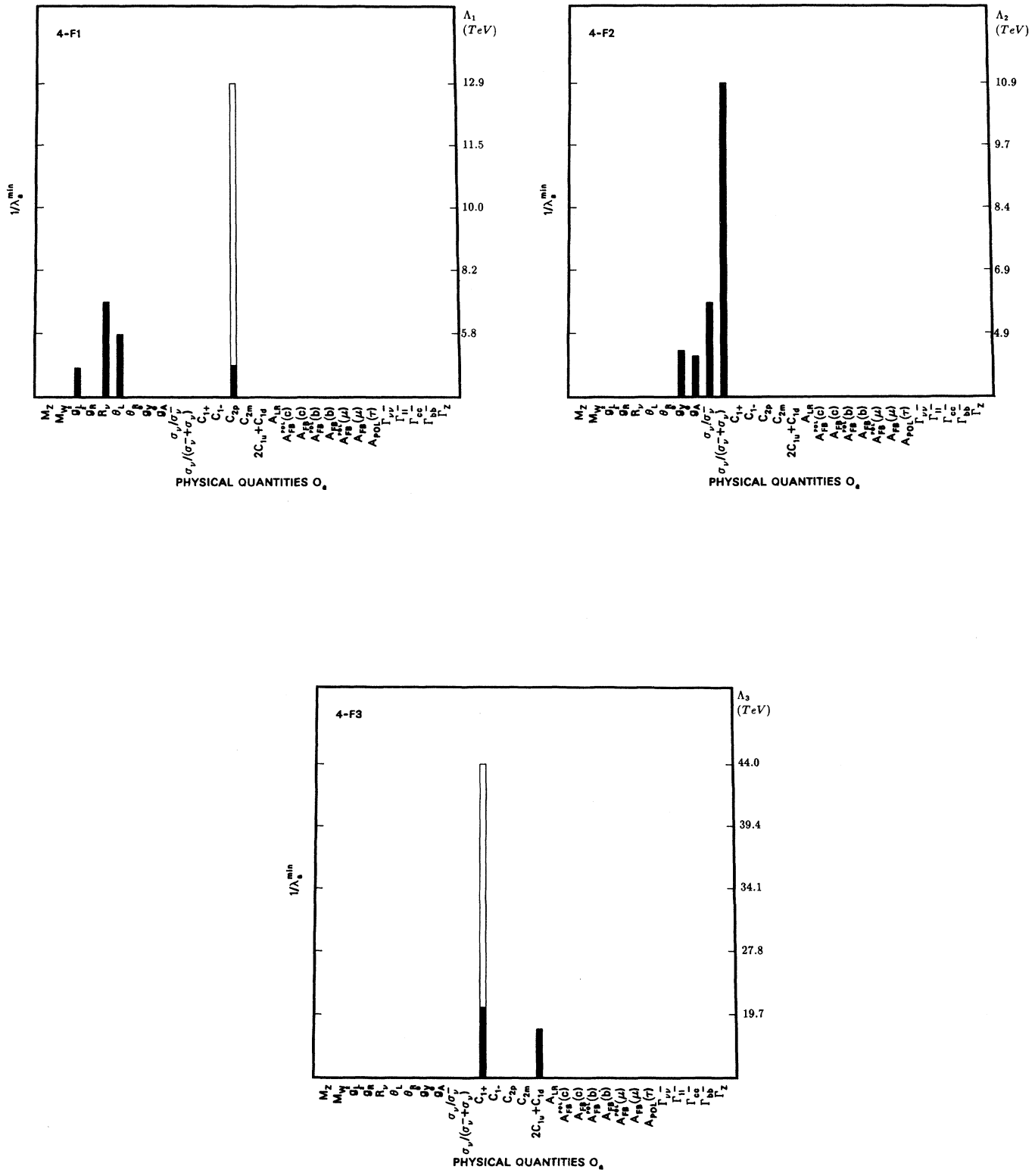

FIG. 56. The new physics of four-fermi operators: (a) four-fermi operator, type I: solid bar for C_{2p}, open bar for $C_{2p}(1)$. The right-hand scale corresponds to the compositeness scale Λ in TeV. (b) Four-fermi operator, type II: solid bar for C_{1+} and A_{LR}(SLC); open bar for C_{1+}(iso) and A_{LR}(LEP). (c) Four-fermi operator, type III: solid bar for C_{1+}, open bar for C_{1+}(iso).

TABLE XXXI. Deviations from the SM due to heavy-particle contributions to loop corrections (h_V). Type: Deviations arising from loop corrections due to heavy-particle physics, e.g., nondegenerate heavy fermion or boson multiplets, with $h_V \neq 0$, $h_{AZ}=0$, $h_{AW}=0$ (Sec. IV.E). Free parameter: $\lambda=\alpha h_V$ ($\alpha=1/137.036$). Inputs: $M_Z=91.177$ GeV, $m_t=100$ GeV, $M_H=100$ GeV ($\sin^2\theta_W^M=0.2306$, $\sin^2\hat{\theta}_W=0.2334$). **Comments:** For the explicit definitions of physical observables, see Sec. III. The inverses of the sixth column $1/\lambda^{\min}$ are plotted in Fig. 57. As expected, the deviation pattern among the observables is exactly the same as that of nonstandard Higgs fields (see Table XIX and Fig. 45). R_ν has $\lambda^{\min}=0.0015$, corresponding to $h_V=0.21$; $A_{\rm LR}$(LEP) has $\lambda^{\min}=0.0017$ ($h_V=0.23$); and M_W has $\lambda^{\min}=0.0018$ ($h_V=0.25$). $A_{\rm LR}$(SLC), $A_{\rm FB}(b)$, and $\sigma_\nu/(\sigma_{\bar\nu}+\sigma_\nu)$ all have $\lambda^{\min}<0.004$.

Quantities	O_a^{SM}	ΔO_a^{exp}	ΔO_a^i $\lambda=0.01$	λ_a^{min}	$\Delta\sin^2\theta_W^{exp}$	$\Delta\sin^2\theta_W^{(a;Z)}$ $\lambda=0.01$
$M_Z(GeV)$	91.1770	0.0200	—	—	0.0003	—
$M_W(GeV)$	79.9832	0.1050	0.5709	0.0018	0.0006	−0.0033
g_L^2	0.2997	0.0042	0.0084	0.0050	0.0057	−0.0114
g_R^2	0.0301	0.0034	−0.0002	0.1366	0.0130	−0.0010
R_ν	0.3117	0.0013	0.0083	0.0015	0.0020	−0.0131
θ_L	2.4640	0.0300	−0.0019	0.1608	—	—
θ_R	5.1765	0.4400	0.0000	—	—	—
g_V^e	−0.0361	0.0220	−0.0069	0.0317	0.0110	−0.0035
g_A^e	−0.5037	0.0250	−0.0050	0.0496	—	—
$\sigma_\nu/\sigma_{\bar\nu}$	1.1515	0.0453	0.0298	0.0152	0.0050	−0.0033
$\sigma_\nu/(\sigma_{\bar\nu}+\sigma_\nu)$	0.1455	0.0026	0.0068	0.0039	0.0025	−0.0065
C_{1+}	0.1291	0.0013	0.0000	—	0.0033	0.0000
$C_{1+}(iso)$	0.1291	0.0003	0.0000	—	0.0009	0.0000
C_{1-}	−0.3633	0.1000	−0.0084	0.1190	0.0689	−0.0058
C_{2p}	−0.0140	0.0460	−0.0001	—	—	—
$C_{2p}(1)$	−0.0140	0.0046	−0.0001	0.3276	—	—
C_{2m}	−0.0537	0.1100	−0.0137	0.0801	0.0274	−0.0034
$2C_{1u}+C_{1d}$	−0.0323	0.0040	−0.0070	0.0058	0.0020	−0.0035
$A_{LR}(SLC)$	0.1306	0.0066	0.0257	0.0026	0.0008	−0.0033
$A_{LR}(LEP)$	0.1306	0.0041	0.0257	0.0017	0.0005	−0.0033
$A_{FB}^{pol}(c)$	0.4725	0.0250	0.0087	0.0288	0.0095	−0.0033
$A_{FB}(c)$	0.0617	0.0070	0.0133	0.0053	0.0017	−0.0033
$A_{FB}^{pol}(b)$	0.6965	0.0200	0.0016	0.1285	0.0423	−0.0033
$A_{FB}(b)$	0.0910	0.0054	0.0181	0.0030	0.0010	−0.0033
$A_{FB}^{pol}(\mu)$	0.0980	0.0090	0.0193	0.0047	0.0015	−0.0033
$A_{FB}(\mu)$	0.0128	0.0035	0.0050	0.0069	0.0023	−0.0033
$A_{pol}(\tau)$	0.1306	0.0110	0.0257	0.0043	0.0014	−0.0033
$\Gamma_{inv}(GeV)$	0.4990	0.0160	0.0050	0.0321	0.0070	−0.0022
$\Gamma_{l\bar l}(GeV)$	0.0835	0.0007	0.0010	0.0070	0.0016	−0.0023
$\Gamma_{c\bar c}(GeV)$	0.2959	0.0300	0.0046	0.0646	0.0161	−0.0025
$\Gamma_{b\bar b}(GeV)$	0.3773	0.0400	0.0053	0.0757	0.0184	−0.0024
$\Gamma_Z(GeV)$	2.4837	0.0150	0.0332	0.0045	0.0011	−0.0024

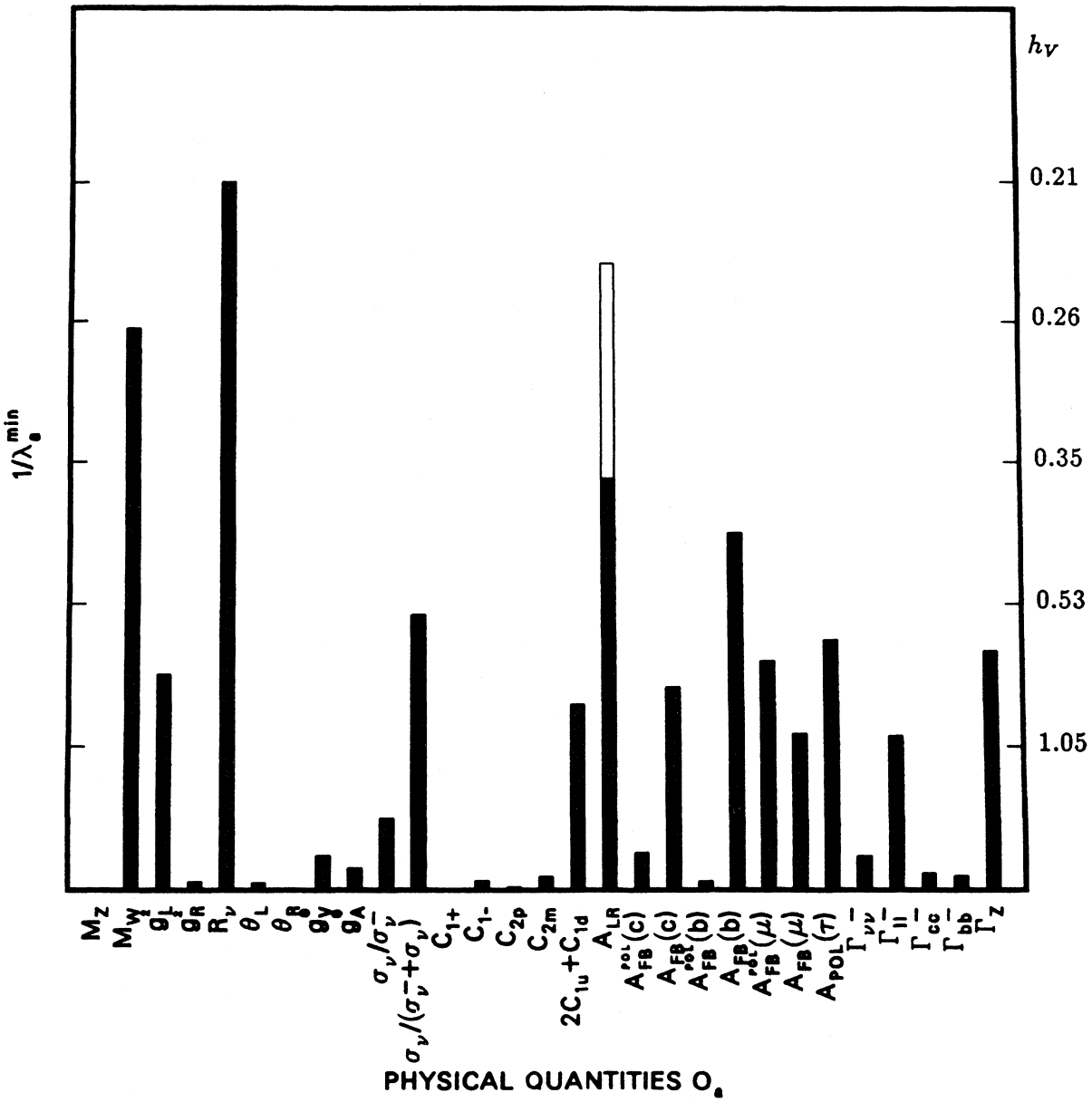

FIG. 57. Heavy physics through loop corrections (h_V): solid bar for C_{2p} and A_{LR}(SLC); open bar for $C_{2p}(1)$ and A_{LR}(LEP). The right-hand scale is h_V.

TABLE XXXII. Deviations from the SM due to heavy-particle contributions to loop corrections (h_A). Type: deviations arising from loop corrections due to heavy-particle physics, e.g., technicolor or degenerate heavy-fermion multiplets, with $h_V=0$, $h_A=h_{AZ}=h_{AW}\neq 0$ (Sec. IV.E). Free parameter: $\lambda=\sqrt{2}G_F M_Z^2 h_A/4\pi$. Inputs: $M_Z=91.177$ GeV, $m_t=100$ GeV, $M_H=100$ GeV ($\sin^2\theta_W^M=0.2306$, $\sin^2\hat{\theta}_W=0.2334$). **Comments:** The inverses of the sixth column $1/\lambda^{\min}$ are plotted in Fig. 58. $A_{\rm LR}$(LEP) has $\lambda^{\min}=0.0017$, corresponding to $h_A=0.16$. $A_{\rm LR}$(SLC), C_{1+}(iso), and $A_{\rm FB}(b)$ all have $\lambda^{\min}\sim 0.003$ ($h_A\sim 0.27$). We have assumed $h_{AZ}=h_{AW}$, which is true for most types of new physics. However, in principle h_{AZ} and h_{AW} are two independent parameters. For $h_{AW}=0$, $\Delta O_{M_W}=-0.57$ GeV rather than -0.26 GeV, while for $h_{AZ}=0$, M_W alone is shifted, by $+0.30$ GeV.

Quantities	O_a^{SM}	ΔO_a^{exp}	ΔO_a^i $\lambda=0.01$	λ_a^{min}	$\Delta\sin^2\theta_W^{exp}$	$\Delta\sin^2\theta_W^{(a;Z)}$ $\lambda=0.01$
$M_Z(GeV)$	91.1770	0.0200	—	—	0.0003	—
$M_W(GeV)$	79.9832	0.1050	−0.2631	0.0039	0.0006	0.0015
g_L^2	0.2997	0.0042	−0.0024	0.0172	0.0057	0.0033
g_R^2	0.0301	0.0034	0.0009	0.0400	0.0130	0.0033
R_ν	0.3117	0.0013	−0.0021	0.0061	0.0020	0.0033
θ_L	2.4640	0.0300	0.0019	0.1608	—	—
θ_R	5.1765	0.4400	0.0000	—	—	—
g_V^e	−0.0361	0.0220	0.0066	0.0334	0.0110	0.0033
g_A^e	−0.5037	0.0250	0.0000	—	—	—
$\sigma_\nu/\sigma_{\bar{\nu}}$	1.1515	0.0453	−0.0298	0.0152	0.0050	0.0033
$\sigma_\nu/(\sigma_{\bar{\nu}}+\sigma_\nu)$	0.1455	0.0026	−0.0034	0.0076	0.0025	0.0033
C_{1+}	0.1291	0.0013	0.0013	0.0101	0.0033	0.0033
$C_{1+}(iso)$	0.1291	0.0003	0.0013	0.0026	0.0009	0.0033
C_{1-}	−0.3633	0.1000	0.0048	0.2095	0.0689	0.0033
C_{2p}	−0.0140	0.0460	0.0000	—	—	—
$C_{2p}(1)$	−0.0140	0.0046	0.0000	—	—	—
C_{2m}	−0.0537	0.1100	0.0132	0.0834	0.0274	0.0033
$2C_{1u}+C_{1d}$	−0.0323	0.0040	0.0066	0.0060	0.0020	0.0033
$A_{LR}(SLC)$	0.1306	0.0066	−0.0257	0.0026	0.0008	0.0033
$A_{LR}(LEP)$	0.1306	0.0041	−0.0257	0.0017	0.0005	0.0033
$A_{FB}^{pol}(c)$	0.4725	0.0250	−0.0087	0.0288	0.0095	0.0033
$A_{FB}(c)$	0.0617	0.0070	−0.0133	0.0053	0.0017	0.0033
$A_{FB}^{pol}(b)$	0.6965	0.0200	−0.0016	0.1285	0.0423	0.0033
$A_{FB}(b)$	0.0910	0.0054	−0.0181	0.0030	0.0010	0.0033
$A_{FB}^{pol}(\mu)$	0.0980	0.0090	−0.0193	0.0047	0.0015	0.0033
$A_{FB}(\mu)$	0.0128	0.0035	−0.0050	0.0069	0.0023	0.0033
$A_{pol}(\tau)$	0.1306	0.0110	−0.0257	0.0043	0.0014	0.0033
$\Gamma_{inv}(GeV)$	0.4990	0.0160	0.0000	—	0.0070	0.0000
$\Gamma_{l\bar{l}}(GeV)$	0.0835	0.0007	−0.0002	0.0411	0.0016	0.0004
$\Gamma_{c\bar{c}}(GeV)$	0.2959	0.0300	−0.0017	0.1783	0.0161	0.0009
$\Gamma_{b\bar{b}}(GeV)$	0.3773	0.0400	−0.0015	0.2646	0.0184	0.0007
$\Gamma_Z(GeV)$	2.4837	0.0150	−0.0084	0.0178	0.0011	0.0006

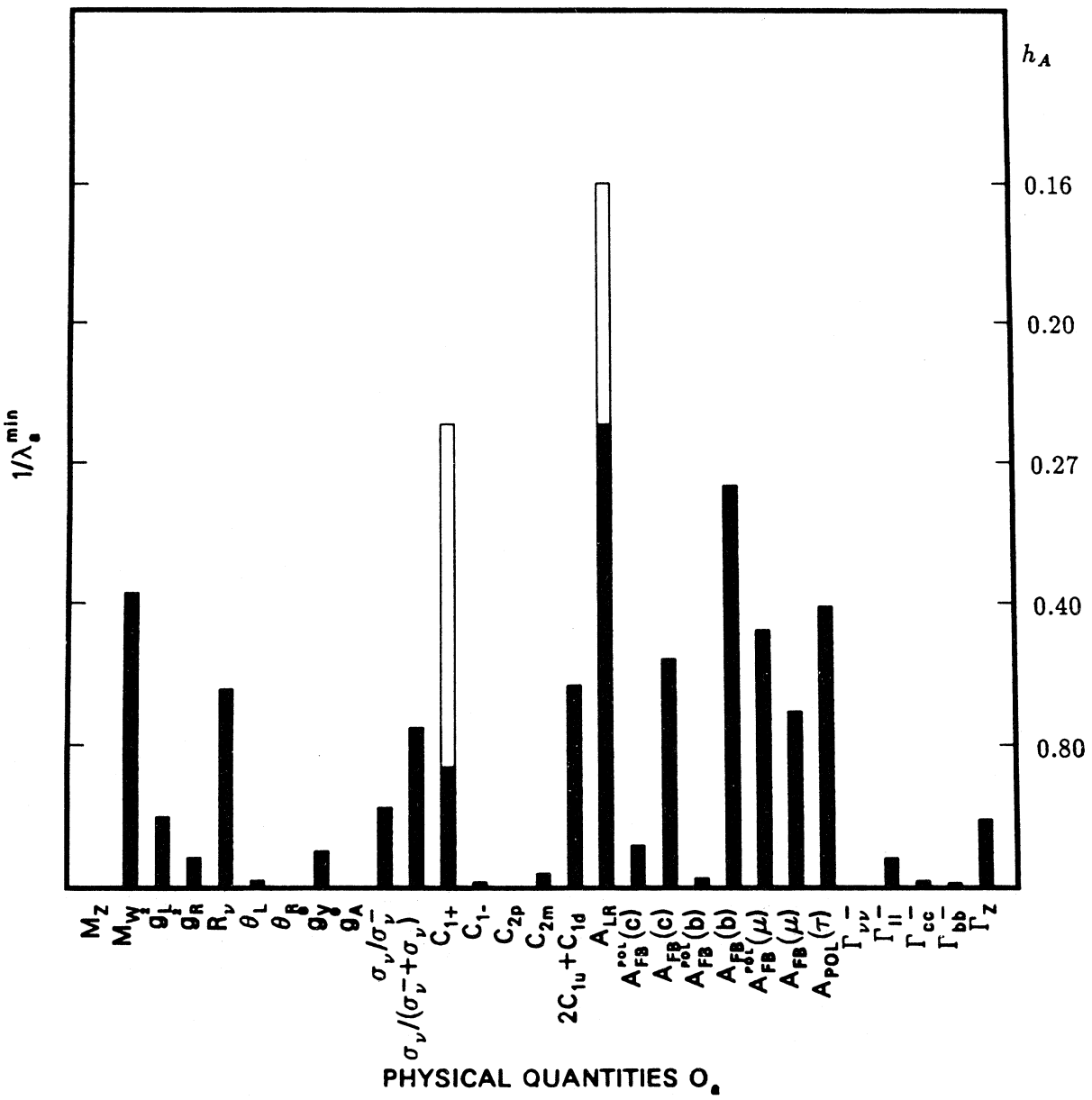

FIG. 58. Heavy physics through loops corrections (h_A): solid bar for C_{1+} and A_{LR}(SLC); open bar for C_{1+}(iso) and A_{LR}(LEP). The right-hand scale is h_A.

TABLE XXXIII. Deviations from the SM due to variation of M_H. Type: deviations arising from the variation in the Higgs mass M_H from the reference value of 100 GeV (see Sec. IV.E). Inputs: $M_Z=91.177$ GeV, $m_t=100$ GeV [$\sin^2\theta_W^M=0.2327(0.2338)$ for $M_H=500$ GeV (1000 GeV); $\sin^2\hat{\theta}_W=0.2342(0.2346)$]. The numbers in parentheses within the table are the values of M_H in GeV. **Comments:** For the explicit definitions of physical observables, see Sec. III. The ratios r_a of the M_H-induced offsets of the values of the observables to the experimental errors ($r_a=|\Delta O_a|/\Delta O_a^{\rm exp}$) are given in column 6 for $M_H=1000$ GeV and are plotted in Fig. 59(a) (for $M_H=500$ GeV) and in Fig. 59(b) (for $M_H=1000$ GeV). For $M_H=1000$ GeV, $r_a\cong 2.9$ for $A_{\rm LR}$(LEP), implying approximately a 3σ shift, while $r_a\sim 1.5-1.8$ for M_W, R_ν, $A_{\rm LR}$(SLC), and $A_{\rm FB}(b)$.

Quantities	O_a^{SM} (100)	ΔO_a^{exp}	ΔO_a^i (500)	ΔO_a^i (1000)	r_a (1000)	$\Delta\sin^2\theta_W^{exp}$	$\Delta\sin^2\theta_W^{(a;Z)}$ (500)	$\Delta\sin^2\theta_W^{(a;Z)}$ (1000)
$M_Z(GeV)$	91.1770	0.0200	—	—	—	0.0003	—	—
$M_W(GeV)$	79.9832	0.1050	−0.1182	−0.1786	1.7002	0.0006	0.0007	0.0010
g_V^2	0.2997	0.0042	−0.0015	−0.0023	0.5379	0.0057	0.0020	0.0031
g_R^2	0.0301	0.0034	0.0002	0.0003	0.0775	0.0130	0.0007	0.0010
R_ν	0.3117	0.0013	−0.0014	−0.0022	1.6866	0.0020	0.0022	0.0034
θ_L	2.4640	0.0300	0.0005	0.0007	0.0246	—	0.0009	0.0013
θ_R	5.1765	0.4400	0.0000	0.0000	0.0000	—	—	—
g_V^e	−0.0361	0.0220	0.0021	0.0030	0.1383	0.0110	0.0010	0.0015
g_A^e	−0.5037	0.0250	0.0006	0.0010	0.0404	—	—	—
$\sigma_\nu/\sigma_{\bar{\nu}}$	1.1515	0.0453	−0.0092	−0.0135	0.2975	0.0050	0.0010	0.0015
$\sigma_\nu/(\sigma_{\bar{\nu}}+\sigma_\nu)$	0.1455	0.0026	−0.0015	−0.0022	0.8590	0.0025	0.0015	0.0022
C_{1+}	0.1291	0.0013	0.0002	0.0002	0.1692	0.0033	0.0004	0.0006
$C_{1+}(iso)$	0.1291	0.0003	0.0002	0.0002	0.7333	0.0009	0.0004	0.0006
C_{1-}	−0.3633	0.1000	0.0017	0.0026	0.0257	0.0689	0.0012	0.0018
C_{2p}	−0.0140	0.0460	0.0002	0.0003	0.0059	—	—	—
$C_{2p}(1)$	−0.0140	0.0046	0.0002	0.0003	0.0587	—	—	—
C_{2m}	−0.0537	0.1100	0.0040	0.0059	0.0533	0.0274	0.0010	0.0015
$2C_{1u}+C_{1d}$	−0.0323	0.0040	0.0018	0.0026	0.6475	0.0020	0.0008	0.0013
$A_{LR}(SLC)$	0.1306	0.0066	−0.0080	−0.0117	1.7790	0.0008	0.0010	0.0015
$A_{LR}(LEP)$	0.1306	0.0041	−0.0080	−0.0117	2.8637	0.0005	0.0010	0.0015
$A_{FB}^{pol}(c)$	0.4725	0.0250	−0.0029	−0.0043	0.1705	0.0095	0.0011	0.0016
$A_{FB}(c)$	0.0617	0.0070	−0.0041	−0.0061	0.8649	0.0017	0.0010	0.0015
$A_{FB}^{pol}(b)$	0.6965	0.0200	−0.0005	−0.0008	0.0393	0.0423	0.0011	0.0016
$A_{FB}(b)$	0.0910	0.0054	−0.0056	−0.0083	1.5316	0.0010	0.0010	0.0015
$A_{FB}^{pol}(\mu)$	0.0980	0.0090	−0.0060	−0.0088	0.9784	0.0015	0.0010	0.0015
$A_{FB}(\mu)$	0.0128	0.0035	−0.0015	−0.0022	0.6277	0.0023	0.0011	0.0016
$A_{pol}(\tau)$	0.1306	0.0110	−0.0080	−0.0117	1.0674	0.0014	0.0010	0.0015
$\Gamma_{inv}(GeV)$	0.4990	0.0160	−0.0006	−0.0010	0.0633	0.0070	0.0003	0.0005
$\Gamma_{l\bar{l}}(GeV)$	0.0835	0.0007	−0.0001	−0.0002	0.3143	0.0016	0.0003	0.0005
$\Gamma_{c\bar{c}}(GeV)$	0.2959	0.0300	−0.0008	−0.0012	0.0410	0.0161	0.0004	0.0007
$\Gamma_{b\bar{b}}(GeV)$	0.3773	0.0400	−0.0009	−0.0014	0.0358	0.0184	0.0004	0.0007
$\Gamma_Z(GeV)$	2.4837	0.0150	−0.0053	−0.0085	0.5686	0.0011	0.0004	0.0006

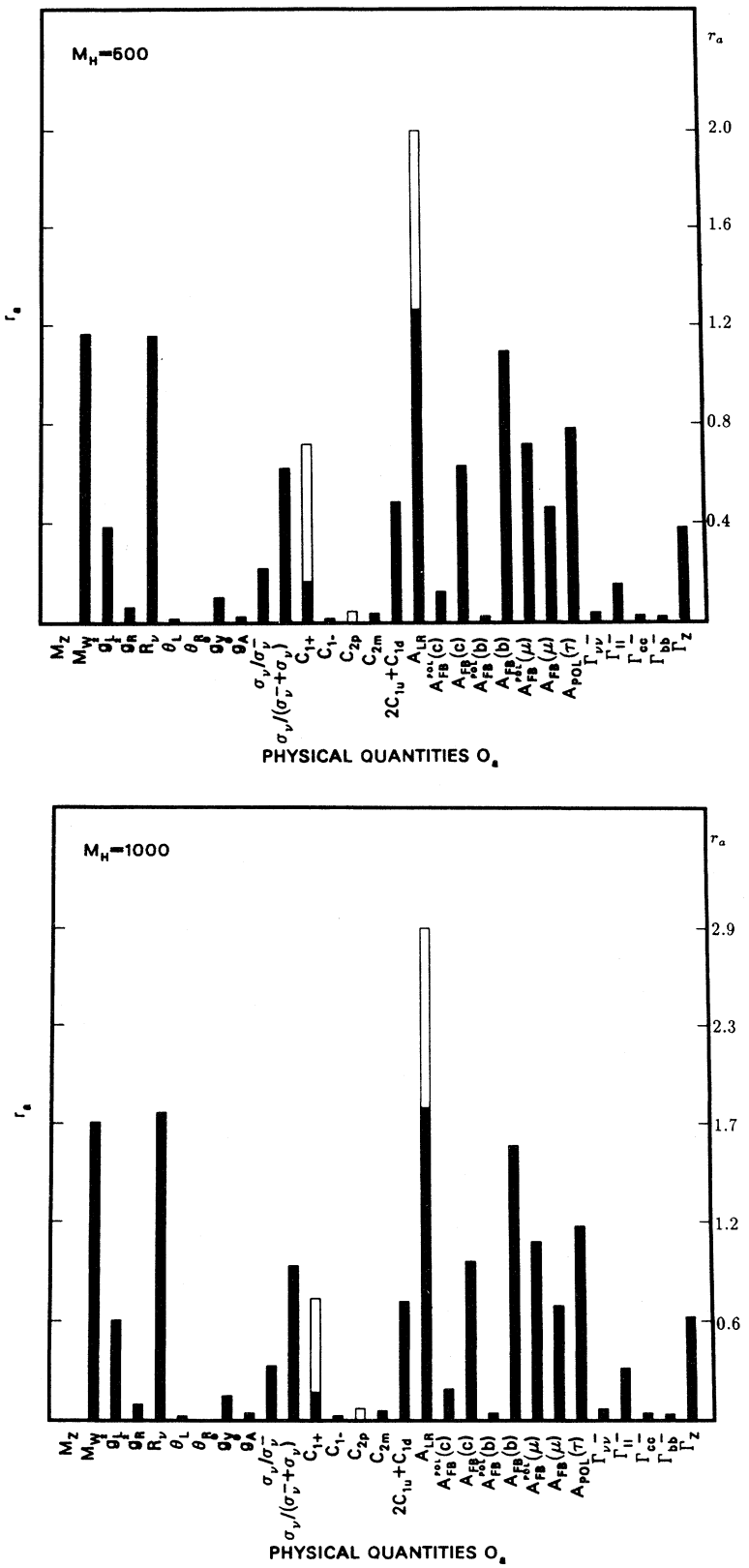

FIG. 59. Effects of the Higgs mass M_H: (a) change in the SM predictions for $M_H = 500$ GeV: solid bar for C_{1+}, C_{2p}, and $A_{\rm LR}$(SLC); open bar for C_{1+}(iso), $C_{2p}(1)$, and $A_{\rm LR}$(LEP). The right-hand scale is $r_a = |\Delta O_a| / \Delta O_a^{\rm exp}$. (b) Change in the SM predictions for $M_H = 1000$ GeV.

TABLE XXXIV. Deviations from the SM due to variation in m_t. Type: deviations arising from the variation in the top quark mass m_t from the reference value of 100 GeV (see Sec. IV.E). Inputs: $M_Z=91.177$ GeV, $M_H=100$ GeV [$\sin^2\theta_W^M=0.2248(0.2178)$ for $m_t=150$ GeV (200 GeV); $\sin^2\hat{\theta}_W=0.2321(0.2302)$]. The numbers in parentheses within the table are the values of m_t in GeV. **Comments:** The ratios r_a of the m_t-induced offsets of the values of the observables to the experimental errors ($r_a=|\Delta O_a|/\Delta O_a^{\rm exp}$) are given in column 6 for $m_t=200$ GeV and are plotted in Fig. 60(a) (for $m_t=150$ GeV) and in Fig. 60(b) (for $m_t=200$ GeV). R_ν, $A_{\rm LR}$ (LEP), and M_W are very sensitive to large m_t, with $r_a\sim 7$ for $m_t=200$ GeV, while $r_a\sim 4.4$ for $A_{\rm LR}$(SLC). g_L^2, $\sigma_{\nu e}/(\sigma_{\nu_e e}+\sigma_{\bar{\nu}e})$, $2C_{1u}+C_{1d}$, $\Gamma_{l\bar{l}}\,\Gamma_Z$, and the Z-pole asymmetries are also sensitive.

Quantities	O_a^{SM} (100)	ΔO_a^{exp}	ΔO_a^i (150)	ΔO_a^i (200)	r_a (200)	$\Delta\sin^2\theta_W^{exp}$	$\Delta\sin^2\theta_W^{(a;Z)}$ (150)	$\Delta\sin^2\theta_W^{(a;Z)}$ (200)
$M_Z(GeV)$	91.1770	0.0200	—	—	—	0.0003	—	—
$M_W(GeV)$	79.9832	0.1050	0.3354	0.7640	7.2757	0.0006	−0.0018	−0.0041
g_L^2	0.2997	0.0042	0.0037	0.0091	2.1756	0.0057	−0.0050	−0.0121
g_R^2	0.0301	0.0034	−0.0003	−0.0006	0.1791	0.0130	−0.0010	−0.0024
R_ν	0.3117	0.0013	0.0036	0.0089	6.9653	0.0020	−0.0056	−0.0137
θ_L	2.4640	0.0300	−0.0009	−0.0021	0.0699	—	−0.0016	−0.0038
θ_R	5.1765	0.4400	0.0000	0.0000	0.0001	—	—	—
g_V^e	−0.0361	0.0220	−0.0041	−0.0096	0.4362	0.0110	−0.0020	−0.0048
g_A^e	−0.5037	0.0250	−0.0020	−0.0049	0.1956	—	—	—
$\sigma_\nu/\sigma_{\bar{\nu}}$	1.1515	0.0453	0.0164	0.0361	0.7960	0.0050	−0.0018	−0.0039
$\sigma_\nu/(\sigma_{\bar{\nu}}+\sigma_\nu)$	0.1455	0.0026	0.0033	0.0077	2.9489	0.0025	−0.0030	−0.0070
C_{1+}	0.1291	0.0013	−0.0001	−0.0004	0.2923	0.0033	−0.0003	−0.0010
$C_{1+}(iso)$	0.1291	0.0003	−0.0001	−0.0004	1.2667	0.0009	−0.0003	−0.0010
C_{1-}	−0.3633	0.1000	−0.0038	−0.0094	0.0940	0.0689	−0.0026	−0.0065
C_{2p}	−0.0140	0.0460	−0.0005	−0.0012	0.0259	—	—	—
$C_{2p}(1)$	−0.0140	0.0046	−0.0005	−0.0012	0.2592	—	—	—
C_{2m}	−0.0537	0.1100	−0.0069	−0.0151	0.1369	0.0274	−0.0017	−0.0037
$2C_{1u}+C_{1d}$	−0.0323	0.0040	−0.0034	−0.0086	2.1375	0.0020	−0.0017	−0.0044
$A_{LR}(SLC)$	0.1306	0.0066	0.0130	0.0288	4.3569	0.0008	−0.0017	−0.0037
$A_{LR}(LEP)$	0.1306	0.0041	0.0130	0.0288	7.0136	0.0005	−0.0017	−0.0037
$A_{FB}^{pol}(c)$	0.4725	0.0250	0.0047	0.0103	0.4133	0.0095	−0.0018	−0.0041
$A_{FB}(c)$	0.0617	0.0070	0.0068	0.0152	2.1762	0.0017	−0.0017	−0.0037
$A_{FB}^{pol}(b)$	0.6965	0.0200	0.0009	0.0019	0.0952	0.0423	−0.0019	−0.0042
$A_{FB}(b)$	0.0910	0.0054	0.0092	0.0203	3.7649	0.0010	−0.0017	−0.0037
$A_{FB}^{pol}(\mu)$	0.0980	0.0090	0.0098	0.0216	2.3963	0.0015	−0.0017	−0.0037
$A_{FB}(\mu)$	0.0128	0.0035	0.0027	0.0063	1.7869	0.0023	−0.0015	−0.0034
$A_{pol}(\tau)$	0.1306	0.0110	0.0130	0.0288	2.6142	0.0014	−0.0017	−0.0037
$\Gamma_{inv}(GeV)$	0.4990	0.0160	0.0019	0.0047	0.2913	0.0070	−0.0008	−0.0018
$\Gamma_{l\bar{l}}(GeV)$	0.0835	0.0007	0.0003	0.0008	1.0861	0.0016	−0.0007	−0.0015
$\Gamma_{c\bar{c}}(GeV)$	0.2959	0.0300	0.0019	0.0045	0.1508	0.0161	−0.0009	−0.0022
$\Gamma_{b\bar{b}}(GeV)$	0.3773	0.0400	−0.0007	−0.0018	0.0461	0.0184	0.0003	0.0008
$\Gamma_Z(GeV)$	2.4837	0.0150	0.0106	0.0250	1.6646	0.0011	−0.0007	−0.0016

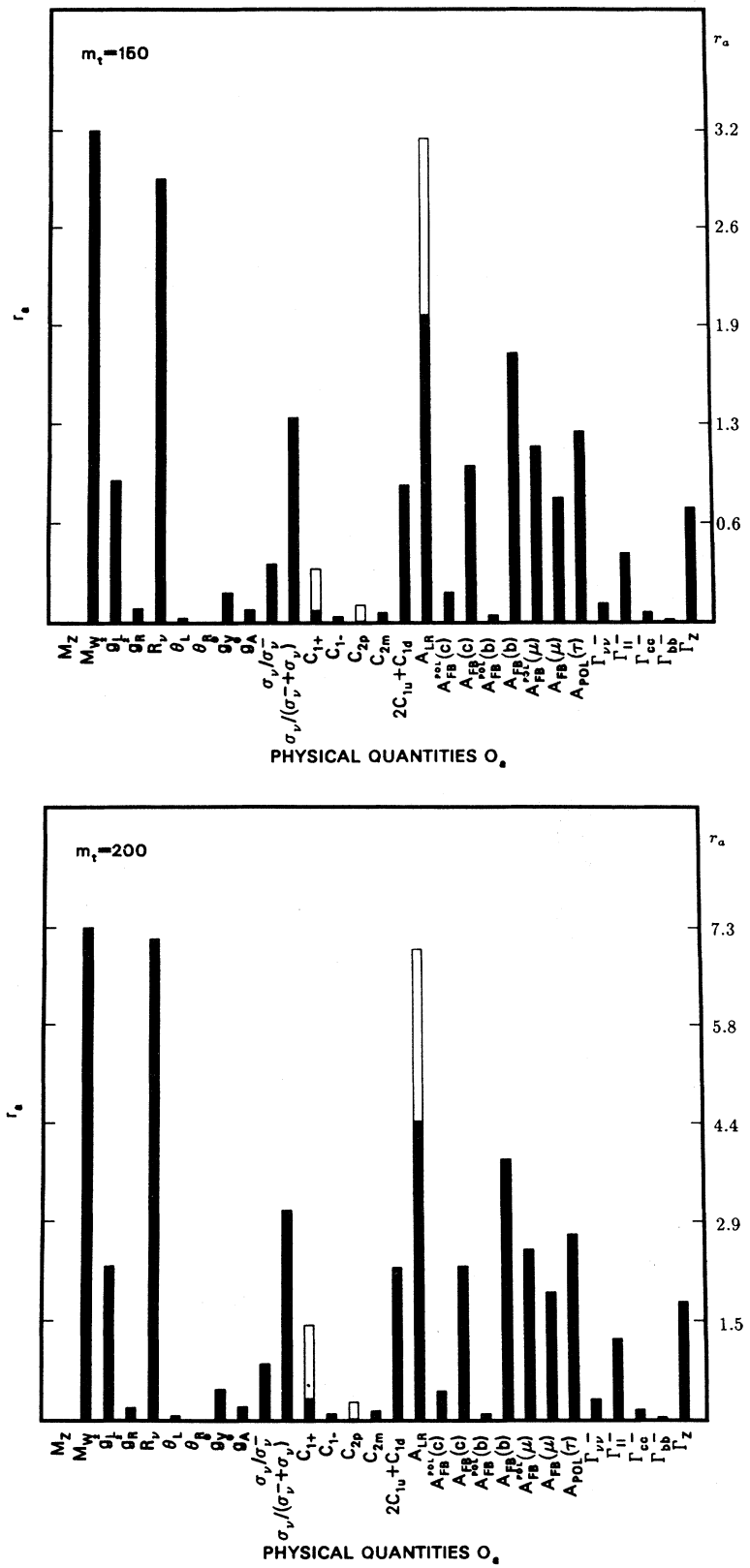

FIG. 60. Effects of the top quark mass m_t: (a) change in the SM predictions for $m_t=150$ GeV: solid bar for C_{1+}, C_{2p}, and $A_{\rm LR}$(SLC); open bar for C_{1+}(iso), $C_{2p}(1)$, and $A_{\rm LR}$(LEP). The right-hand scale is $r_a=|\Delta O_a|/\Delta O_a^{\rm exp}$. (b) Change in the SM predictions for $m_t=200$ GeV.

VI. SUMMARY OF RESULTS

The Standard Model predictions for 28 observables are presented in Table I. These are computed using the experimental value of M_Z as input and assuming the reference values $m_t = M_H = 100$ GeV for the top quark and Higgs masses. Full one-loop electroweak radiative corrections are included. The projected errors to be obtained from future precision measurements of those observables (including theoretical errors and uncertainties in the predictions arising from the input values) are also shown.

The changes in these predictions due to 25 examples of possible new physics, as well as larger values of m_t and M_H, are shown in Tables VIII–XXXIV and the corresponding figures (Figs. 34–60). In each case the changes in the predictions of a given observable and the corresponding value of $\sin^2\theta_W$ extracted from it are calculated for $\lambda = 0.01$, where λ is a parameter that characterizes the strength of the new physics (for m_t and M_H, specific values are chosen). The value $\lambda_a^{\min}$ for which the change in observable O_a is equal to the projected experimental uncertainty is also presented. The bar-graph figures display $1/\lambda_a^{\min}$ for each observable. The higher the bar, the more sensitive that observable is to the particular type of new physics.

A brief summary of the results is given in Tables XXXV–XXXVIII. For each type of new physics considered are given the smallest value of $\lambda^{\min}$ for any of the observables, the corresponding scale of new physics (e.g., M_{Z_2} for an extra Z), and the most sensitive observables. Many of the observables are sensitive to several types of new physics with characteristic scale extending into the TeV range. No single observable is the most sensitive to

TABLE XXXV. Summary of the discussion in Sec. V: implications for extra Z bosons. The smallest $\lambda^{\min}$ is the value of the overall coupling constant $\lambda^{\min} = (g_2^2/M_{Z_2}^2)/(g_1^2/M_Z^2)$ at which the extra Z is manifested in the most sensitive observable. Here g_1, g_2, M_Z, and M_{Z_2} are the coupling constants and masses of the ordinary Z and extra Z_2, and $g_2^2/g_1^2 = \frac{5}{3}\sin^2\theta_W$ is assumed.

New Physics	Smallest λ^{min}	Implications $M_{Z_2}(GeV)$	Most Sensitive Observables
$Z_\chi(C = \sqrt{2/5})$	0.0019	~ 1295	R_ν;
			M_W, g_L^2, $\sigma_{\nu e}/(\sigma_{\nu_e e} + \sigma_{\bar{\nu} e})$,
			$C_{1+}(iso)$, $A_{LR}(LEP)$, Γ_Z
$Z_\chi(C = 0)$	0.0011	~ 1700	$C_{1+}(iso)$;
			C_{1+}, $\sigma_\nu/(\sigma_{\bar{\nu}} + \sigma_\nu)$, $2C_{1u} + C_{1d}$
$Z_\psi(C = \sqrt{2/3})$	0.0017	~ 1370	R_ν;
			M_W, $C_{1+}(iso)$, A_{LR}, $A_{FB}(b)$
$Z_\psi(C = -\sqrt{2/3})$	0.0029	~ 1050	$A_{LR}(LEP)$, M_W;
			R_ν, $C_{1+}(iso)$, $A_{LR}(SLC)$, $A_{FB}(b)$, $\Gamma_{\bar{l}l}$
$Z_\psi(C = 0)$	0.025	~ 357	$\sigma_\nu/(\sigma_{\bar{\nu}} + \sigma_\nu)$
$Z_\eta(C = -\frac{1}{\sqrt{15}})$	0.0075	~ 650	$A_{LR}(LEP)$;
			$C_{2p}(1)$, $A_{LR}(SLC)$, $A_{FB}(b)$
$Z_\eta(C = \frac{4}{\sqrt{15}})$	0.0008	~ 2000	$C_{1+}(iso)$; M_W, R_ν
$Z_\eta(C = 0)$	0.0045	~ 840	$C_{1+}(iso)$; $C_{2p}(1)$
$Z_{3R}(C = \sqrt{3/5}\alpha)$	0.0009	~ 1880	R_ν, $A_{LR}(LEP)$;
			M_W, $A_{LR}(SLC)$, $C_{1+}(iso)$, $A_{FB}(b)$
$Z_{3R}(C = -\sqrt{3/5}/\alpha)$	0.0008	~ 2000	$C_{1+}(iso)$; C_{1+}
Z_{3R} $(C = 0)$	0.0010	~ 1785	$C_{1+}(iso)$; C_{1+}

TABLE XXXVI. Summary of the discussion in Sec. V: implications for exotic fermions. The smallest value $\lambda^{\min}$ is the value of $(\sin^2\theta^i_{L,R})^2$ at which the exotic fermion is manifested in the most sensitive observable. Here $\theta^i_{L,R}$ is the mixing angle between the ordinary and exotic fermions.

New Physics	Smallest λ^{min}	Implications	Most Sensitive Observables
u_L	0.0010	$(\theta^u_L)^2 \sim 0.0010$	$C_{1+}(iso)$;
			R_ν, C_{1+}, $2C_{1u} + C_{1d}$
u_R	0.0010	$(\theta^u_R)^2 \sim 0.0010$	$C_{1+}(iso)$; C_{1+}, $2C_{1u} + C_{1d}$
d_L	0.0009	$(\theta^d_L)^2 \sim 0.0009$	$C_{1+}(iso)$; R_ν, C_{1+}
d_R	0.0009	$(\theta^d_R)^2 \sim 0.0009$	$C_{1+}(iso)$; C_{1+}
e_L	0.0025	$(\theta^e_L)^2 \sim 0.0025$	$C_{1+}(iso)$; $A_{pol}(\tau)$
e_R	0.0021	$(\theta^e_R)^2 \sim 0.0021$	$A_{LR}(LEP)$, $C_{1+}(iso)$;
			C_{1+}, $A_{LR}(SLC)$, $A_{FB}(c)$,
			$A_{FB}(b)$, $A_{pol}(\tau)$
ν_{eL}	0.0033	$(\theta^{\nu_e}_L)^2 \sim 0.0033$	$A_{LR}(LEP)$;
			$\sigma_\nu/(\sigma_{\bar\nu} + \sigma_\nu)$, $A_{LR}(SLC)$,
			$A_{FB}(b)$, $A^{pol}_{FB}(\mu)$.
μ_L	0.0018	$(\theta^\mu_L)^2 \sim 0.0018$	R_ν; g^2_L, $A_{FB}(b)$, A_{LR}
$\nu_{\mu L}$	0.0033	$(\theta^{\nu_\mu}_L)^2 \sim 0.0033$	$A_{LR}(LEP)$;
			$A_{LR}(SLC)$, $A_{FB}(b)$, $A^{pol}_{FB}(\mu)$

all types.

The specific predictions of sensitivity depend on the projected experimental uncertainties, and it is likely that many of the experiments will be more or less precise than anticipated. While keeping this caveat in mind, it is apparent from the Tables VIII–XXXIV and XXXV–XXXVIII that the observables M_W, R_ν, C_{1+}(iso), and $A_{\rm LR}$(LEP) are especially promising, each showing considerable sensitivity to a variety of new physics. The observables $\sigma_\nu/(\sigma_{\bar\nu}+\sigma_{\nu_e})$, $A_{\rm FB}(b)$, $A_{\rm pol}(\tau)$, $\Gamma_{l\bar l}$, Γ_Z, and the existing g^2_L are also especially sensitive; most of the remaining observables are strong probes of one or more types of new physics. New physics at the TeV scale or higher may be observed or excluded if a significant number of these observables are measured precisely. If all the measured values are consistent with the SM pre-

TABLE XXXVII. Summary of the discussion in Sec. V: implications for nonstandard Higgs fields ($\lambda=\rho_0-1$), leptoquarks ($\lambda=2^{1/2}|\eta|^2/8M^2_S G_F$), and four-fermi operators ($\lambda=2^{1/2}\pi/\ G_F\Lambda^2$). The smallest value $\lambda^{\min}$ is the value of λ at which these new physics are manifested in the corresponding most sensitive observable.

New Physics	Smallest λ^{min}	Implications	Most Sensitive Observables
NS Higgs	0.0015	$VEV_{NH} \sim 7\ GeV$	R_ν, $A_{LR}(LEP)$, M_W;
			$A_{LR}(SLC)$, $A_{FB}(b)$
Leptoquark	0.0005	$\frac{M_S}{\lvert\eta_L\rvert} \sim 5.5\ TeV$	$C_{1+}(iso)$; C_+, $2C_{1u} + C_{1d}$
4-Fermi op. (I)	0.0023	$\Lambda_1 \sim 12.9\ TeV$	$C_{2p}(1)$
4-Fermi op. (II)	0.0032	$\Lambda_2 \sim 10.9\ TeV$	$\sigma_\nu/(\sigma_{\bar\nu} + \sigma_\nu)$
4-Fermi op. (III)	0.0002	$\Lambda_3 \sim 44\ TeV$	$C_{1+}(iso)$

TABLE XXXVIII. Summary of the discussion in Sec. V: implications for heavy physics through loops. For h_V, $\lambda=\alpha h_V$; for h_A, $\lambda=2^{1/2}G_F M_Z^2 h_A/4\pi$; for the variations of m_t and M_H, $r_a=|\Delta O_a|/\Delta O_a^{\rm exp}$. The smallest value $\lambda^{\rm min}$ is the value of λ at which these new physics are manifested in the corresponding most sensitive observable.

New Physics	Smallest λ^{min}	Implications	Most Sensitive Observables
h_V	0.0015	$h_V \sim 0.21$	R_ν, $A_{LR}(LEP)$, M_W;
			$A_{LR}(SLC)$, $A_{FB}(b)$, $\sigma_\nu/(\sigma_{\bar\nu}+\sigma_\nu)$
h_A	0.0017	$h_A \sim 0.16$	$A_{LR}(LEP)$;
			$A_{LR}(SLC)$, $C_{1+}(iso)$, $A_{FB}(b)$
$M_H = 500\ GeV$	—	$r_a \sim 2.0$	$A_{LR}(LEP)$;
			M_W, R_ν, $A_{LR}(SLC)$, $A_{FB}(b)$.
$M_H = 1000\ GeV$	—	$r_a \sim 2.9$	$A_{LR}(LEP)$;
			M_W, R_ν, $A_{LR}(SLC)$, $A_{FB}(b)$.
$m_t = 150\ GeV$	—	$r_a \sim 3.2$	R_ν, $A_{LR}(LEP)$, M_W;
			$A_{LR}(SLC)$, g_L^2, $\sigma_{\nu e}/(\sigma_{\nu_e e}+\sigma_{\bar\nu e})$,
			asymmetries
			$2C_{1u}+C_{1d}$, $\Gamma_{l\bar l}$, Γ_Z
$m_t = 200\ GeV$	—	$r_a \sim 7.3$	R_ν, $A_{LR}(LEP)$, M_W;
			asymmetries
			$A_{LR}(SLC)$, g_L^2, $\sigma_{\nu e}/(\sigma_{\nu_e e}+\sigma_{\bar\nu e})$,
			$2C_{1u}+C_{1d}$, $\Gamma_{l\bar l}$, Γ_Z

dictions, then, except for the unlikely possibility of fine-tuned cancellations, various types of new physics will be excluded at scales of the order of those shown in Tables XXXV–XXXVIII.

If, however, deviations are observed, then as much information as possible will be needed to confirm the discrepancy and to determine the nature of the new physics and its strength. From the pattern of the deviations of the various observables it will be possible in most cases to distinguish which type of new physics is responsible, or at least which is most likely out of the set of possibilities considered here. The deviation pattern can also distinguish true new physics from values of m_t and M_H different from the reference values used in the SM predictions. Identification of the origin of deviations is another reason for carrying out a large variety of precision experiments.

To quantify this, it is useful to consider an n-dimensional vector space, each point of which represents the possible outcome of n precise experiments. Let us choose the origin in this space as the SM prediction for the n observables. Then one can define an n-dimensional vector with components:

$$V_a^{\rm exp}=\frac{O_a^{\rm exp}-O_a^{SM}}{\Delta O_a^{\rm exp}}\ , \tag{222}$$

where $V_a^{\rm exp}$ is the deviation of the ath observable from the SM prediction, weighted by the inverse of the experimental uncertainty. Similarly, each type i of new physics predicts a deviation vector with components:

$$V_a^i(\lambda)=\frac{\Delta O_a^i(\lambda)}{\Delta O_a^{\rm exp}},\quad a=1,\ldots,n\ , \tag{223}$$

which has a magnitude proportional to the coupling strength λ and a direction depending on a. If $V_a^{\rm exp}$ is compatible with zero (i.e., the total length is of order n and no single component is much bigger than unity), then there is no evidence for new physics. One can then set upper limits on the magnitude of each $V_a^i(\lambda)$ and therefore on each λ. On the other hand, if $V_a^{\rm exp}\gg n$, then there is evidence for new physics. The most likely type or types can be determined, at least among the possibilities considered, by choosing i such that $V_a^i(\lambda)$ and $V_a^{\rm exp}$ are approximately parallel. The strength λ could be estimated from the requirement that $V_a^i(\lambda)=V_a^{\rm exp}$.

The observables considered in this paper would usually be sufficient to distinguish the nature of new physics from the directions of $V_a^i(\lambda)$. Rather than grapple further with an n-dimensional vector space, however, it is productive as illustration to display the projections onto 36 two-dimensional subspaces as in Fig. 61. These are just those involving pairs of M_W, R_ν, C_{1+}(iso), $A_{\rm LR}$(LEP), $\sigma_\nu/(\sigma_\nu+\sigma_{\nu_e})$, $A_{\rm FB}(b)$, $A_{\rm pol}(\tau)$, $\Gamma_{l\bar{l}}$, and Γ_Z, which are representative of the most sensitive observables. We have also selected a representative sample of 12 types of new physics described in Sec. V. These are $Z_\chi(C=\sqrt{2/5})$; $Z_\psi(C=-\sqrt{2/3})$; $Z_\eta(C=\sqrt{16/15})$; nonstandard Higgs (NH) or h_V; leptoquark (type I, LQ); u_L mixing; ν_{eL} mixing; μ_L mixing; four-fermi (4F) operators (L3); h_A; $M_H \neq 100$ GeV; $m_t \neq 100$ GeV. Each of the 36 plots is a projection onto two observables. The origins

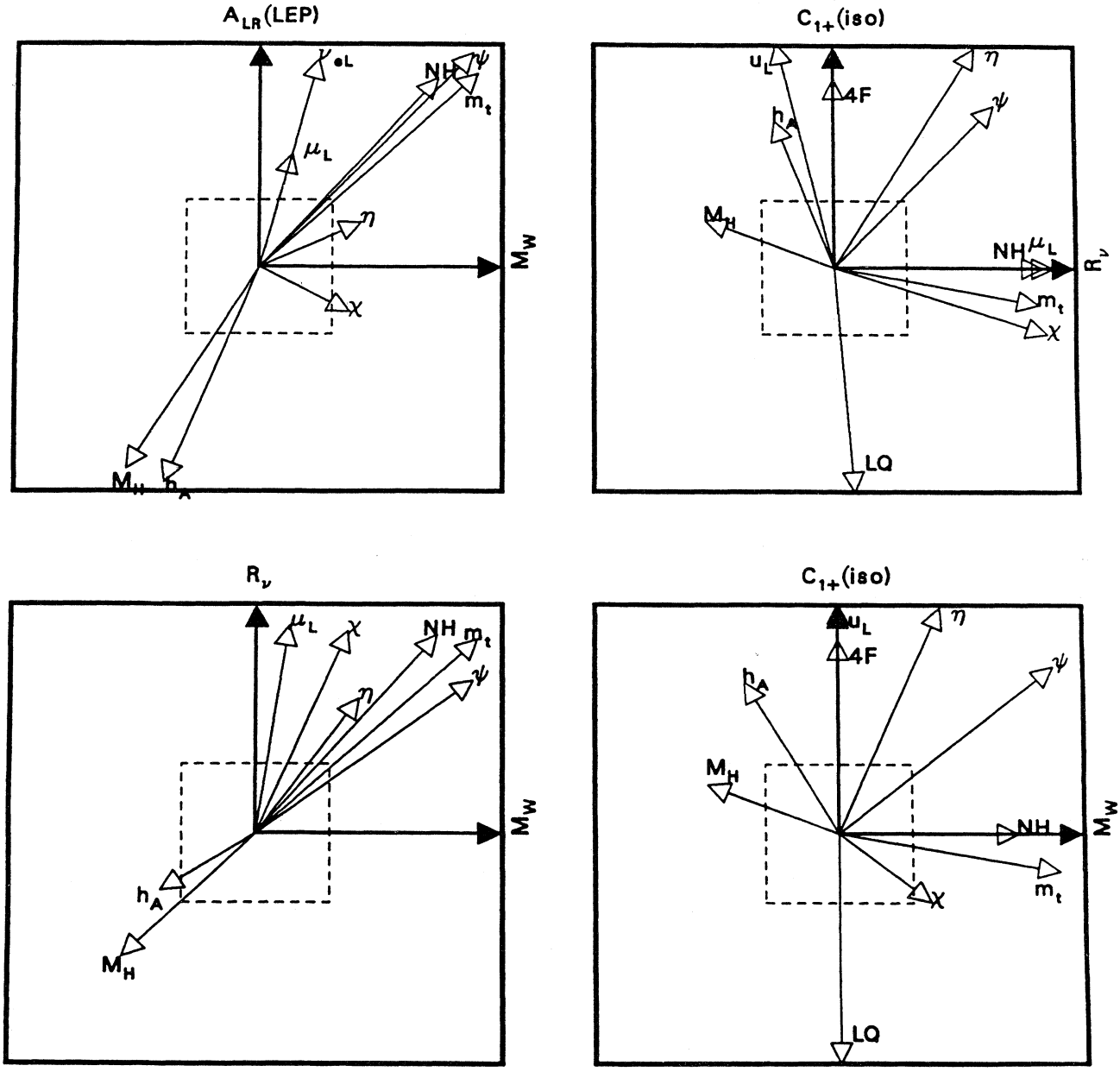

FIG. 61. Deviations from the Standard Model predictions of various combinations of two observables due to a representative sample of new physics. The dash-line boxes represent the projected $\pm 1\sigma$ uncertainties of the measurements, with the scale of the axes chosen accordingly. The strength λ of each new-physics type is selected to provide a 3σ effect in the most sensitive observable.

represent the SM predictions, and the dash-line boxes are the projected $\pm 1\sigma$ uncertainties. The axis scales are chosen so that the boxes all have the same size for convenience, which is not meant to suggest that the precision of all the experiments is the same. The deviations due to new physics are represented by labeled arrows. In each case the overall coupling constant λ^i is chosen so that the largest deviation from the SM in any observable is 3 times the projected uncertainty (i.e., λ^i is 3 times the $\lambda^{\min}$ in Tables XXXV–XXXVIII). Projections of vectors totally covered by the dashline boxes are ignored.

It is apparent from the figures that, given a number of high-precision experiments, it will be possible to distinguish among most of the examples of new physics considered here with reasonable confidence. The types of new physics that manifest themselves at the tree level all have distinctive patterns in Fig. 61. These are different from the patterns induced by loop effects, with the exception of nonstandard Higgs fields, which cannot be distinguished from h_V by the measurements treated here.

Distinguishing new loop effects (h_A and h_V) from M_H and m_t, or even M_H and m_t from each other, is more difficult, though not impossible. It is likely, however, that m_t will be accurately known from direct observation

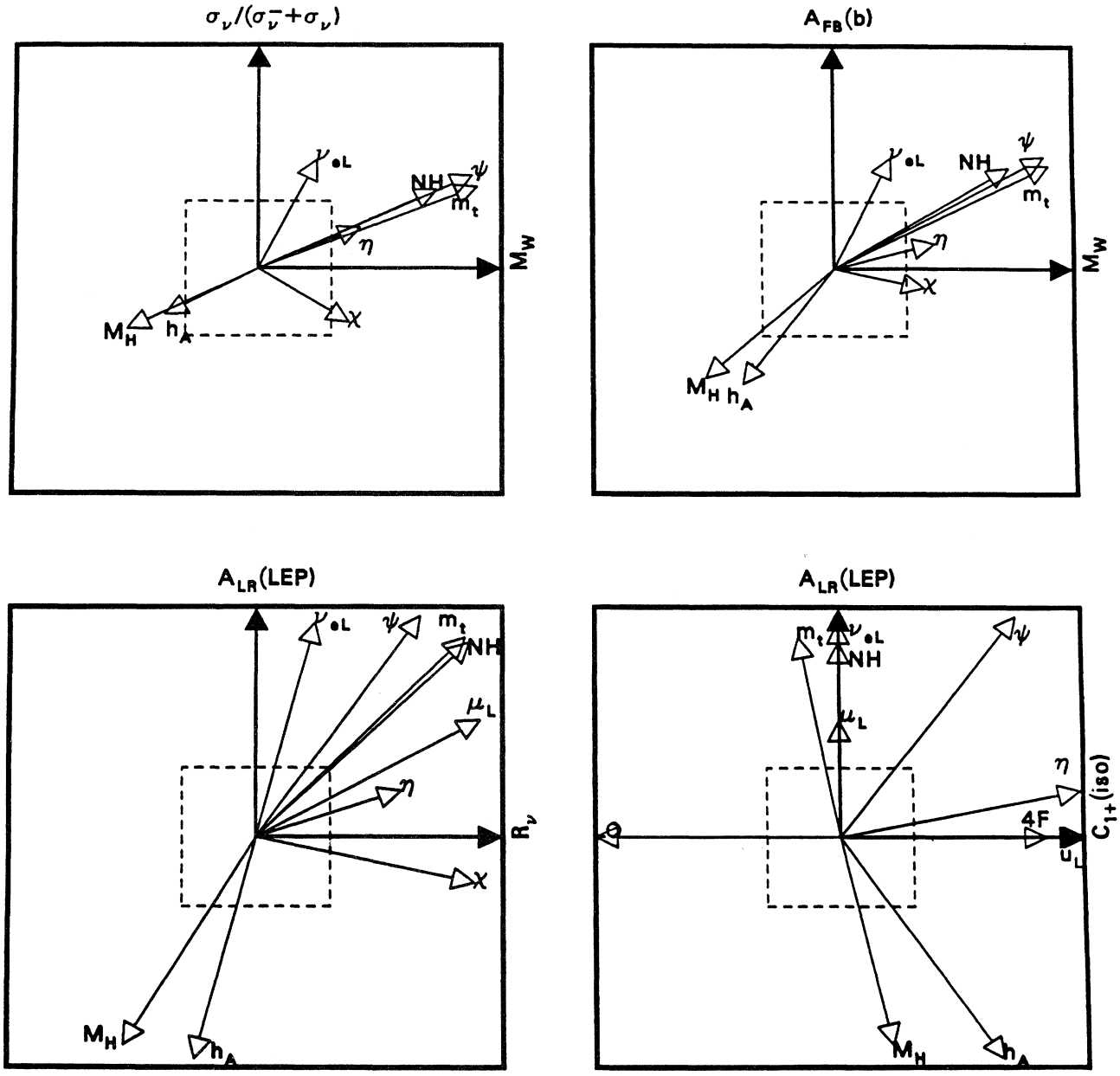

FIG. 61. (*Continued*).

at the Tevatron within a few years. It is also possible that the Higgs boson will be directly observed as well. With that information, one could certainly elicit h_A and h_V. If M_H is not known from direct observation, its effects on the observables considered here are generally small, though non-negligible for $M_H \leq 1$ TeV. Assuming the exact validity of the SM (i.e., $h_A = h_V = 0$), precision measurements could yield an estimate of M_H with a sensitivity of a few hundred GeV.

VII. CONCLUSIONS

Our paper has attempted to provide a framework for interpretation of the high-precision electroweak experiments that are likely to be done in the next ten years. To accomplish this requires several steps.

(a) Using M_Z as input, the predictions of the SM for 28 additional observables encompassing weak neutral-current phenomena and intermediate vector boson masses and decay widths have been calculated numerically to the one-loop level. (b) The modifications of each of these SM predictions, which might be caused by ten general types of possible new physics, have also been calculated numerically for 27 specific examples.

(c) The latter values, each subject to the specification of a single coupling strength parameters, are compared with the projected numerical experimental errors of future

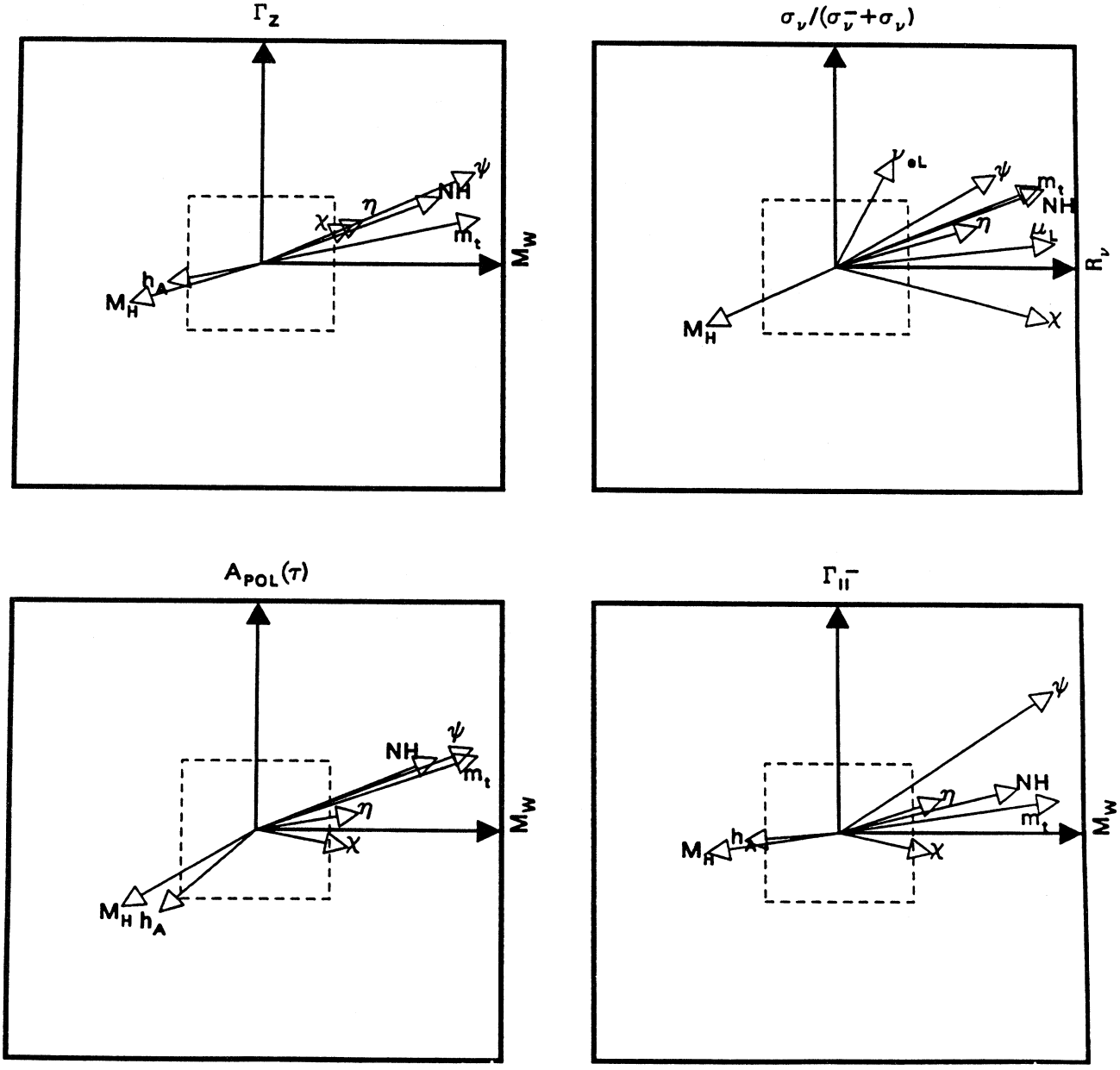

FIG. 61. (*Continued*).

high-precision experiments with a threefold purpose: testing the SM (including radiative corrections) at the highest level of precision, recognizing the relative sensitivities of the several observables to the different types of new physics treated here, and delineating the nature of the new physics if deviations from the SM are found empirically.

The detailed numerical results of the analysis are presented in 27 tables and accompanying figures in Sec. V, each of which is self-contained and follows directly from the discussion of new physics in Sec. IV. For convenience, as well as conciseness, we have summarized those results in the four tables at the beginning of Sec. VI. We have, however, refrained from singling out particular observables as being "most valuable" for the reason mentioned at length below, and because we do not wish to underestimate the inventiveness and ingenuity of the experimentalists who will carry out the future electroweak experiments.

Three general conclusions emerge from our analysis.

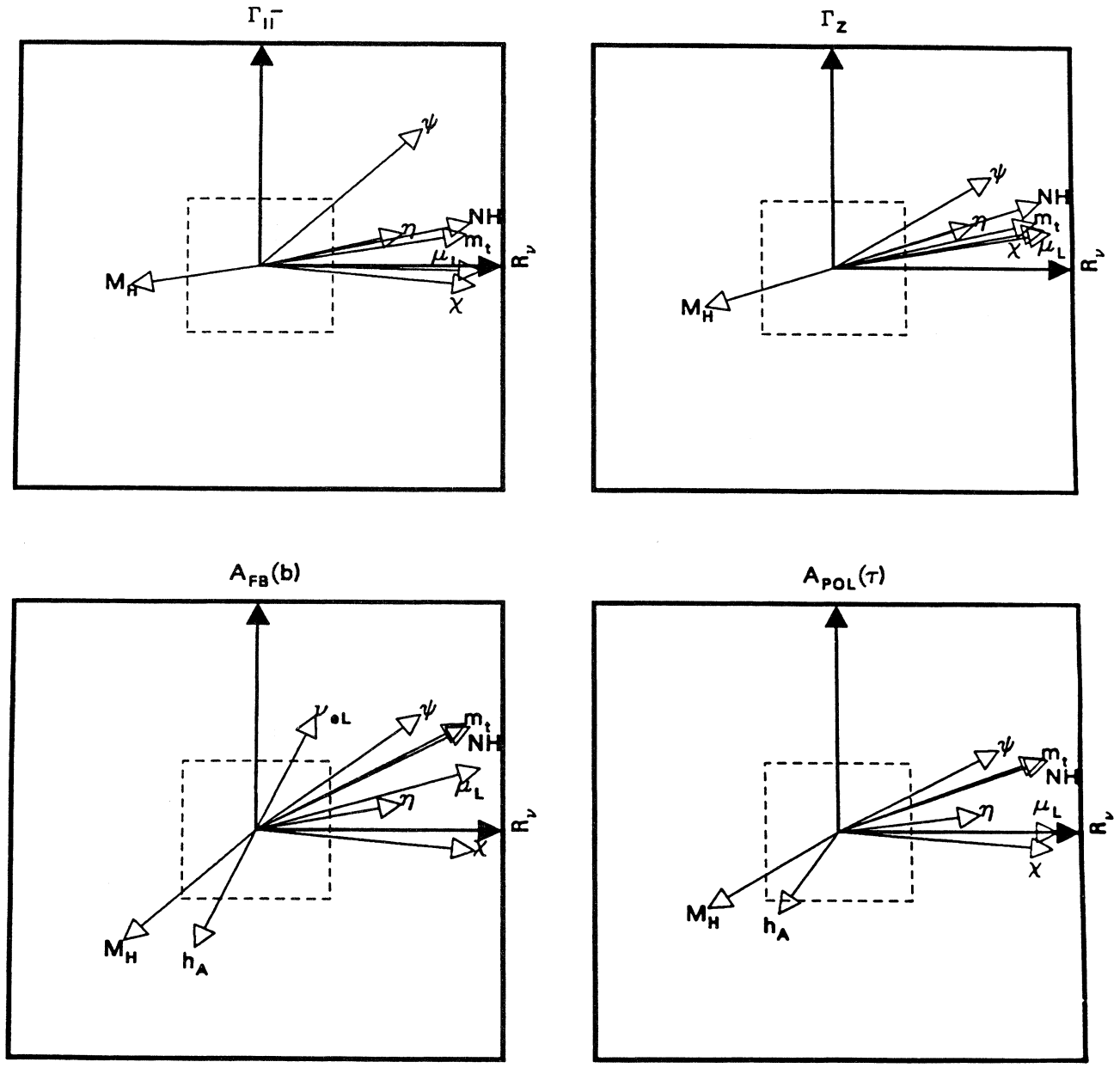

FIG. 61. (*Continued*).

First, the analytic framework presented here, or one similar to it, is necessary for the understanding of future high-precision experiments and their interpretation within the SM. As noted in the Introduction, the results of most electroweak experiments are not predicted absolutely by the SM, but depend on the value of the weak mixing angle, $\sin^2\theta_W$. Any single precision measurement specifies that angle but constrains the theory only through confrontation with the results of equivalent precision measurements of other observables. Furthermore, as has also been pointed out, the sensitivity of different observables to $\sin^2\theta_W$ and to the radiative corrections varies significantly so that comparison of the values of $\sin^2\theta_W$ extracted from several experiments may not by itself provide the most stringent test of their internal consistency. In addition, precise numerical comparison of one experiment with another, or experiment with theory, requires the top quark mass and Higgs mass to be known or at least constrained within reasonably tight limits. All of these difficulties may be overcome with a sufficient

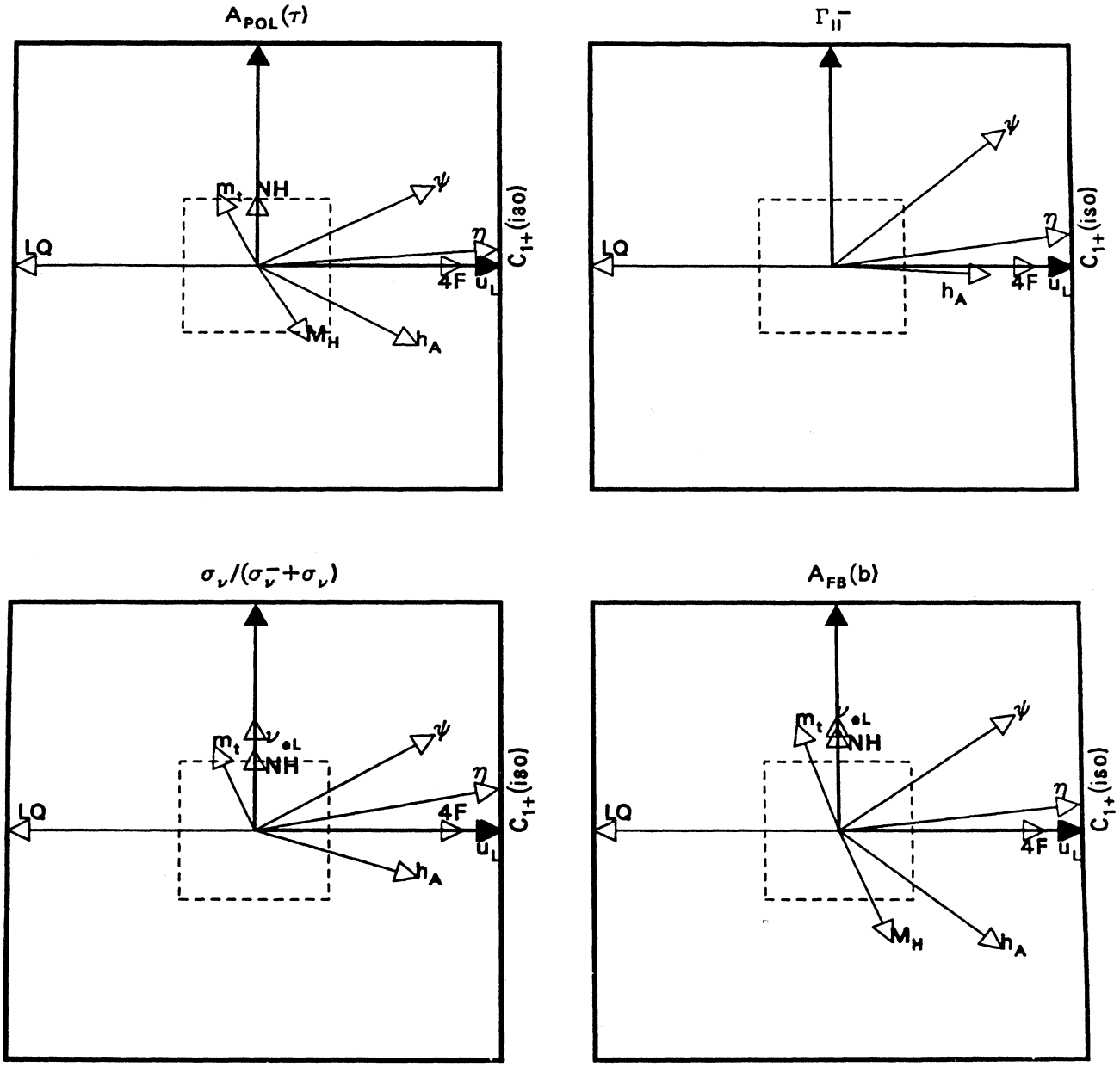

FIG. 61. (*Continued*).

number of high-precision experiments analyzed within a global or general framework such as proposed here. The absence of the framework will lead to a waste of the high precision of these experiments and limit the conclusions to be drawn from them.

A second general conclusion is that the outcome of the global analysis will include accurate determinations of the radiative corrections within the SM, which will test the gauge nature of the theory at its foundation. The high-precision experiments uniquely verify renormalizibility of the theory and the consistency of the calculations of the radiative corrections.

Third, the variety of observables open to precise experimental study and the precise nature of the electroweak theoretical predictions jointly constitute a powerful means of searching for new physics. The wide range of momentum transfers and the varied sensitivities of the electroweak phenomena to new physics form a network through which new physics in the TeV region is unlikely to pass unnoticed. We have tried to furnish examples of this by considering specific instances of possible new physics. In general, all of the measurements we have

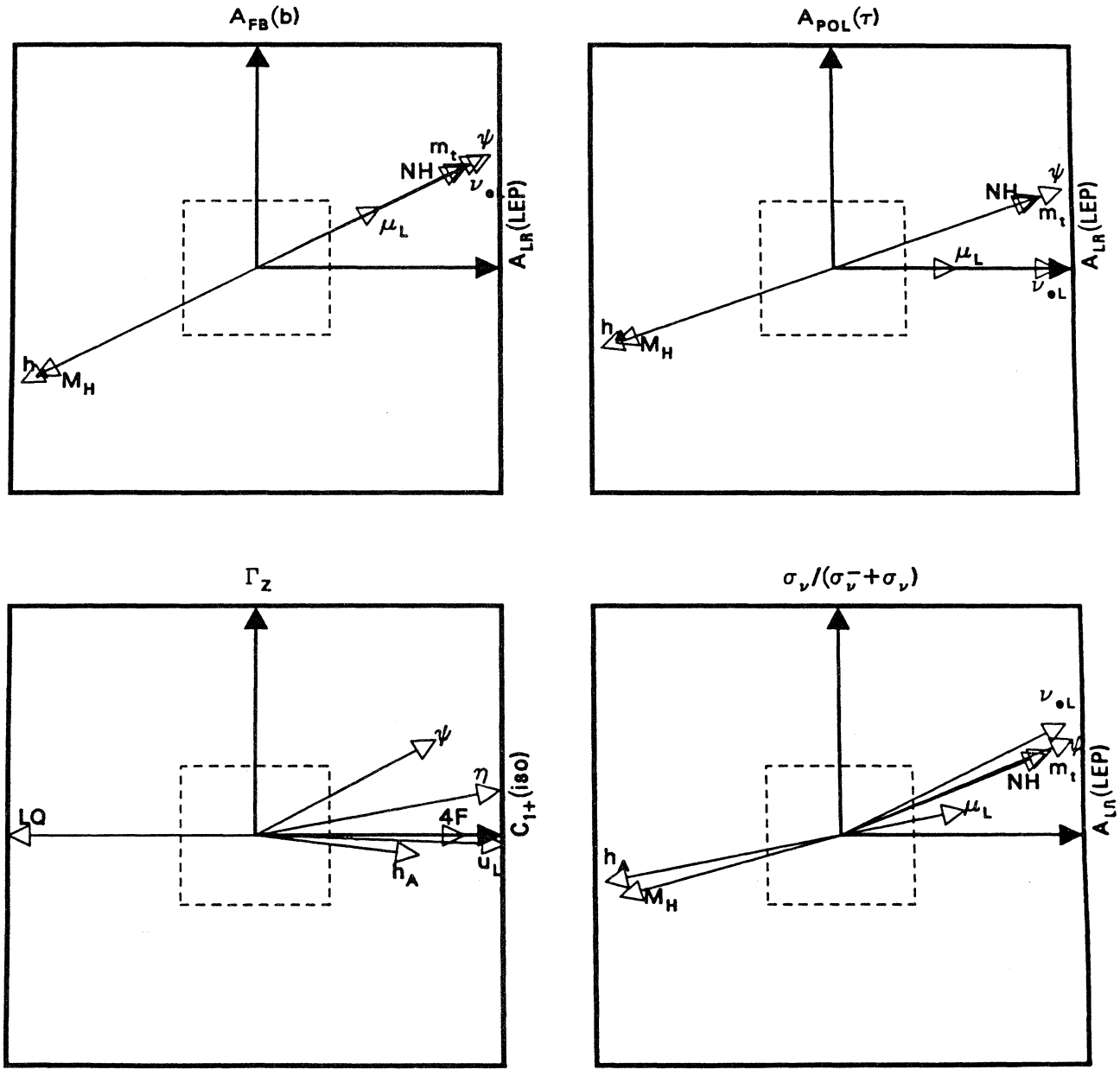

FIG. 61. (*Continued*).

considered show good sensitivity to one or another type of the new physics treated. It is likely, however, that the new physics that nature holds in store for us is not among the examples we have discussed. Recognition of this likelihood offers still another reason to encourage the performance of a multiplicity of measurements. Precision measurements of the masses of Z and W, precise determinations of neutrino-quark and neutrino-electron scattering cross sections, precision measurements of the parameters of atomic parity violation, and precision measurements of the asymmetries in e^+e^- scattering at the Z pole, combined with precise knowledge of the Z-decay widths, are all possible, and to a greater or lesser extent are possible with existing accelerators and, in many cases, with existing detectors.

This circumstance, global in character experimentally and theoretically, presents a window of opportunity through which a view of the future realm of elementary-particle physics may be obtained before we are transported there by the forthcoming high-energy colliders. We must use our resources wisely to take advantage of the opportunity.

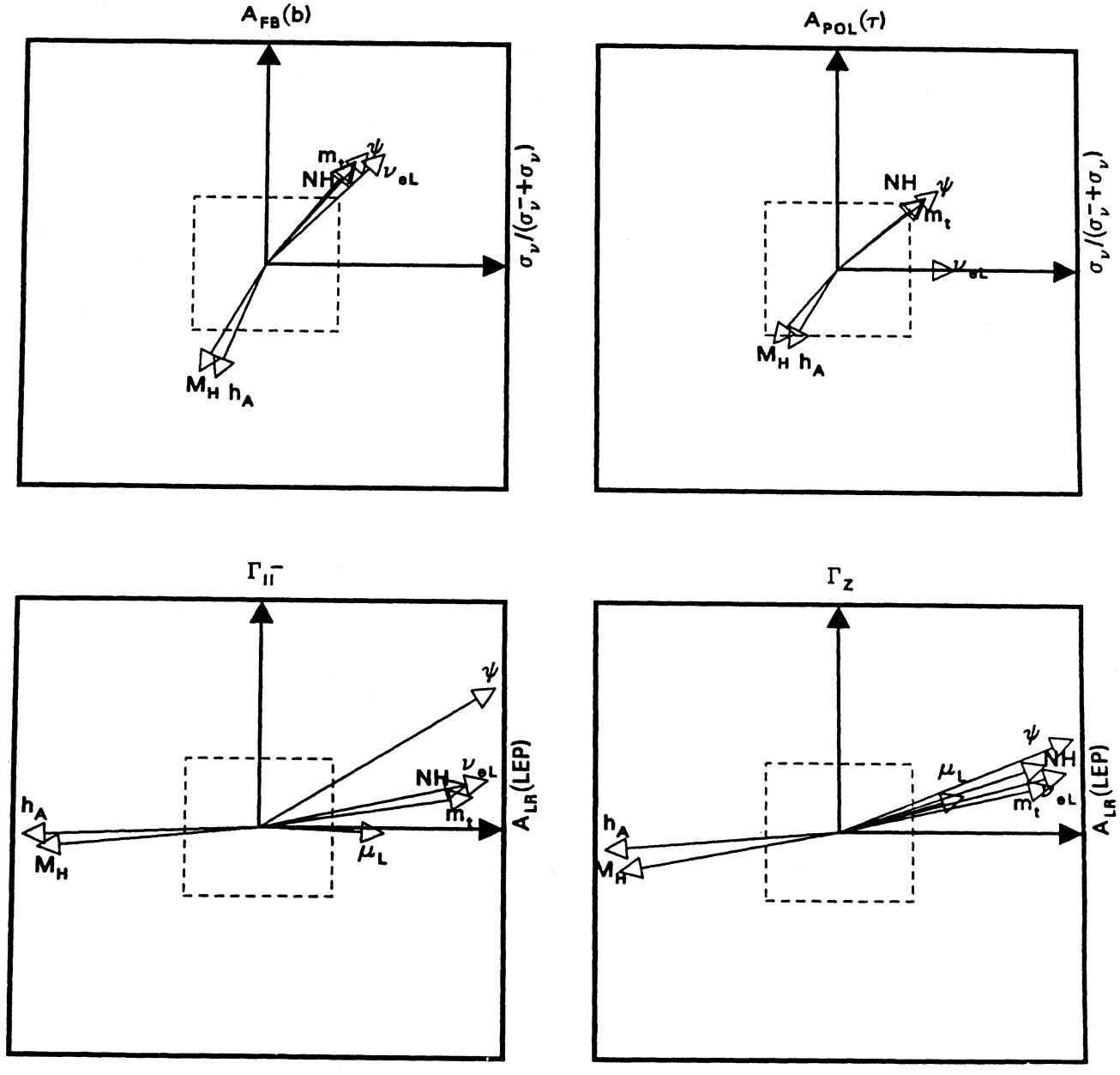

FIG. 61. (*Continued*).

ADDENDUM

Since this paper was written in late 1990, the experimental errors on some of the observables discussed here have been lowered in newly completed experiments beyond the initial estimates of the experimentalists responsible for those measurements. This verifies the wisdom of the precaution stated in Sec. VII that "... we do not wish to underestimate the inventiveness and ingenuity of the experimentalists who will carry out the future electroweak experiments."

In addition to the small change in the value of M_Z from 91.177 to 91.174 GeV, the error on M_Z, ΔM_Z, has been reduced from 0.031 to 0.021 GeV, the latter value corresponding to the error anticipated in the farther future by the experimentalists and given as part of the first entry line of Table I. Furthermore, the errors on the Z widths have been improved as follows: $\Delta\Gamma_Z$ from 0.015 to 0.009 GeV, $\Delta\Gamma_{\bar{l}l}$ from 0.007 to 0.004 GeV, and $\Delta\Gamma_{\text{inv}}$

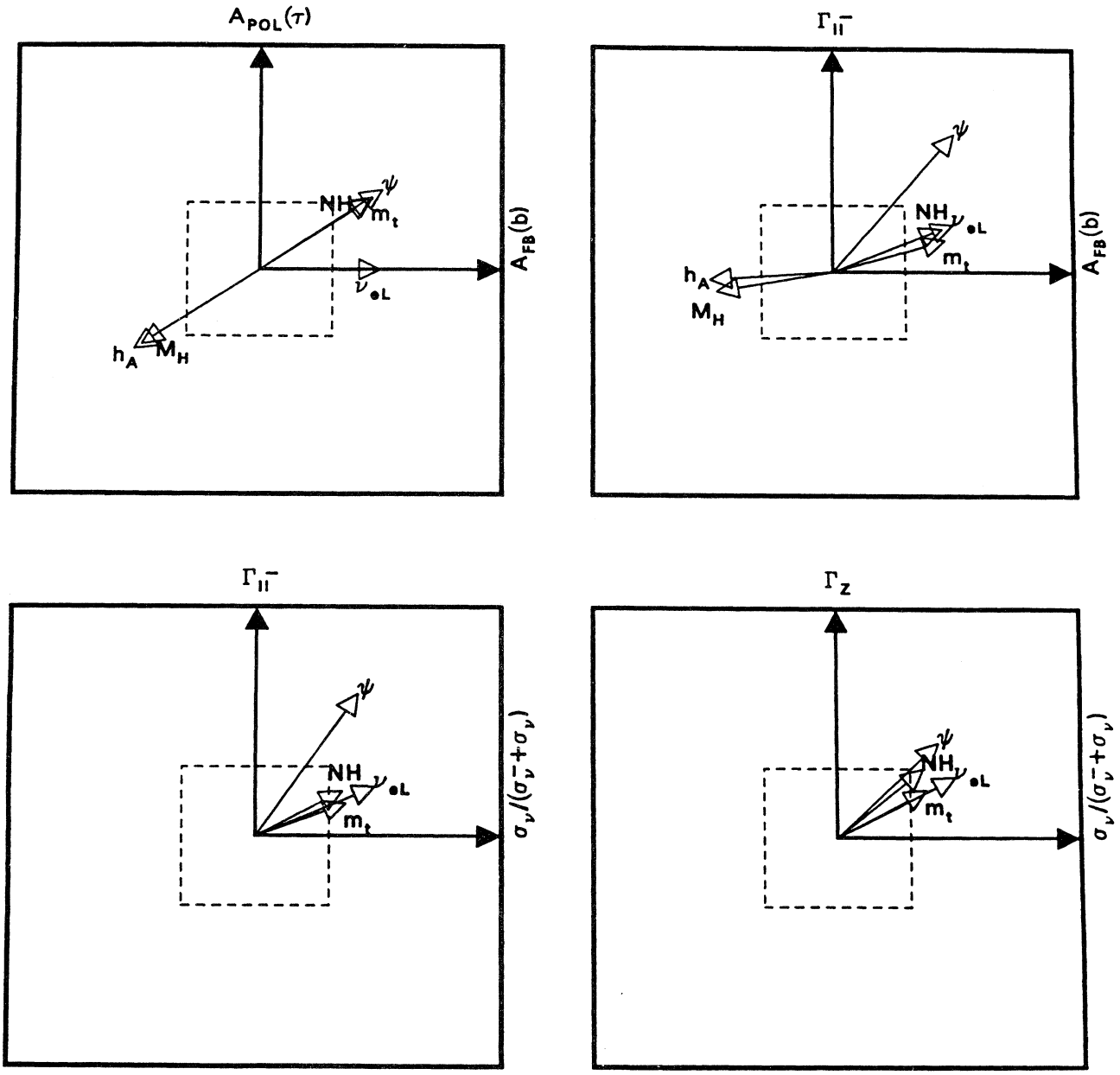

FIG. 61. (*Continued*).

from 0.016 to 0.010 GeV. These lower error values are given in a summary of results by S. Lloyd at the Aspen Winter Conference in Elementary Particle Physics, January, 1991, and are largely due to more accurate determinations of the LEP luminosity than had been foreseen.

The smaller errors on M_Z, Γ_Z, $\Gamma_{l\bar{l}}$, and Γ_{inv} linearly modify the values of $\lambda_a^{\min}$ and $\Delta \sin^2\theta_W^{\exp}$ in Tables VIII–XXXIV and the values of $1/\lambda_a^{\min}$ in the corresponding figures (Figs. 34–60). In particular, the influence of Γ_Z and $\Gamma_{l\bar{l}}$ in Figs. 37, 45, 51, 53, 55, and 57 is enhanced, although the stated conclusions relating to those figures, e.g., in Tables XXXV–XXXVIII are essentially unchanged. The semiquantitative features of those parts of Fig. 61 relating to M_Z, Γ_Z, $\Gamma_{l\bar{l}}$, and Γ_{inv} are also unchanged.

Subsequent improvements in the experimental errors on other observables may be taken into account by the reader in the same linear manner.

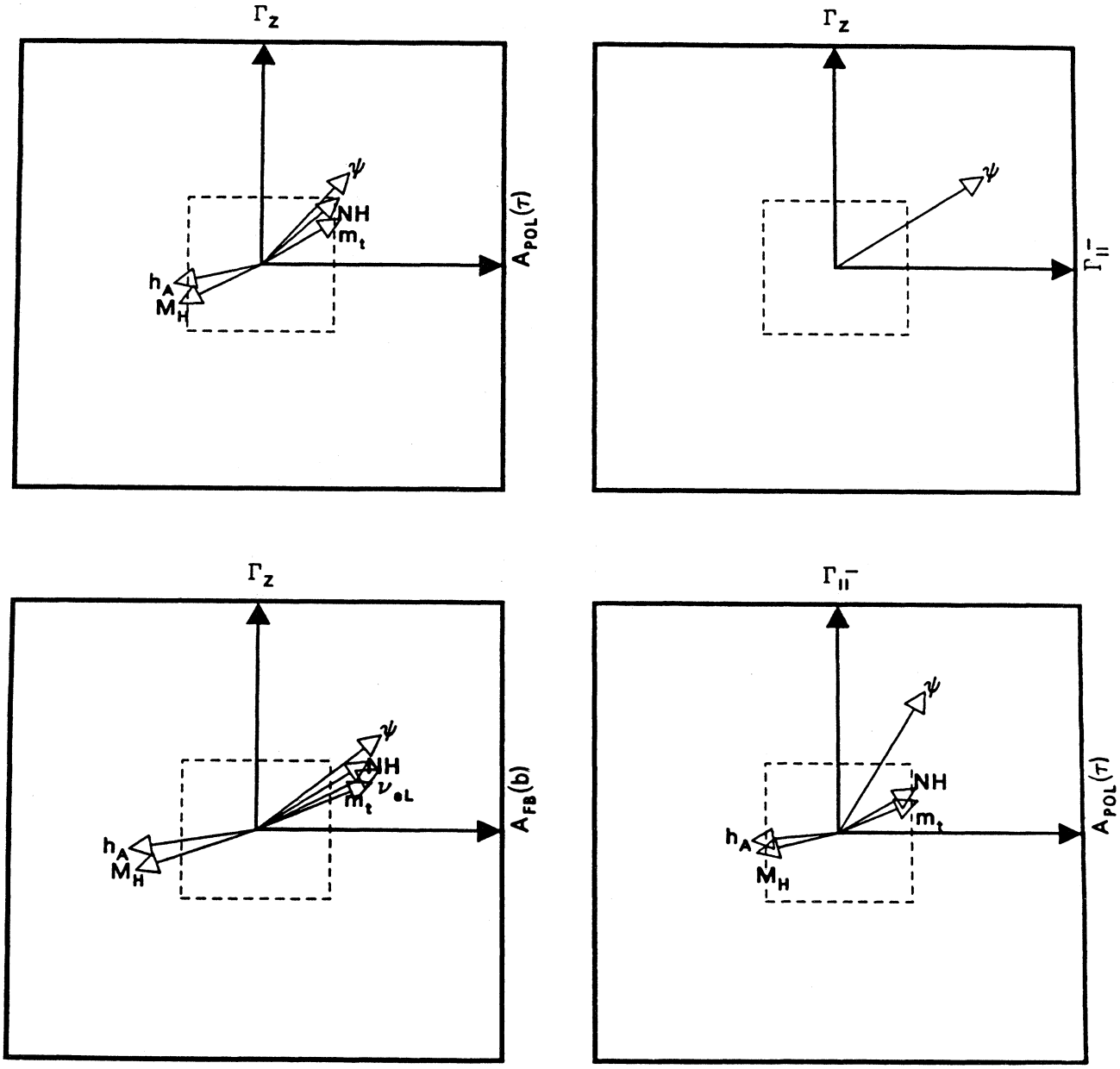

FIG. 61. (*Continued*).

ACKNOWLEDGMENTS

It is a pleasure to thank W. Marciano and A. Sirlin for valuable discussion. This work was supported by the Department of Energy contract DE-AC02-76-ERO-3071. One of us (M.L.) would like to acknowledge the hospitality of Brookhaven National Laboratory during part of the work.

REFERENCES

Abe, F., *et al.*, 1990, Phys. Rev. Lett. **65**, 2243.
Abe, K., 1990, *International Conference on High Energy Physics*, Singapore, KEK Report No. 90-136.
Akhundov, A. A., D. Y. Bardin, and T. Riemann, 1986, Nucl. Phys. B **276**, 1.
Albert, D., W.J. Marciano, D. Wyler, and Z. Parsa, 1980, Nucl. Phys. B **166**, 460.
Alexander, G., G. Altarelli, A. Blondel, G. Coignet, G. Keil, D. E. Plane, and D. Treille, 1988, Eds., *Polarization at LEP* (CERN, Geneva), CERN Report No. 88-06.
Alitti, J., *et al.*, 1990, Phys. Lett. B **241**, 150.
Allaby, J. V., *et al.*, 1987, Z. Phys. C **36**, 611.
Allen, R. C., *et al.*, 1988, "A Proposal for a Precision Test of the Standard Model by Neutrino-Electron Scattering," Los Alamos Report No. LA-11300-PROPOSAL, UC-410.
Altarelli, G., and R. Barbieri, 1991, Phys. Lett. B **253**, 161.
Altarelli, G., R. Casalbuoni, D. Dominici, F. Feruglio, and R. Gatto, 1990a, Nucl. Phys. B **342**, 15.
Altarelli, G., R. Casalbuoni, D. Dominici, F. Feruglio, and R. Gatto, 1990b, Mod. Phys Lett. A **5**, 495.
Altarelli, G., R. Casalbuoni, F. Feruglio, and R. Gatto, 1990a, CERN Report No. CERN-TH.5752/90-ADD.
Altarelli, G., R. Casalbuoni, F. Feruglio, and R. Gatto, 1990b, Phys. Lett. B **245**, 669.
Altarelli, G., R. Kleiss, and C. Verzegnassi, 1989, Eds., *Z Physics at LEP 1* (CERN, Geneva), CERN Report No. 89-08.
Amaldi, U., A. Böhm, L. S. Durkin, P. Langacker, A. K. Mann, W. J. Marciano, A. Sirlin, and H. Williams, 1987, Phys. Rev. D **36**, 1385.
Appelquist, T., and J. Carazzone, 1975, Phys. Rev. D **11**, 2856.
Appelquist, T., D. Karabali, and L. C. R. Wijewardhana, 1986, Phys. Rev. Lett. **57**, 957.
Argento, A,. *et al.*, 1983, Phys. Lett. B **120**, 245.
Argento, A., *et al.*, 1984, Phys. Lett. B **140**, 142.
Barbieri, R., M. Frigeni, F. Giuliani, and H. E. Haber, 1990, Nucl. Phys. B **341**, 309.
Bardin, D. Y., M. S. Bilenky, G. V. Mitselmakher, T. Riemann, and M. Sachwitz, 1989, Z. Phys. C **44**, 493.
Bardin, D. Y., A. Leike, T. Riemann, and M. Sachwitz, 1988, Phys. Lett. B **206**, 539.
Beck, D. H., 1989, Phys. Rev. D **39**, 3248.
Beenakker, W., and W. Hollik, 1988, Z. Phys. C **40**, 141.
Berends, F. A., G. Burgers, W. Hollik, and W. L. van Neervan, 1988, Phys. Lett. B **203**, 177.
Berends, F. A., W. L. van Neervan, and G. J. H. Burgers, 1988, Nucl. Phys. B **297**, 429.
Bernabeu, J., A. Pich, and A. Santamaria, 1990, Nucl. Phys. B **363**, 326.
Bertolini, S., 1986, Nucl. Phys. B **272**, 77.
Bertolini, S., and A. Sirlin, 1984, Nucl. Phys. B **248**, 589.
Bilal, A., J. Ellis, and G. L. Fogli, 1990, Phys. Lett. B **246**, 459.
Blochus, D., *et al.*, 1986, "SLC Polarization Proposal," SLAC-PROPOSAL-SLC-01.
Blondel, A., 1989, CERN-EP/89-84.
Blondel, A., 1990, CERN-EP/90-10.
Blondel, A., *et al.*, 1990, Z. Phys. C **45**, 361.
Blondel, A., B. W. Lynn, F. M. Renard, and C. Verzegnassi, 1988, Nucl. Phys. B **304**, 438.
Blümlein, J., A. Leike, and T. Riemann, 1990, PHE90-30.
Blundell, S. A., W. R. Johnson, and J. Sapirstein, 1990, Phys. Rev. Lett. **65**, 1411.
Bolton, T., *et al.*, 1990, "Precision Measurements of Neutrino Neutral Current Interactions Using a Sign-Selected Beam," Fermilab Proposal P815.
Borrelli, A., M. Consoli, L. Maiani, and R. Sisto, 1990, Nucl. Phys. B **333**, 357.
Borrelli, A., L. Maiani, and R. Sisto, 1990, Phys. Lett. B **244**, 117.
Bouchiat, M. A., 1990, *12th International Atomic Physics Conference*, Ann Arbor, MI.
Bouchiat, C., and C. A. Piketty, 1991, Z. Phys. C **49**, 91.
Bouchiat, M. A., and A. Pottier, 1986, Science **234**, 1203.
Boudjema, F., F. M. Renard, and C. Verzegnassi, 1988, Phys. Lett. B **214**, 151.
Boudjema, F., F. M. Renard, and C. Verzegnassi, 1989, Nucl. Phys. B **314**, 301.
Brock, R., 1988, in *New Directions in Neutrino Physics at Fermilab*, edited by R. Bernstein (Fermilab, Batavia), p. 57.
Buchmuller, W., R. Rückl, and D. Wyler, 1987, Phys. Lett. B **191**, 442.
Buchmuller, W., and D. Wyler, 1986a, Nucl. Phys. B **268**, 621.
Buchmuller, W., and D. Wyler, 1986b, Phys. Lett. B **177**, 377.
Burckhardt, H., F. Jegerlehner, G. Penso, and C. Verzegnassi, 1988, in *Polarization at LEP*, edited by G. Alexander, G. Altarelli, A. Blondel, G. Coignet, G. Keil, D. E. Plane, and D. Treille (CERN, Geneva), CERN 88-06, Vol. 1, p. 145.
Campbell, B. A., J. Ellis, and R. A. Flores, 1989, Phys. Lett. B **225**, 419.
Chanowitz, M., 1988, Annu. Rev. Nucl. Part. Phys. **38**, 323.
Chanowitz, M. S., M. A. Furman, and I. Hinchliffe, 1978, Phys. Lett. B **78**, 285.
Consoli, M., S. LoPresti, and L. Maiani, 1983, Nucl. Phys. B **223**, 474.
Costa, G., J. Ellis, G. L. Fogli, D. V. Nanopoulos, and F. Zwirner, 1988, Nucl. Phys. B **297**, 244.
Cvetic, M., and P. Langacker, 1990, Phys. Rev. D **42**, 1797.
Cvetic, M., and B. Lynn, 1987, Phys. Rev. D **35**, 51.
de Boer, W., 1989, *Brighton Conference on Electroweak Radiative Corrections*, DESY 89-111.
Degrassi, G., S. Fanchiotti, and A. Sirlin, 1991, Nucl. Phys. B **351**, 49.
Degrassi, G., and A. Sirlin, 1989, Phys. Rev. D **40**, 3066.
Degrassi, G., and A. Sirlin, 1991, Nucl. Phys. B **352**, 342.
del Aguila, F., Ll. Garrido, and R. Miquel, 1990, Barcelona Report No. UAB-FT-237/90.
del Aguila, F., J. M. Moreno, and M. Quiros, 1989, Phys. Rev. D **40**, 2481.
del Aguila, F., J. M. Moreno, and M. Quiros, 1990, Phys. Rev. D **41**, 134.
del Aguila, F., J. M. Moreno, and M. Quiros, 1991, Phys. Lett. B **254**, 497.
Denner, A., R. J. Guth, and J. H. Kühn, 1990, Phys. Lett. B **240**, 438.
Djouadi, A., J. H. Kühn, and P. M. Zerwas, 1990, Z. Phys. C **46**, 411.

Drees, M., and K. Hagiwara, 1990, Phys. Rev. D **42**, 1709.
Durkin, L. S., and P. Langacker, 1986, Phys. Lett. B **166**, 436.
Dydak, F., 1990, in *25th International Conference on High Energy Physics, Singapore, 1990,* edited by K. K. Plana and Y. Yamaguchi (World Scientific, Singapore, 1991).
Dzuba, V. A., V. V. Flambaum, and O. P. Sushkov, 1989, Phys. Lett. A **141**, 147.
Eichten, E., I. Hinchliffe, K. Lane, and C. Quigg, 1984, Rev. Mod. Phys. **56**, 579.
Eichten, E. J., K. D. Lane, and M. Peskin, 1983, Phys. Rev. Lett. **50**, 811.
Einhorn, M. B., D. R. T. Jones, and M. Veltman, 1981, Nucl. Phys. B **191**, 146.
Eliasson, E., 1984, Phys. Lett. B **147**, 65.
Ellis, J., and G. L. Fogli, 1988, Phys. Lett. B **213**, 526.
Ellis, J., and G. L. Fogli, 1990, Phys. Lett. B **249**, 543.
Ellis, J., and R. Peccei, 1986, Eds., *Physics at LEP,* Vols. 1 and 2 (CERN, Geneva), CERN-86-02.
Englert, F., and R. Brout, 1964, Phys. Rev. Lett. **13**, 321.
Fanchiotti, S., and A. Sirlin, 1990, Phys. Rev. D **41**, 319.
Fernandez, E., 1990, *Neutrino '90,* June 1990 (CERN, Geneva), CERN-PPE/90-151.
Fogli, G. L., and D. Haidt, 1988, Z. Phys. C **40**, 379.
Frantsuzov, P. A., and I. B. Khriplovich, 1988, Z. Phys. D **7**, 297.
Geiregat, D., *et al.*, 1989, Phys. Lett. B **232**, 539.
Georgi, H., and G. L. Glashow, 1974, Phys. Rev. Lett. **32**, 438.
Glashow, S. L., J. Iliopoulos, and L. Maiani, 1970, Phys. Rev. D **2**, 1285.
Golden, M., and L. Randall, 1991, Nucl. Phys. B **361**, 3.
Gonzales-Garcia, M. C., and J. W. F. Valle, 1990a, Nucl. Phys. B **345**, 312.
Gonzales-Garcia, M. C., and J. W. F. Valle, 1990b, Phys. Lett. B **236**, 360.
Gonzales-Garcia, M. C., and J. W. F. Valle, 1991, Phys. Lett. B **259**, 365.
Grifols, J., and J. Sola, 1985, Nucl. Phys. B **253**, 47.
Gunion, J., H. Haber, G. Kane, and S. Dawson, 1990, *The Higgs Hunter's Guide* (Addison-Wesley, Redwood City).
Guralnik, G., C. Hagen, and T. Kibble, 1964, Phys. Rev. Lett. **13**, 585.
Haber, H., 1990, in *Testing the Standard Model,* edited by M. Cvetic and P. Langacker (World Scientific, Singapore, 1991), p. 340.
Haber, H. E., and G. Kane, 1985, Phys. Rep. C **117**, 75.
Hall, L. J., and L. J. Randall, 1986, Nucl. Phys. B **274**, 157.
Halzen, F., and B. A. Kniehl, 1991, Nucl. Phys. B **353**, 567.
Hartley, A. C., and P. G. H. Sandars, 1990, J. Phys. B, in press.
Heil, W., *et al.*, 1989, Nucl. Phys. B **327**, 1.
Herczeg, P., 1989, *International Symposium on Fundamental Symmetry in Nuclei and Particles, Caltech.*
Higgs, P. W., 1964, Phys. Rev. Lett. **12**, 132.
Higgs, P. W., 1966, Phys. Rev. **145**, 1156.
Hioki, Z., 1983, Nucl. Phys. B **229**, 284.
Hioki, Z., 1989, Prog. Theor. Phys. **82**, 875.
Hioki, Z., 1991, Z. Phys. C **49**, 287.
Holdom, B., 1985, Phys. Lett. B **150**, 301.
Holdom, B., 1987, Phys. Lett. B **198**, 535.
Holdom, B., and J. Terning, 1990, Phys. Lett. B **247**, 88.
Hollik, W., 1986, Z. Phys. C **32**, 291.
Hollik, W., 1988, Z. Phys. C **37**, 569.
Hollik, W., 1990, Fortschr. Phys. **38**, 165.
Hurst, P. T., 1990, Ph.D. thesis (University of Illinois).
Jegerlehner, F., 1986a, Z. Phys. C **32**, 425.
Jegerlehner, F., 1986b, Z. Phys. C **32**, 195.
Kaplan, D., and A. Manohar, 1988, Nucl. Phys. B **310**, 527.
Kennedy, D. C., 1991, Nucl. Phys. B **351**, 81.
Kennedy, D. C., and P. Langacker, 1990, Phys. Rev. Lett. **65**, 2967.
Kennedy, D. C., and P. Langacker, 1991, Phys. Rev. D **44**, 1591.
Kennedy, D. C., and B. Lynn, 1989, Nucl. Phys. B **322**, 1.
Kennedy, D. C., B. W. Lynn, C. J. C. Im, and R. Stuart, 1989, Nucl. Phys. B **321**, 83.
Kibble, T., 1967, Phys. Rev. **155**, 1554.
Kiesling, C., 1988, *Standard Theory of Electroweak Interactions* (Springer-Verlag, Berlin).
Kim, J. E., P. Langacker, M. Levine, and H. H. Williams, 1981, Rev. Mod. Phys. **53**, 211.
Kniehl, B. A., 1990a, Nucl. Phys. B **347**, 86.
Kniehl, B. A., 1990b, Comput. Phys. Commun. **50**, 293.
Kniehl, B. A., M. Krawczyk, J. H. Kühn, and R. G. Stuart, 1988, Phys. Lett. B **209**, 337.
Kniehl, B. A., and J. H. Kühn, 1989, Phys. Lett. B **224**, 229.
Kniehl, B. A., and J. H. Kühn, 1990, Nucl. Phys. B **329**, 547.
Kniehl, B. A., J. H. Kühn, and R. G. Stuart, 1988a, Phys. Lett. B **214**, 621.
Kniehl, B. A., J. H. Kühn, and R. G. Stuart, 1988b, in *Polarization at LEP,* Vol. I, edited by G. Alexander, G. Altarelli, A. Blondel, G. Coignet, G. Keil, D. E. Plane, and D. Treille (CERN, Geneva), p. 158.
Langacker, P., 1981, Phys. Rep. C **72**, 185.
Langacker, P., 1984, Phys. Rev. D **30**, 2008.
Langacker, P., 1988, in *Ninth Workshop on Grand Unification,* edited by R. Barloutand (World Scientific, Singapore), p. 3.
Langacker, P., 1989a, Phys. Rev. Lett. **63**, 1920.
Langacker, P., 1989b, in *Weak and Electromagnetic Interactions in Nuclei,* edited by P. Depommier (Editions Frontiéres, Gif sur Yvette), p. 5.
Langacker, P., 1990a, Phys. Lett. B **239**, III-56.
Langacker, P., 1990b, Nucl. Phys. B (Proceedings Supplement) **13**, 344.
Langacker, P., 1991a, in *Particles, Strings, and Cosmology,* edited by P. Nath and S. Reucroft (World Scientific, Singapore), p. 237.
Langacker, P., 1991b, Phys. Lett. B **256**, 277.
Langacker, P., and D. London, 1988a, Phys. Rev. D **38**, 886.
Langacker, P., and D. London, 1988b, Phys. Rev. D **38**, 907.
Langacker, P., and M. Luo, 1991a, Phys. Rev. D **44**, 817.
Langacker, P., and M. Luo, 1991b, University of Pennsylvania Preprint No. UPR-0476T.
Langacker, P., and A. K. Mann, 1989, Phys. Today, **42** (12), 22.
Langacker, P., R. Robinett, and J. Rosner, 1984, Phys. Rev. D **30**, 1470 and references therein.
Langacker, P., and R. Rückl, 1991, unpublished.
Langacker, P., and S. Umasankar, 1989, Phys. Rev. D **40**, 1569.
Layssac, J., F. M. Renard, and C. Verzegnassi, 1990, Annecy Preprint LAPP-TH-290/90(REV).
Lee, B. W., 1972, *XVIth International Conference on High Energy Physics* (FNAL) Vol. IV, p. 266.
Lim, S., T. Inami, and N. Sakai, 1984, Phys. Rev. D **29**, 1488.
Lynn, B., 1984, SLAC-PUB-3358.
Lynn, B., M. Peskin, and R. Stuart, 1986, in *Physics at LEP,* Vol. 1, edited by J. Ellis and R. Peccei (CERN, Geneva), CERN-86-02, p. 90.
Lynn, B. W., F. M. Renard, and C. Verzegnassi, 1988, Nucl. Phys. B **310**, 237.
Lynn, B., and J. F. Wheater, 1984, Eds., *Radiative Corrections*

in SU(2)×U(1) (World Scientific, Singapore).
Maalampi, J., and M. Roos, 1990, Phys. Rep. **186**, 53.
Mahanthappa, K. T., and P. K. Mohapatra, 1991, Phys. Rev. D **43**, 3093.
Marciano, W., 1979, Phys. Rev. D **20**, 274.
Marciano, W., 1990a, TASI-90, unpublished.
Marciano, W., 1990b, private communication.
Marciano, W., and J. Rosner, 1990, Phys. Rev. Lett. **65**, 2963.
Marciano, W., and A. Sirlin, 1980, Phys. Rev. D **22**, 2695.
Marciano, W., and A. Sirlin, 1981, Nucl. Phys. B **189**, 442.
Marciano, W., and A. Sirlin, 1983, Phys. Rev. D **27**, 552.
Marciano, W., and A. Sirlin, 1984a, Phys. Rev. D **29**, 75.
Marciano, W., and A. Sirlin, 1984b, Phys. Rev. D **29**, 945.
Marshall, R., 1989, Z. Phys. C **43**, 607.
Martyn, H. U., 1987, in *DESY HERA Workshop, 1987,* Proceedings of the workshop held in Hamburg, Germany, edited by R. Peccei (DESY, Hamburg), p. 801. SLAC call number QCD 161:H15:1987.
Mattison, T. S., *et al.*, 1990, Phys. Rev. D **42**, 1311.
Missimer, J., and L. M. Simons, 1985, Phys. Rep. **118**, 179.
Missimer, J., and L. M. Simons, 1990, Z. Phys. D **17**, 275.
Mohapatra, R. N., 1986, *Unifications and Supersymmetries* (Springer, New York).
Mohapatra, R. N., and G. Senjanovic, 1980, Phys. Rev. Lett. **44**, 912.
Mohapatra, R. N., and G. Senjanovic, 1981, Phys. Rev. D **23**, 165.
Mori, Y., *et al.*, 1989, Phys. Lett. B **218**, 499.
Nardi, E., and E. Roulet, 1990, Phys. Lett. B **248**, 139.
Nilles, H. P., 1984, Phys. Rep. C **110**, 1.
Nilles, H. P., 1990, in *Testing the Standard Model,* edited by M. Cvetic and P. Langacker (World Scientific, Singapore, 1991), p. 633.
Noecker, M. C., *et al.*, 1988, Phys. Rev. Lett. **61**, 310.
Passarino, G., and M. Veltman, 1979, Nucl. Phys. B **160**, 151.
Pati, J. C., and A. Salam, 1974, Phys. Rev. D **10**, 275.
Peskin, M., 1987, "Looking Beyond the *Z*," Lecture at 1987 SLAC Summer Institute, edited by E. C. Brennan, SLAC-PUB-5210.
Peskin, M., and T. Takeuchi, 1990, Phys. Rev. Lett. **65**, 964.
Prescott, C. Y., *et al.*, 1979, Phys. Lett. B **84**, 524.
Randall, L., and R. S. Chivukula, 1989, Nucl. Phys. B **326**, 1.
Renard, F. M., and C. Verzegnassi, 1989, Phys. Lett. B **217**, 199.
Reutens, P. G., *et al.*, 1990, Z. Phys. C **45**, 535.
Riemann, T., and M. Sachwitz, 1988, Phys. Lett. B **212**, 488.
Riemann, T., M. Sachwitz, and Z. Was, 1990, CERN-TH.5964/90.
Robinett, R., 1982, Phys. Rev. D **26**, 2388.
Robinett, R., and J. Rosner, 1982a, Phys. Rev. D **25**, 3036.
Robinett, R., and J. Rosner, 1982b, Phys. Rev. D **26**, 2396.
Rosner, J., 1987, Phys. Rev. D **35**, 2244.
Rosner, J., 1989, Phys. Lett. B **221**, 85.
Rosner, J., 1990, in *Testing the Standard Model,* edited by M. Cvetic and P. Langacker (World Scientific, Singapore, 1991), p. 91.
Ross, G. G., 1985, *Grand Scientific Unified Theories* (Benjamin, New York).
Ross, G. G., 1988, Nucl. Phys. B (Proceedings Supplement) **3**, 743.
Rückl, R., 1983, Phys. Lett. B **129**, 363.
Salam, A., 1969, in *Elementary Particle Theory,* edited by N. Svartholm (Almqvist & Wiksells, Stockholm), p. 367.
Sarantakos, S., A. Sirlin, and W. Marciano, 1983, Nucl. Phys. B **217**, 84.
Shaevitz, M., 1990, *Neutrino '90,* Nevis Laboratories, Columbia University, Preprint R1482.
Shanker, O., 1982, Nucl. Phys. B **206**, 253.
Siegel, R., 1987, Ed., *1986 Parity Violation Workshop* (CEBAF, Newport News).
Sirlin, A., 1980, Phys. Rev. D **22**, 971.
Sirlin, A., 1984, Phys. Rev. D **29**, 89.
Sirlin, A., 1989, Phys. Lett. B **232**, 123.
Sirlin, A., 1990, Nucl. Phys. B **332**, 20.
Souder, P. A., *et al.*, 1990, Phys. Rev. Lett. **65**, 694.
Swartz, M., 1987, in SLAC Summer Institute 1987 SLAC call number QCD 161:S76:1987.
Toussaint, D., 1978, Phys. Rev. D **18**, 1626.
van der Bij, J. J., and F. Hoogeveen, 1987, Nucl. Phys. B **283**, 477.
Veltman, M., 1977, Nucl. Phys. B **123**, 89.
Weinberg, S., 1967, Phys. Rev. Lett. **19**, 1264.